Report Title:	**SOFC Prototype System Test**
Type of Report:	Final Technical Report
Reporting Period:	October 1, 2015 to December 31, 2020
Principal Investigator:	Hossein Ghezel-Ayagh
Date Report Issued:	March 31, 2021
Report Prepared for:	U. S. Department of Energy (DOE) – National Energy Technology Laboratory (NETL)
DOE Award No.:	DE-FE0026199
Report Prepared by:	FuelCell Energy, Inc. 3 Great Pasture Road Danbury, CT 06810
Subcontractors:	Versa Power Systems, Ltd 4852 - 52nd Street SE Calgary, AB T2B 3R2

DISCLAIMER

This Technical Progress Report was prepared with the support of the U.S. Department of Energy, under Award No. DE-FE0026199. However, any opinions, findings, conclusions, or recommendations expressed herein are those of the author(s) and do not necessarily reflect the views of the DOE.

TABLE OF CONTENTS

LIST OF FIGURES

LIST OF TABLES

EXECUTIVE SUMMARY

The SOFC Prototype System has achieved 5000 hours of hot operation as of September 9, 2020 fulfilling the final outstanding project milestone. After the 5000 hours was achieved, the system was brought up to 100% load where overall stack performance continued to remain stable. The system continued to operate at 100% load through the end of the test campaign.

This Final report encompasses several topics over the course of this project including the results from demonstration testing and post-test stack analysis. Below is a comprehensive list of the requested test report topics:

- History/Background
- Project Purpose
- R&D On-Cell Development
- Cell Manufacturing
- Cell Yield
- Test plan, test deviations
- Issues and Problems
- Test Results (Relevant Test Data)
- Post Test Final Analysis of the system
- Lessons Learned
- Research and Technology Gaps
- Steps forward
- Stack and system cost analysis

Operation in Danbury was focused at 90% load to provide direct comparison to the operation in Pittsburgh and due to the lingering effects of the sulfur poisoning experienced there. As a result, higher stack temperatures were experienced which demanded higher air flow to provide additional cooling. The gross fuel efficiency was ~58% instead of the projected values of 64% and net fuel efficiency was around 36-38% during operation in Danbury as a direct consequence of the sulfur poisoning. The “projected net efficiency” which removes the added parasitic loads of the startup electric heaters was 46-48%.

GC samples were taken from the system at 100% load operation, which continued to show low levels of reforming in the reformer due to the sulfur poisoning. However, stack reforming did improve compared to the GC’s taken previously at 60% load. Temperatures inside the reformer and stacks remained high and stable, which suggests no significant recovery from the sulfur poisoning.

Post-test analysis for the five stacks from Module A were completed. Analyses showed overall good electrical contact in all layers, no or small trace of carbon at the fuel inlets, and broken cells. The early hours of the initial factory acceptance testing proved to be detrimental as indicated by the direct comparison of the stack that was replaced to that of the new one prior to the Pittsburgh operation. Sulfur was found in the cells that operated in Pittsburgh, while the stack that only ran in Danbury showed no signs of sulfur.

1. INTRODUCTION

The goal of this U.S. Department of Energy (DOE) sponsored project is to test a 200 kWe thermally self-sustaining atmospheric-pressure solid oxide fuel cell (SOFC) prototype system at a prominent site. Fuel Cell Energy Inc. (FCE) utilized the state-of-the-art SOFC technology of its wholly-owned subsidiary Versa Power Systems (VPS) to design, fabricate and test the 200 kW prototype system. The specific objectives of this project were to achieve an SOFC stack power degradation rate of ≤1.5% per 1000 hours for the 400 kW stand-alone prototype power system undergoing ≥ 5000 hours of steady state tests at thermally self-sustained normal operating conditions (NOC), and to verify the prospects for a high volume SOFC stack production cost below the DOE target of 225 dollars per kilowatt. Achieving these goals enables commercial natural gas fueled SOFC system deployment in the 2020 timeframe, which will eventually lead to SOFC technology that is viable for large scale central power generation applications.

The project initially was targeting a 400 kW SOFC system, albeit due to budgetary concerns, the scope of work was altered to target a single 200kWe prototype system.

In support of the aforementioned goals and project objectives, activities to be conducted during this project are as follows:

- Design and fabricate a 200 kWe SOFC prototype system, including the SOFC stacks, Modular Power Block (MPB) module(s), mechanical balance-of-plant (MBOP) and electrical balance-of-plant (EBOP).
- Install the 200 kWe SOFC prototype system at a prominent host site to maximize visibility of the demonstration.
- Commission and operate the 200 kWe SOFC prototype system for at least 5,000 hours at NOC using natural gas fuel and with stack operating temperature greater than 700°C, to demonstrate stack degradation of ≤1.5% per 1000 hours.
- Estimate SOFC stack cost, based on high-volume manufacturing levels and the experimentally-observed stack performance at normal operating conditions, towards the goal of $225/kW (based on system net AC power in year 2011 dollars).
- Estimate the Power Block cost (exclusive of fuel supply, contaminant removal, and CO2 capture subsystems) for an Integrated Gasification Fuel Cell system, towards the goal of $900/kW (based on system net AC power, in year 2011 dollars).

The Milestone Status Report, showing the planned and actual completion dates, is presented in Table 1-1.

Table 1-1 Milestone Status

Id.	Task / Subtask No.	Milestone Description	Planned Completion	Actual Completion	Verification Method
1	3.2	Complete Stack Module Final Design and Fabrication Plan	5/31/16	5/31/16	Quarterly Report
2	3.1	Complete Detailed Prototype System Electrical Design	8/24/16	8/24/16	Quarterly Report
3	3.1	Complete Detailed Prototype System Mechanical Design	10/17/16	10/17/16	Quarterly Report
4	3.1	Complete Detailed Prototype System Process Design	11/3/16	11/3/16	Presentation to DOE PM/ Quarterly Report
5	2.2	Complete Stack Block Fabrication for Prototype System	12/8/16	7/17/17	Presentation to DOE PM/ Quarterly Report
6	4.2	Complete 200 kW SOFC Prototype System Fabrication and Assembly	4/23/18	4/23/18	Quarterly Report/ Letter to DOE PM
7	5	Complete Validation of Stack & IGFC System Costs to Meet DOE's Goals	7/23/19	7/23/19	Quarterly Report
8	4.4	Complete Tests of 200 kW SOFC Prototype System for > 5,000 hours of Operation	9/30/20	9/9/20	Quarterly Report

2. SYSTEM DESIGN

The objective of this task was to complete the detailed design for the 200 kWe SOFC Prototype system. A modular approach to the 200 kW system architecture, in which multiple stack module building blocks are arrayed to generate higher power levels, will be employed. Four nominal 100 kW stack modules, named “Modular Power Block” (MPB), will be utilized for the 200 kWe SOFC prototype system. In order to meet the project goals of less than 1.5% per 1000 hours power degradation over 5000 hours of system operation, the emphasis for system design activities will be placed on: 1) improving the BoP equipment and instrumentation reliability, 2) improving system control and protection logic functions to protect the SOFC stacks during normal operating conditions, as well as during off-design conditions, and 3) integration of thermal management strategies into the MPB to reduce stack temperature gradients. The work will be divided in two subtasks as follows:

Objective:

- Develop detailed, approved-for-construction, engineering and design package for the 200 kW SOFC prototype system
- Conduct an interdisciplinary safety review of the 200 kW system

Approach:

The results of the detailed engineering design activities will include a complete set of documents encompassing analyses, fabrication drawings, specifications, vendor data, and instructions required to construct the power plant. Detailed engineering will be performed for three disciplines: process, mechanical and electrical. The safety review will be conducted, utilizing the Hazard and Operability Analysis (HAZOP) method, to ensure that the 200 kW system includes all required safety features. The detailed design will also address site preparations and installation requirements for the identified demonstration site.

Results & Discussion:

<u>System Layout</u>

The system design effort under this subtask leverages the 200 kW SOFC system design developed under the parallel project ‘Reliable SOFC Systems’ (ReliSS), DOE Award No. DE-FE0023186. Design modifications required based on the host site selection for the 200 kW SOFC system were investigated.

The 200 kW system architecture is comprised of two 200 kW skids, each skid containing two nominal 100 kW stack modules or “Modular Power Blocks” (MPBs). Further, each skid is mechanically autonomous, containing the balance-of-plant equipment necessary to support 2x100 kW MPBs.

In this manner, the process design incorporates 200 kW SOFC subsystem (Figure 2-2) elements into the 200 kW system design. The design elements, and documentation are summarized below:

- Design Basis
- Heat and Material Balances
    - At Full Power and ISO (ambient) Conditions
    - At Rated Power and ISO (ambient) conditions

    - At Rated Power and 95°F ambient temperature
- Piping & Instrumentation Diagrams
    - Natural Gas Desulfurization (subsystem)
    - Anode Recycle System
    - Cathode Air Supply (subsystem)
    - Cathode Air Preheat (subsystem)
    - SOFC Modules and Prereformer
    - SOFC (stack) Towers
    - Purge Gas Supply (subsystem)
    - Demineralized Water Treatment (subsystem)
    - Water Vaporizer
- Major BOP Equipment Specifications
    - Dehumidifier
    - Desiccant Reactivation Blower
    - Desulfurizers
    - Fresh Air Blower
    - Anode Recycle Blower
    - Radiative Fuel Reformer
    - Catalytic Air Preheater
- Water Treatment System
- Instrument Index and Specifications

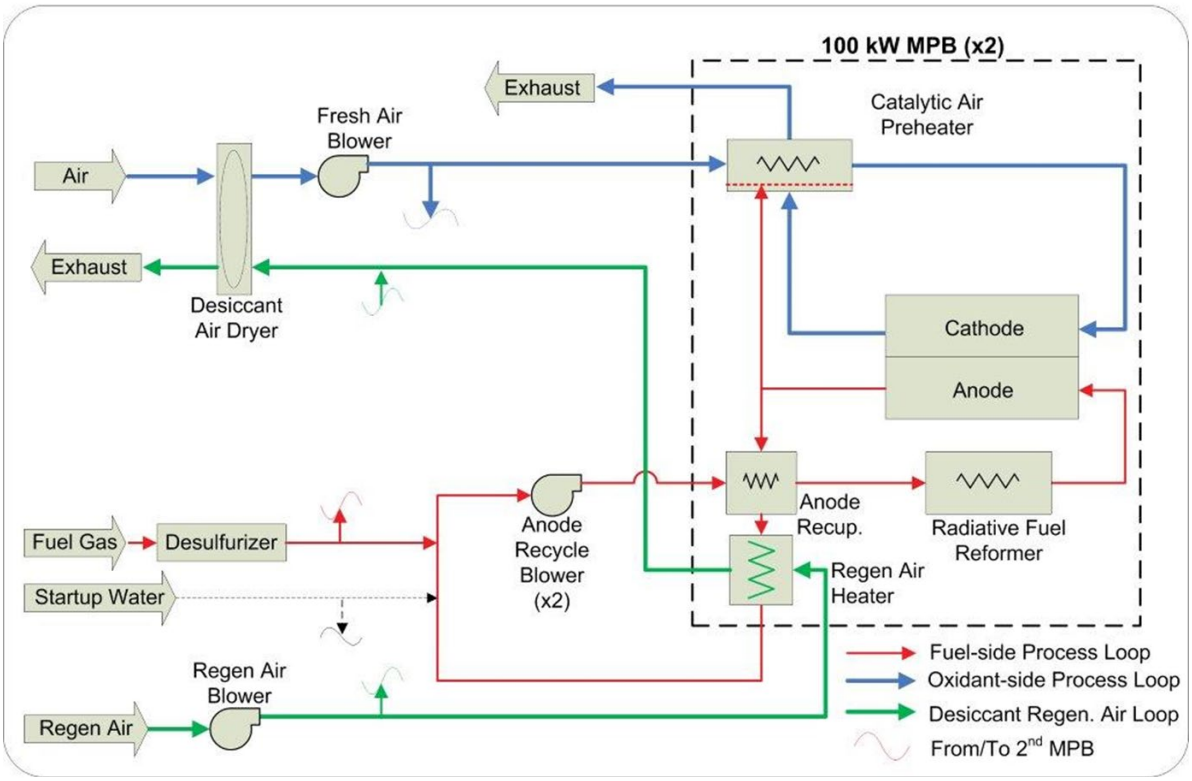

Figure 2-1 200kW SOFC Power Plant Block Flow Diagram

The 200 kW BoP was designed such that, wherever possible, various subsystems would be constructed in parallel and be integrated later in the build in order to reduce schedule risk. The air box assembly is one such subsystem that can be constructed separately from the structural skid. The air box houses many system components and performs many tasks so the ability to construct it in parallel with the structural skid greatly benefited the schedule. The air box not only houses the process and reactivation air blowers, but it also provides cooling for those blowers, a common air pre-filter, a drop-on interface for the environmental protection for sensitive electronics and process piping. Housing process air lines within the air box allows for the use of light-weight materials for the airlines which reduced complexity and cost while allowing for easier maintenance.

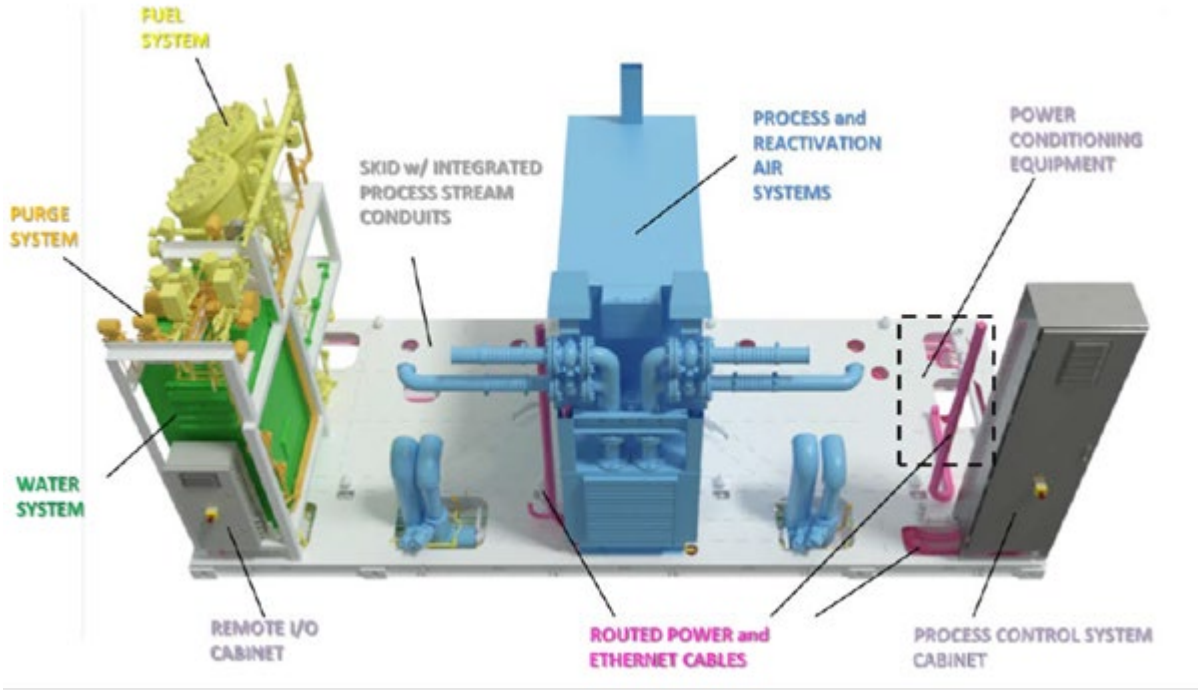

Figure 2-2 200kW Balance of Plant Layout

The purge gas subsystem design required 1500 gallon tank was found to be appropriate for the 200 kW SOFC system, allowing for one complete shutdown with a 30 day refill interval.

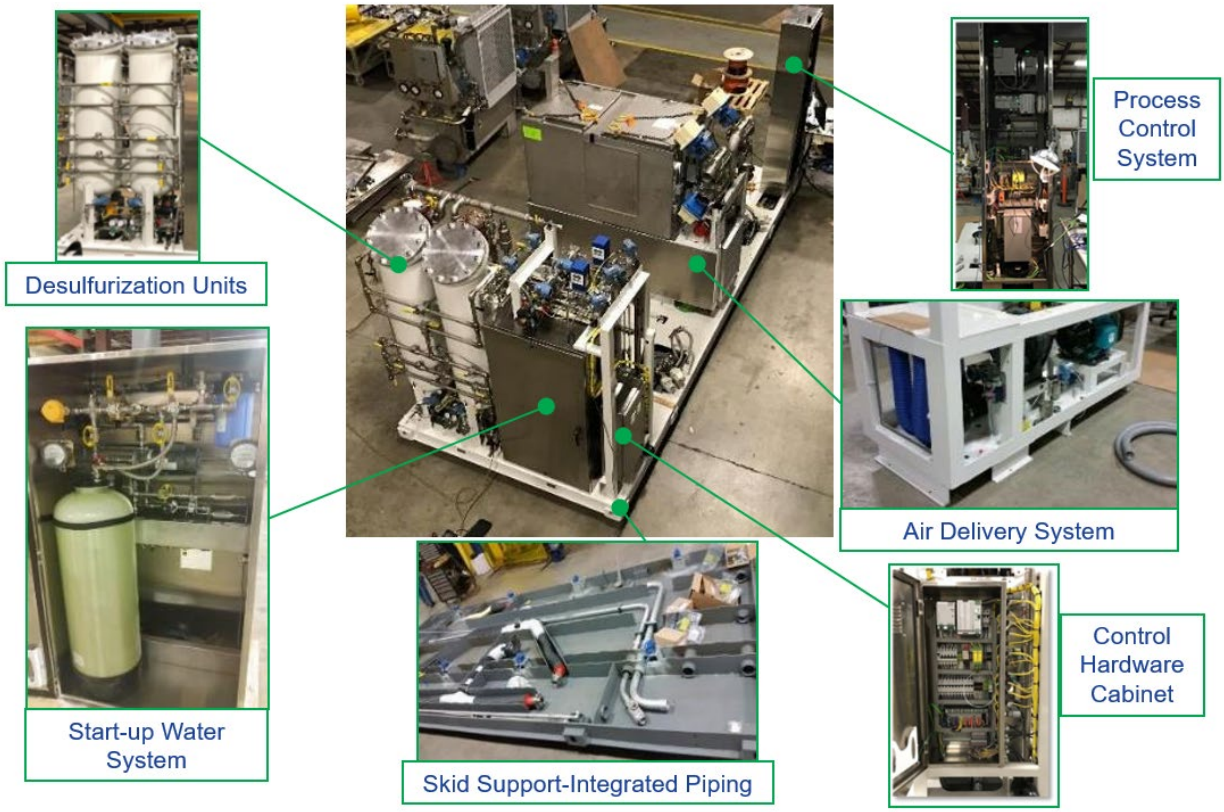

Figure 2-3 200kW BOP Sub-System Fabrication/Assembly

The Modular Power Block highlights the collective efforts of several engineering disciplines, providing the benefits of incorporating a number of BOP sub-system process and control elements. The resulting design layout (Figure 2-4) provides a very compact 100 kW MPB with significantly increased functionality. The critical upgrades that had the biggest impact on reducing the size of the plant were: moving the MPB controller and power distribution hardware onto compact retractable panel arrangements within a high voltage cabinet; moving instrumentation I/O hardware onto compact retractable panel arrangements with a low voltage cabinet; and an anode recycle stream heat exchanger placed within the hot zone allowing to replace the high temperature large fabrication blower (located on the skid) with a lower temperature blower (installed on the MPB). Some of the major benefits to this stack module architecture are as follows:

- Fully integrates all hot BoP equipment within the module
- Eliminates high-temperature plant piping & valves
- Reduces Cr evaporation protective coatings within plant/module
- Integrated anode blower & module-specific instruments greatly decreases plant footprint

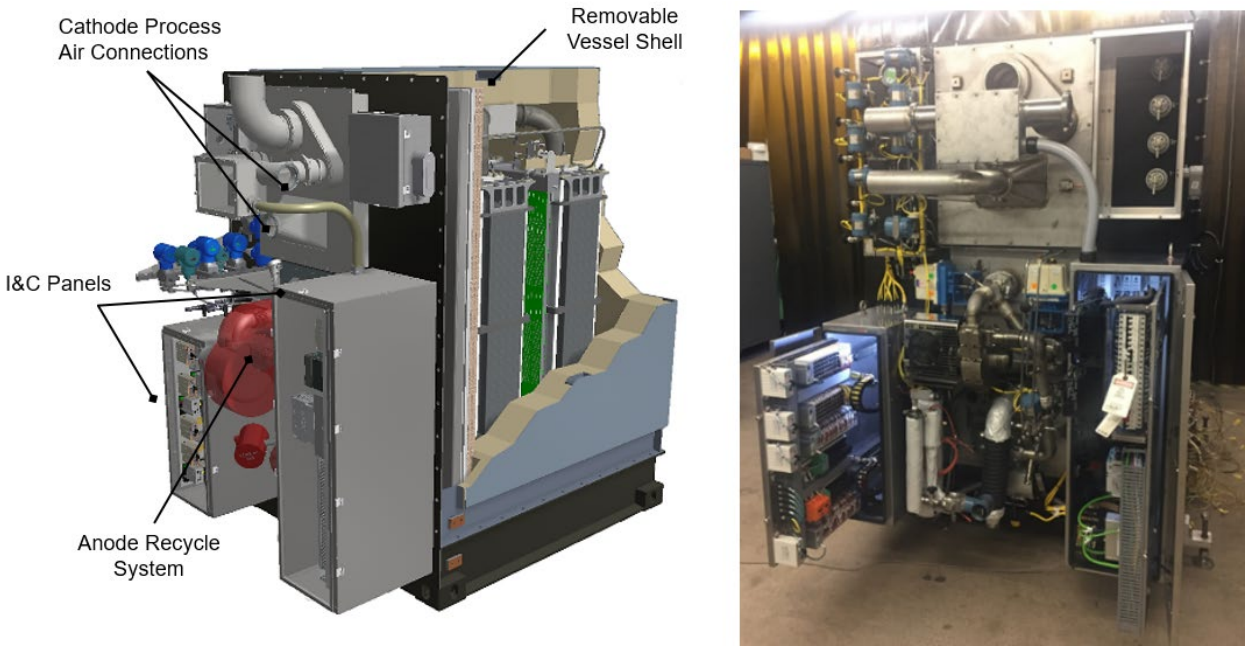

Figure 2-4 Module Power Block Compact Arrangement (Left) & Assembly at FCE facility in Danbury, CT (Right)

Because the first article being used for the 100 kW system is identical to the units planned for the 200 kW plant, a very thorough design documentation effort is being made for the MPB project (ReliSS).

Figure 2-5 illustrates the sub-systems that are part of the top level integrated MPB module. A documentation tree is also provided in the figure. The base module sub-assembly 23600-000 includes all the internal integrated hot components such as the SOFC stacks, radiative fuel reformer, high-temperature electrical heaters, catalytic oxidizer, recuperator/regenerator and all hot piping. The remaining blocks in the documentation tree cover sub-systems mounted externally to the module and include low temperature sub-systems, instrumentation, anode recycle, water vaporization and all module-specific electrical components.

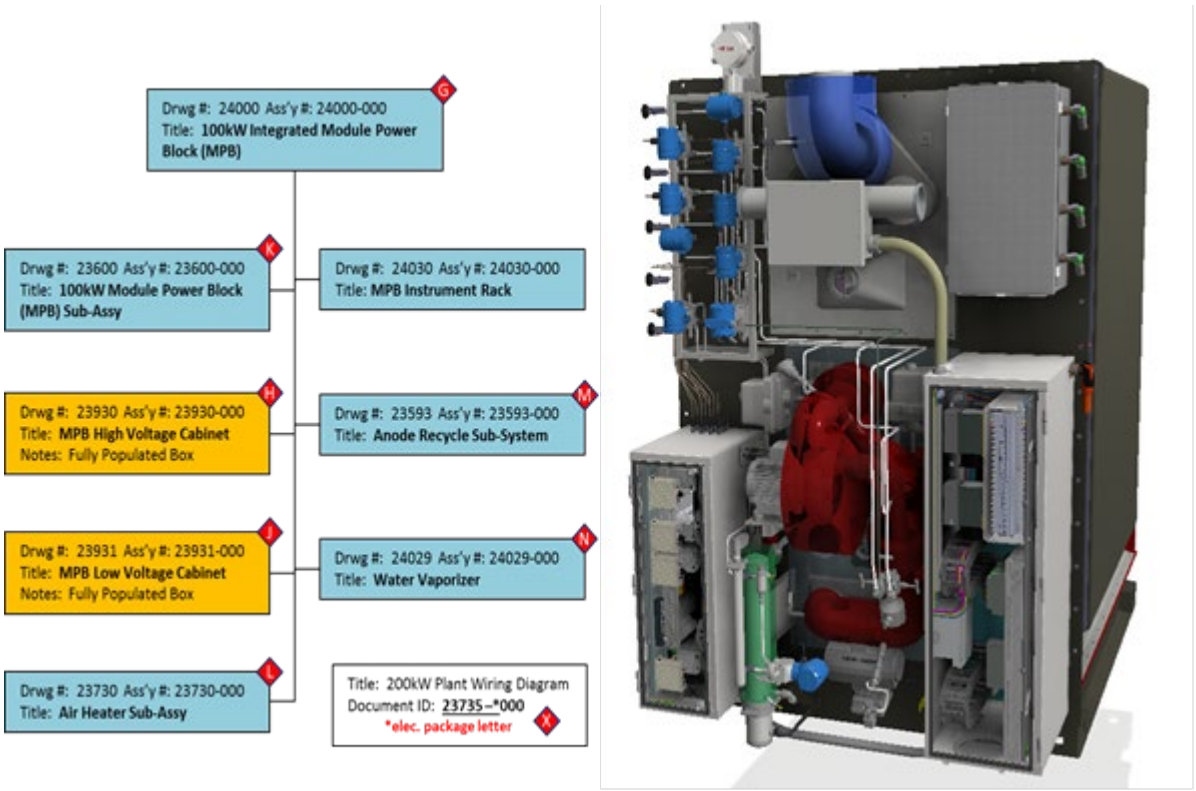

Figure 2-5. 100 kW Module Power Block (MPB) & Documentation Tree

Because the major module components for this project (200 kW SOFC) are being procured in parallel with the first article 100 kW unit, the main focus in the last two quarters has been the detailed development of the CAD (computer aided design/drafting) 3D models to ensure that these modules will go together as planned with minimal deviations between the initial build and the follow-on units. Part of this more complete documentation of the MPB design includes a detailed electrical drawing package. In order to minimize risk, one of the pivotal aspects of the electrical design effort includes modelling of every electrical component, even to the level of every fuse, terminal board, DIN rail, breaker, PLCs, I/O boards, VFDs, heater controllers, fans, smoke detectors, wire ways, pass-through, interconnects, etc. Even wires in some cases are 3D modeled where either large gauges are needed, or high wire count bundles that take up significant volume can affect the ability to package all the electrical equipment.

Mechanical and Electrical Design Cost Reduction:

One of the biggest targets for cost reduction was main process air flow control valves. The units currently being used are industrial 4" flanged ball valves which are very large and heavy requiring significant mounting support, and also are very expensive. At $5,000.00 a piece it made sense to spend time figuring out how to reduce the size, weight and cost of these valves. During the 200 kW design process, a similar problem of cost and space constraints was solved for the reactivation air system by developing a lightweight damper-style valve. This smaller valve was able to meet all the process flow control conditions and is currently included in our 200 kW plant. The success of this small valve gives confidence that the same style valve and smaller actuator could be used for the cathode flow control valves. A larger, 4" version of the valve has been designed and would have been implemented in our 400 kW plant build. As shown in

Figure 2-6, the size difference in the valves is significant. The weight is also reduced by 80% which allowed for the use of lighter-weight tubing for the air lines. The biggest difference was in the price, which was reduced by 75% for a total cost savings of $30,000.00 in the 400 kW plant.

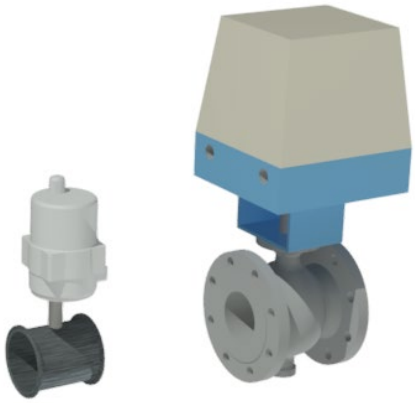

Figure 2-6. Cathode Air Flow Control Valve Size Comparison - 400 kW vs 200 kW System

The same improvement mindset was used to target the natural gas safety shutoff valves, which are also large and very expensive. Instead of relying on industrial valves for this function, FCE explored the industries that require the same level of safety in a smaller valve package. Burner shutoff valves incorporating the required double block valve setup housed within a single unit were found which reduced size, cost and complexity. Several other cost reductions, found during the 200 kW plant build, in smaller components that were suggested by our manufacturer would have been implemented in the 400kW design as well.

In addition to BoP improvements, the design team investigated the layout of the two skids that comprise the 400 kW design. The original idea of housing both skids under a single façade is being investigated as opposed to using two separate facades (from the 200 kW design). This would create a more streamlined and cleaner look for the 400 kW plant.

On the electrical side of the design, the team identified an opportunity to improve communication with the blowers on the plant. The VFD's implemented in the 200 kW design required a translation between different communications protocol. The added unnecessary complexity to the setup and required extra hardware in the Plant Control System enclosure. New VFD's were chosen for the 400 kW design that will eliminate this added layer of complexity and also reduce the overall cost of the installation.

Since the 400 kW design relies on two 200 kW skids each with their own Power Conditioning Unit (PCU), provisions are included in the PCU for synchronization of multiple connected skids.

Skid & Facade:

To provide the structural foundation of the plant, an innovative structural skid was designed to accommodate conduit, cables and process line plumbing below the top surface in order to reduce the overall footprint of the SOFC Plant while maintaining the strength and rigidity to support the BOP during assembly, transportation, installation, and operation. Several packaging updates to the plant design were necessary to accommodate final instrument selections and to address corrective actions resulting from the team's hazard and operability study (HAZOP). The detailed design documentation was used to complete the activities for fabrication of the BOP sub-assembly, which includes both MBOP and EBOP functional sub-systems.

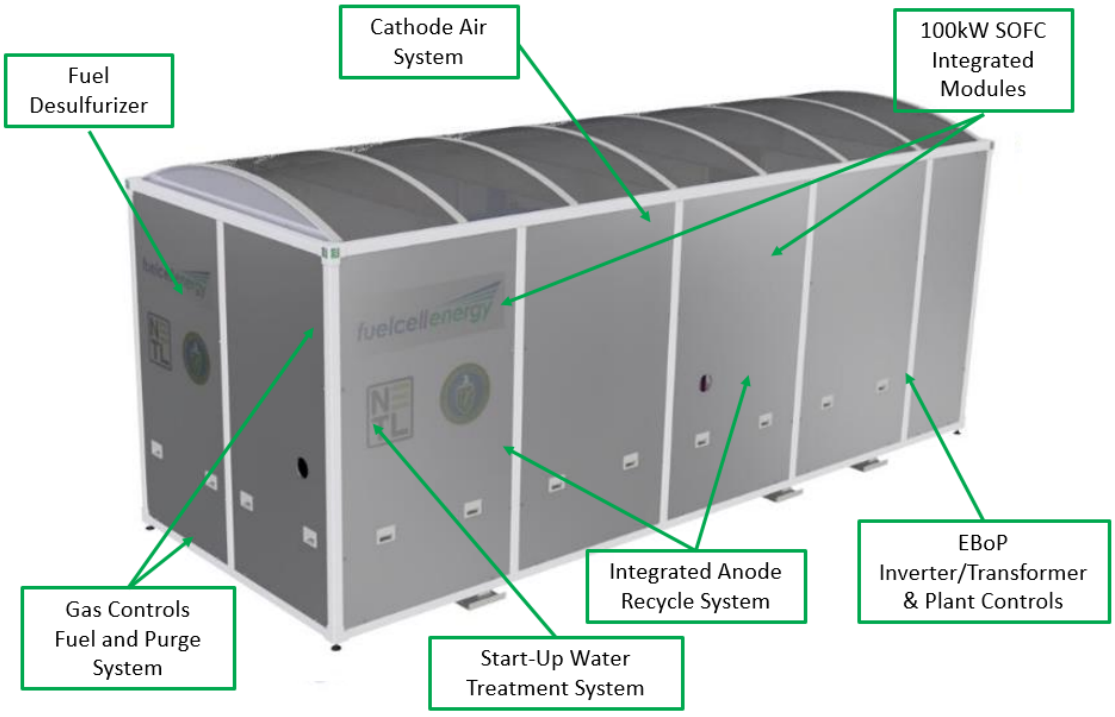

Figure 2-7 SOFC Power System Overview

SITE INSTALLATION

The mechanical contractor managed the installation work in collaboration with NRG and FCE. A local rigging contractor was hired by the mechanical contractor to supply the crane and rigging work. Logistics for hoisting and landing the plant involved closing the road, staging the crane, trucking the plant into position and careful rigging. The SOFC system was set by the rigging contractor (Figure 2-8) under the direction of FCE's engineering team who were onsite during the installation. All resources onsite worked collaboratively, which facilitated a smooth and safe placement of the plant. Planning and coordination prior to and during the lift was essential.

Figure 2-8. Landing the SOFC Unit at the NRG Site in Pittsburgh, PA

Once the plant was landed and all connections were made, all team members worked together to install the façade to provide its finished look, as shown in

Figure 2-9.

Figure 2-9. Fully Assembled SOFC System with Façade at NRG site in Pittsburgh, PA

The nitrogen storage tank and hydrogen bottles, which make up the purge system, were installed at the site after the SOFC unit was installed and fully assembled. The wiring for the nitrogen tank telemetry unit (to allow remote monitoring of tank level by Airgas) was completed early the next quarter and its communication to the PLC was also confirmed at that time.

After the SOFC unit was installed on-site, the electrical contractor applied for the electrical permit. However, it was denied by the City of Pittsburgh as they also required a zoning approval and HVAC permit. When permit requirements were first discussed, the City only advised that an approval from the Fire Marshall would be necessary. As a result, the contractor worked on obtaining zoning approval and the HVAC permit, a typical 30 day process once the application is submitted. Once the zoning permit was approved, the electrical permit application was resubmitted, including the zoning permit number, which allowed the electrical inspection to take place.

3. CELL & STACK MANUFACTURING (AND CELL YIELD)

The objective of this task is to fabricate and deliver the required SOFC stacks for a 200 kWe SOFC demonstration system. In order to meet the project goals of less than 1.5% per 1000 hours power degradation over 5000 hours of system operation, the emphasis will be placed on quality, yield, repeatability, and reliability. Opportunities for manufacturing efficiency improvement and cost reduction will also be addressed as appropriate.

The main technical work will focus on the following subtasks:

Objective:

- Fabricate full area (550 cm^2 active area) cells for the deliverable stack blocks
- Fabricate compressive ceramic seals

Approach:

The cell manufacturing will be based on the established baseline TSC3 cell design, formulations, process technologies and specifications. The TSC3 cell design is based on anode-supported thin electrolyte planar cell platform offering higher power density at intermediate operating temperature (600-800°C). Traditional materials, such as Ni/YSZ anodes, YSZ electrolytes and perovskite cathodes have been utilized in the basic cell structure. The cell configuration for the deliverable stack blocks corresponds to a cell active area of 550 cm^2 and a cell thickness of ~0.6 mm. The estimated power output is 250 mW/cm^2 at system normal operating conditions (NOC).

TSC3 cell manufacturing process is the third generation fully integrated manufacturing process developed for the individual SOFC cell design. It has three major unit operations: Tape-casting, Screen printing and Co-firing. TSC3 cell has an anode substrate ~0.6 mm in thickness, and is produced by a single-step tape casting process. The anode functional layer (AFL) and electrolyte are screen-printed directly on the green anode substrate tape. The multi-layer green cells are sintered into half-cells through a co-firing process. The subsequent barrier layer and cathode are screen printed and fired on half-cells. A total of 120 full-cells will be batched for each single stack block. It is estimated that a total of 4000 cells will be manufactured for this project.

Cell manufacturing process standardization will be performed. Existing cell production capacity at the pilot plant will be optimized to meet the required cell production volume. Incremental process equipment, tooling and fixtures will be procured or fabricated. Cell manufacturing quality control steps will be fully implemented based on controlled documentation (Drawing Specifications, Material Specifications, Work Instructions, and Incoming Inspection Plans). In addition to cell fabrication, compressive ceramic seals composed of a mixture of alumina fiber and powder will be fabricated using the tape casting process to meet the requirements of stack design and build.

Results & Discussion:

CELL PRODUCTION TOOLING

As reported previously under DOE Project DE-FE0023186 (Reliable SOFC Systems, aka ReliSS project), a new device was designed, built and implemented to improve cell thickness measurement. This measurement is an important parameter in the current large area stack manufacturing. The new device has been used to measure cells fabricated for 16-Cell Technology stacks. Based on stack test results and post-test examination, no cell damage was encountered. Thus, this new device was qualified and ready for production use in 120-cell stacks.

A new cell press QC tool for ½ cell measurement was also built which is a replicate to the previous set-up except for the PLC-control and coupler addition. Prior to the switch-over to the new device, a half cell (fired anode substrate, anode functional layer and electrolyte) thickness measurement comparison was performed on the two cell presses to determine if there was any significant difference in average measurements. Based on the results, the individual measurement differences were negligible and no difference was observed for a sample size of 10 (see Figure 3-1).

Cell Thickness Comparison Data

	Z Avg (mm)		
Cell No.	Cell Press 1	Cell Press 2	Delta
1	0.607	0.603	0.004
2	0.584	0.586	-0.002
3	0.552	0.553	-0.001
5	0.590	0.591	-0.001
6	0.588	0.590	-0.002
7	0.589	0.590	-0.001
8	0.587	0.588	-0.001
9	0.611	0.611	0.000
10	0.558	0.558	0.000
Average	*0.585*	*0.585*	*0.000*
Max	*0.611*	*0.611*	
Min	*0.552*	*0.553*	
Std Dev	*0.0195*	*0.0190*	

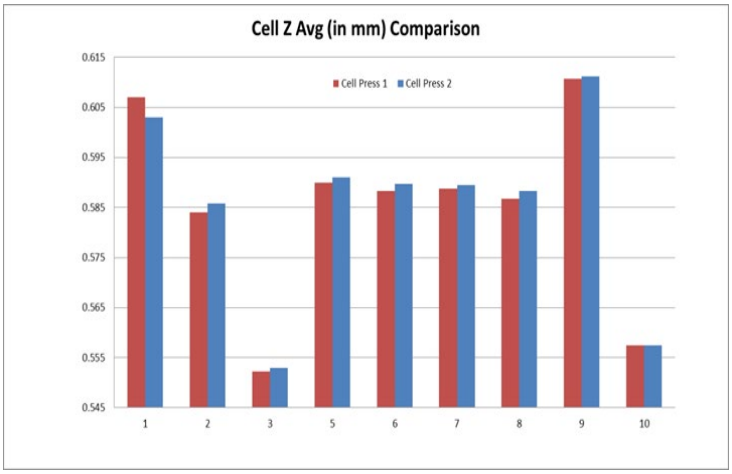

Figure 3-1. Comparison of ½ Cell Thickness Measurements from Two Cell Press QC tools

Thus, the new cell press (PLC-controlled) is now dedicated for ½ cell thickness measurement and its leak testing capability can be evaluated. This will be the final phase to enhance the device, by adding the half-cell leak test measurement to investigate fired electrolyte integrity. Currently this measurement is being completed in another press device. With the intent of having simultaneous cell thickness and leak testing capability on the new device (i.e. press the cell once), the initial plan is to install rotameter (same as on the current leak tester) and evaluate. For the longer term plan, VPS assessed the possibility of installing a stand-alone electronic leak tester based on either mass flow or pressure decay method.

For the cell curvature (edge lip) testing as well as quantification of in-part thickness variation or contour, the team is now considering another strategy. It focuses on other (such as laser-type) measurement technologies from different equipment or device suppliers, which can effectively measure this parameter considering a practical cost of the device. This was considered a longer-term initiative to resolve.

The new cell press (PLC-controlled) dedicated for half-cell thickness measurement was being evaluated for half-cell leak test/measurement (to be used for investigating fired electrolyte integrity). In April 2016, the PLC-controlled cell measuring device was further upgraded to incorporate additional cell (electrolyte) leak test capability. The upgraded device used a rotameter to measure the leak flow rate and is shown in Figure 3-2.

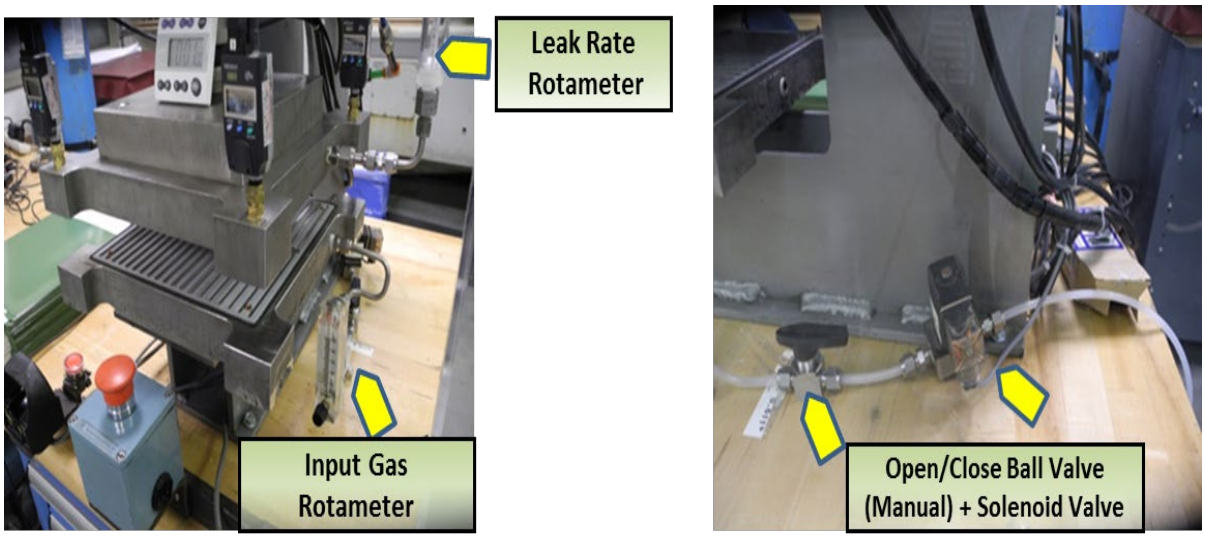

Figure 3-2. Cell Press QC tool with Leak Testing Capability

Gage R&R study for half-cell leak was performed on this upgraded cell measuring device and the result was 18%. The device passed the test by meeting the Gage R&R requirement of < 30% (see

Figure 3-3).

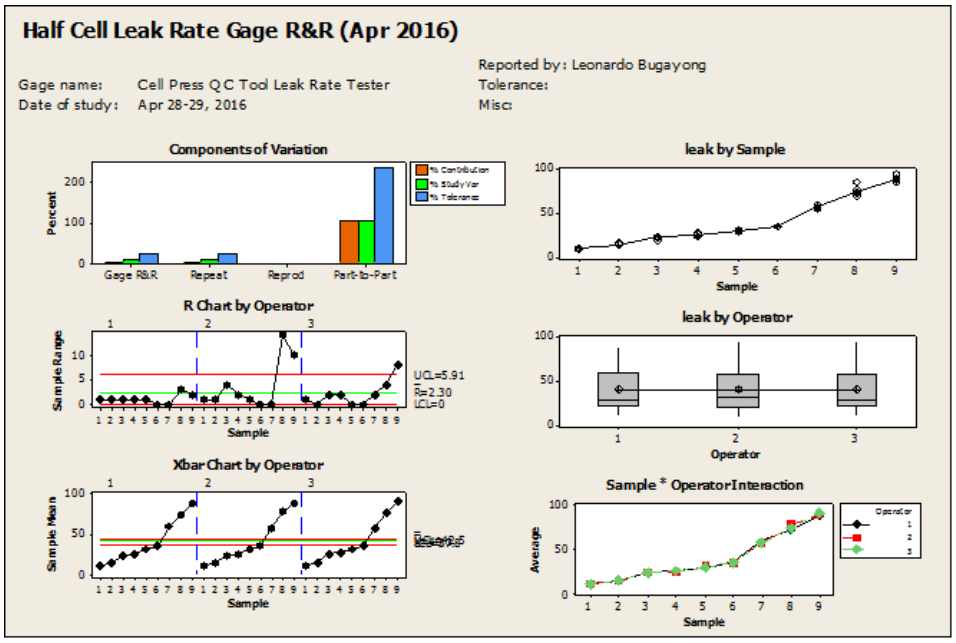

Figure 3-3. Half Cell Leak Measurement Related Gage R&R Result from Upgraded Cell Press QC tool

As an additional long term improvement, FCE-Calgary planned to replace the rotameter which measures leak rate with a stand-alone leak tester. The new tester was received at FCE-Calgary (see

Figure 3-4) and was installed and evaluated. Additional objective for using the new leak tester relates to a possible conversion from helium to air as the leak-test gas medium, which would lead to cost and safety improvements.

Figure 3-4. New Stand-alone Leak Tester from ZAxis

One stage of the qualification included a correlation study between helium leak data from the rotameter (previous set-up) and air leak/pressure decay data (in psig) from the new leak tester. After determining the regression equation, an air leak/pressure decay (psig) upper specification limit (USL) equivalent was computed. This cell leak upper spec limit (USL) was then used for qualifying cells to be used for production build starting October 2016. In November 2016, further improvements were made to minimize leak in the system. These included addressing the leak between the fitting and top platen port opening, and replacing the top platen seal, as shown in Figure 3-5.

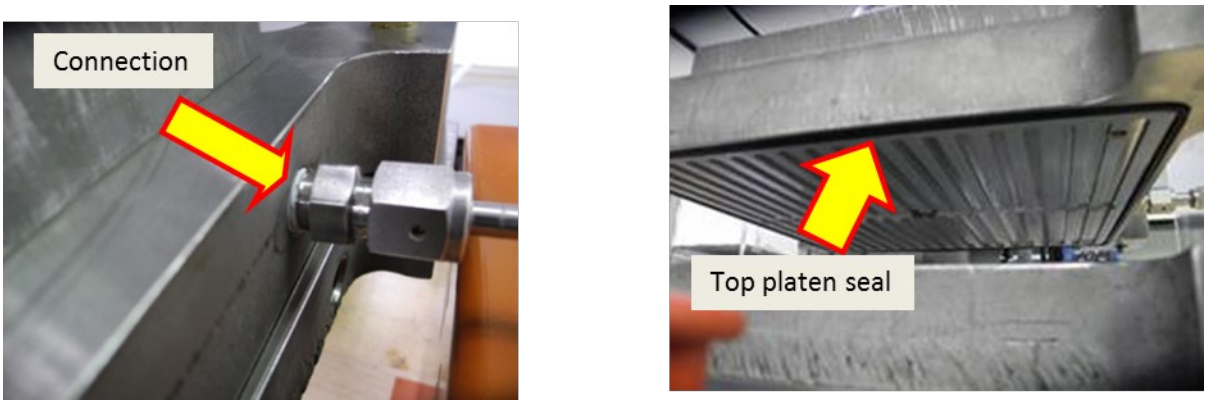

Figure 3-5. Half Cell Leak Tester Improvements (November 2016)

To quantify the leak reduction improvement in the system, a metal cell sample was used in comparing the system leak before and after improvement. The test results in Table 3-1 show that there was a 90% (very significant) reduction of base equipment leak in the system after the improvement.

Table 3-1. System leak comparison before and after improvement

	Leak Tester Parameters: TP=1.6 psig, FT= 8 s ,ST= 4 s ,TT =14 s	
Trial	Metal Cell Air Leak-psig Before (Sept 2016)	Metal Cell Air Leak-psig After (Nov 2016)
1	0.0023	-0.0001
2	0.002	0.0004
3	0.002	0.0005
4	0.0021	0.0004
5	0.0021	-0.0002
6	0.0019	0.0005
7	0.0018	0.0005
8	0.002	0.0005
9	0.0023	0.0002
10	0.0022	0.0001
11	0.0017	0.0005
12	0.0024	0.0000
13	0.0022	0.0000
14	0.0023	0.0000
15	0.0023	0.0005
16	0.0021	-0.0001
17	0.0024	0.0002
18	0.0026	0.0002
19	0.002	0.0003
20	0.0022	0.0001
Average	*0.0021*	*0.0002*
Max	*0.0026*	*0.0005*
Min	*0.0017*	*-0.0002*
Std Dev	*0.0002*	*0.0002*
Range	*0.0009*	*0.0007*
% Improvement	89.51%	

Cell Quality Control (Measurement) Device

For the new leak tester, the leak measurement technique changed from a flow rate measurement to pressure-decay for quantification of the leak. During this quarter, qualification process for this automated Z Axis unit (stand-alone leak tester) was initiated. For the initial stage, the objective was to minimize the "zero leak" of the device by selecting the best connections to maximize measurement accuracy. Three different connecting tubes including (a) transparent PVC tube, (b) black PVC tube, and (c) corrugated metal tube were evaluated. The corrugated metal tube was selected as the best option with least leak. It was then used for the connection as shown in

Figure 3-6.

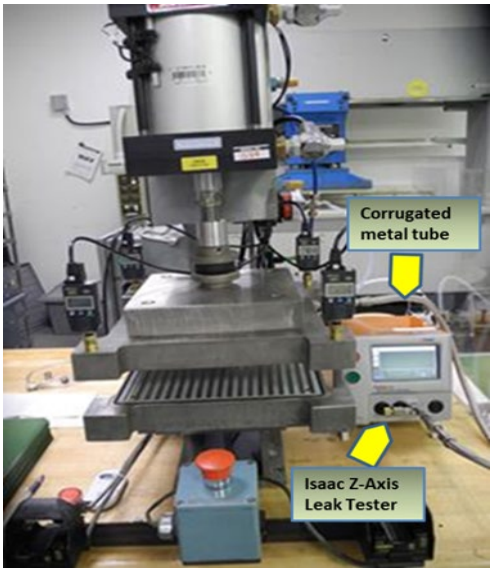

Figure 3-6. Leak Tester Connection Using Corrugated Metal Tube

For the second stage of the qualification, the objective was to characterize the input parameters and identify the best parameter combination that will result in small measurement error and a reasonable test time. During this stage, correlation study between helium leak data from the rotameter (previous set-up) and air leak/pressure decay data (in psig) from the new leak tester was conducted using the same half-cell test samples. After determining the regression equation, air leak/pressure decay upper specification limit equivalent can be computed considering a safety offset of 5 from the previous helium leak limit of 60 on the rotameter (as shown below).

Equation 3-1 Air Leak/Pressure Decay Upper Specification Limit Equivalent

$$y = 0.0004x - 0.001$$

Let : x - helium leak (rotameter)

y - air leak - pressure decay in psig (Z-Axis tester)

if x = 60 , then y = 0.0230 psig

if x = 55 , then y = 0.0210 psig (propose upper spec limit)

For the last stage of the qualification, the objective was to perform the Gage R&R (Repeatability and Reproducibility) study on ½ cell air leak/pressure decay from this upgraded cell measuring device. The result was 28%, thereby passing the Gage R&R requirement of < 30%.

The new leak tester can also be identified and implemented as a Go/No-Go QC tool by just defining the pressure decay limit. Setting the upper specification limit at 0.0210 as shown in

Figure 3-7, the tester can easily identify the passing or failing cells.

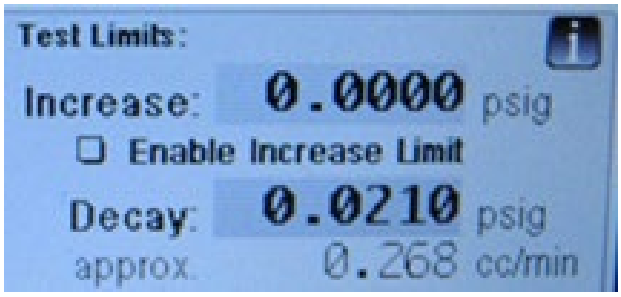

Figure 3-7. X-Axis Leak Tester Pressure Decay Variable Setting

If the green light is triggered, it means that the half-cell sample passed the air leak test and pressure decay value is below the upper specification limit as shown in

Figure 3-8.

Figure 3-8. Green Light and Monitor Display for Half Cell Passing the Air Leak/Pressure Decay Limit

However, if the red light is triggered, then the half-cell failed the air leak test as shown in

Figure 3-9.

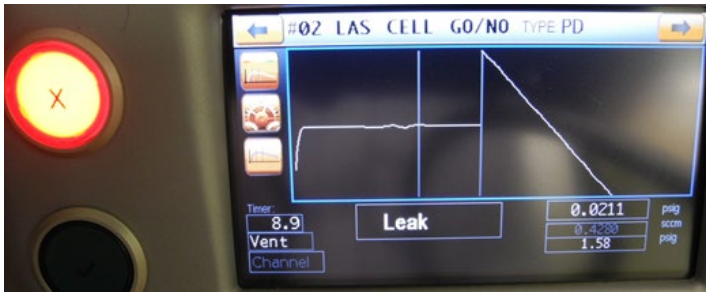

Figure 3-9. Red Light and Monitor Display for Half Cell Failing the Air Leak/Pressure Decay Limit

The use of different light colors in indicating the result of the leak test was a good approach in assisting operator during the cell QC. The upgraded cell measuring device with new leak tester will be endorsed to production for use.

CELL MANUFACTURING YIELD STUDY

The formal monitoring of manufacturing yield, with basic corrective action capability integrated for issue tracking and continuous improvement, was performed on a weekly basis throughout the stack production for the 200 kW System Demonstration project. As of the end of September 2017, completion of cell production, the running (including work in progress) product cell yield (cumulative since March 2015) was 63%, and the completed (closed lots) product yield was 53% and the breakdown over the time of the production run is given in

Figure 3-10.

The major manufacturing issue encountered which resulted in the significant decrease in yield was cell cracking detected after co-firing. This problem has been addressed and the rejection rate is now being minimized after adjustment and fine tuning of Harrop electric kiln temperature and the cell load travel time (or push rate). Cell yield was recovering. Previous (prior to the problem) overall cell yield performance level would be achieved, through improving co-firing results of the recent cell batches.

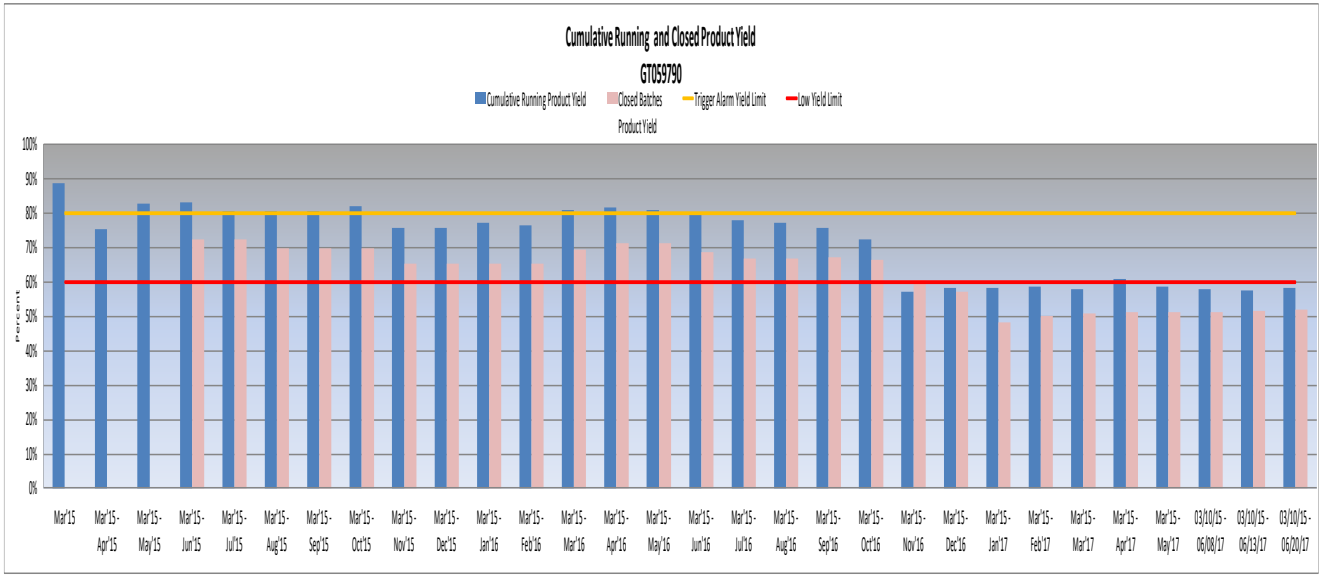

	Mar'15	Mar'15 - Apr'15	Mar'15 - May'15	Mar'15 - Jun'15	Mar'15 - Jul'15	Mar'15 - Aug'15	Mar'15 - Sep'15	Mar'15 - Oct'15	Mar'15 - Nov'15	Mar'15 - Dec'15	Mar'15 - Jan'16	Mar'15 - Feb'16	Mar'15 - Mar'16	Mar'15 - Apr'16	Mar'15 - May'16	Mar'15 - Jun'16	Mar'15 - Jul'16	Mar'15 - Aug'16	Mar'15 - Sep'16	Mar'15 - Oct'16	Mar'15 - Nov'16	Mar'15 - Dec'16	Mar'15 - Jan'17	Mar'15 - Feb'17	Mar'15 - Mar'17	Mar'15 - Apr'17	Mar'15 - May'17	03/10/15 - 06/08/17	03/10/15 - 06/13/17	03/10/15 - 06/20/17
Cumulative Running Product Yield	88.6%	75.3%	82.6%	83.1%	80.5%	80.5%	80.5%	81.9%	75.7%	75.6%	77.1%	76.3%	81.0%	81.6%	80.8%	80.0%	77.8%	77.4%	75.9%	72.5%	57.2%	58.2%	58.3%	58.7%	57.8%	60.9%	58.8%	57.9%	57.6%	58.1%
Closed Batches Product Yield				72.3%	72.3%	69.8%	69.8%	69.8%	65.1%	65.1%	65.1%	65.1%	69.5%	71.1%	71.1%	68.8%	66.9%	66.9%	67.1%	66.5%	60.5%	57.2%	48.4%	50.3%	51.0%	51.1%	51.2%	51.2%	51.7%	52.0%
Trigger Alarm Yield Limit	80.0%	80.0%	80.0%	80.0%	80.0%	80.0%	80.0%	80.0%	80.0%	80.0%	80.0%	80.0%	80.0%	80.0%	80.0%	80.0%	80.0%	80.0%	80.0%	80.0%	80.0%	80.0%	80.0%	80.0%	80.0%	80.0%	80.0%	80.0%	80.0%	80.0%
Low Yield Limit	60.0%	60.0%	60.0%	60.0%	60.0%	60.0%	60.0%	60.0%	60.0%	60.0%	60.0%	60.0%	60.0%	60.0%	60.0%	60.0%	60.0%	60.0%	60.0%	60.0%	60.0%	60.0%	60.0%	60.0%	60.0%	60.0%	60.0%	60.0%	60.0%	60.0%
No. of Good Cells	450	472	774	810	813	813	813	892	1128	1216	1352	1337	1774	1893	1909	2139	2252	2435	2475	2447	2110	2313	2590	2849	2922	3436	3389	3338	3321	3399
No. of Tape Cuts	508	627	937	975	1010	1010	1010	1089	1490	1608	1753	1753	2191	2321	2362	2673	2894	3148	3263	3376	3686	3973	4443	4853	5059	5641	5763	5763	5763	5846
No. of Rejects	58	155	163	165	197	197	197	197	344	369	378	391	394	405	430	511	607	678	753	894	1541	1625	1818	1969	2102	2170	2339	2390	2407	2412
No. of Recycled									18	23	23	23	23	23	23	23	35	35	35	35	35	35	35	35	35	35	35	35	35	35
Out to Projects	4	4	4	4	4	4	4	4	5	6	10	30	158	164	164	169	196	196	196	196	196	196	196	196	198	198	198	198	198	198

Figure 3-10. Cell Product Yield Performance for Cumulative Running and Closed Batches

SCALE-UP PREPERATION

As reported previously under DOE Project DE-FE0023186 (ReliSS project), the use of Vendor-supplied cathode contact powder is being evaluated to prepare for high volume cell and stack production required to meet the project deliverable. During this reporting period, a number of processing trials were conducted in the areas of calcination and milling to achieve the same specification as the feedstock. Two different tests were run, one using 7-day ball-milled Vendor-supplied powder with surface area of 5.4 m^2/g, and the other with 8-hour attrition milled Vendor-supplied powder with surface area of 8.6 m^2/g. Some improvement was seen in the power curve and thermal cycle performance especially for attrition milled powder. The performance during steady-state holds also improved a little. It seems that at higher current densities in the power curve, the VPS powder is slightly better for thermal cycling performance. But during the steady-state hold at lower current density, there is very little difference and the Vendor-supplied powder should be fine to use.

A large area stack was built with half of the cells fabricated using Vendor-supplied powder and the remaining cells fabricated using VPS powder for comparison. Figure 3-11 shows the cell voltage drop over 3 thermal cycles at all conditions tested, for the individual cells in the 16-cell stack where odd numbered cells have VPS powder and even numbered cells have Praxair powder. There was no discernible difference between the two powders. Figure 3-12 shows a steady state hold at VPS gas replacement test conditions for this stack after 4 thermal cycles with cells using Praxair powder in red and cells using VPS powder in blue (end cell removed since there were problems from the start of test not related to the pastes). Again there was no discernible difference, so it appears that the Vendor-supplied powder should be a reasonable replacement for the VPS powder.

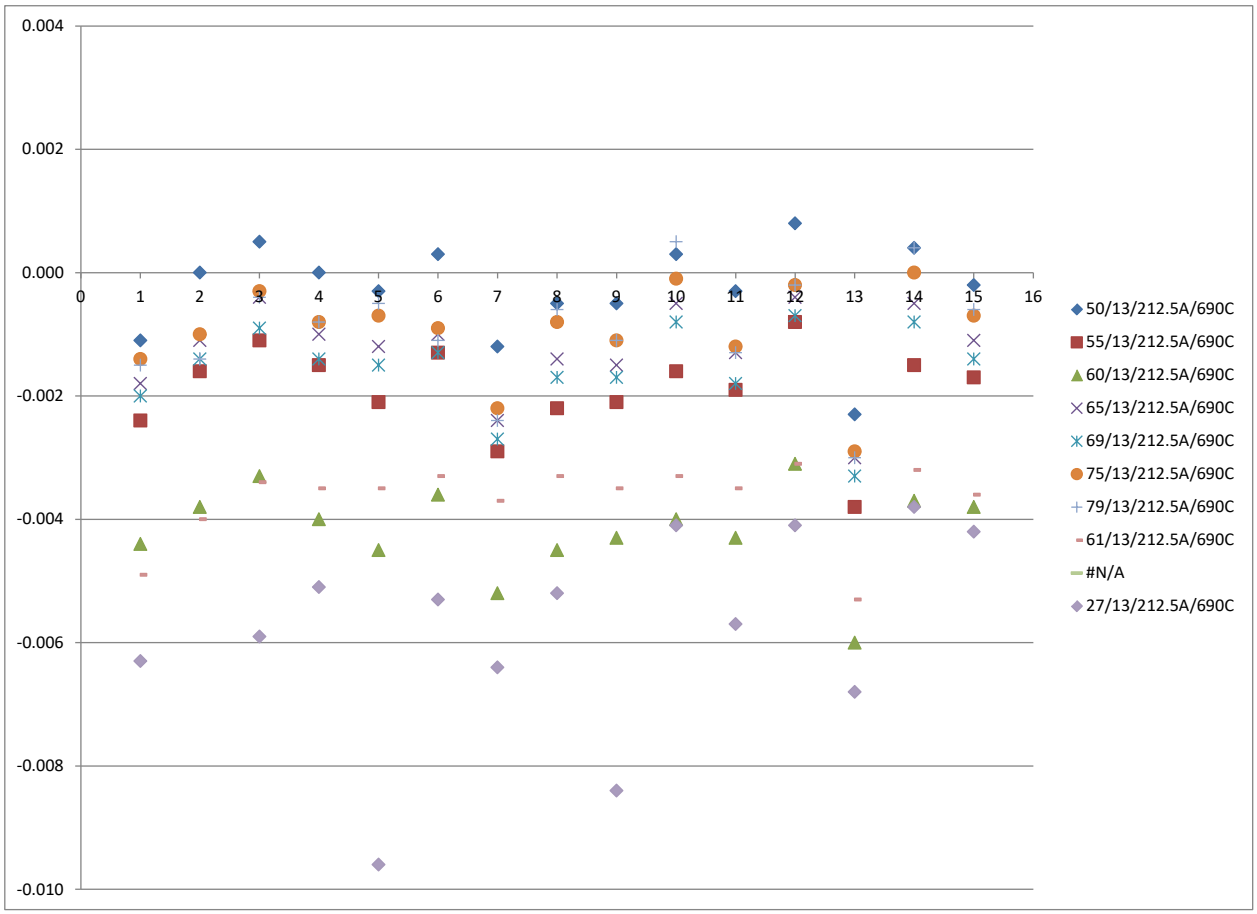

Figure 3-11. Individual Cell Voltage Drop (volt, at 50–79% Fuel Utilizations) Over 3 Thermal Cycles for 16-Cell Stack GT057235-0123 (odd cells fabricated using VPS powder, even cells using Vendor-supplied powder)

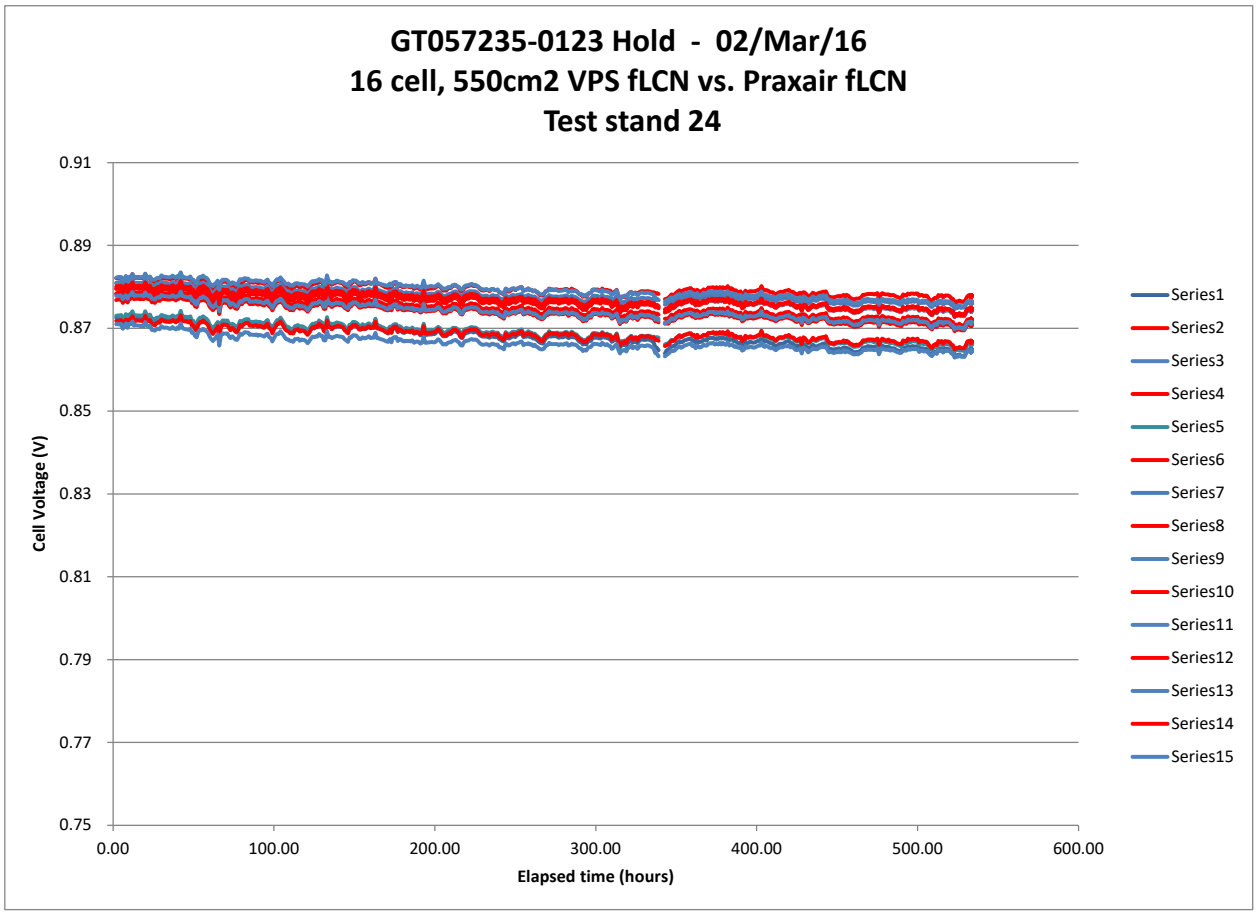

Figure 3-12. Performance of Stack GT057235-0123 during Steady State Hold at VPS GR Conditions (odd cells fabricated using VPS powder (blue), even cells using Vendor-supplied powder (red), end cell excluded)

Prior to receiving the powder from Praxair, a package containing ~100 g powder was shipped from VPS. Particle size, surface area (BET) and XRD analyses were carried out on the sample at VPS prior to shipping. Praxair repeated the analysis at their facility and results were compared. Particle size analysis results were almost identical. Surface area analysis results showed an offset, with Praxair measuring lower surface area than VPS by almost 1 m^2g^{-1}. The specifications were set with Praxair based on discrepancies in surface area measurements at the two laboratories. Praxair supplied 50 kg material using this specification. SEM analysis of the powder was performed to compare it with in-house LCN powder. Figure 3-13 shows a comparison of the powder morphology at different magnifications. The morphology, as expected, is rather different due to the preparation differences. The Praxair powder is prepared from solution via spray pyrolysis and so should have a finer microstructure than the solid state reaction material from VPS.

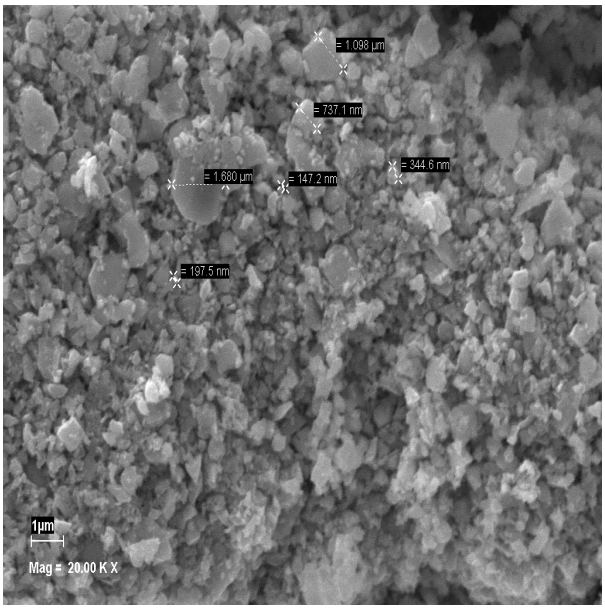
1.098 µm
737.1 nm
1.680 µm
147.2 nm
344.6 nm
197.5 nm
1µm
Mag = 20.00 K X

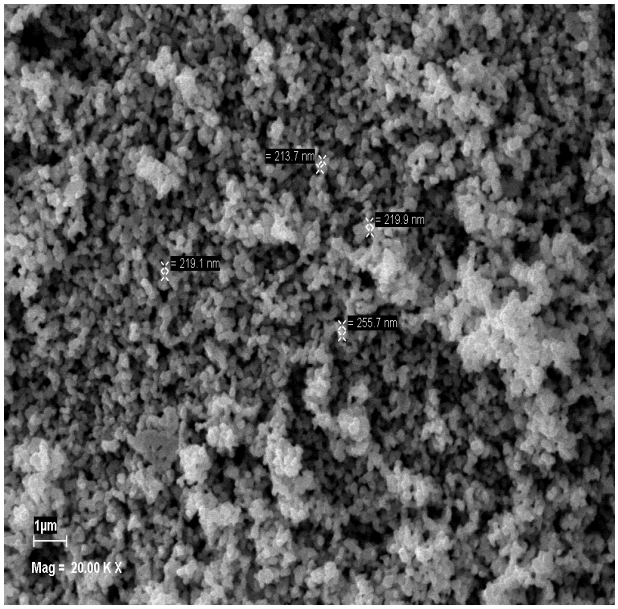
213.7 nm
219.9 nm
219.1 nm
255.7 nm
1µm
Mag = 20.00 K X

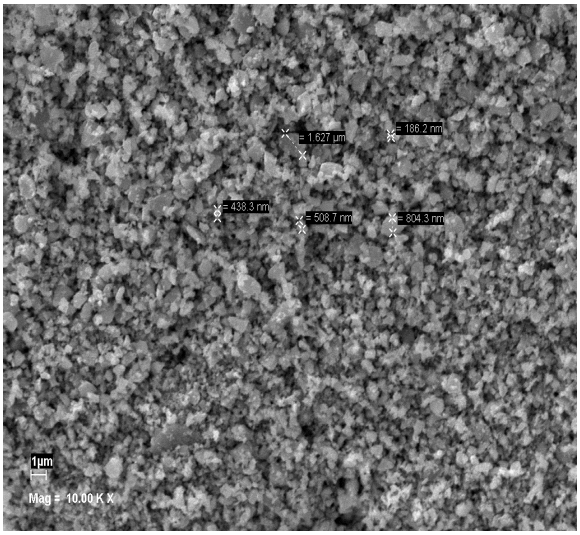
1.627 µm
186.2 nm
438.3 nm
508.7 nm
804.3 nm
1µm
Mag = 10.00 K X

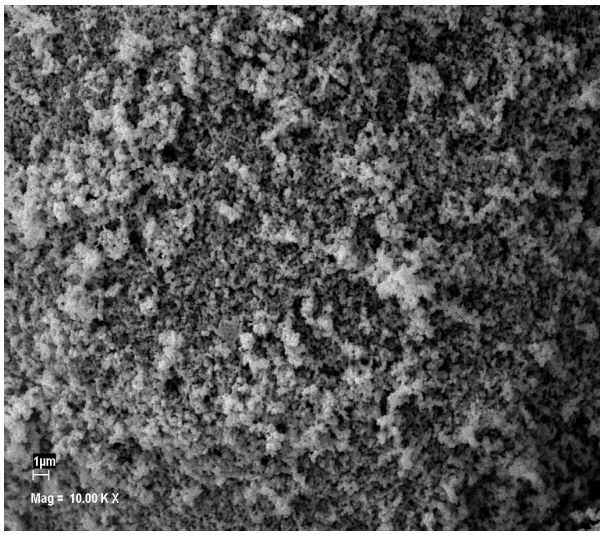
1µm
Mag = 10.00 K X

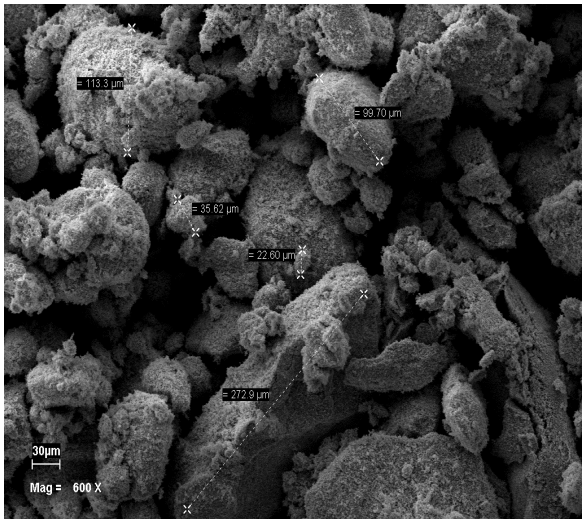
113.3 µm
99.70 µm
35.62 µm
22.60 µm
272.9 µm
30µm
Mag = 600 X

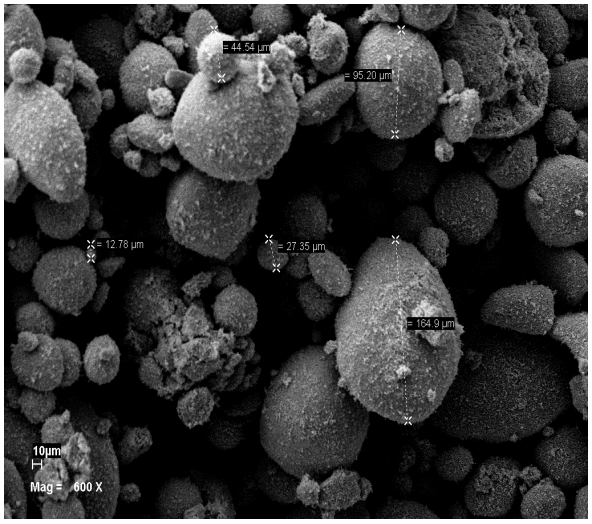
44.54 µm
95.20 µm
12.78 µm
27.35 µm
164.9 µm
10µm
Mag = 600 X

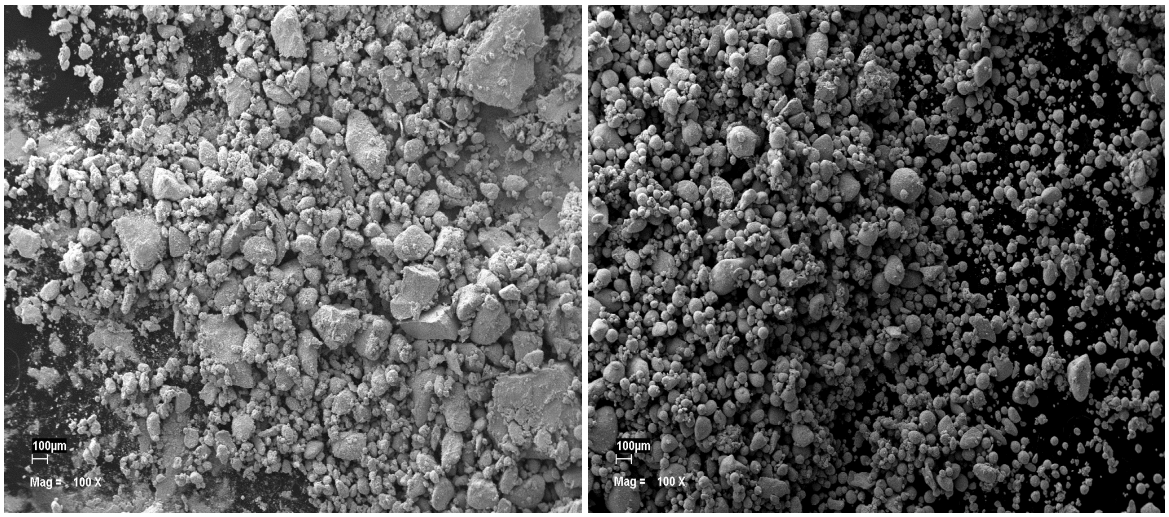

Figure 3-13. SEM Showing Morphology of (a) VPS and (b) Praxair powders at 20k, 10k, 600 and 100 X magnifications

A number of processing trials were conducted (with the Praxair-supplied powder) in the areas of calcination to achieve the same specification as the feedstock. A detailed design of experiment study was carried out. Single cell tests Glob101988 and 101989 were conducted to further evaluate the Praxair powder in the area of electrochemical performance as well as thermal cycle performance.

Figure 3-14 shows results from single cell test Glob101988 evaluating the performance degradation rate at steady-state hold conditions, after 10 thermal cycles.

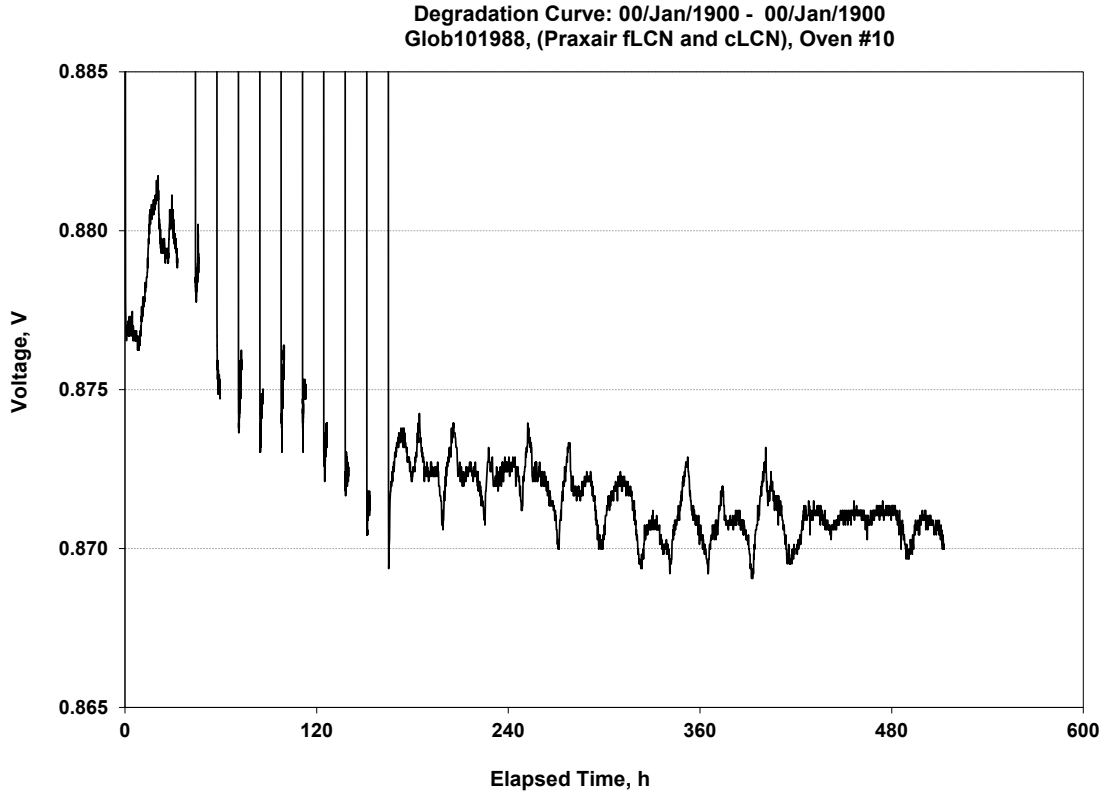

Figure 3-14. Steady state test of cell with Praxair powder at 750°C after 10 thermal cycles

A typical degradation rate of 0.5% per 1000 hours was observed for the cell, showing no issues with the material composition and stability for the Praxair powder. However, the thermal cycle losses were unacceptably high, indicating a problem with the particle size and/or powder morphology for the Praxair powder.

It was decided to mill the powder until it meets specification and rerun the test 101985 configuration to confirm that this is the only modification required to achieve acceptance with the Praxair powder. Two different tests were run, one using ball-milled Praxair powder with smaller surface area (101992), and one using attrition milled Praxair powder with larger surface area (101995). Some improvement was seen in the power curve - thermal cycle performance especially for attrition milled powder, and steady-state hold performance had also improved a little.

After the initial 5 single cell tests for performance comparison and specification fine tuning, the powder qualification was further expanded to study the performance repeatability with different test stands. From this repeat testing, it seems that at higher current densities in the power curve the VPS fLCN powder is slightly better for thermal cycling. Whereas, during the steady-state hold at lower current density, there is very little difference. Further processing trials have begun to achieve the same specification for the Praxair powder as the feedstock material.

In addition to qualifying Praxair as the vendor for the cathode powder, a number of other cell materials were tested for potential replacement. One is fine mesh screened green NiO to remove free Ni. Single cell test results are shown in

Figure 3-15. The performance was not significantly different compared to that with non-sieved NiO. It was decided to continue to use NiO with previous specification for the deliverable stacks.

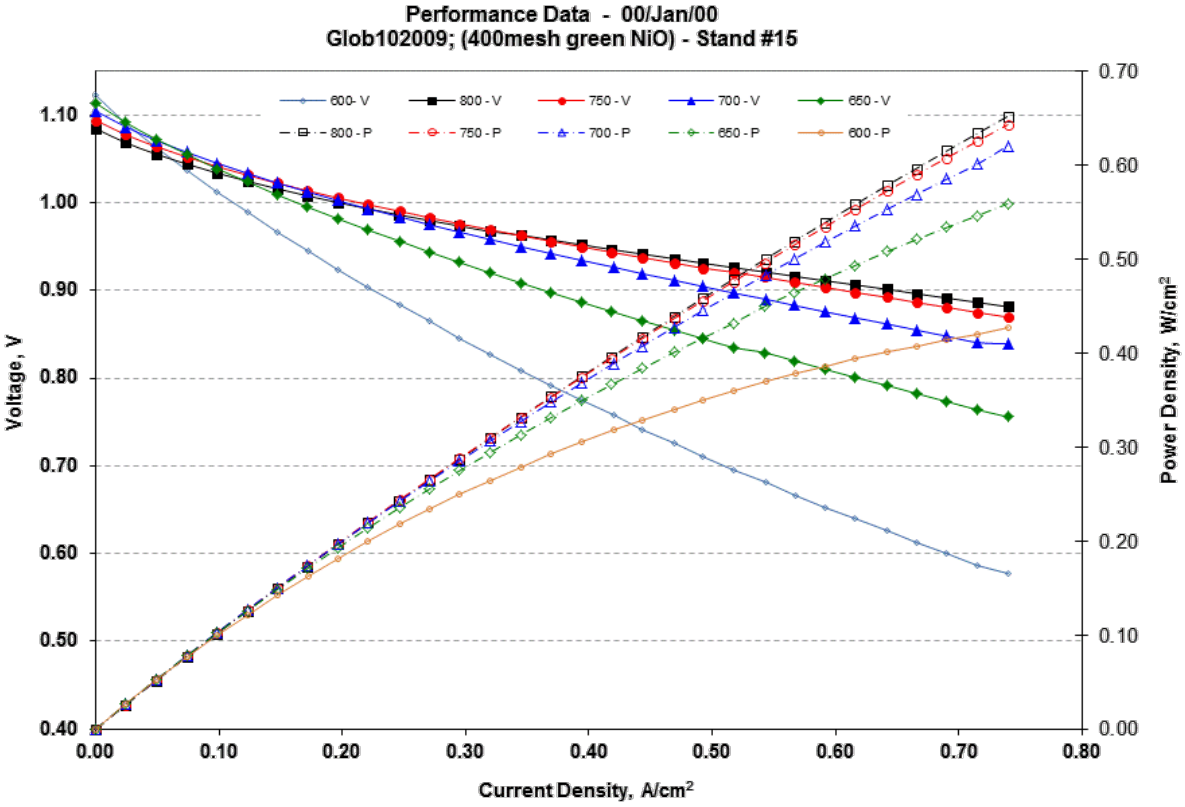

Figure 3-15. Performance Characteristics and Power Curves for Cell 102009 Evaluating 400 mesh green NiO (in Temperature Range 600 to 800°C)

Materials (NiO for Anode Functional Layer and GDC for interlayer) from different vendors were also tested in single cells with the purpose to lower the cost while maintaining the performance level same.

Figure 3-16 and

Figure 3-17 present the results with GDC10 interlayers from Solvay featuring low surface area and high surface area, respectively.

Figure 3-18 shows the results with Sumimoto NiO for AFL. The performance was lower than that with standard NiO currently used for AFL.

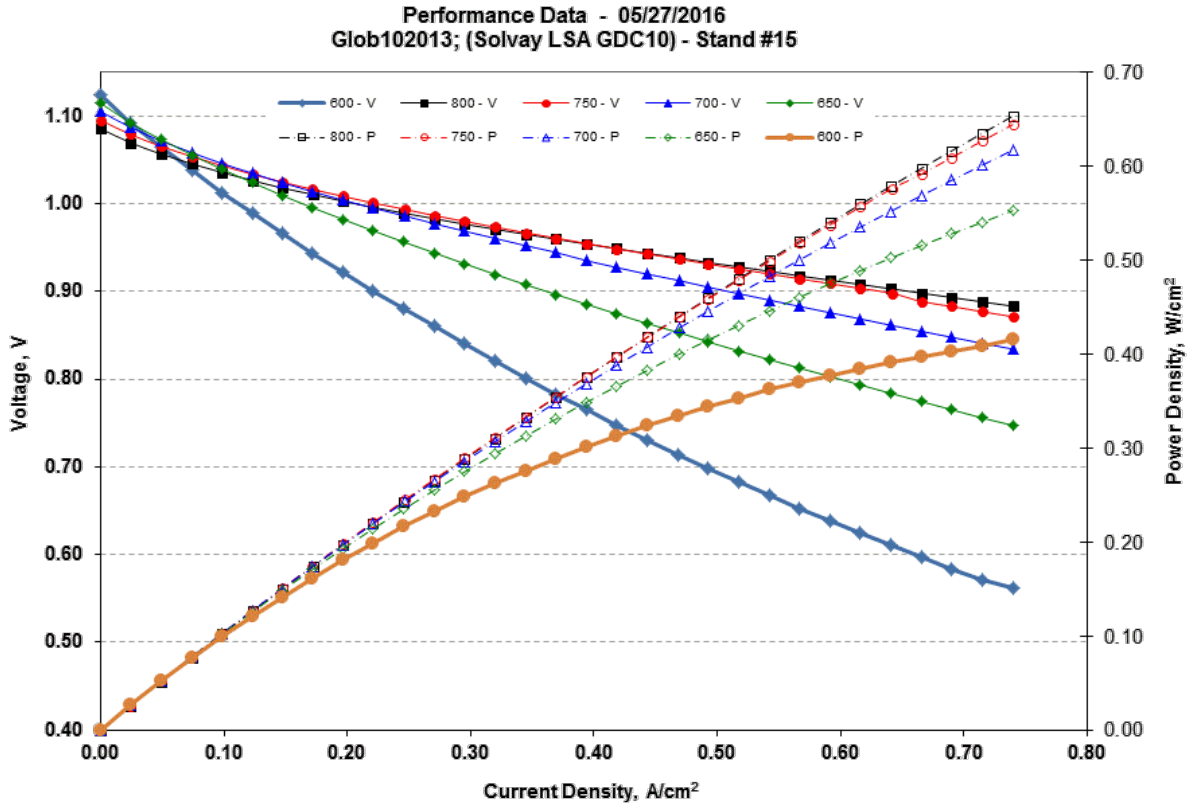

Figure 3-16. Performance Characteristics and Power Curves for Cell 102013 Evaluating Solvay low surface area GDC10 interlayer (in Temperature Range 600 to 800°C)

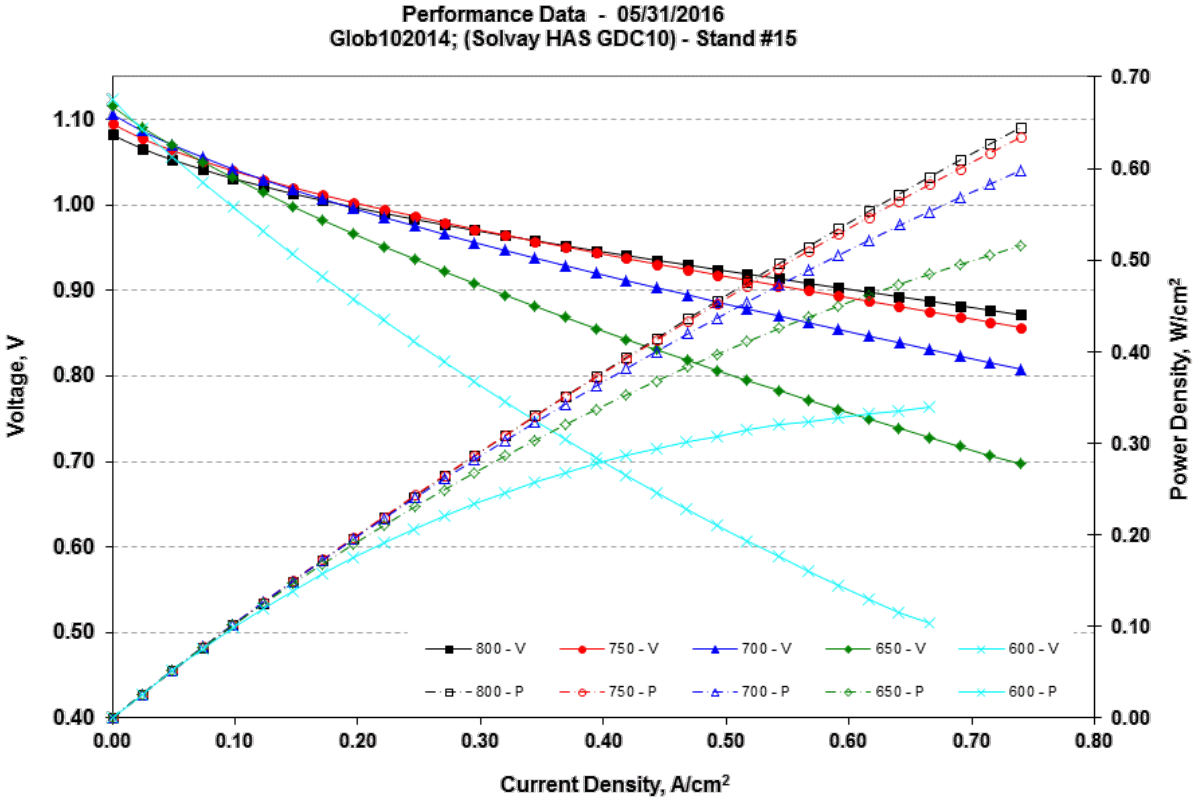

Figure 3-17. Performance Characteristics and Power Curves for Cell 102014 Evaluating Solvay high surface area GDC10 interlayer (in Temperature Range 600 to 800°C)

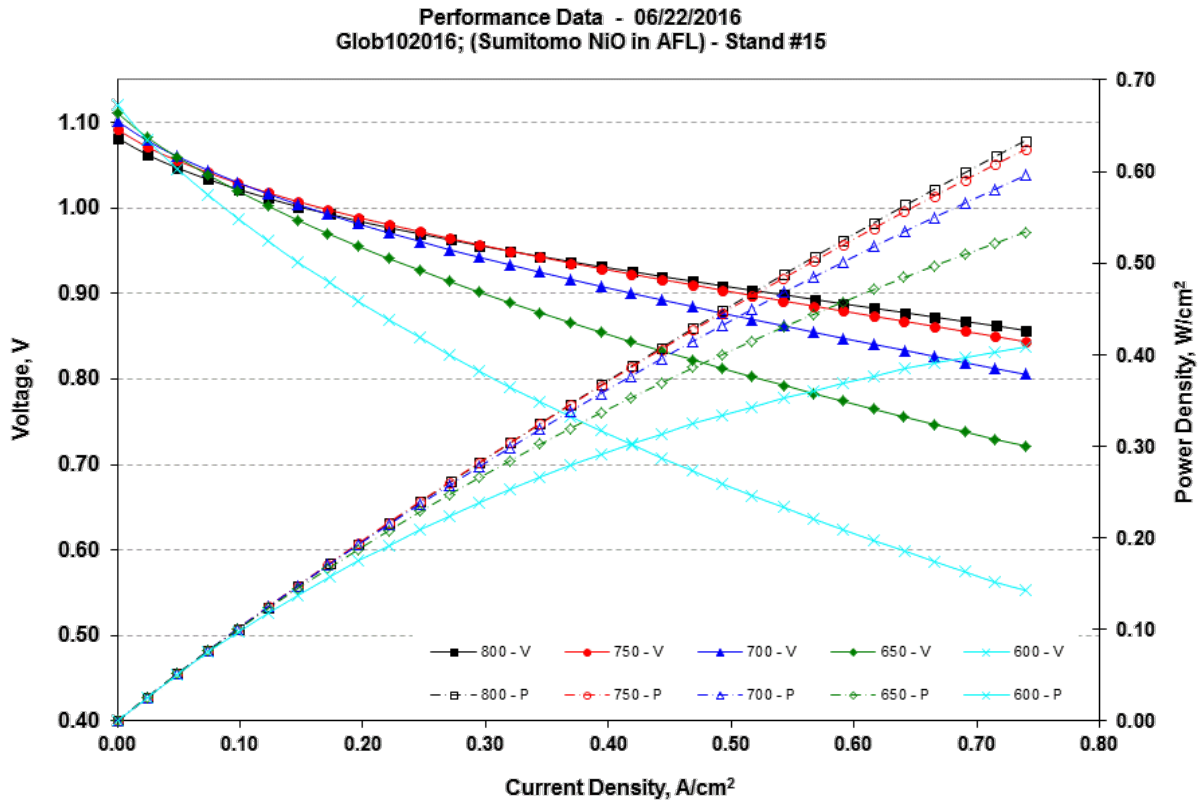

Figure 3-18. Performance Characteristics and Power Curves for Cell 102016 Evaluating Sumitomo NiO AFL (in Temperature Range 600 to 800°C)

STACK MANUFACTURING

Objective:

- Fabricate up to 32 SOFC stack blocks for the 200 kW Prototype system
- Perform conditioning and factory (performance) testing of the assembled stacks

Approach:

The stacks will be 120 cells in size and will be based on VPS-FCE's large area stack (LAS) block design and specifications. In the baseline LAS stack design, TSC3 cells are stacked in a cross-flow gas configuration with manifolds integrated into interconnects. The stack design utilizes a metallic cell holder component to surround a TSC3 cell. The cell and metallic cell holder are matched in thickness which allows for a balancing reference for other unit-cell components on both anode and cathode sides of the cell. Ferritic stainless steel flow field components are formed utilizing conventional metal forming techniques. These components interface mechanically and electrically between repeating cells and interconnects, providing electrical path as well as producing the cross-flow geometry in the stack. Separate forms are utilized for anode and cathode streams. Thin physical vapor deposition (PVD) cobalt-coatings are applied on the cathode flow fields. This coating forms a dense manganese cobalt oxide spinel (MCO) layer in-situ during stack operation to limit chromium volatilization (that can occur

in presence of moisture present in cathode gas) as the chromium species can poison the cell. Other metallic repeat stack components are formed using laser cutting of ferritic stainless steel sheets. Seals for use in the stack will be manufactured by tape casting under Task 2.1. The green seal tape is die-cut to form stack seal assemblies. The stack also includes machined SS430 grade end plates which have been designed to interface with the stack module environment allowing for easy stack installation. The stack design incorporated and operational performance demonstrated in previous DOE project will be reviewed to ensure that critical degradation and performance expectations are achieved or exceeded when improvements are implemented for the 200 kWe prototype system.

During the 120-cell stack block build, all kitted stack components will be assembled by a pick-and-place process according to assembly drawings. Total quality control will be applied to ensure that design drawings and specifications are complete and up-to-date and represent the item being manufactured. All stacks will be conditioned and performance tested in factory. Stack consolidation follows the stack build. It occurs during the cold-stack compression and the (first) stack heat-up in conditioning. The stack achieves final height, intimate electrical contact in the stack core and quality seals for both anode and cathode chambers. In order to deliver high quality and reliable stacks, all stacks will follow a regimented acceptance qualification procedure. The stack's voltage-current performance will be characterized. This will include measuring open circuit voltages as well as voltage as a function of current and fuel utilization. A 50-hour hold (steady state testing) and a full deep thermal cycle will also be included in this qualification procedure. In order to assess manufacturing variance and suitability of the stack to operate in parallel flow schemes with other stacks in the system environment, pressure drop characterization of anode and cathode sides of each stack will be completed. Additional quality control steps, such as leak testing and physical dimension checks. Following acceptance testing, the stacks will be prepared for shipment to FCE's Danbury, CT facility.

Results & Discussion:

USE OF CELL PRESS-TYPE QC DEVICE FOR THE SMALLER METALLIC COMPONENTS

One idea that was considered for thickness measurement of smaller cell active area metallic components such as anode and cathode flow fields was the option of extending usage of the current cell press-type QC device. A new press was built (a replicate) for ½ cell measurement and the older cell press-type QC device was qualified for measurement of smaller area metallic components (see

Figure 3-19). The solid top and bottom platens were installed and QC qualified for small area metallic components in January 2016.

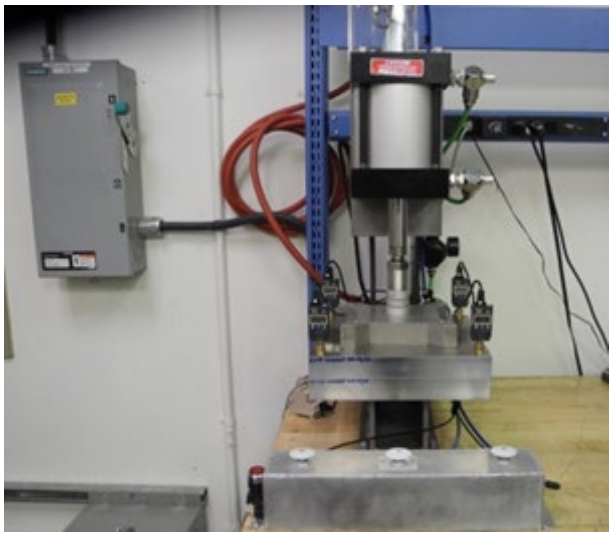

Figure 3-19. Modified Cell Press-Type QC Device with Coupler and New Solid Top and Bottom Platens

80-cell Pre-Production Stack

Prior to the 120-cell stack production, an 80-cell pre-production stack was to be fabricated to represent all the (frozen) technology, engineering and quality control aspects for the upcoming build campaign. The 200 kW build project was at an early phase as the 80-cell pre-product configuration stack was yet to be built, which was a key anchor point in the schedule. Thus, there was an unplanned addition of three 16-cell stacks undertaken in order to finalize stack design and quality control specifications as well as verifying Praxair powder for cathode contact layers in the stacks. Design validation of 16-cell stacks -0127, -0128 and -0129 to confirm the technical approach was delayed by approximately 3 months.

Large-area Stack GT059914-0001 containing 80 cells was built on August 17, 2016 and testing was initiated. Test results from this stack were utilized to validate 120-cell stack technology and unit cell configurations. During initial performance characterization testing, all individual cell voltages at 75% Uf (the most aggressive test condition) before thermal cycle (TC0 performance shown in Figure 3-20) and after the first deep thermal cycle (TC1 performance shown in Figure 3-21) were stable. The maximum cell voltage differential considering the lowest and the highest cell performance (voltage spread/range dv is shown as secondary Y-axis in the figures) for both periods was small (17 mV).

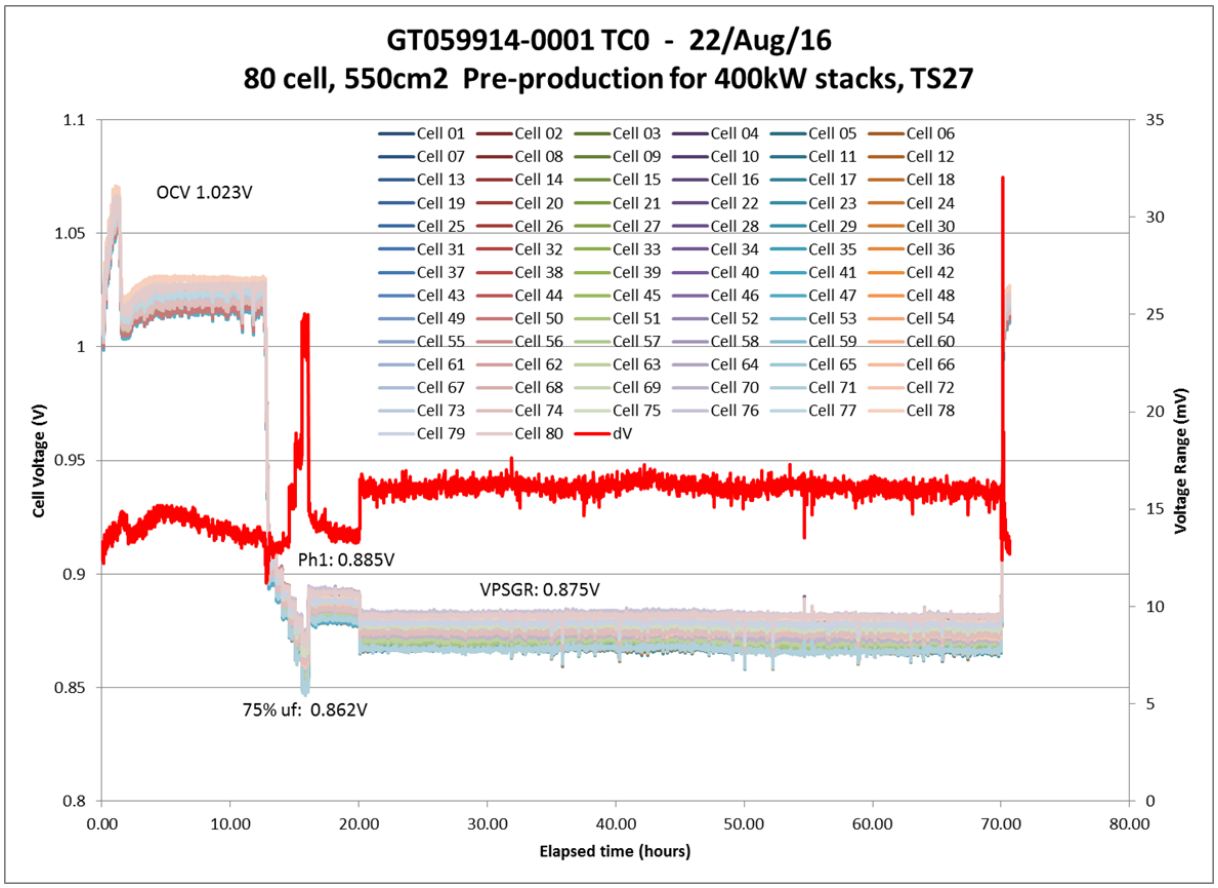

Figure 3-20. Stack GT059914-0001 Individual Cell Voltage and Voltage Spread (dV) Trends Before Thermal Cycle (TC0)

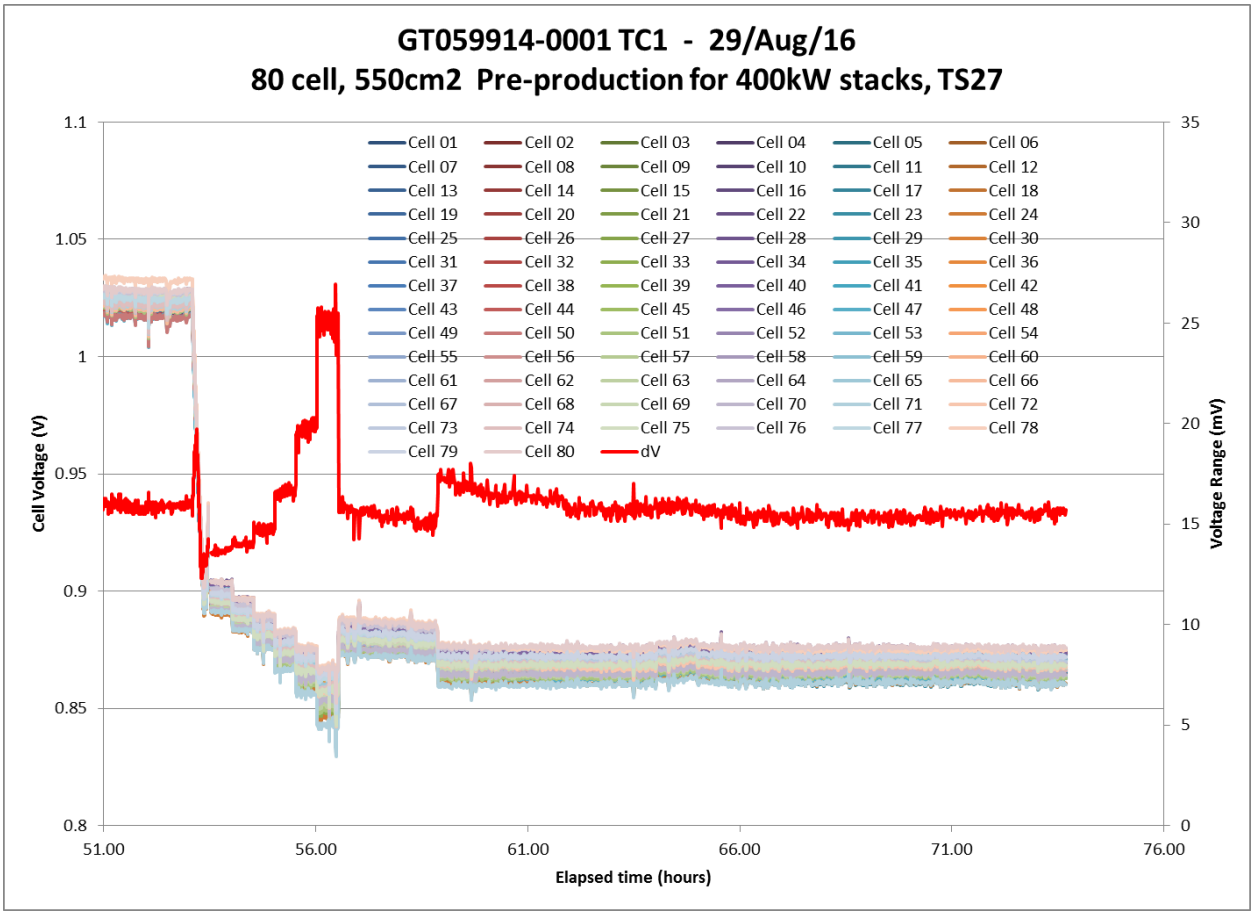

Figure 3-21. Stack GT059914-0001 Individual Cell Voltage and Voltage Spread (dV) Trends After Thermal Cycle (TC1)

Following the conditioning/acceptance testing, the steady state testing was initiated. Test conditions were: 160 A (291 mA/cm^2), fuel utilization (Uf) of 68%, air (oxidant) utilization of 15%, stack environment temperature of 690°C, and a fuel composition (aligning to that of the FCE systems) of 44.43% H_2, 6.37% CH_4 (Natural Gas), 23.26%N_2, and 25.94% H_2O.

Figure 3-22 to Figure 3-24 show the individual cell voltage trends, average cell voltage trend and the individual cell performance degradation rate distribution, respectively. The performance degradation rate observed over the 964-hour test period was 1.1 % (9.7mV) /1000h. However as was expected, the degradation rate was decreasing as more time accumulates. 500 hours more of holding, degradation was observed to be 0.88% (7.6mV)/1000h.

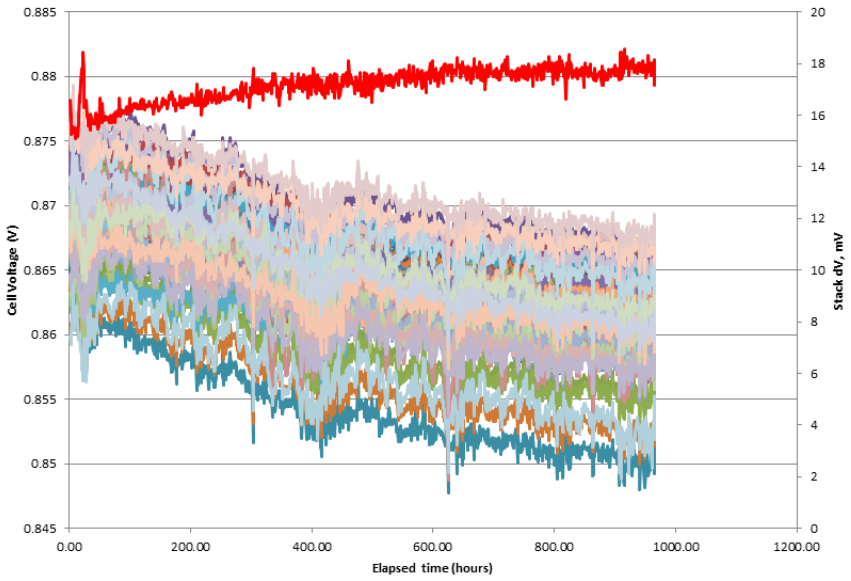

Figure 3-22. Stack GT059914-0001 Individual Cell Voltage and Voltage Spread (dV) Trends

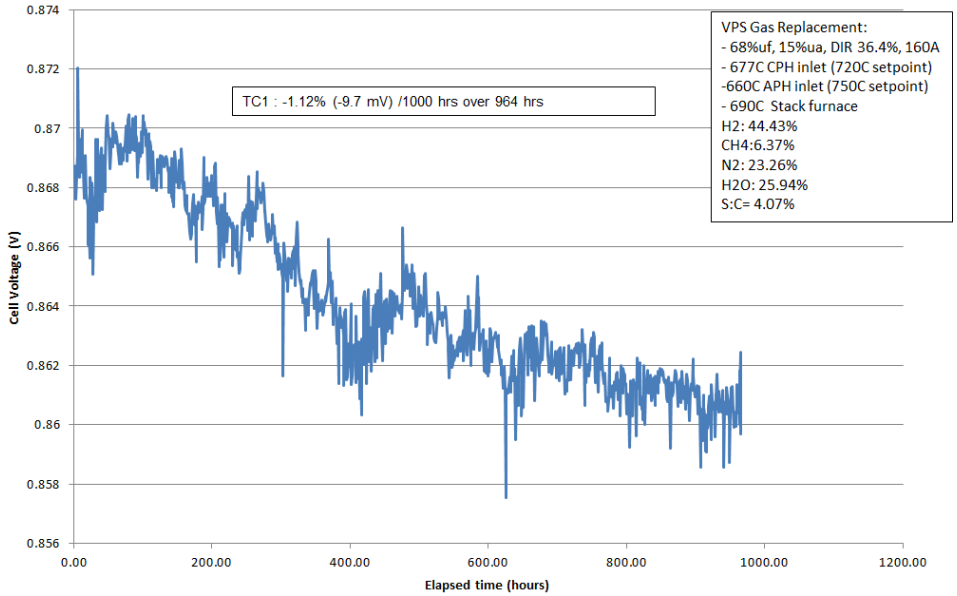

Figure 3-23. Performance Stability of Stack GT059914-0001 during Steady State Testing

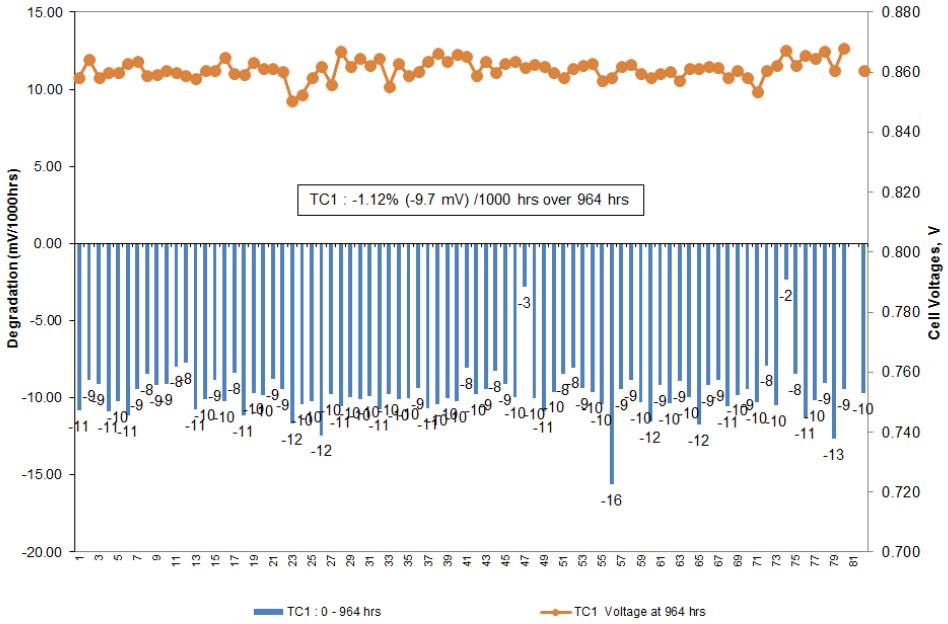

Figure 3-24. Stack GT059914-0001 Individual Cell Performance and Degradation Rate Distribution

Long-term steady-state testing of large-area Stack GT059914-0001 containing 80 cells was continued. Test results from this stack were utilized to validate 120-cell stack technology and unit cell configurations (frozen for 200 kW SOFC system modules). The test conditions used were: 160 A (291 mA/cm^2), fuel utilization of 68%, air (oxidant) utilization of 15%, stack environment temperature of 690℃, and fuel composition of 44.43% H_2, 6.37% CH_4 (Natural Gas), 23.26%N_2, and 25.94% H_2O (aligning to that of the FCE SOFC systems). The stack was

being tested in Test Stand #27. The stack performance degradation rate was observed to be 0.85 % (7.4mV) /1000h over 1615 hours (with a slight second order decreasing trend over time).

While in Test Stand 27 (for TC1 hold), the stack experienced humidifier pump communication errors at 1062 and 1615 hours. The humidifier pump adds water to a steam vessel which provides steam to the incoming fuel mix. Following the second interruption, the stack was shut down, cooled and physically moved to neighboring test stand #28 (see Figure 3-25). This was done to have both Test Stand 29 (lead) and Test Stand #27 (alternate) available for 120-cell stack conditioning and acceptance testing.

Figure 3-25. Tall (25 kW) Large Area Stack Test Stands

After resuming the test in Test Stand #28, the stack had accumulated over 550 hours at the same test conditions. The test results are shown in Figure 3-26 (elapsed time excludes time taken up by the test interruption).

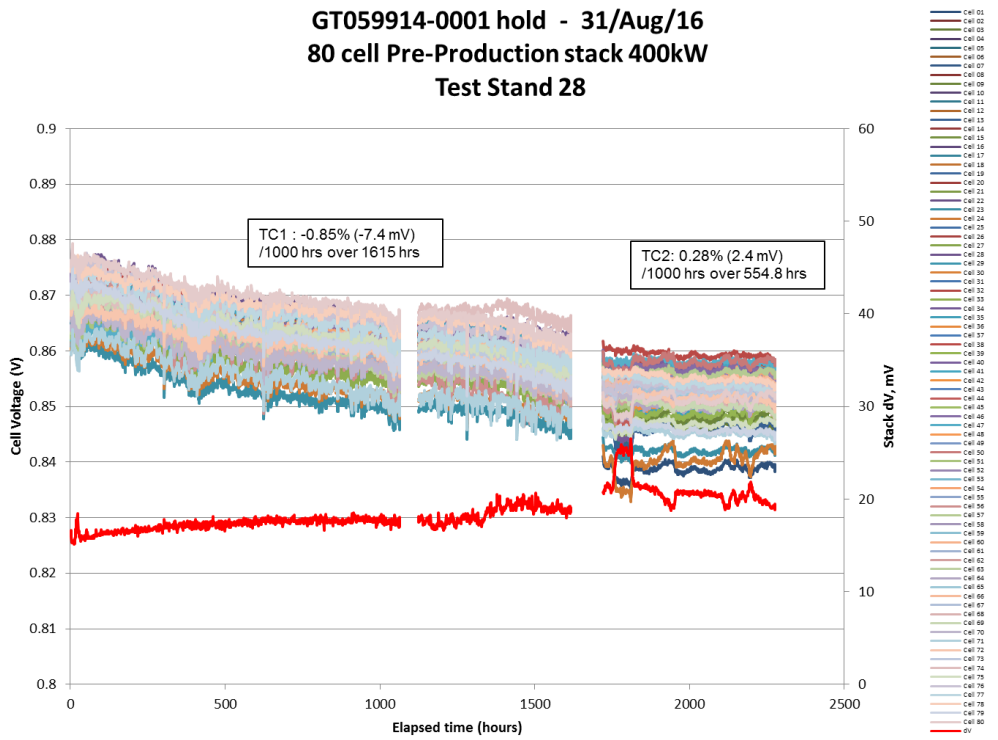

Figure 3-26. Stack GT059914-0001 (80 cells) Individual Cell Voltage and Voltage Spread (dV) Trends (TS #27 + TS #28)

The stack had been performing at a lower voltage. However, the stack performance was improving (voltage improved slightly). In a closer review and comparison of the test stand temperatures (shown in Figure 3-27), though the preheater set-points for both test stands are the same (730°C), the actual stack inlet temperature is considerably cooler (645°C v. 675°C) in Test Stand #28. Efforts went to see if a matched temperature can be achieved (increase to 675°C) which would allow for a better comparison of the stack results in both test stands.

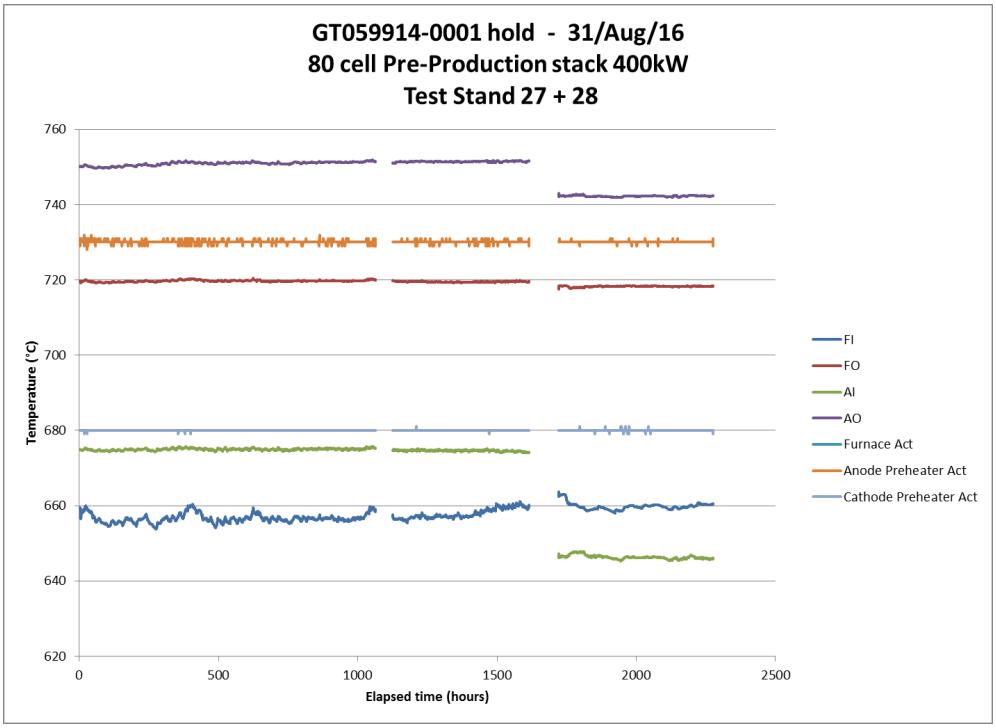

Figure 3-27. Stack GT059914-0001 (80 cells) Key Temperatures (TS #27 + TS #28)

A comparison of the individual cell performance degradation rates and stack average cell voltage profiles (cell 1 is at top of the stack), is shown in Figure 3-28.

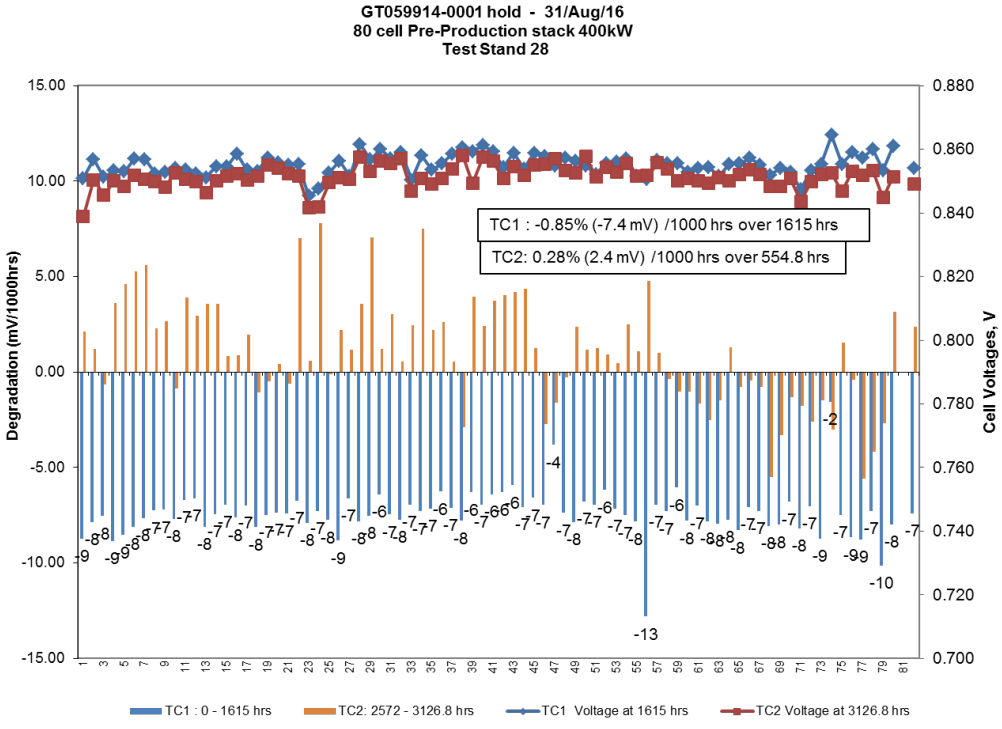

Figure 3-28. Stack GT059914-0001 (80 cells) Individual Cell Performance Degradation Rate Distributions (in TS #27 and TS #28)

After moving the stack to Test Stand #28, the test had accumulated additional 2048 hours at the same test fuel and stack current conditions. The combined test results are shown in Figure 3-29.

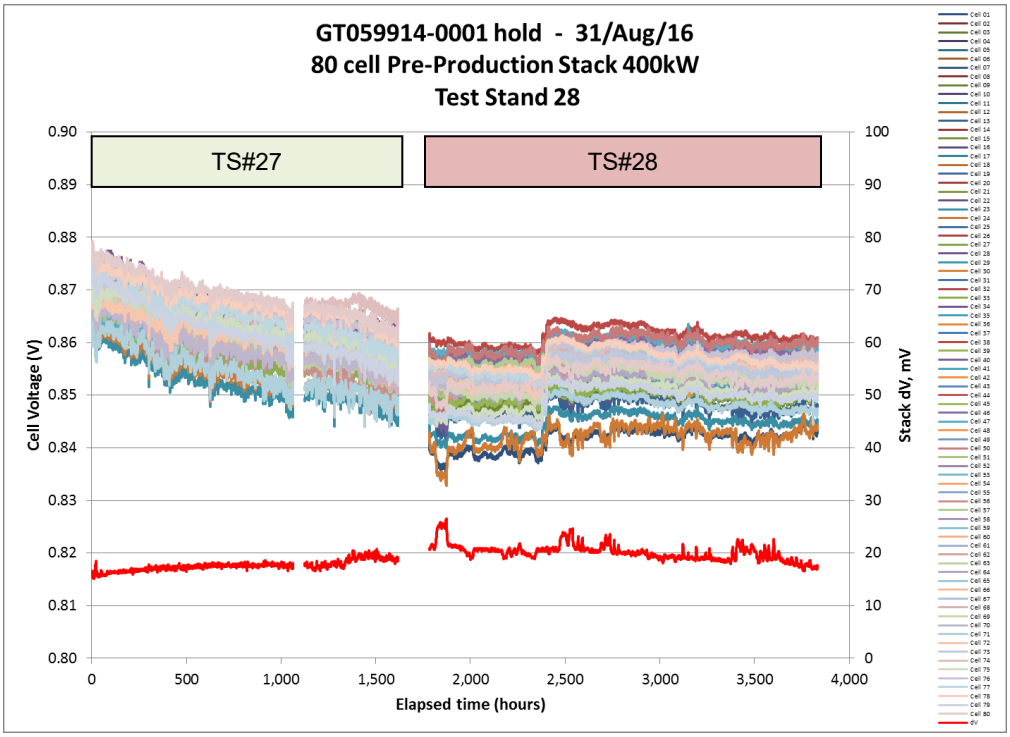

Figure 3-29. Stack GT059914-0001 (80 cells) Individual Cell Voltage and Voltage Spread (dV) Trends (TS #27 + TS #28)

Over the first 590 hours in Test Stand #28, the stack demonstrated 0.07% (0.6 mV)/kh or nearly a negligible change in average voltage. In a closer review and comparison of the test stand temperatures (shown in Figure 3-30), it was identified that although the preheater set-points for both test stands were the same (730°C), the actual stack air inlet (AI) temperature was considerably cooler (645°C v. 675°C) in Test Stand #28. Soon after, the air inlet preheater set point was increased to better match the actual air inlet temperature. Overall, this has a cooling effect on the stack as can be seen in the air outlet temperature. After the temperature adjustment to the air inlet, the stack has improved performance, similar voltage performance to that demonstrated in Test Stand #27. The stack has impressively low performance degradation rate of 0.22% (1.8 mV) / 1000h over the most recent 1,421 hour period.

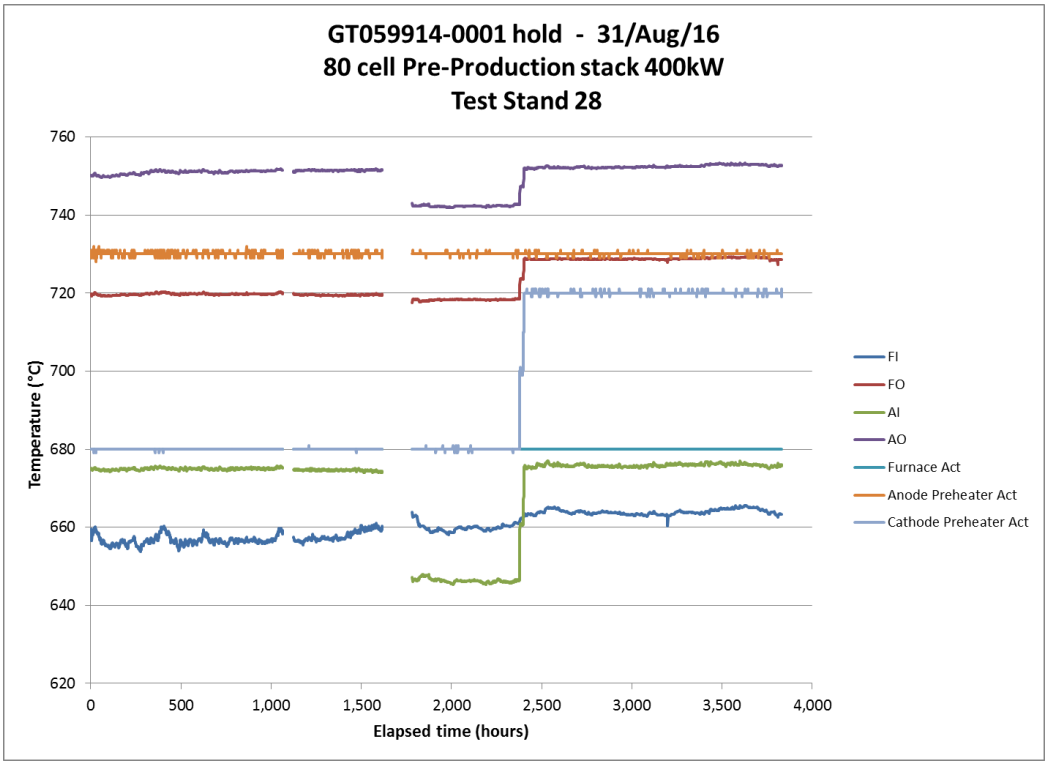

Figure 3-30. Stack GT059914-0001 (80 cells) Key Temperatures (TS #27 + TS #28)

The estimated average cell performance degradation rates are as shown in Figure 3-31.

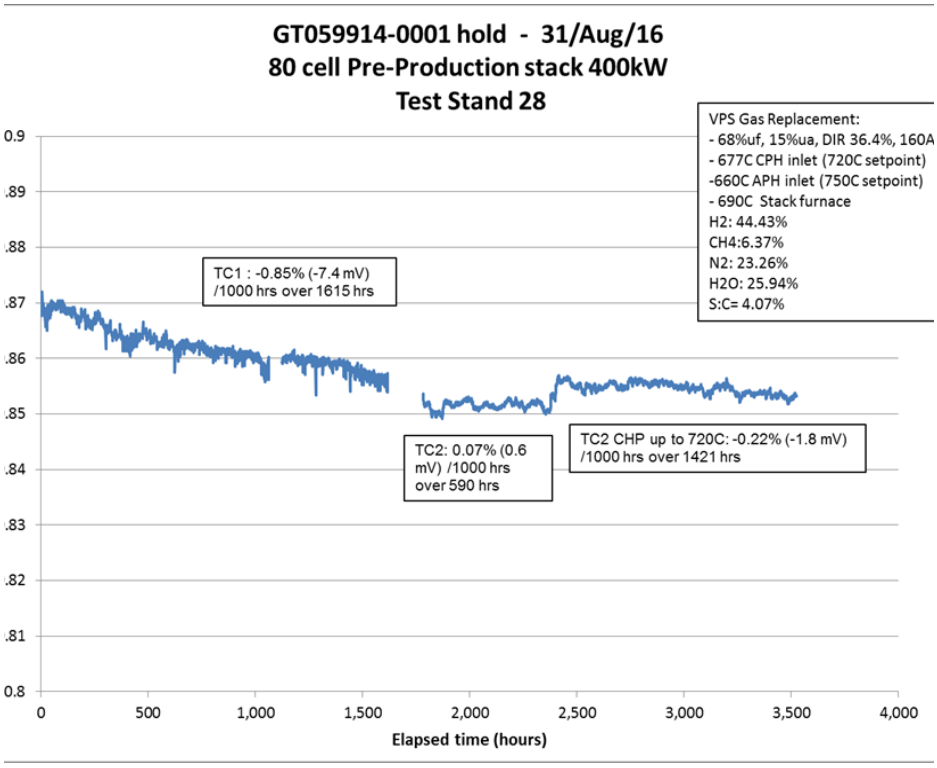

Figure 3-31. Stack GT059914-0001 (80 cells) Average Cell Performance Degradation Rate (in TS #27 and TS #28)

During Q7 (April-June, 2017), test stand issues were encountered with the stack furnace ground fault protection leading to four additional thermal cycles (TC3-TC6) with this test. The ground fault protection sub-system ensures safe operation of the 600 VAC powered stack furnace by monitoring leakage current to the electrical ground. The issue was not fully resolved, and the stack will now be moved to Test Stand #29 to continue long term testing with greater test stand confidence. It is expected that this test will extend into Y2019 when long term test results will validate the 120-cell stack technology and unit cell configurations selected (design frozen) for 200 kW SOFC system modules.

As reported previously, the stack test was initiated in Test Stand #27. The stack was shut down, cooled and physically moved to neighboring Test Stand #28, where the test has accumulated additional hours at the same fuel and stack current test conditions. The combined test results are shown in Figure 3-32.

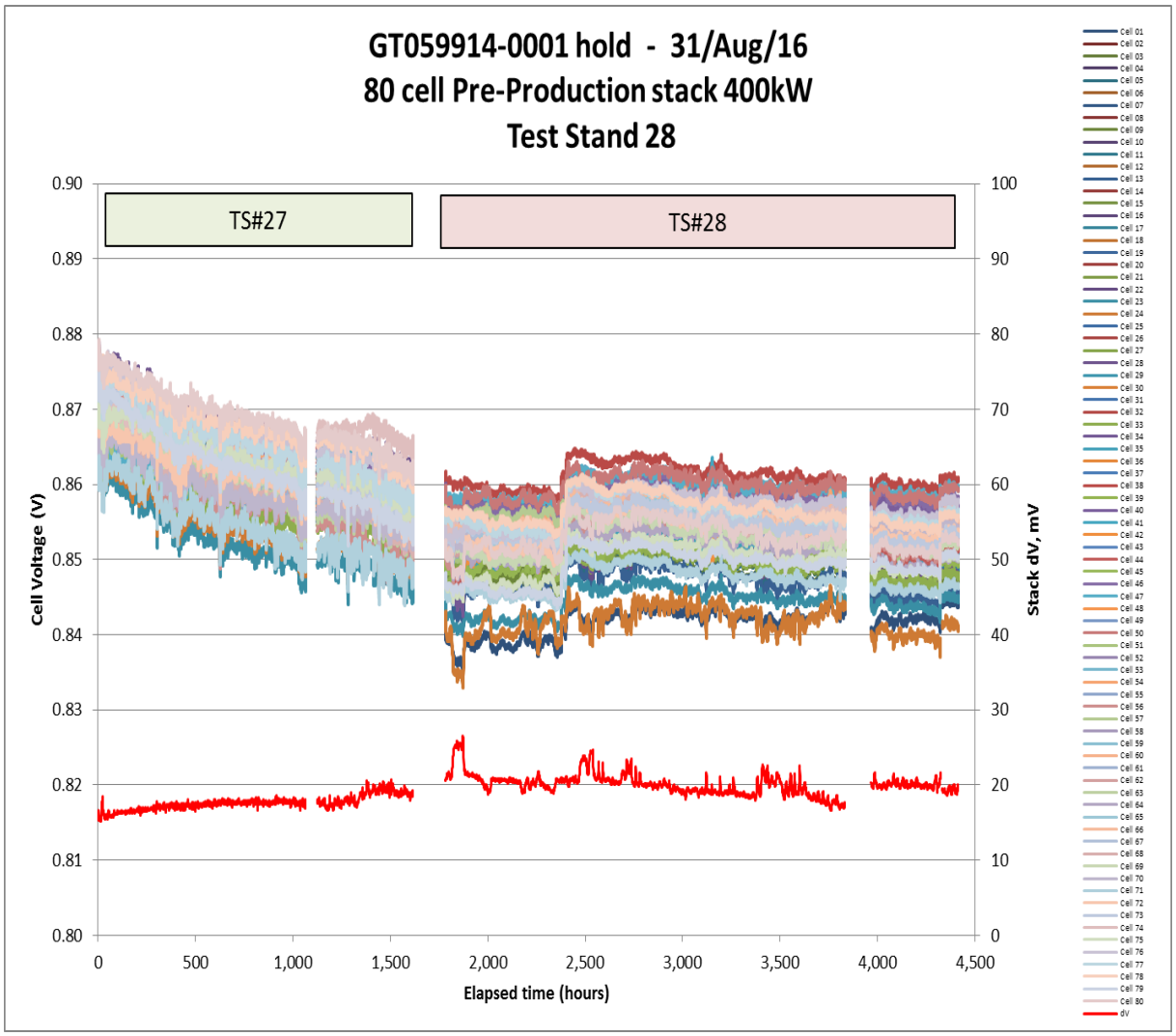

Figure 3-32. Stack GT059914-0001 (80 cells) Individual Cell Voltage and Voltage Spread (dV) Trends (TS #27 + TS #28)

The air inlet preheater set point was increased to match the actual air inlet temperature observed while the stack was in Test Stand #27. Since this thermal adjustment in Test Stand #28, the stack has accumulated an additional 2001 hours which allows for a better comparison of the stack results in both test stands. Figure 3-33 shows the comparison of key temperatures.

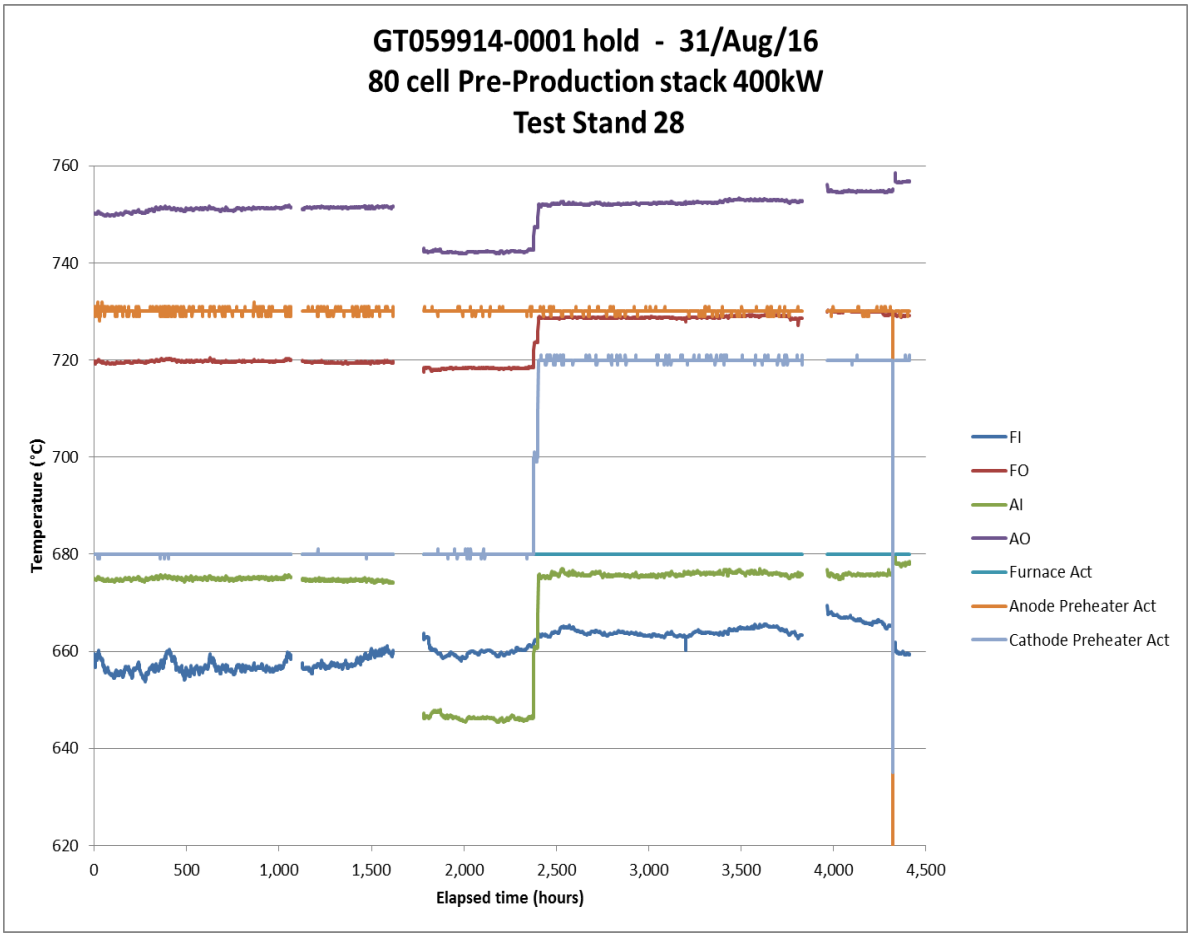

Figure 3-33. Stack GT059914-0001 (80 cells) Key Temperatures (TS #27 + TS #28)

The average cell performance degradation rates estimated for different test periods are shown in Figure 3-34.

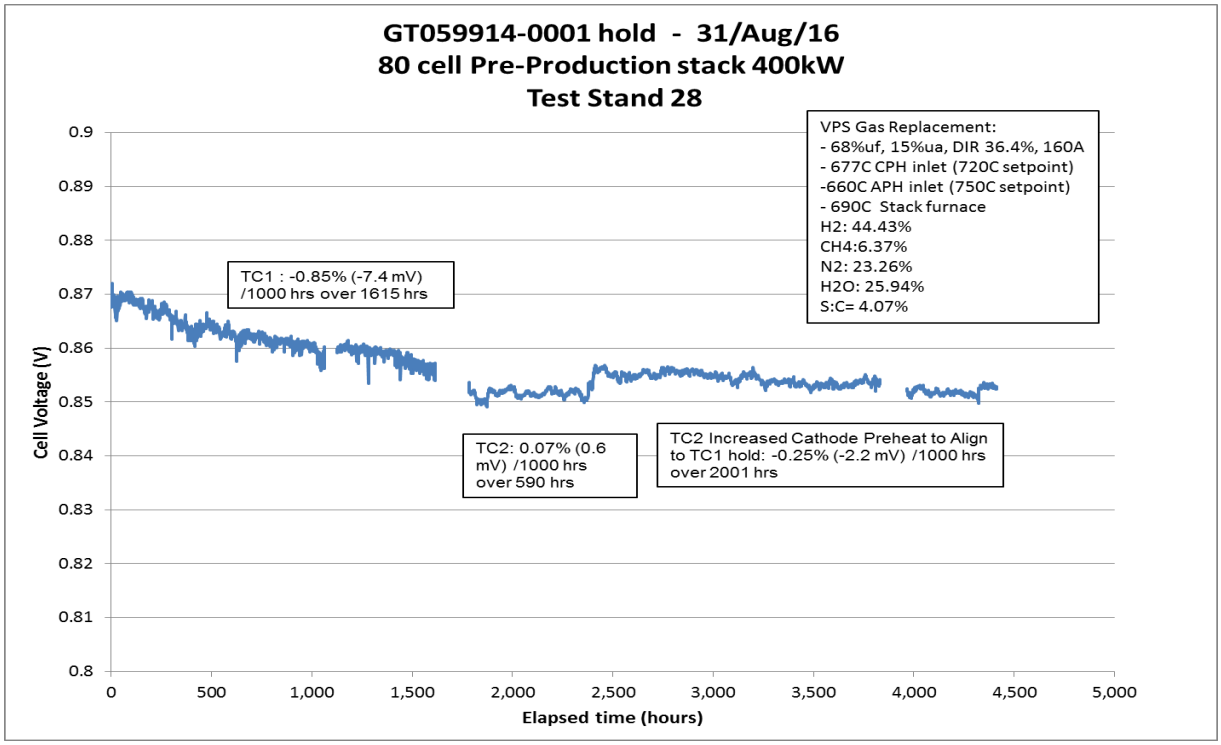

Figure 3-34. Stack GT059914-0001 (80 cells) Average Cell Performance Degradation Rate (in TS #27 and TS #28)

During the first 590 hours (at lower temperature) in Test Stand #28, the stack demonstrated 0.07% (0.6 mV)/1000 h or nearly a negligible change in average voltage. After the temperature adjustment to the air inlet, the stack has improved voltage and performance similar to that demonstrated in Test Stand #27. In addition, the stack has continued with impressive low degradation performance rate of 0.25% (2.2 mV) / 1000 h over the most recent 2,001 hour time period.

Long-term steady-state testing of the large-area stack (GT059914-0001) was re-started quarter Q3 2017. The overall testing to date is as shown in

Figure 3-35. Testing began in Test Stand #27, changed to Test Stand #28, and then reverted back to Test Stand #27 complete with 9 deep thermal cycles and a relatively low 6,252 hours of test time thus far whereas more than 1 year of calendar time has passed. Simply looking at the beginning voltage 0.869 V initial and 0.842 V (@6252 h), this equates to 4.3 mV (0.50%) / kh over the duration of testing including steady-state and thermal cycles thus far.

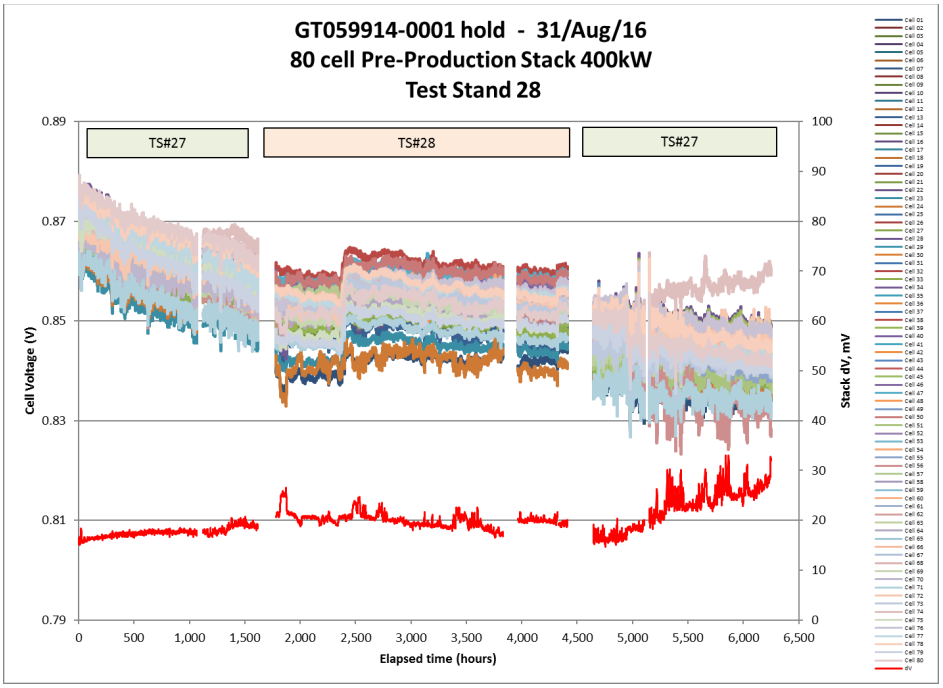

Figure 3-35. Stack GT059914-0001 (80 cells) Individual Cell Voltage and Voltage Spread (dV) Trends (TS #27 + TS #28)

At the beginning in Test Stand #27, the stack performance degradation rate was observed to be 0.85 % (7.4mV) /1000h over 1615 hours (with a slight second order decreasing trend over time). During this time, the test stand experienced humidifier pump communication errors and stack test interruptions at 1062 and 1615 hours. Following the second interruption, the stack was shut down, cooled and physically moved to neighboring Test Stand #28 (see Figure 3-36). This was done to have both Test Stand #29 (lead) and Test Stand #27 (alternate) available for 120-cell stack conditioning and acceptance testing for the main stack production effort.

Figure 3-36. Tall (25 kW) Large Area Stack Test Stands

After resuming the test in Test Stand #28, the stack accumulated an additional 2,628 hours at the same test fuel and stack current conditions. Over the first 590 hours (hour 1780 to hour

2370) in Test Stand #28, the stack was performing at a lower, although quite constant operating voltage. In a closer review and comparison of the test stand temperatures (shown in Figure 3-37), it was identified that although the preheater set-points for both test stands were the same (730°C), that the actual stack air inlet (AI) temperature was considerably cooler (645°C v. 675°C) in Test Stand #28. After this was better realized, the air inlet preheater set point was increased to match the actual air inlet temperature compared to the test condition in Test Stand #27. After this thermal adjustment in Test Stand #28, the stack accumulated an additional 2001 hours which allowed for a better comparison of the stack results in both test stands.

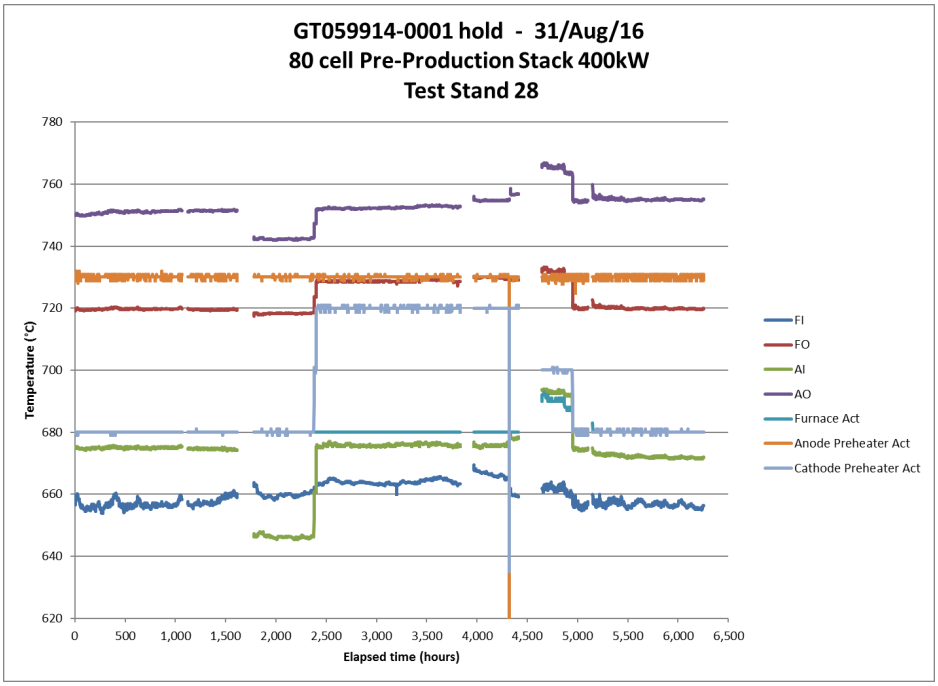

Figure 3-37. Stack GT059914-0001 (80 cells) Key Temperatures (TS#27+TS#28+TS#27)

Limited hot testing occurred from April 5 through early August in 2017 as substantial test stand issues were encountered related to the stack furnace ground fault protection system leading to 4 (TC3-TC6) thermal cycles on the stack while attempts to resolve the issue were made including new GFI equipment and wiring. The ground fault protection ensures safe operation of the 600 VAC powered stack furnace by monitoring leakage current to the electrical ground. Ultimately, the decided solution was to move the test back to Test Stand #27. As of August 8, 2017, long term testing resumed. Calculations of the average cell performance degradation rates are as shown in
Figure 3-38. Over TC2, when including the temperature increase, basically no degradation was observed. In TC8, and when considering the last 1,102 h of testing, the stack is still performing very well with a measured decay rate of -0.20% (1.7 mV)/kh.

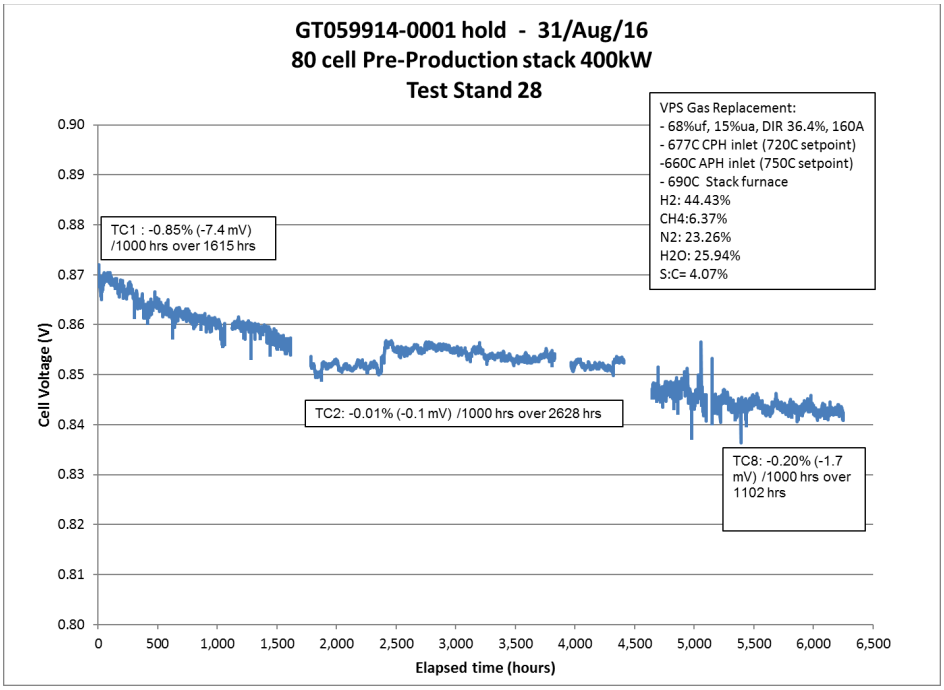

Figure 3-38. Stack GT059914-0001 (80 cells) Average Cell Performance Degradation Rate (in TS #27 and TS #28)

Overall, it is expected that this test will last into 2019 where long term test results will validate the same 120-cell stack technology and unit cell configurations frozen for the 200 kW system demonstration in Pittsburgh, PA.

The overall average cell voltage test performance to date is as shown in Figure 3-39.

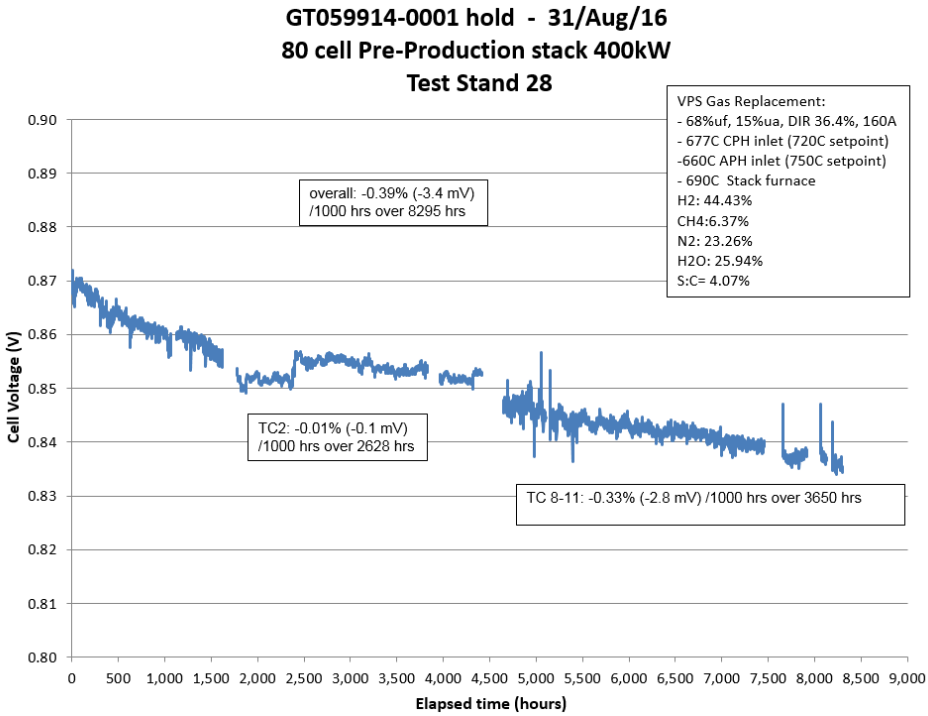

Figure 3-39. Stack GT059914-0001 (80 cells) Average Cell Performance Degradation Rate (in TS #27 and TS #28)

Thus far, the stack has completed 12 deep thermal cycles and 8,295 hours of test time at operating conditions, whereas more than 1 year of calendar time has passed due to test stand interruptions. From simply looking at the beginning (initial) voltage of 0.869 V and final voltage of 0.834 V (at 8295 h), 4.2 mV (0.49%) / kh is calculated over the duration of testing including both steady-state and thermal cycles considered thus far.

In TC8 to 11 (when considering the last 3,145 h of testing), the stack is still performing well with a measured decay rate of -0.33% (2.8 mV) / kh.

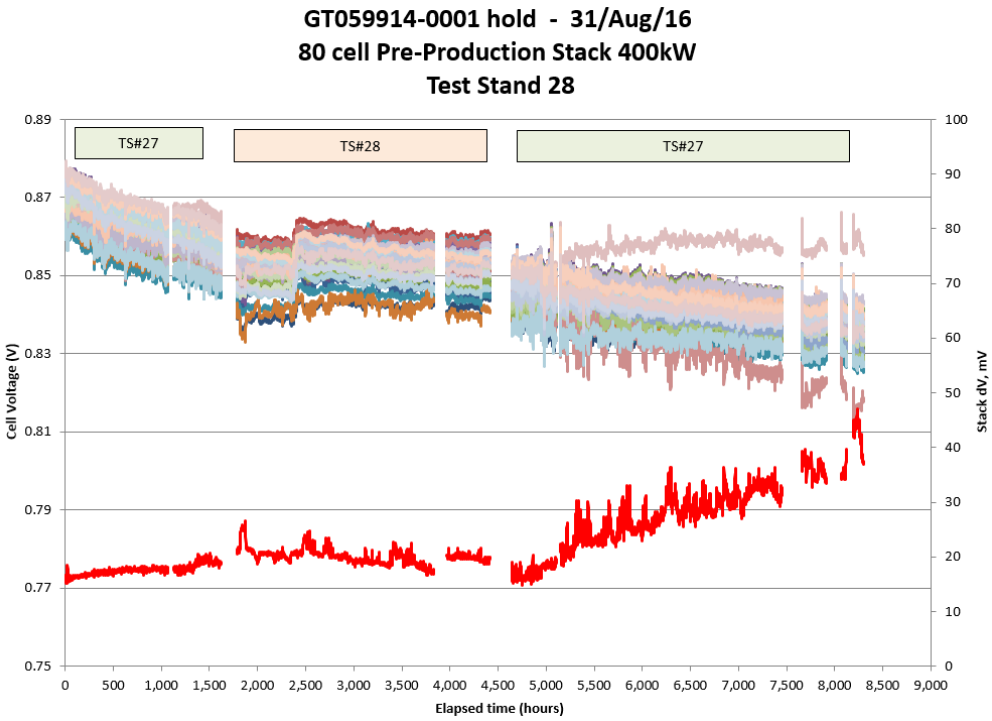

Figure 3-40. Stack GT059914-0001 (80 cells) Individual Cell Voltage and Voltage Spread (dV) Trends (TS #27 + TS #28)

Long-term steady-state testing of this large-area stack (GT059914-0001) was re-started twice in Q4 2017. The anode preheat over-temperature protection controller was the cause of these restarts, which was not suspected until the second restart where the controller went into an error loop. The controller was replaced before the fourth restart (TC11) and has been running well since. Figure 3-41 shows a zoomed in view of the last 1200 hours of operation including the restarts.

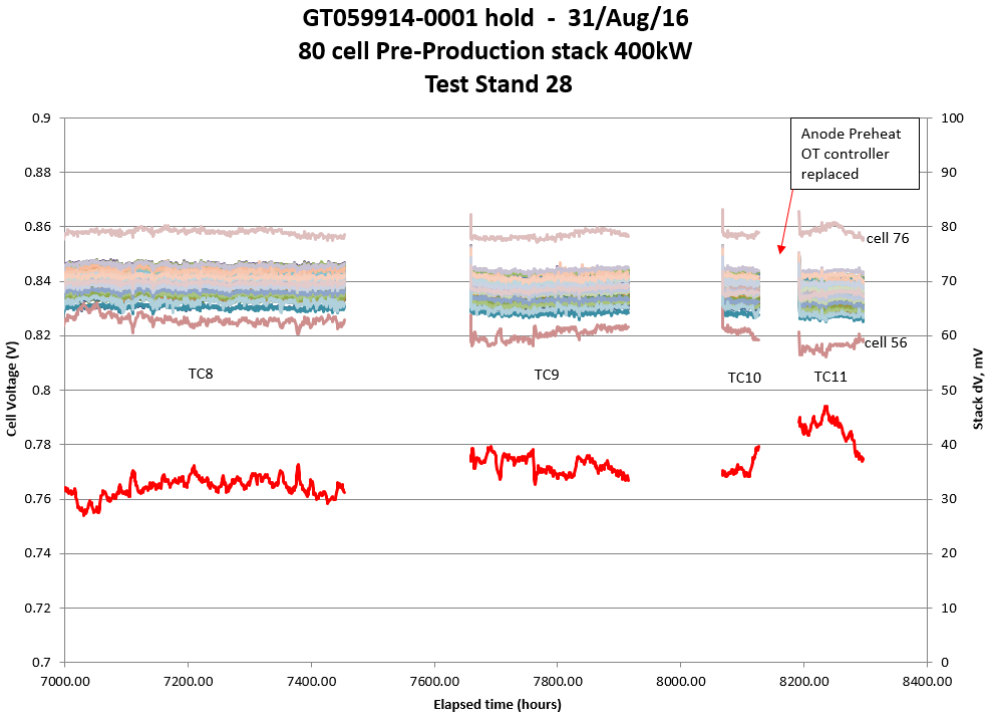

Figure 3-41. Stack GT059914-0001 (80 cells) Last 1200 hours hold of Individual Cell Voltage and Voltage Spread (dV) Trends

Since approximately 6000 h elapsed time, Cell 76 has been observed to be the highest voltage out the pack and Cell 56 the lowest cell voltage. During TC11 and the most recent test time, both cells now seem to be converging towards the pack as the stack dV trend dictates.
Overall, it is expected that this test will last into 2019 where long term test results will validate the same 120-cell stack technology and unit cell configurations frozen for the 200 kW prototype system demonstration test.

120-cell Production Stacks

To guide stack conditioning and performance testing, a factory acceptance test document was generated. The document contains metrics to graduate and accept the stacks for 100 kW modules. All stack conditioning will be conducted using the FuelCell Energy – Calgary 25 kW Test Stand fleet (Test Stands 27, 28 and 29). The conditioning will include TC0 (before thermal cycle) fuel utilization testing and (TC0) testing at VPS Gas Replacement (system representative) operating conditions. No TC1 (after thermal cycle) testing is included which is a simplification compared to past stack conditioning practice. The 16-cell and 80-cell stacks of the same configuration have validated that the stack can thermal cycle and therefore deliverable stacks are not required to be thermal cycled further for the stack factory acceptance. Major conditioning and test steps are listed in Table 3-2.

Table 3-2. Hot Test Overview - Major Steps

Step #	**TC0** (Before Thermal Cycle) Test Description
1	Initial Mechanical loading to 600 lbf
2	1st Heating Phase
3	Final Mechanical Loading and dwell (hold)
4	Air and N_2 Supplied & 2nd Heating Phase
5	3rd Heating Phase-750°C furnace and 730°C preheats & hold *(test prime to release hold manual after checkout)*
6	Reduction
7	Ramp Temp to 700°C furnace, 720°C cathode preheat, 750°C anode preheat (@ 3°C/min) and dwell
8	Set / Re-confirm flows and Load to 160A for fuel utilization testing
9	Hold at Phase 1 system conditions for 1 hour
10	VPS GR system conditions and 160A dwell for 50 hours
11	Electrically unload the stack and cooldown

Eleven in-cell thermocouples (TC) have been specified. TCs are labelled with FuelCell Energy - Danbury module thermocouple identification number (FCE TC ID #) and Calgary test stand (TC ID) number for reference. Thermocouple information is presented in Table 3-3.

Table 3-3. Stack Thermocouples (11 per stack)

Test Stand (TC ID) #	Cell #	(FCE) TC ID	TC Location	Manifold Penetration	Hot Sheath Length (in)	Cold Extension Length (in)
1	1	001B	B	A/I	72	12
2	1	001E	E	A/I	72	12
3	1	001I	I	A/I	72	12
4	60	060B	B	A/I	72	12
5	60	060b	B (spare)	A/I	72	12
6	60	060E	E	A/I	72	12
7	60	060e	E (spare)	A/I	72	12
8	60	060I	I	A/I	72	12
9	120	120B	B	A/I	72	12
10	120	120E	E	A/I	72	12
11	120	120I	I	A/I	72	12

A variety of acceptance criteria is included relating to the geometry and configuration of the cells and stacks as well as the cold measured leak rate. Anode and cathode (cold) flow test (pressure drop) variation for stacks is also included for combining stacks as a family or set for a particular module. For hot test results, the acceptance criteria are as described **Error! Not a valid bookmark self-reference.** in
.

Table 3-4. Stack Hot Test Results - Acceptance Criteria

Hot Testing	Acceptance (/cell or /double cell block)
Initial reduction at 750°C	All in-stack thermocouples below 800°C at all times
OCV	> 1.00 V (minimum) – at hold condition prior to power curve (electrical load-up)
Cell Voltage at 75% Uf, 13.5% Ua, 160 A, 25% DIR	> 0.84 V (average) > 0.80 V (minimum)
Stable cell voltages over 50 h hold	< 10 mV decrease in individual cell voltage during hold when compared to stack cell average over same time period

Actual build dates for the 5 stacks built in this reporting quarter are shown in Table 3-5, along with the planned dates for stacks to be built in the next quarter.

Table 3-5. Stacks Built During Reporting Quarter & Planned for the Next Quarter

	Stack ID	Build Date
Completed	GT060322-0004	April 18, 2017
	GT060322-0005	April 26, 2017
	GT060322-0006	May 10, 2017
	GT060322-0007	May 30, 2017
	GT059879-0010	June 26, 2017
Forecast	GT060322-0008	Plan - July 4, 2017
	GT060322-0009	Plan – August 2017 *Start of Set 3*
	GT060322-0010	Plan – September 2017
	…	Plan – September 2017

The build date for the last stack built in Q3 - Calendar 2017 is as shown in Table 3-6, initially module 3 stacks were scheduled for building. However in a mutual decision with DOE and FuelCell Energy, any further module or spare stacks is delayed into the future.

Table 3-6. Stacks Built During Reporting Quarter & Forecast

	Stack ID	Build Date
Completed	GT060322-0008	July 4, 2017

Stack GT060322-0008 was stable in performance at 75% fuel utilization condition and passed acceptance criteria. From September 2016 to July 2017, 120-cell cell and stack production was active. As of September 30, 2017 the effort was completed as presented in Table 3-7 for the required 16 stacks contained within the 200 kW prototype system. Also in Q3 2017, stacks were delivered to Danbury for module builds.

Table 3-7. Stack Build Status

Set 1 (Module 1)	Set 2 (Module 2)
GT059879-0001	GT060322-0001
GT059879-0002	GT060322-0002
GT059879-0003	GT060322-0003
GT059879-0004	GT060322-0004
GT059879-0005	GT060322-0005
GT059879-0006 (spare)	GT060322-0006
GT059879-0007	GT060322-0007
GT059879-0008	GT060322-0008
GT059879-0009	
GT059879-0010	
Module 1: 8/8 =100%	Module 2: 8/8 =100%
200 kW Overall: 16/16 =100%	

In the above table, color coding is utilized with green denoting a pass and red to yield a loss. For Set 1 (Module 1), 10 stacks were required, as a single stack was lost due to a component build error and a spare was built (as desired). For Set 2 (Module 2), 8 of 8 stacks were built and passed factory acceptance testing to produce a 100% yield achieved.

100 kW Stack Module Modeling and Related Testing

The 100 kW stack module included four 240-cell stack towers (each tower built using two 120-cell stack blocks), a radiator (preheater + reformer) and vessel. A cross-section is shown conceptually in Figure 3-42. There were several key modeling questions such as to find out how the radiator reforming duty change affects stack thermal performance and the direct in-stack reforming (DIR) level, what the temperature profiles and heat flux will be on surfaces of the preheater and reformer, and what the optimal operable design point should be for the stack module.

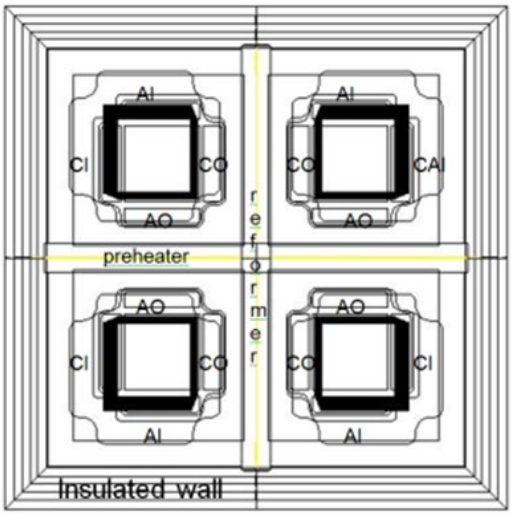

Figure 3-42. 100 kW Module Featuring Four Cross-flow 240-cell Stacks with a Radiant Reformer and a Preheater System

The radiator was designed to sit in the middle of module and separates the four stack towers into independent thermal zones. The 50 kW module radiator is composed of two sections, the reformer facing the cathode exhaust manifold and the preheater facing the anode exhaust manifold. Whereas in the 100 kW stack module, the second pass preheater was converted also to an active radiant reformer to reduce catalytic space velocity and increase hydrocarbon conversion.

FCE Calgary developed a reformer kinetics model for the catalytic inserts used inside the radiant reformer. Which required kinetics' parameters special to the reformer and catalysts to be applied. To develop this information, testing has been conducted on 4 different catalysts of interest: JM 3496 (Ni), Nov Foam, JM 3825 (Ru) and Nexceris), as shown in Figure 3-43. The best catalyst was JM 3496, which was the focus for modeling efforts. For JM 3496, a long term 1500-hour test has also been completed as shown in Figure 3-44 with good and stable results over this time period. The plot shows the reformer bed temperatures in addition to the reforming level.

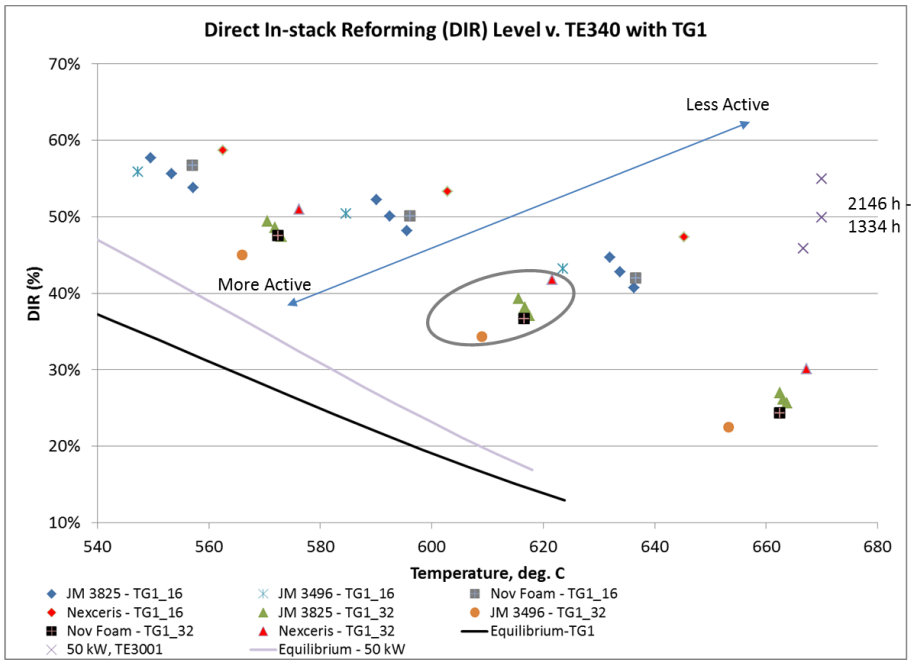

Figure 3-43. Catalyst Test Data for Reforming Inserts

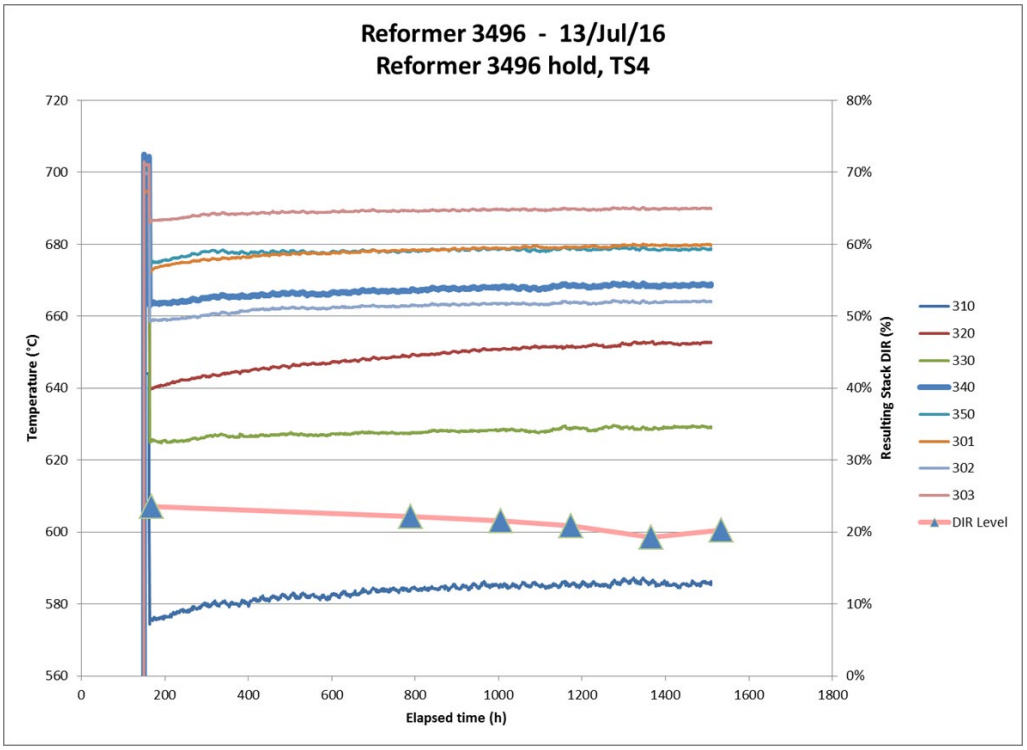

Figure 3-44. Performance of JM 3496 Catalyst during 1500-h Hold

Based on the test data, a reforming kinetics model has been developed and applied in 3D CFD (computational fluid dynamics) simulations of reformer insert. Figure 3-45 shows the test set-up used and the CFD simulation.

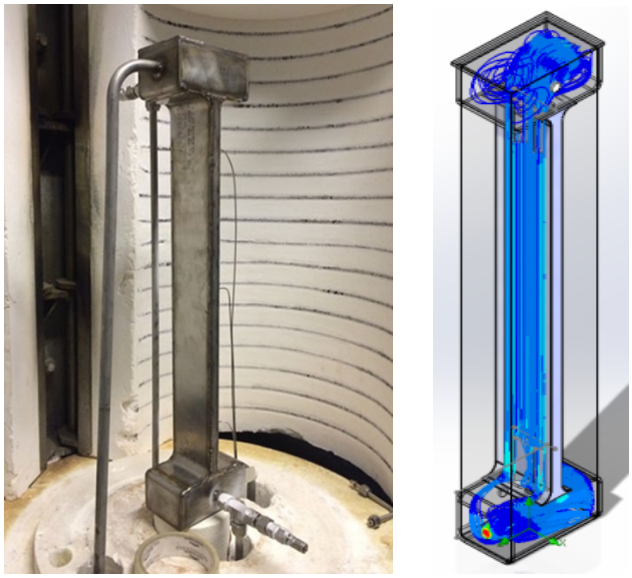

Figure 3-45. Reforming Test Set-up and CFD Simulation

Module 1 Stacks – (Stacks GT059879-0001 to -0006)

The first 120-cell stack for Module 1 of the 200 kW system was built (shown in Figure 3-46) on September 14, 2016 and conditioned with no thermal cycle.

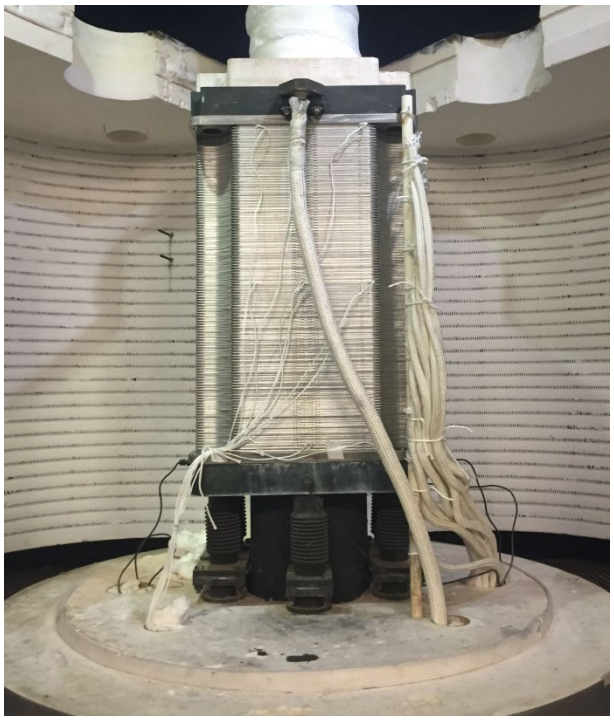

Figure 3-46. 120-cell Stack GT059879-0001 (After Installation)

The stack performance was stable at 75% Uf (fuel utilization testing) with average cell voltage 4 mV higher than the 80-cell stack and at the VPS GR conditions (steady state hold) with average cell voltage 2 mV higher. The results are shown in Figure 3-47 and Figure 3-48, respectively. The average voltage range (spread) at the VPS GR conditions was 23 mV over the 50-hour hold. At said time of testing, the stack had passed all hot performance criteria set in the factory acceptance test plan.

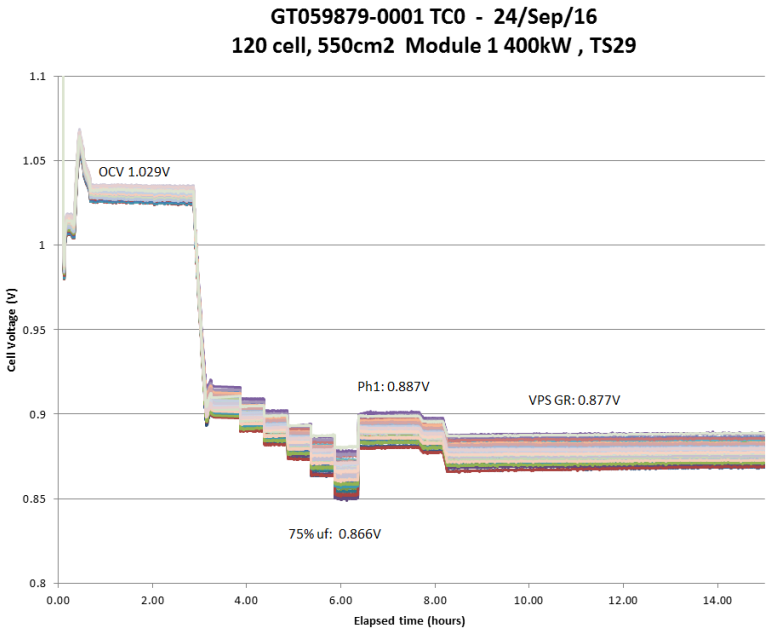

Figure 3-47. Performance of Stack GT059879-0001 During Fuel Utilization Testing

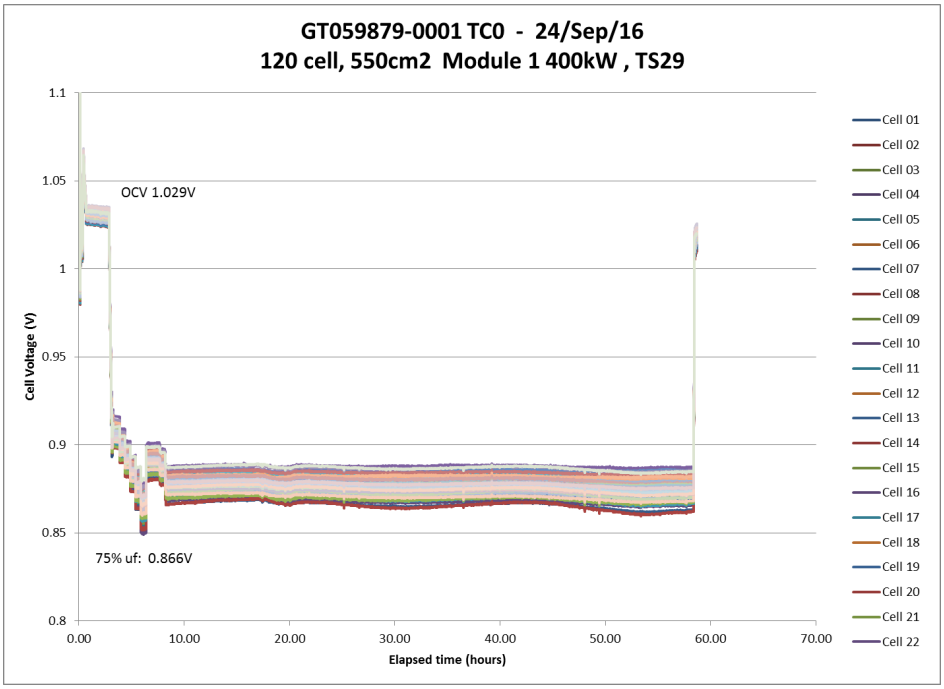

Figure 3-48. Performance Stability of Stack GT059879-0001 During 50-hour Hold at VPS GR System Conditions

For the six 120-cell stacks that have been built, Figure 3-49 illustrates the electrochemical performance aligned on a single time-plot. At ~15 hours, the stacks were first electrically loaded, and then run through fuel utilization steps (50 through 75%). This was followed by a 50 hour hold at a system representative condition (160 Amperes, 291 mA/cm^2).

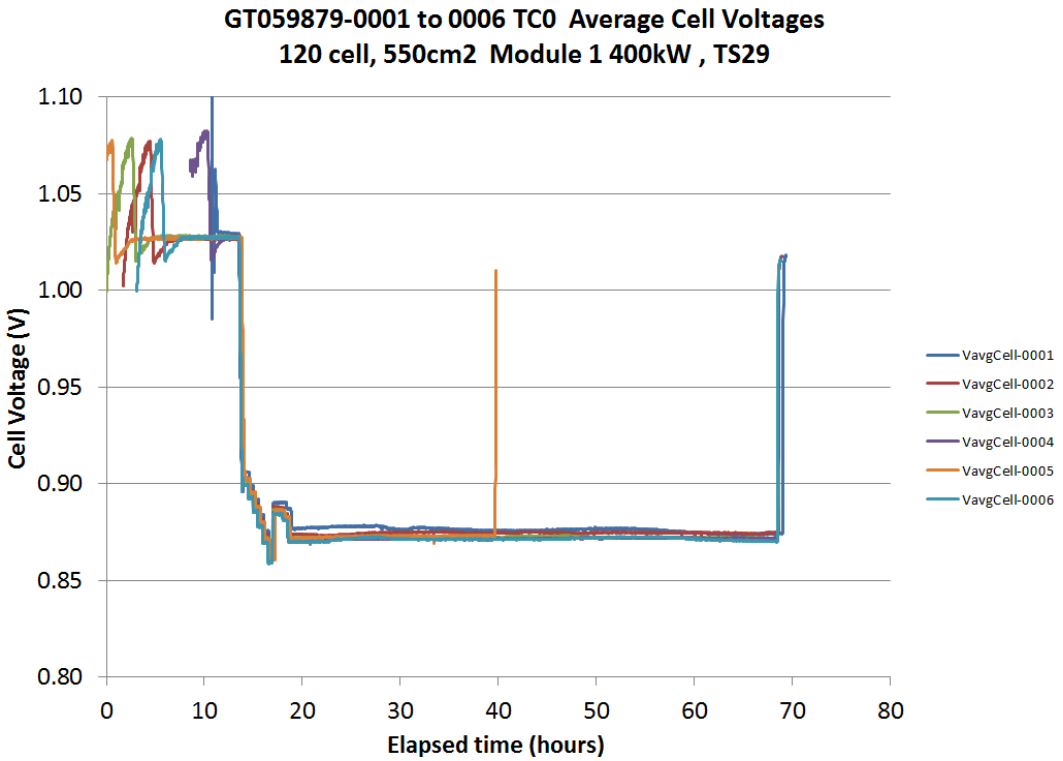

Figure 3-49. Average Cell Voltage during Fuel Utilization Testing for Stacks GT059879-0001 to -0006

The average cell voltage results are shown numerically in Table 3-8 and graphically in Figure 3-50 for comparison. The stack performance compares well, with all results within 7 mV or <1% variation between the highest and lowest performing stacks.

Table 3-8. Performance of 120-cell Stacks built for Module 1

	OCV	75%uf	Ph1	VPS GR
GT059879-0001	1.029	0.866	0.887	0.877
GT059879-0002	1.027	0.864	0.885	0.875
GT059879-0003	1.027	0.862	0.883	0.872
GT059879-0004	1.028	0.862	0.882	0.871
GT059879-0005	1.028	0.861	0.881	0.872
GT059879-0006	1.027	0.859	0.881	0.870

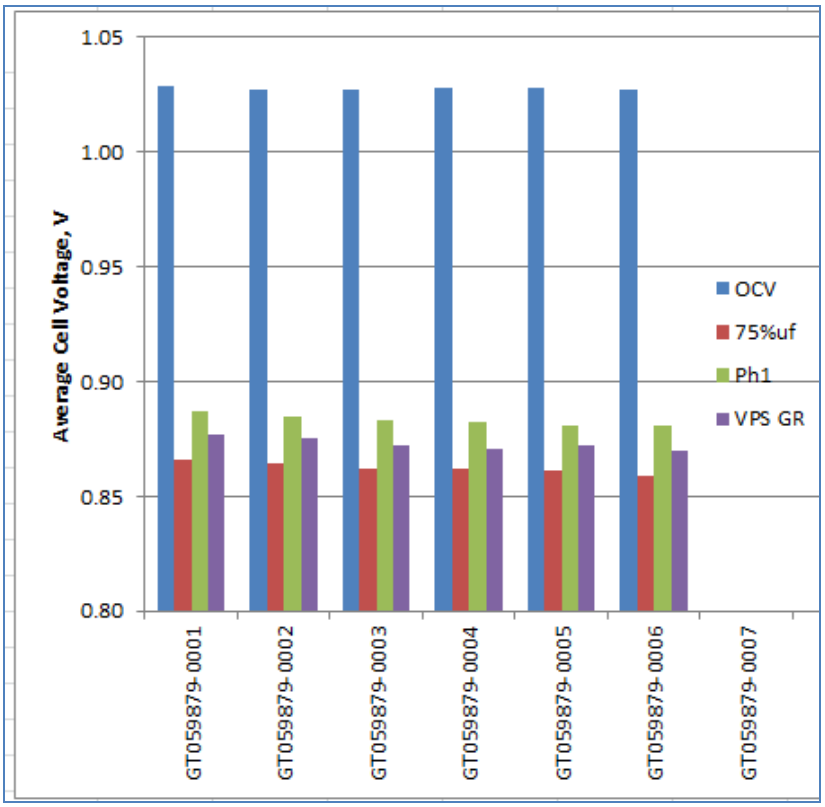

Figure 3-50. Performance Comparison of 120-cell Stacks built for Module 1

Stack GT059879-0005 had issues observed early on in the electrochemical testing as shown Figure 3-51.

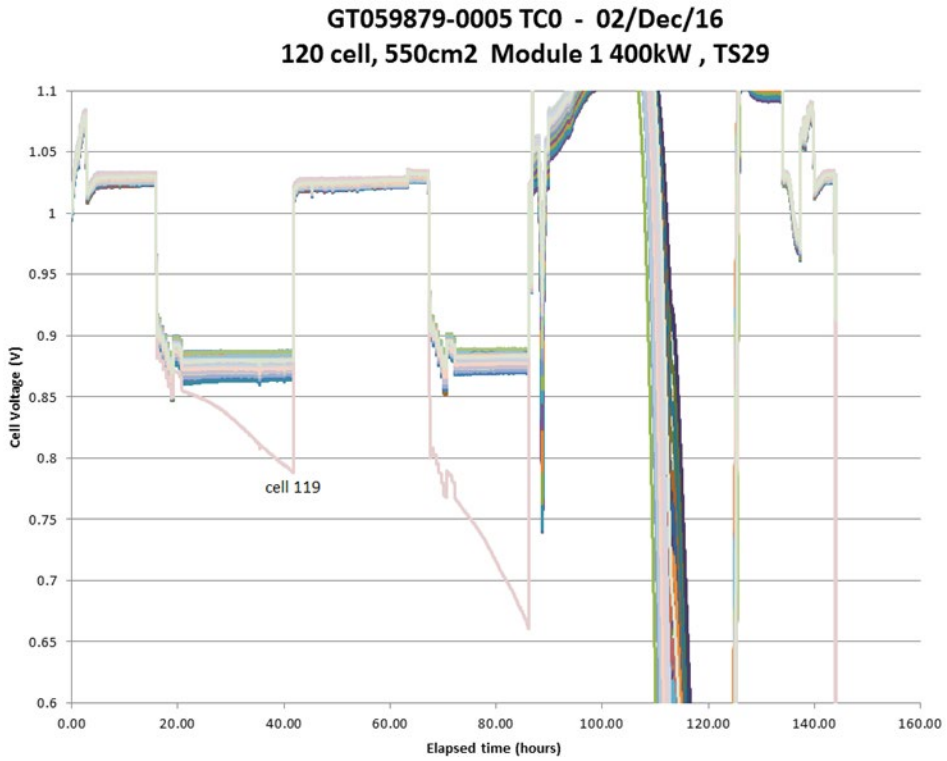

Figure 3-51. Stack GT059879-0005 Performance during Fuel Utilization Testing

The test electrical load was manually interrupted after 24 hours on load, as performance of Cell 119 was degrading quickly. The stack electrical load was re-applied (160 A) after a 24 h stabilization period at open circuit conditions. Cell 119 voltage, however, continued to degrade at rapid rate until 0.66 V was measured on this weak cell. The stack was then thermally cycled to investigate if the contact in Cell 119 in particular could be improved. After the thermal cycle, Cell 119 contact worsened and the stack was only loaded up to 144 A point.

During post-test examination, Cell 119 issue was further traced to a human error in build relating to an up-side down anode flow field / anode contact sub-assembly within the stack. As the issue was very near the stack end, the stack did not require disassembly. The component was observed via the stack gas manifold openings. Although 119 of 120 cells, as well as the stack average voltage, demonstrate acceptable performance, the stack will not be used for Module 1. This stack also has a cross leak outside the acceptance criteria (see Table 3-9).

Table 3-9. Leakage Rates (sccm – air) of Stacks built for Module 1

	Raw Data			Calculated		
	Cathode total	Anode Total	Both	Cathode	Anode	Cross
GT059879-0001	8360	9870	8470	3480	4990	4880
GT059879-0002	7840	9270	6230	2400	3830	5440
GT059879-0003	6080	8480	5160	1380	3780	4700
GT059879-0004	8370	10160	4970	1590	3380	6780
GT059879-0005	12870	16410	660	-1440	2100	14310
GT059879-0006	7380	16270	14640	2875	11765	4505

As Module 1 stacks must work together as a single unit, the anode and cathode pressure drop characteristics must be very similar. To investigate this, cold flow testing was performed with air for both anode and cathode sides of the stack. The test results are shown in Figure 3-52. All 6 stacks have similar anode and cathode pressure drop characteristics. Stack 0001 has somewhat higher cathode side pressure drop at higher flow rates.

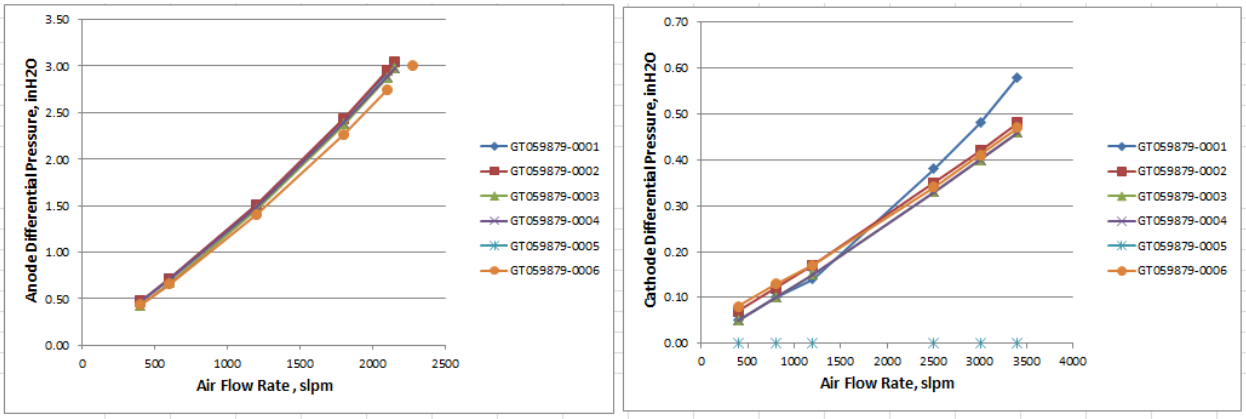

Figure 3-52. Stack Anode and Cathode dP Trends of Stacks built for Module 1

All stacks also met the stack height acceptance criteria. Figure 3-53 shows the measured stack height (average of the 4 corners) compared to the upper and lower specification limits. In addition, the chart also shows the contribution of cell height to the total stack height. In the large area stack design, the cell thickness makes up approximately 12% of the overall stack height including stack end plates.

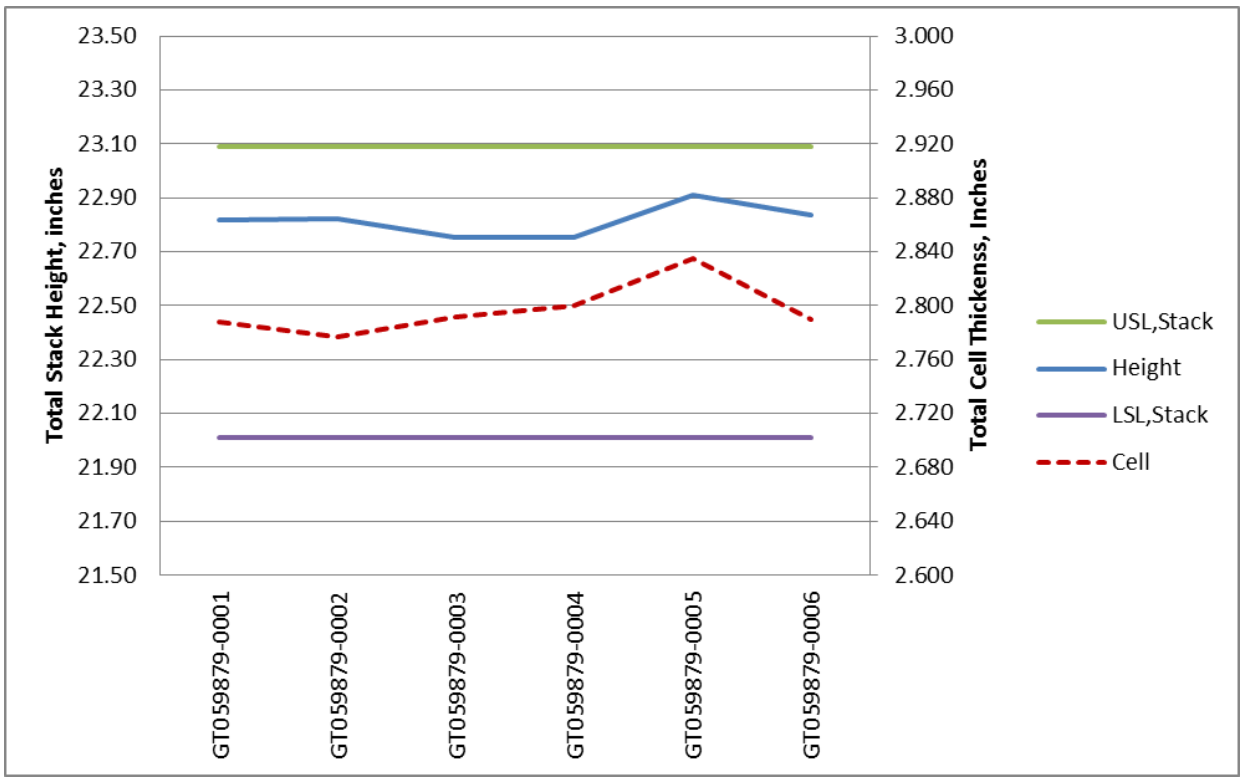

Figure 3-53. Comparison of Stack Height and Cell Thickness for Stacks GT059879-0001 to -0006

Module 1 Stacks – (Stacks GT059879-0001 to -0009)

For the eight accepted 120-cell stacks, Figure 3-54 illustrates the electrochemical performance on a single time-plot. At ~15 hours, the stacks were first electrically loaded, and then run through fuel utilization steps (50 through 75%). All stacks, except for Stack -0005, were stable in performance at 75% fuel utilization condition. This was followed by a 50-hour hold at a system representative condition (160 Amperes, 291 mA/cm^2) to demonstrate stack stability.

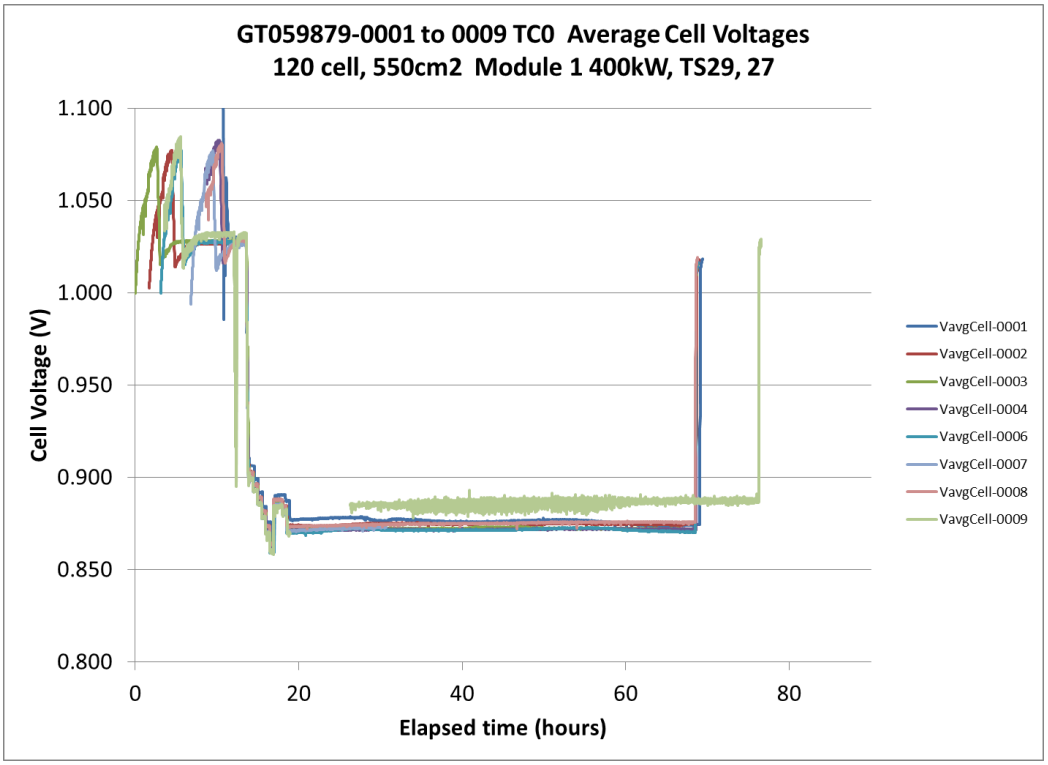

Figure 3-54. Average Cell Voltage during Fuel Utilization Testing for Stacks GT059879-0001 to -0009 with -005 excluded

The average cell voltage results are shown numerically in Table 3-10 and graphically in Figure 3-55 for comparison. The stack performance compares well, with all results within 7 mV or <1% variation between the highest and lowest performing stacks.

Table 3-10. Performance of 120-cell Stacks built for Module 1

	Hot testing							
Stack #	OCV	OCV σ (mV)	75%uf	75%uf σ (mV)	Ph1	Ph1 σ (mV)	VPS GR	VPS GR σ (mV)
Acceptance	>1.00 V (min)		> 0.84 V (average cell)					
-0001	1.029	2.3	0.866	5.3	0.887	3.7	0.877	4.0
-0002	1.027	2.5	0.864	4.9	0.885	4.1	0.875	4.6
-0003	1.027	2.3	0.862	5.6	0.883	4.5	0.872	4.5
-0004	1.028	2.4	0.862	5.3	0.882	3.7	0.871	4.2
-0006	1.027	2.0	0.859	5.8	0.881	3.8	0.870	4.4
-0007	1.026	2.0	0.861	5.3	0.882	3.5	0.871	4.1
-0008	1.028	1.7	0.864	5.5	0.884	3.8	0.873	4.5
-0009	1.032	1.8	0.860	6.7	0.880	4.4	0.870	5.0

For the 8 deliverable stacks, the cell voltage deviation was found to range from 1.7 to 2.5 mV at open circuit, and between 4.0 and 5.0 mV at VPS Gas Replacement (VPS GR) condition which represents the 200 kW system.

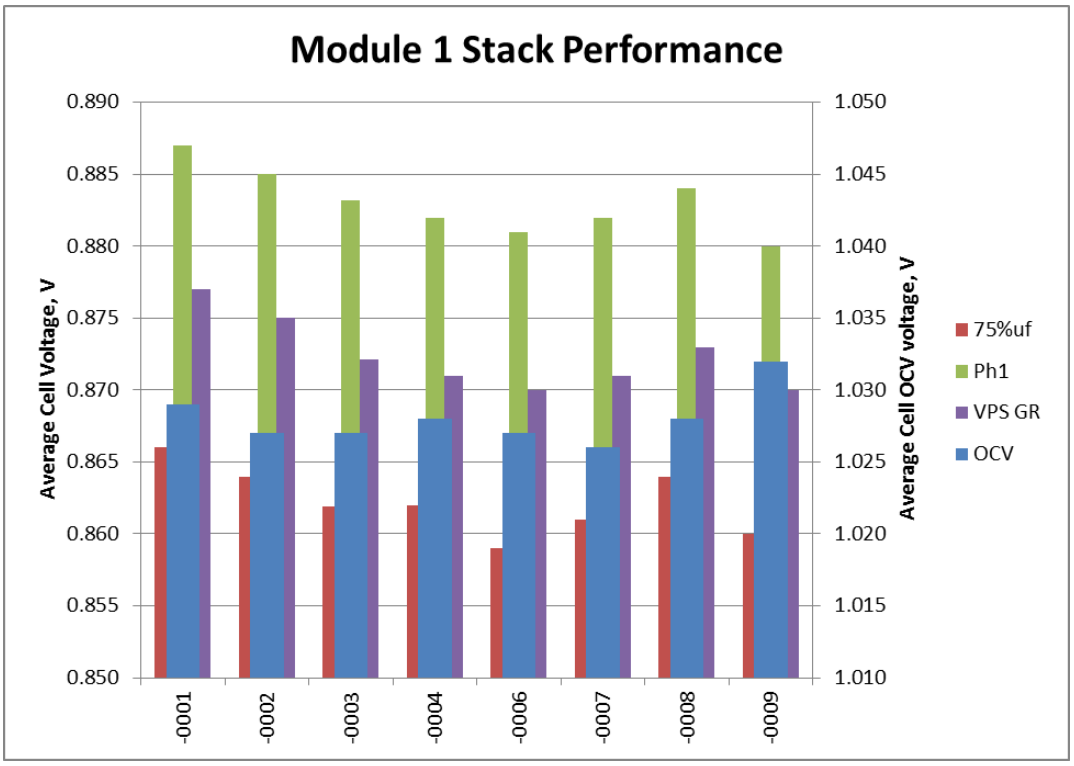

Figure 3-55. Performance Comparison of 120-cell Stacks built for Module 1

The stacks had cold leakage measurements as shown in Table 3-11. Cross leakages were all less than 12000 sccm which is the pass / fail criteria.

Table 3-11. Leakage Rates (sccm – air) of Stacks built for Module 1

	Raw Data				
Stack #	Cathode Total	Anode Total	Both	Anode	Cross
-0001	8360	9870	8470	4990	4880
-0002	7840	9270	6230	3830	5440
-0003	6080	8480	5160	3780	4700
-0004	8370	10160	4970	3380	6780
-0006	7380	16270	14640	11765	4505
-0007	9030	11830	8590	5695	6135
-0008	9280	11400	8920	5520	5880
-0009	12460	15490	10390	6710	8780

Within Module 1, the eight stacks must work together. As anode and cathode flow paths are all in parallel, both anode and cathode pressure drop characteristics must be similar. Less than 2% dP variation at 2100 SLPM and 3400 SLPM respectively is a design target. To obtain accurate data related to stack pressure drop, each stack is cold flow tested after conditioning with a large flow rate of air. For the anode side, Figure 3-56 shows a comparison of the stack anode side pressure drop. The results are shown for a variety of air flow test points.

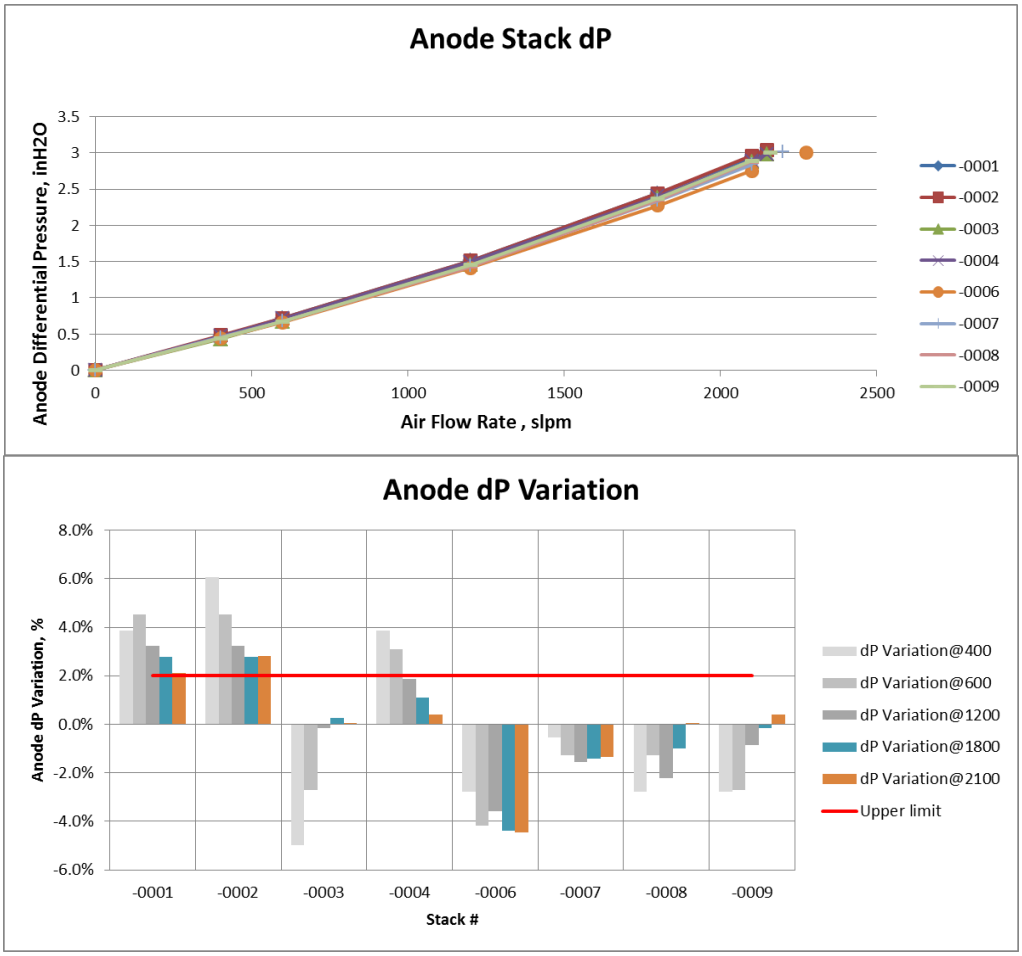

Figure 3-56. Anode Pressure Drop (dP) (Cold Flow) Comparison for Module 1 Stacks

Stack results of interest include Stacks -001 and -002 for high dP and Stack -006 for low dP. For the stack module, fuel is both fed and exhausted from the bottom of the module towers. As such, it is expected that fuel flow will be slightly lower in the top stack location due to the tower and manifolding design, as well as the expectation that the top stack will be slightly warmer than the bottom stack. As such, the high anode dP stacks were placed in the bottom position (Stacks -001 and -002) and Stack -006 were placed in the top position. This way, the stack characteristics are utilized to improve in-module stack-to-stack performance. The stack cathode dP test results for cold flow testing are as shown in Figure 3-57.

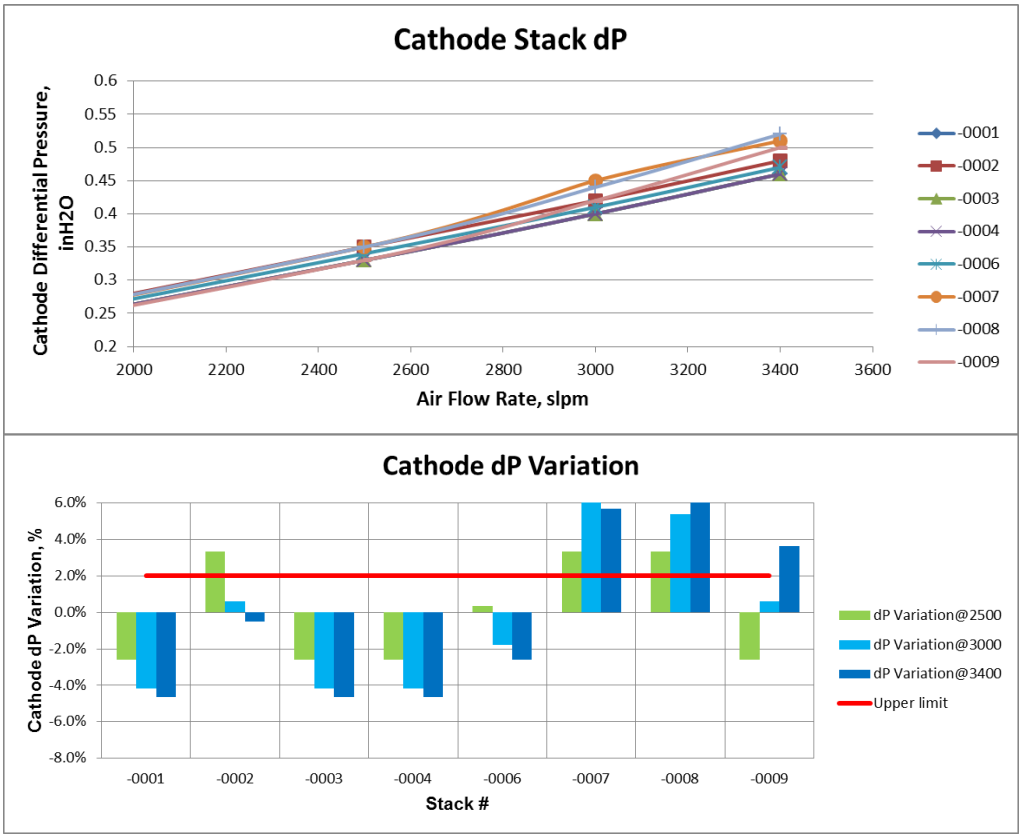

Figure 3-57. Cathode Pressure Drop (dP) (Cold Flow) Comparison for Module 1 Stacks

Air is both fed and exhausted from the bottom of the module towers. As such, it is expected that air flow will be slightly higher in the top stack location due to the tower and manifolding design. As such, the high cathode dP stacks were placed in the top position (Stacks -007 and -008) and Stacks -001, -003, and 004 were placed in the bottom position. This way, the stack characteristics are utilized to improve in-module cathode flow distribution. Stack -002 exceeded the anode dP design limit and Stacks -007 and -008 exceeded the cathode dP design limit. However, at this point, additional engineering and flow adjustment features are not deemed necessary.

Additionally, all stacks met the stack height acceptance criteria as shown in Figure 3-58. The data shown is the total height (average of the four corners) compared to the upper and lower specification limits. The chart also shows the contribution of cell height to the total stack height. In the large area stack design, the cell thickness makes up approximately 12% of the overall stack height including stack end plates.

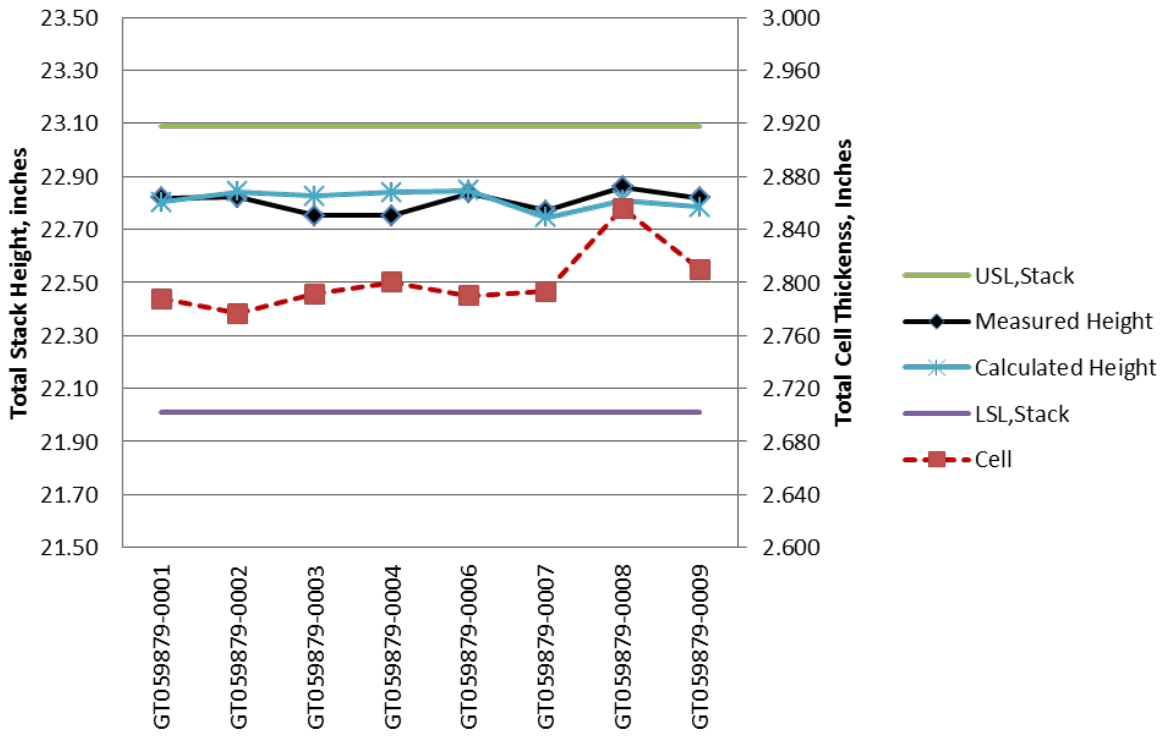

Figure 3-58. Comparison of Stack Height and Cell Thickness for Module 1 Stacks

Overall, 8 stacks passed all the performance criteria set in the factory acceptance test plan.

Set 1 (Module 1 Stacks) – (Stacks GT059879-0001 to -0010)

For the Set 1 (Module 1) 120-cell stacks, Figure 3-59 illustrates the electrochemical performance aligned on a single time-plot. At ~15 hours, the stacks were first electrically loaded, and then run through fuel utilization steps (50 through 75%). This was followed by a 50-hour hold at a system representative condition (160 Amperes, 291 mA/cm^2) to demonstrate stack stability.

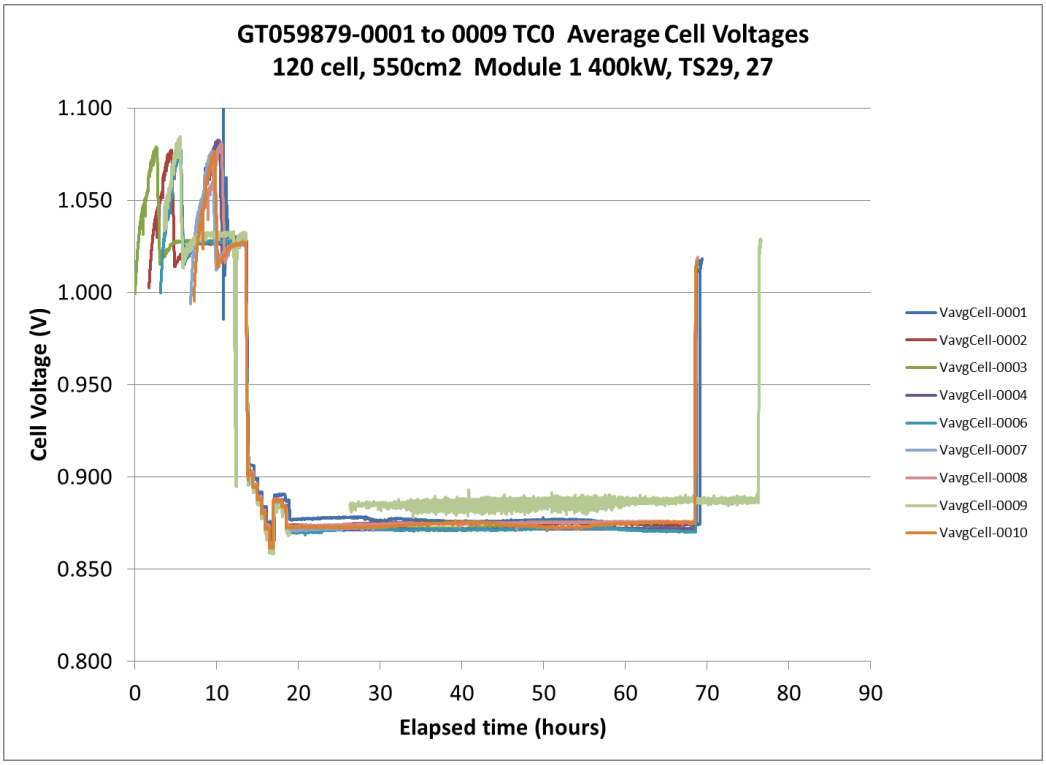

Figure 3-59. Average Cell Voltage during Fuel Utilization Testing for Stacks GT059879-0001 to -0010 with -005 excluded

The average cell voltage results are shown numerically in Table 3-12 and graphically in Figure 3-60 for comparison. The stack performance compares well, with all results within 7 mV or <1% variation between the highest and the lowest performing stacks.

Table 3-12. Performance of 120-cell Stacks built for Module 1 (Set 1)

Stack #	OCV	OCV σ (mV)	75%uf	75%uf σ (mV)	75%uf σ min cell	Ph1	Ph1 σ (mV)	VPS GR	VPS GR σ (mV)
Req't	> 1.0 V (min)		> 840 mV (min)		> 800 mV (min)				
-0001	1.029	2.3	0.866	5.3	0.851	0.887	3.7	0.877	4.0
-0002	1.027	2.5	0.864	4.9	0.854	0.885	4.1	0.875	4.6
-0003	1.027	2.3	0.862	5.6	0.850	0.883	4.5	0.872	4.5
-0004	1.028	2.4	0.862	5.3	0.849	0.882	3.7	0.871	4.2
-0006	1.027	2.0	0.859	5.8	0.847	0.881	3.8	0.870	4.4
-0007	1.026	2.0	0.861	5.3	0.846	0.882	3.5	0.871	4.1
-0008	1.028	1.7	0.864	5.5	0.849	0.884	3.8	0.873	4.5
-0009	1.032	1.8	0.860	6.7	0.840	0.880	4.4	0.870	5.0
-0010	1.027	2.5	0.862	6.4	0.843	0.884	4.4	0.873	5.1

For the Set 1 deliverable stacks, the cell voltage deviation (σ) was found to range from 1.7 to 2.5 mV at open circuit condition and between 4.0 and 5.1 mV under the System Gas / VPS Gas Replacement (VPS GR) condition representative of the 200 kW system.

.

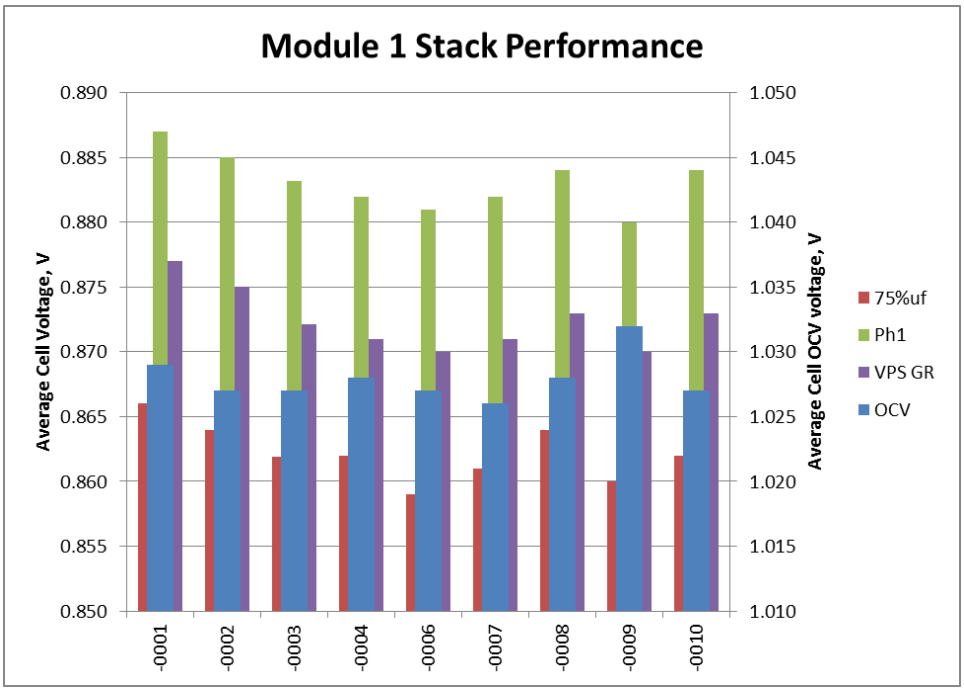

Figure 3-60. Performance Comparison of 120-cell Stacks built for Set 1 (Module 1)

The stacks had cold leakage measurements as shown in Table 3-13. Cross leakages were all less than 12,000 sccm which is the pass/fail criteria.

Table 3-13. Leakage Rates (sccm – air) of Stacks built for Module 1

	Raw Data			Calculated	
Stack #	Cathode Total	Anode Total	Both	Anode	Cross
-0001	8,360	9,870	8,470	4,990	4,880
-0002	7,840	9,270	6,230	3,830	5,440
-0003	6,080	8,480	5,160	3,780	4,700
-0004	8,370	10,160	4,970	3,380	6,780
-0006	7,380	16,270	14,640	11,765	4,505
-0007	9,030	11,830	8,590	5,695	6,135
-0008	9,280	11,400	8,920	5,520	5,880
-0009	12,460	15,490	10,390	6,710	8,780
-0010	10,800	12,480	7,640	4,660	7,820

Within each stack module, 8 deliverable stacks must work together. As anode and cathode flow paths are all in parallel, both anode and cathode pressure drop characteristics must be similar. Less than 2% dP variation at 2100 SLPM and 3400 SLPM respectively is a design target. To obtain accurate data related to stack pressure drop, each stack is cold flow tested after

conditioning with a large flow rate of air. Figure 3-61 shows a comparison of the stack anode side pressure drop. The results are shown for a variety of air flow test points.

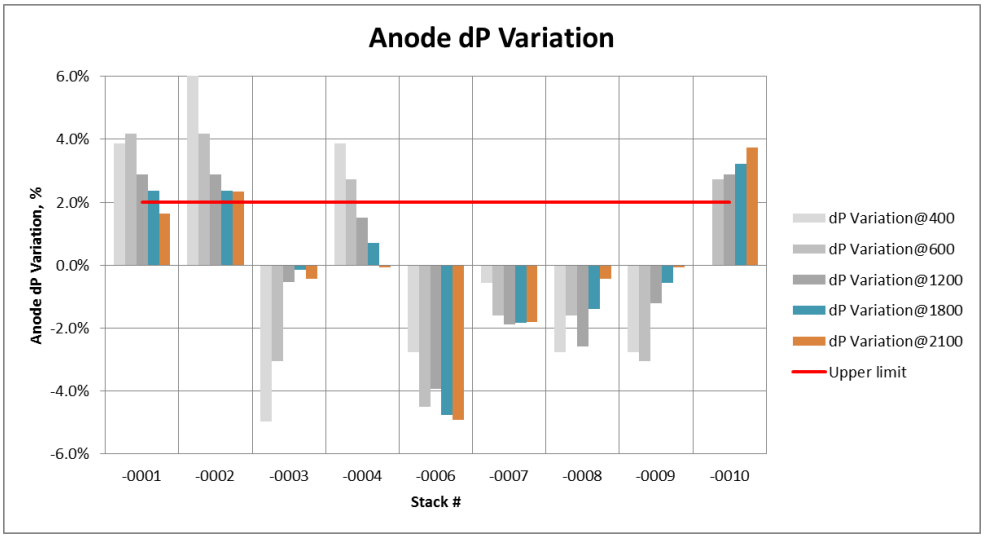

Figure 3-61. Anode Pressure Drop (dP) (Cold Flow) Comparison for Module 1 Stacks

Stack results of interest include Stacks -010, -001 and -002 with high dP and Stack -006 with low dP. For the stack module, fuel is both fed and exhausted from the bottom of the module towers. It is expected that fuel flow will be slightly lower in the top stack location due to the tower and manifolding design, as well as the expectation that the top stack will be slightly warmer than the bottom stack. Therefore, the high anode dP stacks (Stacks -010, -001 and -002) were placed in the bottom position, and Stack -006 (if utilized) was placed in the top position. That way, the stack characteristics are utilized to improve in-module stack-to-stack performance.

The stack cathode dP test results for cold flow testing are as shown in Figure 3-62.

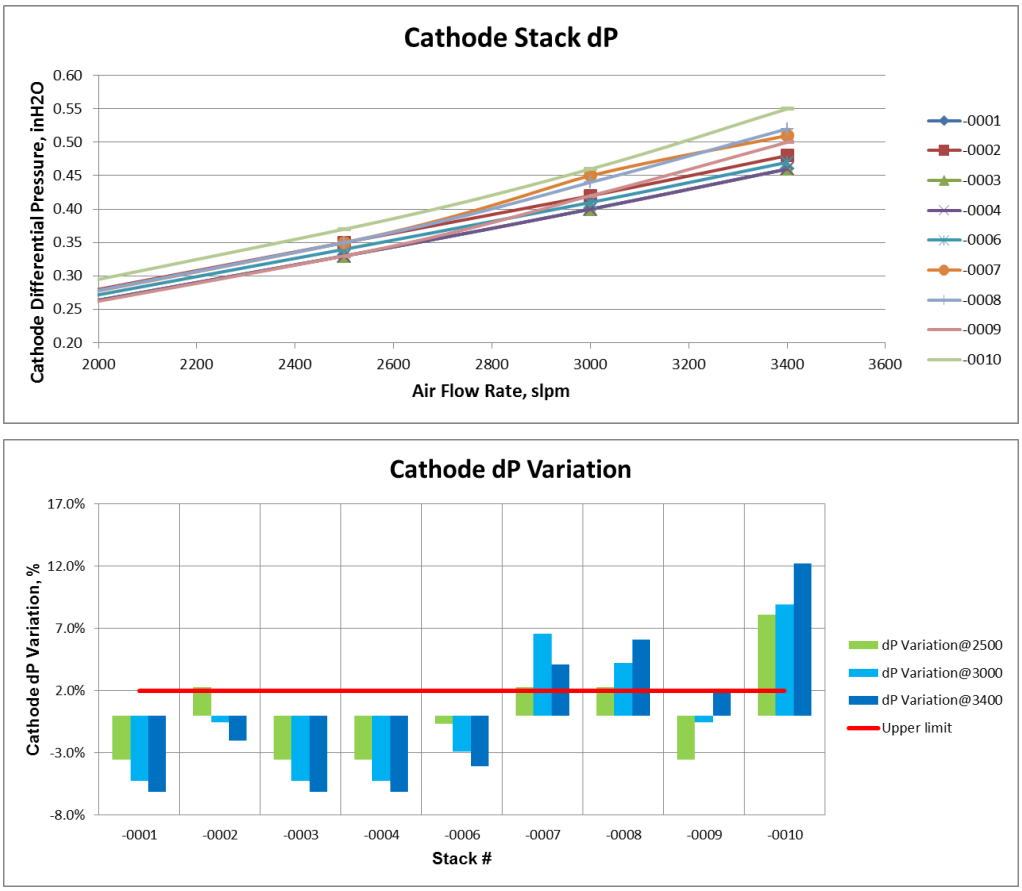

Figure 3-62. Cathode Pressure Drop (dP) (Cold Flow) Comparison for Module 1 Stacks

Air is both fed and exhausted from the top of the stack towers. As such, it is expected that air flow will be slightly higher in the top stack location due to the tower and manifolding design. Therefore, the high cathode dP stacks (Stacks -007 and -008) were placed in the top position and Stacks -001, -003, and 004 were placed in the bottom position. Stack -0010 would also be placed in the top location, although the anode dP characteristic is more important and overrides this logic. That way, the stack characteristics are utilized to improve in-module cathode flow distribution. Stacks -002 and -010 exceeded the anode dP design limit and Stacks -007, -008, and -010 exceeded the cathode dP design limit. However, at this point, additional engineering and flow adjustment features are not deemed necessary.

Additionally, all stacks met the stack height acceptance criteria as shown in Figure 3-63. The data shown is the total height (average of the 4 corners) compared to the upper and lower specification limits. The chart also shows the contribution of cell height to the total stack height. In the large area stack design, the cell thickness makes up approximately 12% of the overall stack height including stack end plates.

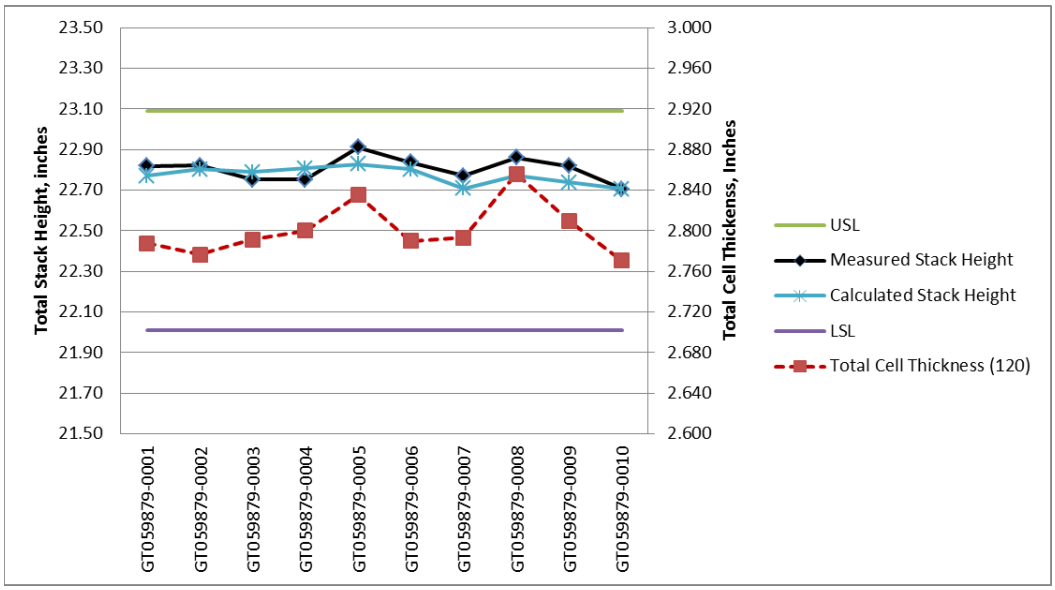

Figure 3-63. Comparison of Stack Height and Cell Thickness for Module 1 Stacks

Overall, 9 stacks passed all the performance criteria set in the factory acceptance test plan. Eight stacks will be selected for the Module 1 build with 1 stack reserved as spare. Figure 3-64 illustrates the tentative Module 1 build configuration under review.

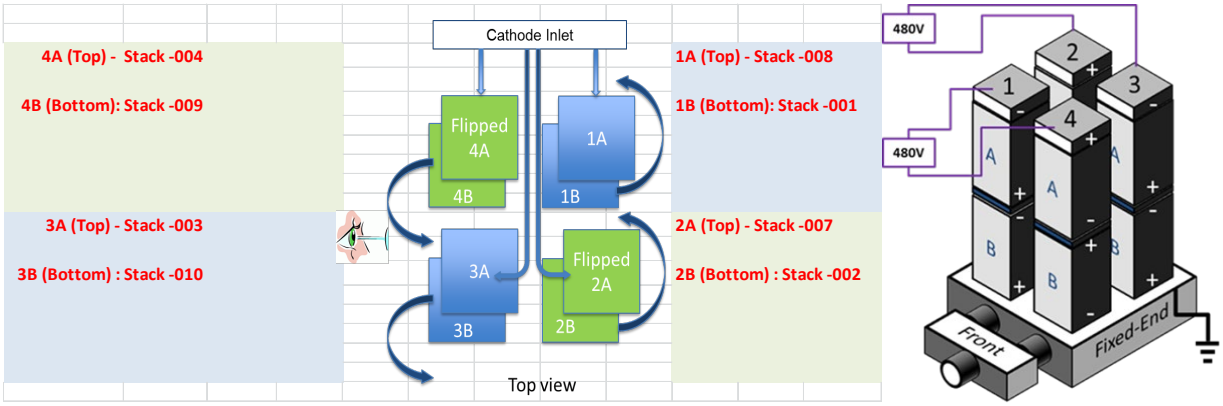

Figure 3-64. Module 1 Stack Build Configuration (Tentative)

Towers 2 and 4 contain flipped stacks (anode or negative terminal down) with the A-position denoting a top location in each tower, and the B-position the lower position.

Set 2 (Module 2) Stacks – (Stacks GT060322-0001 to -0008)

As of September 30, 2017, all eight (8) of the required deliverable stacks for Set 2 (Module 2) were been built, QC tested and delivered to Danbury, CT for stack module build. As noted in the stack part number, a new part number (GT060322) was utilized to highlight some subtle technology changes introduced with the stacks planned for Module 2. These changes include: a) the base cathode flow field metal (noting that this is a coated part) changing from Sanergy HT to SS441 and b) the anode flow field metal changing from SS444 (UNS44400 by Alegheny USA) to SS444 (UNS44400 by Aperam – France (K44)). These metals have been previously

characterized and stack tested by FuelCell Energy in technology stacks. In addition, a 16-cell technology stack (GT057235-0131) is currently running matching the complete GT060322 design configuration. This result is as reported in the next report section.

As identically tested per Set 1 stacks, the 120-cell Set 2 stacks were first electrically loaded, and then run through fuel utilization steps (50 through 75%). This was followed by a 50 hour hold at a system representative condition (160 Amperes, 291 mA/cm^2). This is as shown in

Figure 3-65 and

Figure 3-66.

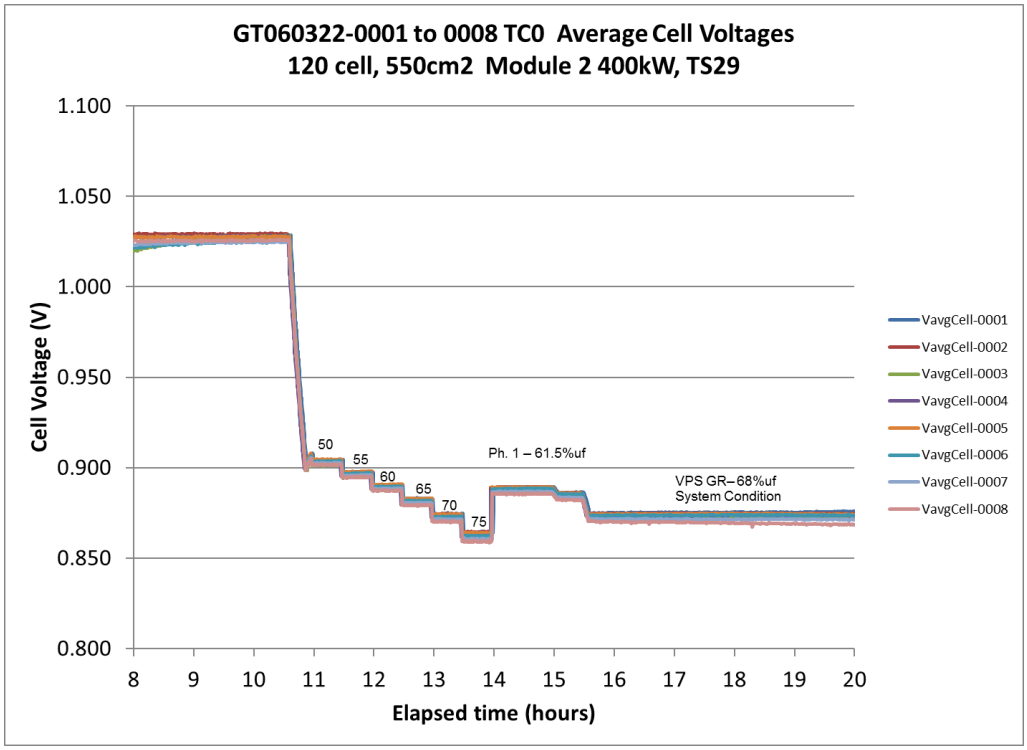

Figure 3-65. Average Cell Voltage during Fuel Utilization Testing for Stacks GT60322-0001 to -0008 (Close-Up)

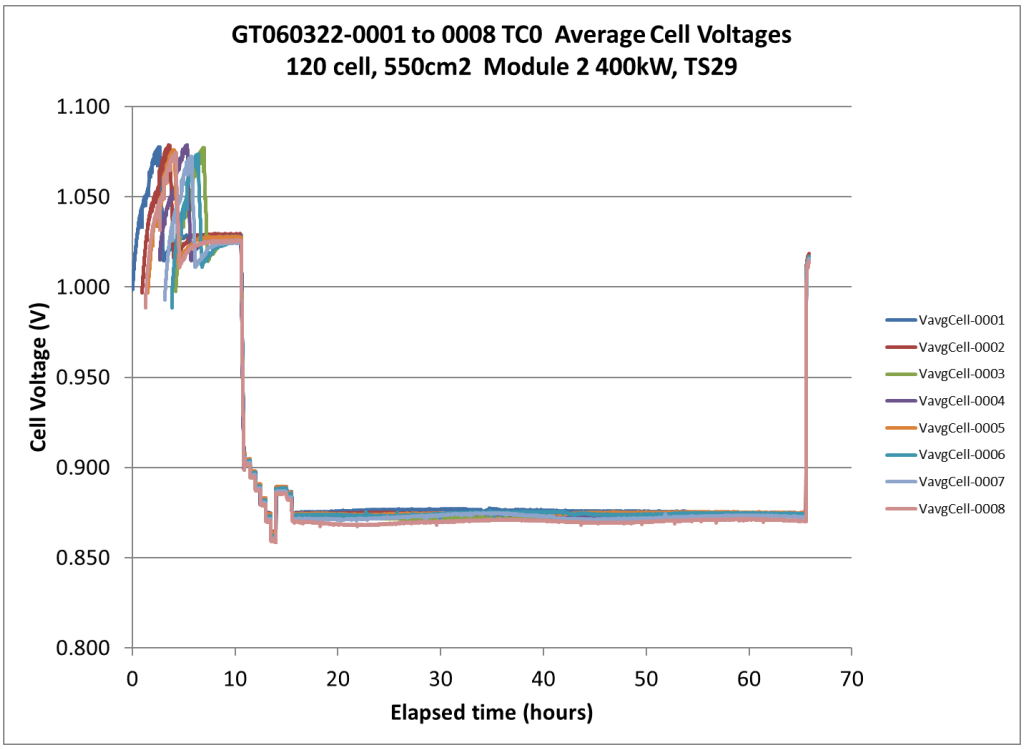

Figure 3-66. Average Cell Voltage during Fuel Utilization Testing for Stacks GT60322-0001 to -0008

The average cell voltage results are shown numerically in Table 3-14 and graphically in

Figure 3-67 for comparison. The stack performance compares well, with all results within 5 mV or <1% variation between the highest and lowest performing stacks at VPS GR or System Gas condition.

Table 3-14. Performance of 120-cell Stacks built for Set 2 (Module 2)

Stack #	OCV	OCV σ (mV)	75%uf	75%uf σ (mV)	75%uf σ min cell	Ph1	Ph1 σ (mV)	VPS GR	VPS GR σ (mV)
Req't	> 1.0 V (min)		> 840 mV (min)		> 800 mV (min)				
-0001	1.028	2.0	0.865	4.8	0.862	0.886	3.8	0.875	4.2
-0002	1.029	1.7	0.864	5.4	0.851	0.886	4.0	0.874	4.4
-0003	1.028	2.1	0.861	5.9	0.839	0.884	4.2	0.872	4.5
-0004	1.028	1.8	0.861	4.5	0.849	0.884	3.3	0.874	3.6
-0005	1.028	2.1	0.864	4.6	0.851	0.886	3.1	0.874	3.5
-0006	1.025	2.2	0.862	4.6	0.853	0.885	3.1	0.874	3.4
-0007	1.025	2.8	0.860	5.0	0.847	0.883	3.5	0.872	3.8
-0008	1.026	2.9	0.859	4.2	0.845	0.882	4.1	0.870	4.6

For the Set 2 deliverable stacks, the cell voltage deviation was found to range from 1.7 to 2.9 mV at open circuit and between 3.4 and 4.6 mV at VPS GR (System Gas) test conditions, a slight improvement versus the Set 1 stacks

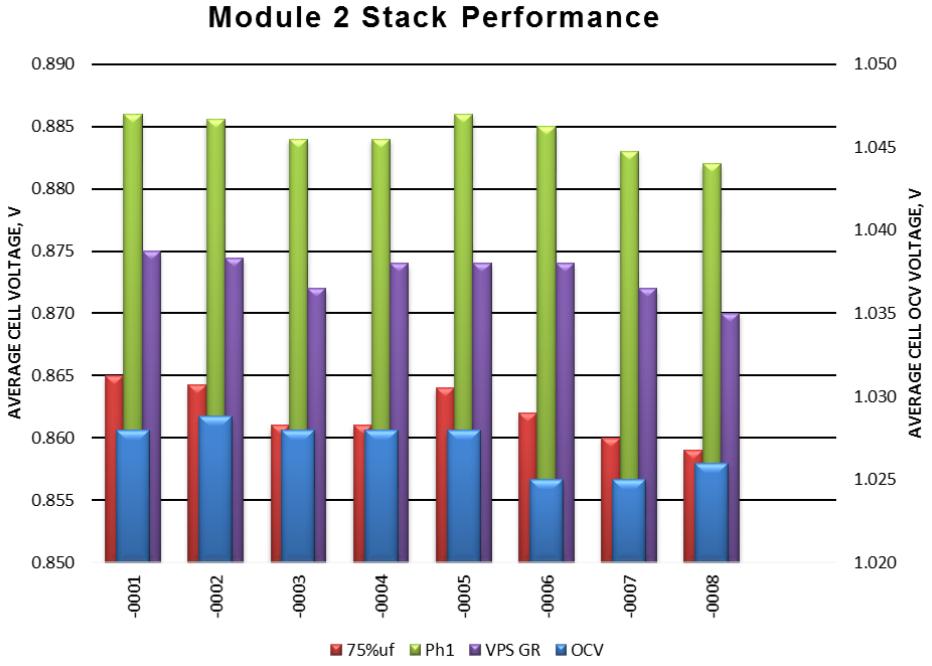

Figure 3-67. Performance Comparison of 120-cell Stacks built for Set 2 (Module 2)

These stacks had cold leakage measurements as shown in Table 3-15 with calculated cross leakage all less than 12,000 sccm.

Table 3-15. Leakage Rates (sccm – air) of Stacks for Set 2 (Module 2)

	Raw Data			Calculated		
	Cathode total	Anode Total	Both	Cathode	Anode	Cross
-0001	10,200	9,610	8,260	4,425	3,835	5,775
-0002	7,830	7,830	5,540	2,770	2,770	5,060
-0003	11,410	11,300	9,660	4,885	4,775	6,525
-0004	9,700	10,280	9,290	4,355	4,935	5,345
-0005	9,800	9,030	8,210	4,490	3,720	5,310
-0006	11,530	10,730	9,670	5,235	4,435	6,295
-0007	12,000	11,002	10,590	5,794	4,796	6,206
-0008	8,670	10,980	8,780	3,235	5,545	5,435

As with Module 1, Module 2 stacks must also work together as a single operating unit, and thus anode and cathode pressure drop characteristics must be similar with preferably less than 2% (upper) dP variation as design target.

Different from the Module 1 set of stacks, all Module 2 stack were re-flow tested in Danbury. Due to the long time difference (multiple months) between the early and late stack measurements in Calgary for the production stacks, it is believed that the Danbury data is more accurate and is the focus for technical discussion here. The data for 8 of 8 stacks is as shown in Figure 3-68, where low flow points are shown (down to the left, for Reynolds number matching) as well as high flow points (dP matching) points. Due to the improved resolution and matching of Calgary's test conditions and current stack qualification methodology, the higher flow points where analysis of stack flow differences.

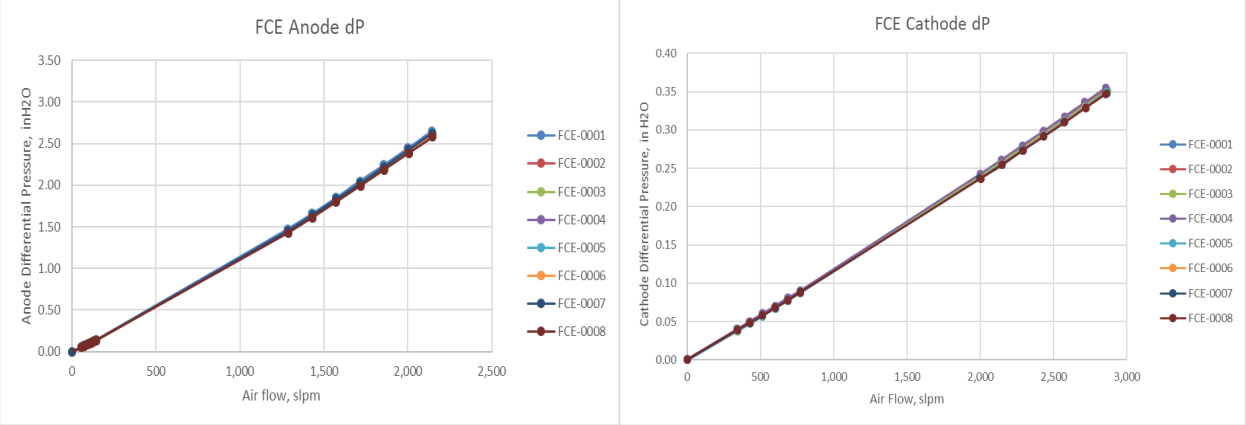

Figure 3-68. Anode and Cathode Stack Pressure Drop Characteristics for Set 2 Stacks

The final comparative analysis is as shown in Figure 3-69. All stacks met the set upper limit requirement of no more than 2% higher than the set mean.

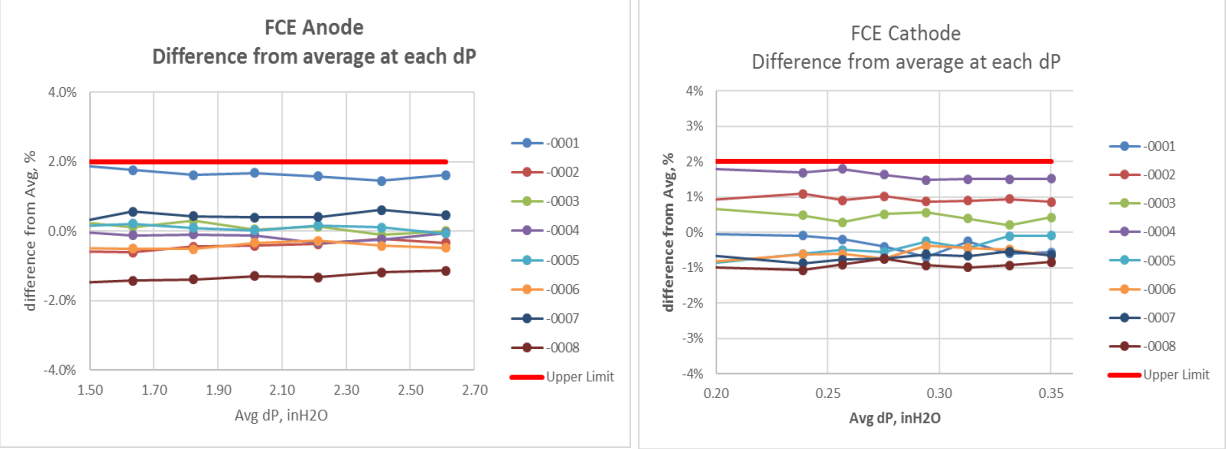

Figure 3-69. Anode and Cathode Stack Pressure % Difference in Drop Characteristics for Set 2 Stacks

For the anode pressure drop, a detailed stack-to-stack comparison at 2.6 inches water column pressure (647 Pa) or 2140 SLPM - noted that Stack 1 had the highest pressure drop (1.6% above mean) and Stack -008 had the lowest at 1.1 % below mean. For the cathode side pressure drop at 0.35 inches water column (87 Pa) or 2860 SLPM, Stack -004 had the highest pressure drop at +1.5% and Stack -008 had the lowest at -0.8% from mean. A tabular summary of this information is as shown in Figure 3-70 following with all stacks acceptable.

	Cold testing		
Stack #	Stack leakage (sLpm) -Calgary data	Between stacks fuel dP variation at same cold flow on Air	Between stacks AIR dP variation at same cold flow on Air
Acceptance	Stack cross leak <12 SLPM at 14 in*H2O	<2% dP variation (from mean of set) at~ 2140 SLPM AIR	<2% dP variation (from mean of set) at ~2860 SLPM AIR Danbury Testing
-0001	5.8	+1.6% (highest)	-0.6%
-0002	5.1 (min)	-0.3%	+0.9%
-0003	6.5 (max)	+0.0%	+0.4%
-0004	5.3	-0.1%	+1.5% (highest)
-0005	5.3	-0.1%	-0.1%
-0006	6.3	-0.5%	-0.7%
-0007	6.2	+0.5%	-0.6%
-0008	5.4	-1.1% (lowest)	-0.8% (lowest)

(-) denotes more flow, less dP

Figure 3-70. Tabular Stack Set 2 Cross Leak and Pressure Drop Comparison

All stacks also met the stack height acceptance criteria.

Figure 3-71 shows the measured stack height (average of the 4 corners) compared to the upper and lower specification limits. In addition, the chart also shows the contribution of cell height to the total stack height.

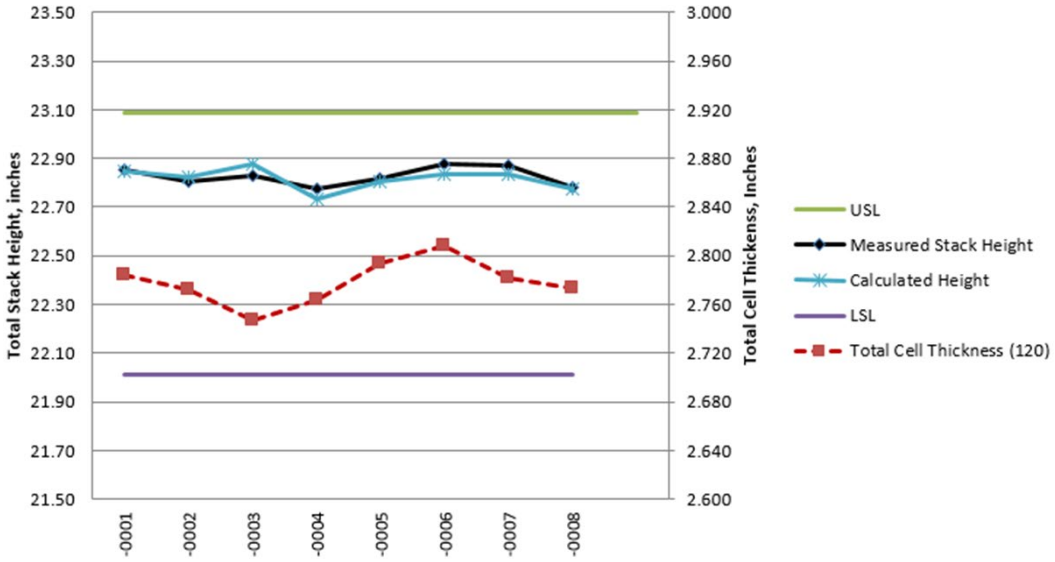

Figure 3-71. Comparison of Stack Height and Cell Thickness for Module 2 Stacks

Overall, all 8 stacks passed all performance criteria set in the factory acceptance test plan. Figure 3-72 illustrates the Module 2 stack build configuration completed. As a reminder, all of these stacks contained the GT060322 part number.

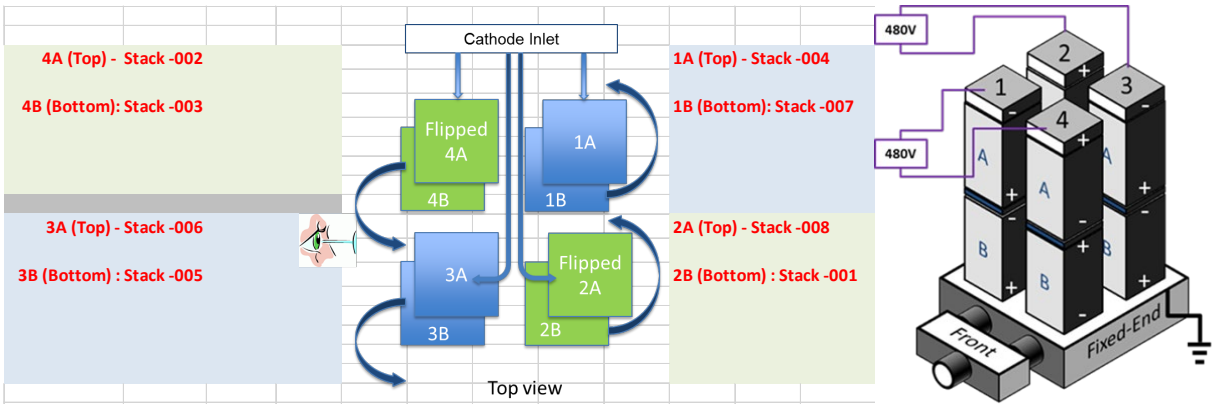

Figure 3-72. Module 1 Stack Build Configuration (Tentative)

Towers 2 and 4 contain flipped stacks (anode or negative terminal down) with the A-position denoting a top location in each tower, and the B-position the lower position. The team looks forward to system testing with these high quality stacks.

Technology Stack – GT057235-0131

A 16-cell technology stack matching the Module 2 through 4 design configuration (GT060322 design configuration) was tested. The performance degradation rate was <1% /1000h which is normally expected.

The initial Thermal Cycle 1 (TC1) and TC2 steady-state performance is as shown in Figure 3-73.

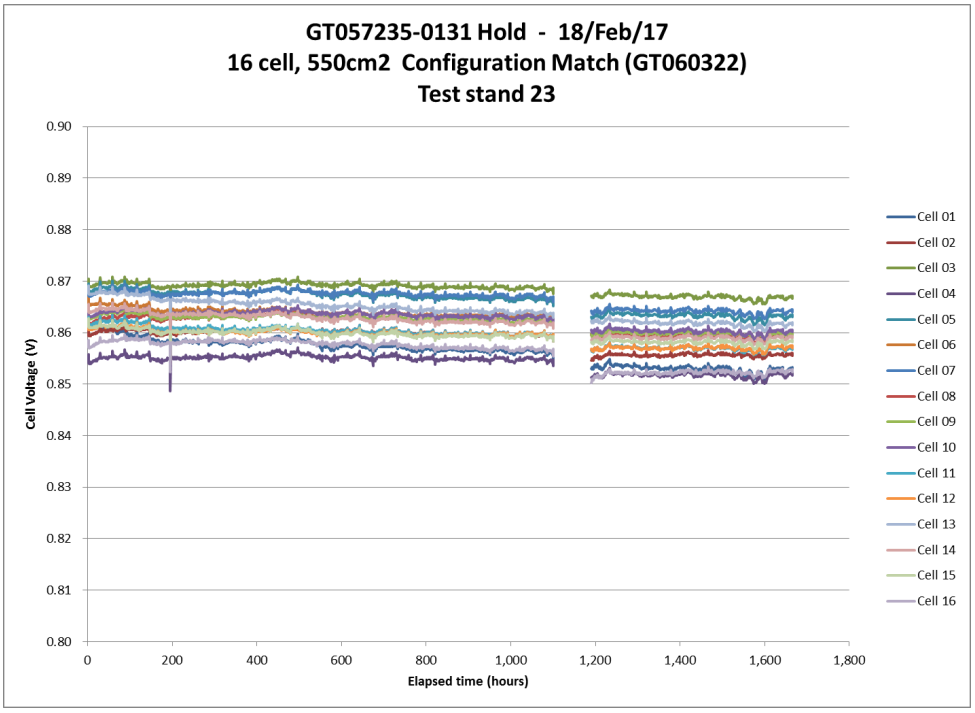

Figure 3-73. Performance Stability of Stack GT057235-0131 During Steady State Testing

The stack test had accumulated 1099 hours (TC1 hold) with performance degradation rate of 0.23 % (2.0 mV) / 1000 hours. Then a hard test stand shutdown occurred including the loss of mechanical load on the stack, caused by a power outage with a failed transfer switch breaker which was not able to supply any power to the test stands for approximately 2 hours.

After the facility repair, the stack was restarted and the stack continued testing at the system gas condition. The long term testing conditions are a stack current of 160 A (291 mA/cm^2), fuel utilization of 68%, air (oxidant) utilization of 15%, stack environment temperature of 690 ℃, and fuel composition of 44.43% H_2, 6.37% CH_4 (Natural Gas), 23.26% N_2, and 25.94% H_2O (aligning to that of the FCE SOFC system).

An additional 16-cell technology stack was tested matching the Stack Set 2 design configuration (GT060322). The initial Thermal Cycle 1 (TC1) and TC2 steady-state performance is as shown in

Figure 3-74.

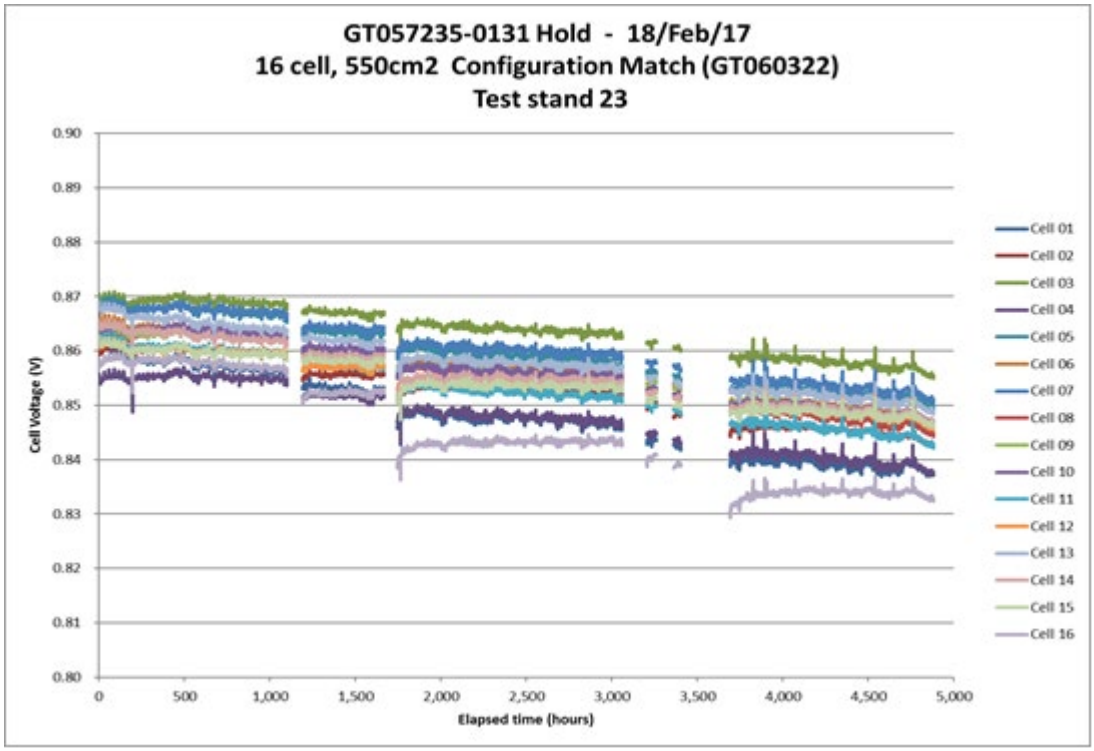

Figure 3-74. GT057235-0131 Degradation Performance

In the first 1180 hours in TC1, the degradation performance was 0.22 % (1.9 mV) / 1000 hours and then a hard test stand shutdown occurred including the loss of mechanical load (very concerning for the physical and electrical contact within the stack) on the stack caused by a power outage with a failed transfer switch breaker, which was not able to supply any power to the test stands for approximately 2 hours. From hour 1200 to 4480, the stack experienced quite a number of electrical unloads due to issues with the electronic load, until the load was replaced at hour 3693. After this point, the test ran without fault, until the stack was shutdown to accommodate another technology stack. From hour 1200 to 4480, the stack demonstrated a 0.43% (3.7 mV) / kh degradation rate, however, a significant portion of the voltage loss occurred due to the hard transient events and interrupts. In addition, the loss of mechanical top load on the stack may have aggravated and caused increased degradation compared to what the unit cell technology is capable of. For additional background, the stack test is at the system gas condition and stack current of 160 A (291 mA/cm^2), fuel utilization of 68%, air (oxidant) utilization of 15%, stack environment temperature of 690 ℃, and fuel composition of 44.43% H_2, 6.37% CH_4 (Natural Gas), 23.26% N_2, and 25.94% H_2O (aligning to that of the FCE SOFC systems).

Set 3 Stacks – (Stacks GT060322-0009+):

Purchase orders were issued for anode and cathode flow fields. QC will take place for the flow fields in July and August 2017. Stack builds will commence in late August 2017.

During July and August, 1107 cells total were in process with 805 at the tape stage (after tape cast), and 302 cells at fired half-cell. Stack builds were planned to commence in late August.

However, DOE project management decided to halt and place a hold on this effort. Thus, for the 200 kW system, only one replacement stack was available (GT059879-0006).

Stack Build Process Improvements

Up until May 2017, stacks were built on a mobile scissor cart that was not exactly parallel to the floor. Without a perfect reference, it was suspected that this may allow the stack layers to slightly shift towards the low side as the stack was built taller. Additionally, alignment posts aged and became less true over time. A step stool was also required to allow the stack builder to work at a necessary ergonomic height for the highest regions of these 120-cell stacks (scissor cart could not go lower once at its stop). This was not ideal and caused undue operator stress. Previously, once a stack was built, it was wheeled away and turned 90 degrees to be placed under the pre-compression stand several feet away. Centering the stack with the pneumatic cylinder piston was difficult since the cart wheels are not very agile. An additional scissor jack was used to level the cart more accurately prior to stack pre-compression. This drove the need for process and equipment improvement.

Stack build room improvements were rolled out and integrated after Module 2 - Stack 5. The addition of a stationary scissor lift table allowed the stack to be built at a constant ergonomic working height. This robust table provides a level and stable working platform to ensure repeatable and consistent stack builds (as shown in Figure 3-75). New alignment build posts (inside stack manifolds) with heavier-duty joining threads were manufactured consistently allowing stacks to be built straighter throughout the entire height. Metal rails were added to allow a smooth short transfer of the stack to the stack pre-compression stand.

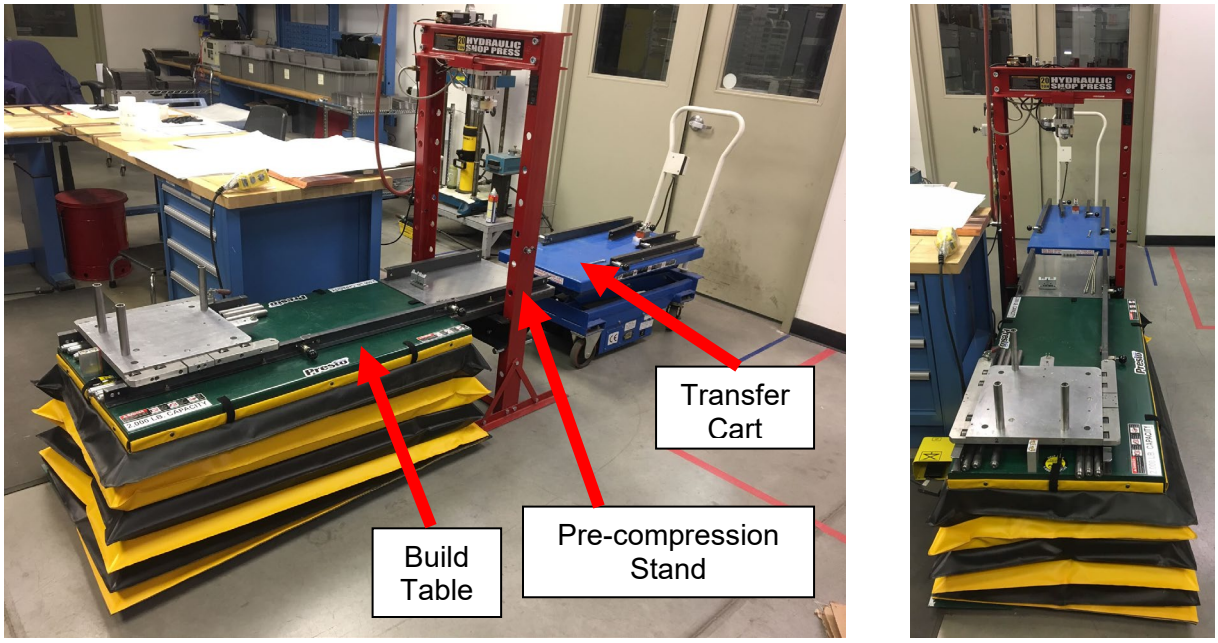

Figure 3-75. Stack Build Setup Improvement

Additionally, the pneumatic piston cylinder now is allowed to move to locate the true center of the stack before compressing to full pressure (Figure 3-75). This ensures that the stack is compressed vertically.

Figure 3-76. Stack Mechanically Loaded in Pre-compression Stand

Once pre-compression is complete, the stack is rolled over to the scissor cart opposite side of the build table. The table and cart were strategically aligned with the door leading to the test stand area for installation. Operator feedback with the new set-up has been very good.

4. PROTOTYPE SYSTEM TESTING

The objective of this task is to fabricate, install, and test the 200 kWe SOFC prototype system. The work will be divided in subtasks as follows:

The 200kW prototype system testing began after installation and completion of all commissioning activities at the host site. The test outline is provided below:

i. Enable plant
ii. Purge all subsystems with air/nitrogen as required
iii. Initiate heat-up sequence and monitor progressions into subsequent steps
    a. Verify required equipment/instruments turn on/off at the appropriate steps
iv. Once Hot Standby is entered, verify all required conditions are met
v. Enter power generation and monitor load ramp to 100% (or other load if desired)
    a. Hold for ≥ 5000 hours of steady-state operation
    b. Respond to alarms and system trips as necessary
vi. Once test duration is complete, decommission the plant
    a. Ramp down electrical load to zero

Cooldown the system to ambient conditions

MODULE POWER BLOCK (MPB) ASSEMBLY

Installation of the HV and LV cabinets, required the thermocouple and voltage lead harnesses to be routed through the penetrations in the vertical wall of the base. The catalytic air preheater (CAPHx) subassembly weldments and ducts were welded. Accurate placement of the ducts were critical to allow the process piping interfaces to be located properly. Once the welding was completed, the CAPHx assembly was insulated and installed.

Figure 4-1 CAPHx Subassembly Weldments

The pressure transducer rack assembly, which consists of a welded frame, pressure transducers (PTs) and pressure differential transducers (PDTs), were installed on the welded frame as a subassembly on the bench before it was installed on the module. Plumbing and wiring was then completed, which can be seen in

Figure 4-2.

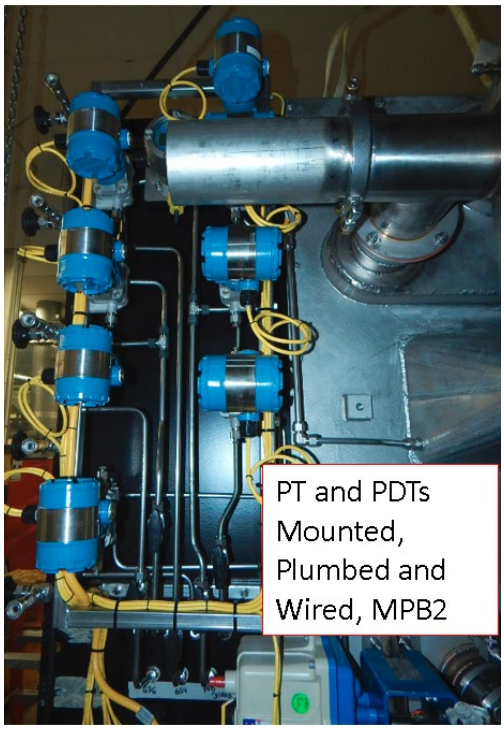

Figure 4-2 Pressure Transducer Rack

The recuperator was installed and the water vaporizer and anode recycle blower systems were mounted. Quad Tower Assembly 2 (QTA2) was stacked and compressed before being integrated onto the MPB2 base. Voltage leads were routed from the stack towers to the terminal blocks, which reside beneath the deck insulation and connect to the VL harness. On-cell thermocouples and module environment thermocouples were routed through the deck plate and plugged into the TC wire harness in the lower purgatory zone. Module interior anode piping spools were field fit, bench welded and installed. The cathode inlet distributor and piping spools were also field fit, bench welded and installed. Hot bus bars were installed and routed through the vertical purgatory zone and connected to the bushing assemblies, which serve as the DC connections for the EBoP DC power interface. A module instrumentation checkout was completed, then the enclosure was installed and a final leak test performed. The insulation kit, was installed as soon as the final tests were completed. As shown in

Figure 4-3, insulation for the Anode Recycle System, which includes the anode recycle blower, steam generator and associated piping, was completed by an outside contractor.

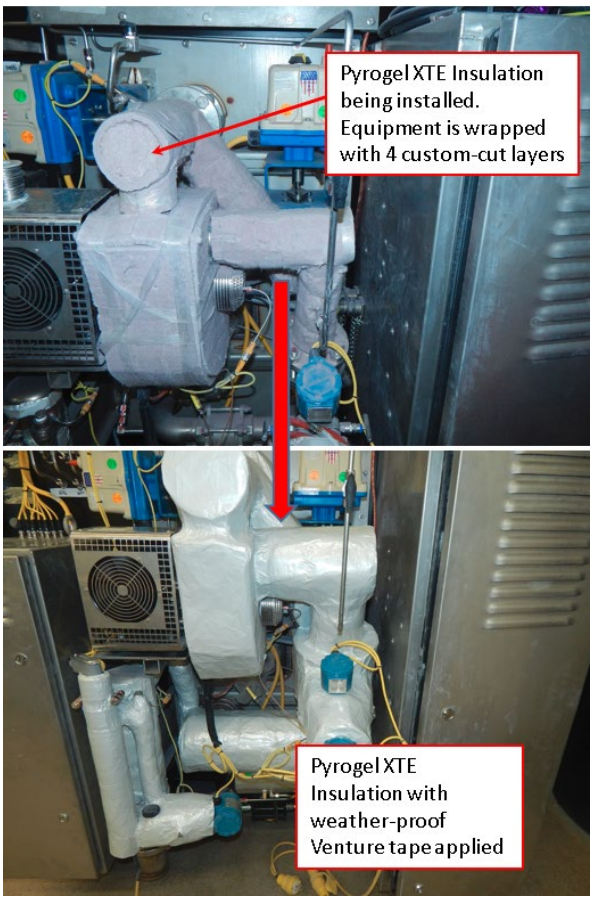

Figure 4-3 Insulated Anode Recycle System and Water Vaporizer

Figure 4-4 Completed Modular Power Block 1

SKID ASSEMBLY

Integrating the two Module Power Blocks onto the skid required a crane and a heavy duty forklift. Once all assembly and check out activities for both modules were completed, Industrial Riggers from Waterbury, CT was engaged to complete the modules transportation and placement onto the skid. The riggers transported the modules from the loading dock to the plant using the heavy duty forklift. Swivel hoist rings, shackles and slings were installed to connect each module to the hook on the crane. The crane picked up and placed the modules onto the skid with ease (

Figure 4-5), as all of the interface points aligned perfectly.

Figure 4-5 Module Power Black 2 (B) Integration

FCE received all parts for and fabricated the Power Conditioning Unit (PCU) as shown in Figure 4-6. The functions of the 200kW PCU include DC to AC power conversion, AC plant output power distribution and net AC plant export to the electric utility grid.

Figure 4-6 200kW Power Conditioning Unit

Final Assembly & Integration:

Both MPBs were landed onto the skid and all mechanical and electrical connections were made. Electrical loop checks and functional checks were been performed to validate proper wiring, communication, and operation of all equipment. The fully assembled 200 kW SOFC Prototype System is shown below in Figure 4-7.

Figure 4-7 Fully Assembled 200 kW SOFC Prototype System

PROTOTYPE SYSTEM TESTS

The purpose of the system testing is to advance FCE's SOFC technology towards commercialization. Factory testing will be performed in accordance with the "Stack Metric Test and Cost Estimation Guidance", included in DE-FOA-0001244 Section I-C. A test plan will be developed and submitted for DOE approval prior to the test start. The average stack operating temperature will be greater than 700°C at NOC. The experimentally-observed stack performance at NOC will be utilized as input to develop the stack and system cost Analysis under Task 5.0 [Section 11].

Summary of test plan deviations are found below. However, a detailed overview of the test plan was submitted as a topical report under this project.

PCU Commissioning Test Results:

FCE utilized field support from Princeton Power to evaluate, repair and commission the two inverters at FCE's facility, as the sensor isolation boards of both inverters were damaged during initial testing. With the help of Princeton Power's field service engineer, the root cause was determined to be leaving certain connectors on the boards in place that should have been unplugged. The sensor isolation boards were replaced and the proper connections were made. The inverters were then successfully validated by using DC power supplies and sending various power demands locally to each inverter to export power to the grid (Table 4-1); the pre-charge

assemblies for each inverter were also tested for proper operation. A Master-Master configuration for the inverters was used to allow either inverter to run without the other.

Table 4-1 Inverter A&B Power Export Results

	AC kW	VAC	AC Amps	DC kW	VDC	DC Amps	Total Losses (kW)	Effy %
INVERTER A	5	476.6	29.7	6.6	477.9	14	1.6	75.76%
	10	482.0	34.7	11.7	478.3	24.8	1.7	85.47%
	25	478.4	40.4	27.4	397.5	69	2.4	91.24%
	50	482.6	67.9	54	396.5	136.2	4	92.59%
	80	484.7	104.3	86.6	394.8	219.4	6.6	92.38%
INVERTER B	AC kW	VAC	AC Amps	DC kW	VDC	DC Amps	Total Losses (kW)	Effy %
	5	478.2	30.9	6.6	477.9	14	1.6	75.76%
	10	483.4	30.3	11.8	479.2	24.5	1.8	84.75%
	50	484.7	69.7	53.6	395.2	135.7	3.6	93.28%
	82	484.2	107	88.5	394.7	224.2	6.5	92.66%

Modbus communication from the PLC to both inverters were established and verified. Functionality and electrical loop checks to all PCU related instrumentation, such as DC and AC contactors and current transducers, were also validated. The inverters were then able to undergo a PLC automated load ramp through DC current control, equivalent to what the fuel cells would actually experience; the DC power supplies were set to a constant voltage of 400 VDC to closely mimic the fuel cells. A screenshot of the HMI is shown in Figure 4-8, where both inverters are running at 50% Load.

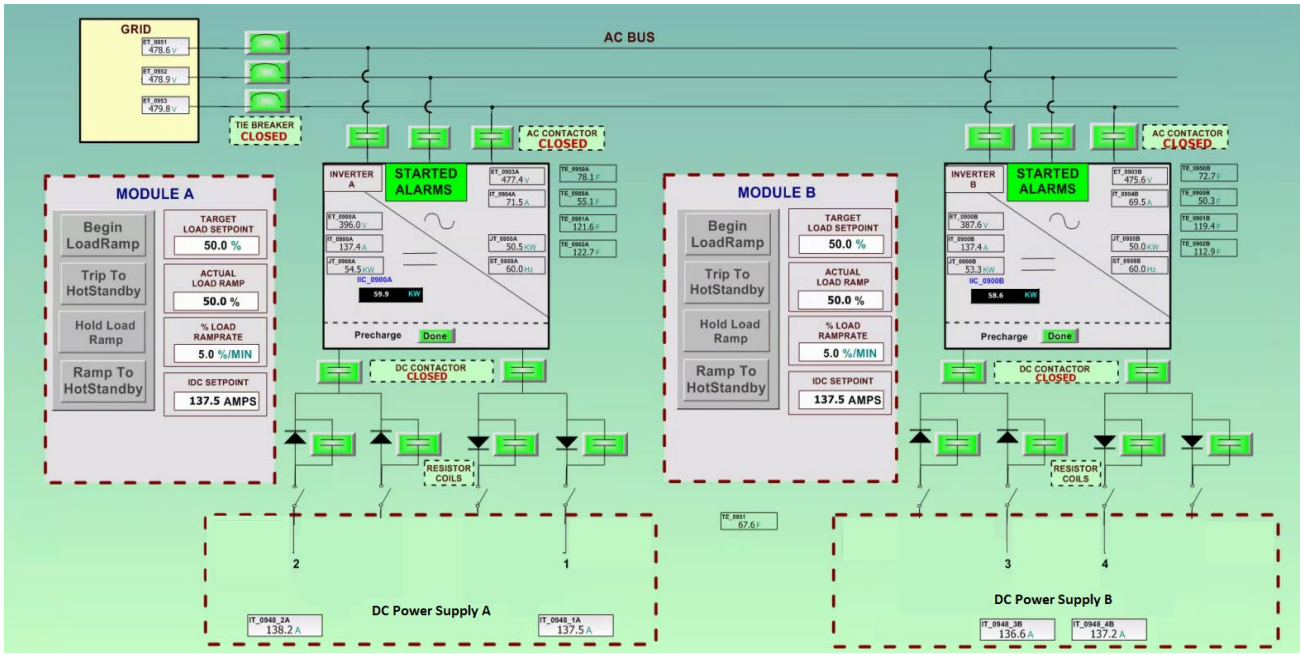

Figure 4-8 HMI Screenshot of Inverter A&B Exporting 50kW AC Each

Various trip scenarios were also performed to validate proper actions by the PLC and inverters. The following tests were performed:

- Inverter A only load ramp & trip to Cooldown (Figure 4-9 & Figure 4-10)
- Inverter B only load ramp
- Simultaneous load ramp
- Trip to ESD with both inverters on-load
- Trip to NRC on Inverter B while Inverter A continues to export power
- Trip to HSB on Inverter A while Inverter B continues to export power
- Grid-tie synchronization

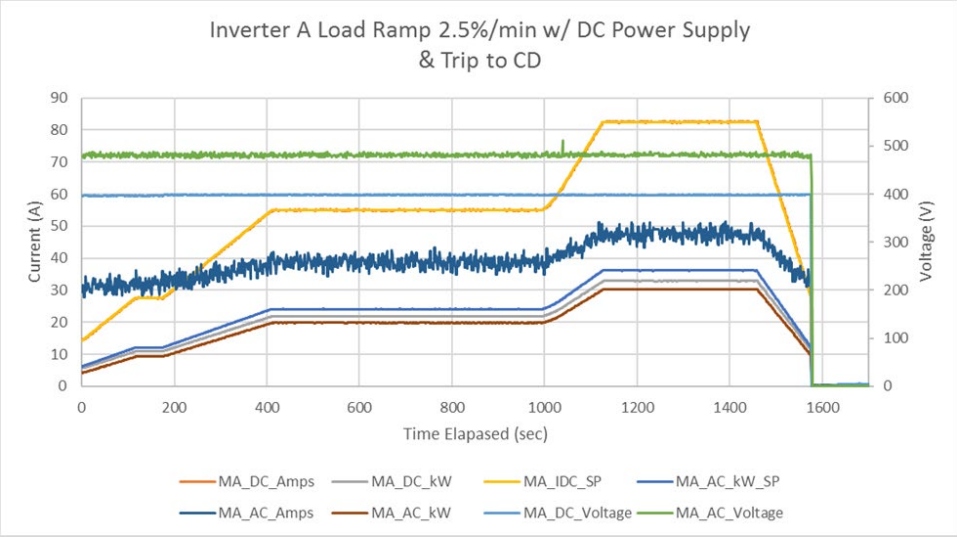

Figure 4-9 Inverter A Load Ramp & Trip to Cooldown

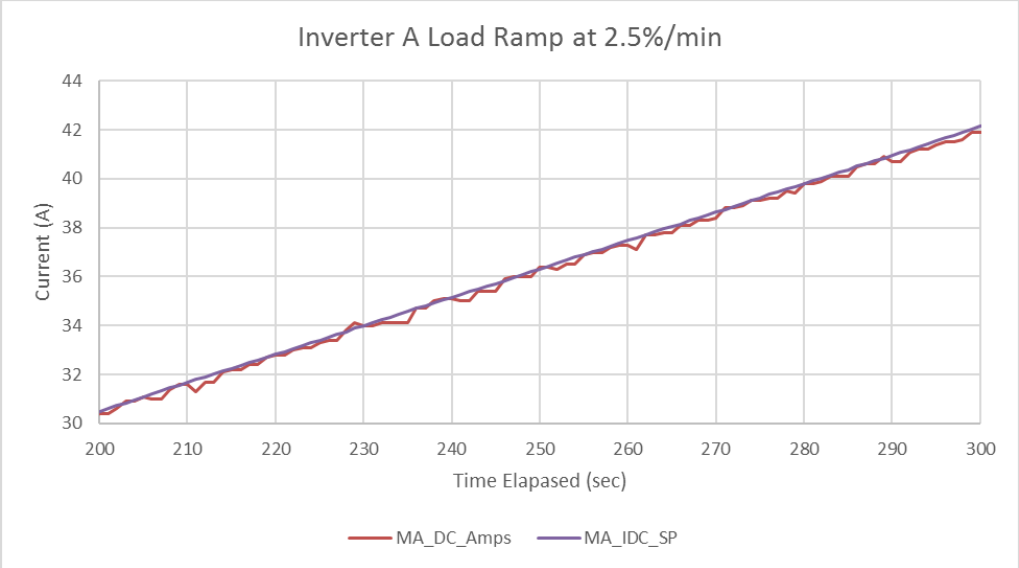

Figure 4-10 Inverter A Load Ramp – 2.5%/min

To simulate a loss of the grid network, the main disconnect to the test pad was opened while both inverters were exporting power. As a result, the plant lost 480 VAC power which caused the plant to trip resulting in zero power export. The grid-tie contactor remained closed but opened as soon as power was reestablished to the plant by closing the main disconnect. Shortly after, the inverter commanded the grid-tie to close as the grid was back online. FCE worked with Princeton Power to determine the proper settings necessary for the inverter to immediately open the grid-tie contacts per IEEE and UL standards.

Factory Acceptance Testing:

A final plant electrical loop checkout and functionality test were completed to validate all updates. This included IO configuration updates, the new cathode air purge system, upgraded water enclosure heaters and new redundant fuel shutoff valves. The cathode purge system performance was satisfactory. The set-points of the regulators were adjusted to maximize the performance of the air motor, which slightly changed the nitrogen pressure for the anode cover gas at different modes of operation. The hydrogen concentration is slightly different as a result at these various modes but is never a concern in terms of safety or performance. One of the nitrogen regulators failed open and was believed to be a defective unit. A replacement was ordered and the factory acceptance test ran as planned by adjusting the upstream regulators accordingly to cause no further delays. The replacement regulator was installed once it was received.

The factory acceptance test sequence was as follows:

1. Startup Module B
    a. Validate sequential logic and control scheme throughout heatup
    b. Enter Power Generation – 50% Load (137.5 DC Amps)
    c. Ramp down load and transition to Hot Standby
2. Hold Module B in Hot Standby and Startup Module A
    a. Validate sequential logic and control scheme throughout heatup
3. Enter Power Generation on both Module A&B and ramp to 100% Load (275 DC Amps)
4. Hold both modules at full load for one day
5. Ramp down load on both modules and transition to Hot Standby
6. Hold Module A in Hot Standby and cool down Module B
    a. Validate sequential logic and control scheme throughout cool down
7. Cool down Module A
8. Validate sequential logic and control scheme throughout cool down

The PCU factory acceptance will be broken down into five tests, as outlined below.

The PCU design underwent checkout testing to validate that it is fully capable of meeting the 200kW prototype system's design requirements. As shown in Figure 4-12, two DC power supplies were rented to simulate two 100kW MPBs for the purpose of this test and

I. Figure 4-13 shows a sketch of the proposed test setup. The two GTIB-125(1.5) inverters will be tested to validate their ability to operate at the 200kW prototype system's full load capacity. They will also be tested for the following parameters:

- Current waveform
- DC current ripple level
- Power efficiency
- Grid/System level total harmonics distortion (THD)
- Synchronization and resynchronization of paralleled inverters to comply with IEEE1547/UL1741 recommended set operating voltage, current and frequency limit waveforms per electric utility company approved application of interconnection at POI/PCC operating site agreement.

Figure 4-11 MTA/MTD-600VDC 240A DC Power Supplies

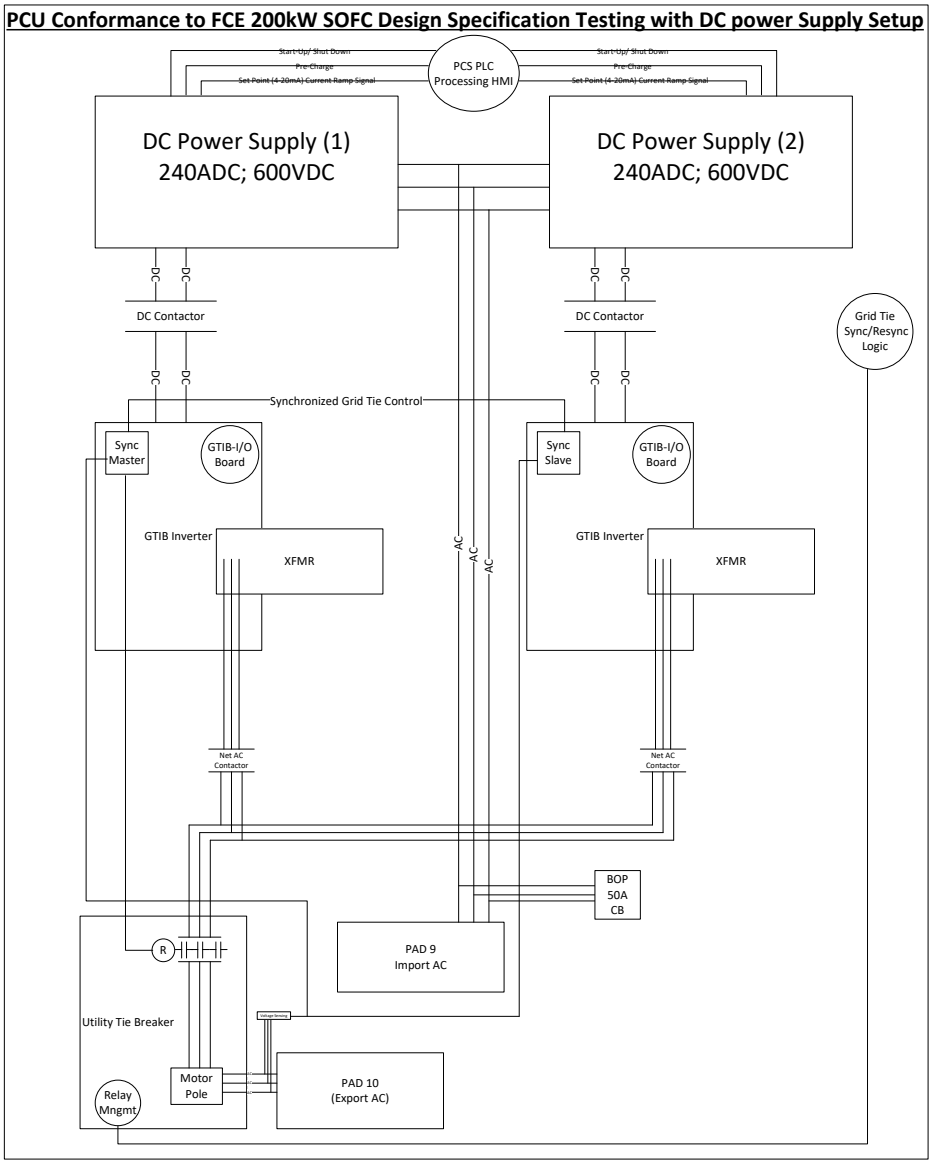

Figure 4-12 PCU Test Setup with DC Power Supplies

II. The 200kW prototype system factory acceptance test went through power generation with the validated inverters. The PCU DC/AC disconnects, diodes, bypass contactors, current sensors, DC/AC inverters, AC transformers, net AC bus bars, grid tie breaker, IEEE compliant tie breaker relay/aux contact switchgear, motorized automatic bus transfer (BoP load) switch and BoP main/distribution load circuit breaker were fully tested to validate their desired functions.

III. The communication between the PCU and PLC was validated and tested at various modes of operation. Trip scenarios was tested to ensure that the system, including the inverters, takes the appropriate corrective actions. This includes the monitoring the time response of these actions.

IV. The PCU net AC power exportation capabilities will be tested at various loads. This also validated the PLC's power demand commands to the inverters and ensure the inverters operate accordingly.

The transition from Hot Standby Mode to Power Generation Mode will be tested to validate that there is no time delay between all components involved. This includes the interaction between the PLC command to transition to grid-connected power generation mode and PCU's respective actions to synchronize to the utility grid network and allow power exportation.

V. Figure 4-13 shows a sketch for the test setup with the actual 200kW prototype system to complete Tests IV-V.

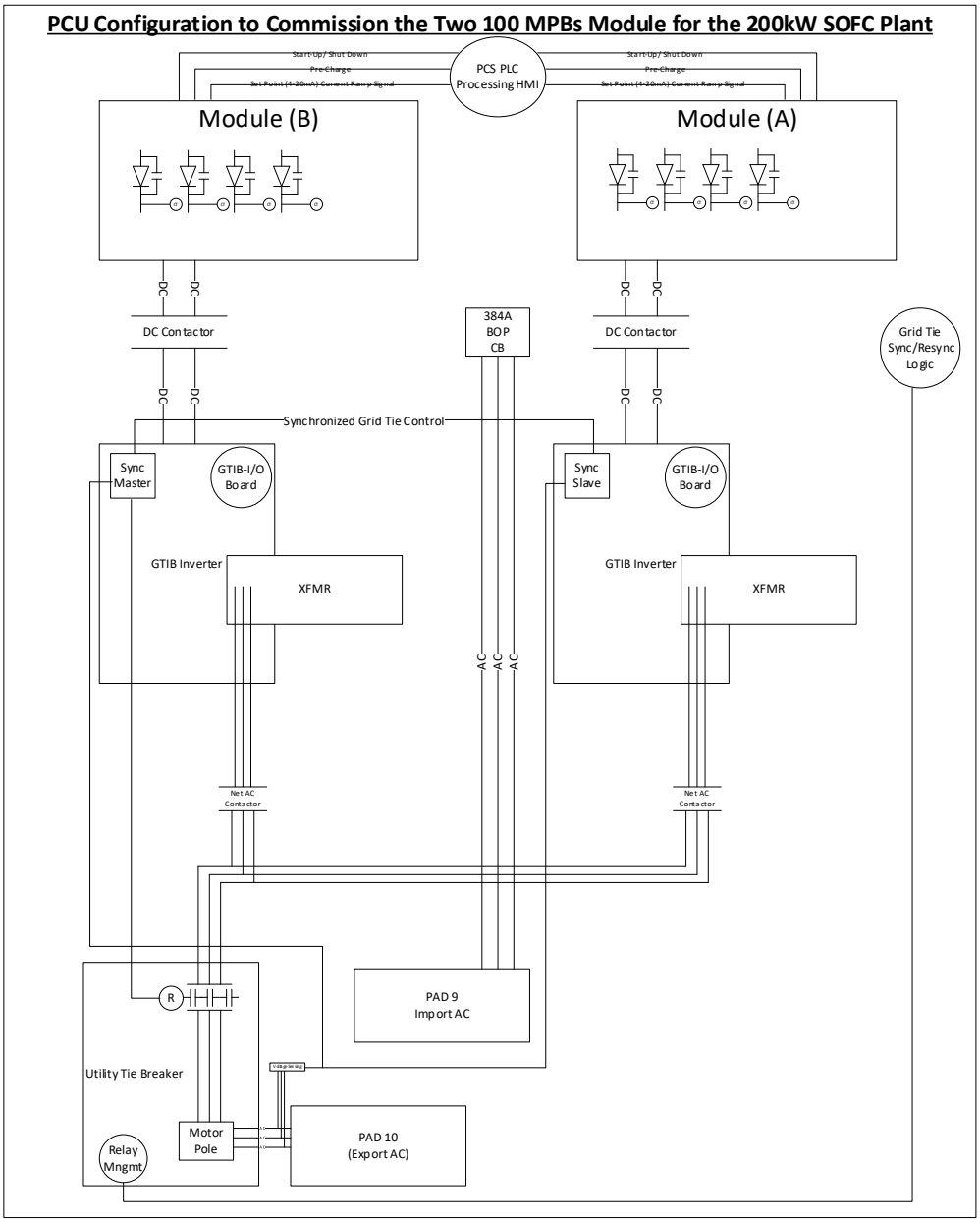

Figure 4-13 PCU Test Setup with Complete 200kW Prototype System

Cathode Air Purge System Overview*:* A fail-safe cathode air purge strategy was developed to protect the cathodes during a shutdown, including loss of power. This system delivers an adequate amount of air to the cathodes by utilizing the work from the expansion of on-site compressed nitrogen, which is part of the anode cover gas system. This work comes from the reduction of compressed nitrogen pressure to the system's design pressure so as a result, there is no impact to the anode cover gas system.

The cathode purge system was tested on the bench and produced satisfactory results. The design of the 200kW prototype system was replicated on the bench to effectively test this system, which included required nitrogen pressure and flow and expected pressure drop. The

nitrogen flow was kept constant while regulating the pressure to define the requirements of the cathode purge system to deliver the necessary amount of air to the cathodes.

Factory Acceptance Testing & Results:

An end-to-end electrical loop checkout for the MPBs (independent of the BoP) as assembly work was completed. This ensures that all instruments read correctly back to the HMI. The checkout also included verifying successful operation of all equipment, such as blowers and heaters.

The anode recycle flow transmitter (which was operated during MPB0 testing) did not pass testing due to its calibration. The unit was sent back to the manufacturer for evaluation and repair. The diagnosis included damage to its sensor module, which is being replaced under warranty. To close out MPB1, the flow transmitter from MPB2 was installed on MPB1 and MPB2 will receive the repaired unit once received.

Factory acceptance test, which included commissioning, evaluated the sequential logic and control system which includes the following modes:

- Purge
- Plant Heatup
- Water & Fuel Enable
- Hot Standby/Trip to Hot Standby
- Power Generation
- Hot Restart
- Cooldown
- Non-Recycle Cooldown
- Shutdown/Emergency Shutdown

Because the system allows for single module operation, that functionality will also be tested by allowing the MPBs to run in different modes simultaneously. The full operability range of the system was validated during the FAT.

The factory acceptance test (FAT) included heating up both modules and exporting AC power to the grid. Gas Chromatography (GC) samples were also taken at various operating modes to compare test results to process simulations. Throughout the test, operating parameters were adjusted to improve stack performance. Some issues were encountered, which required bringing the modules back inside the facility to undergo slight rework. Those issue did cause a delay to the completion of the FAT. However, the rework activities are ultimately expected to result in a more reliable system. For more information regarding these issues, refer to section 5 of the report for a more in-depth review of problems/delays and actions to overcome them.

Upon initial startup of the FAT, ground shorts were evident on MPB-B which were noticed at intermediate temperatures (approximately 400˚F). Because they were discovered immediately at relatively low temperatures, the stacks seemed unlikely to have experienced any damage. While MPB-B was cooling down, MPB-A progressed through heat-up and was determined to have a fuel leak within the module due to a disconnected pressure sensing tube. This was noticed through a faulty pressure measurement and unusual GC samples. As a result, both modules were brought inside for further evaluation and repair.

Several modifications were made as a result of initial FAT testing, refer to section 5 for delays and resolution strategies. MPB-A and MPB-B were both re-integrated with the BoP and heated back up for power testing. MPB-A reached full load, but one of the stacks (Stack 4A Upper) was underperforming, as it experienced an area of low cell voltage and high in-cell temperature. Figure 4-14, Figure 4-15 and Figure 4-16 show the performance of the module during this test run. Performance was expected to improve once the stack was replaced, which was demonstrated in the final FAT.

Once MPB-B was on-load, multiple thermocouples began to fail including critical ones used for control. Since both modules experienced issues, they were both cooled down and brought back inside the facility for final repair.

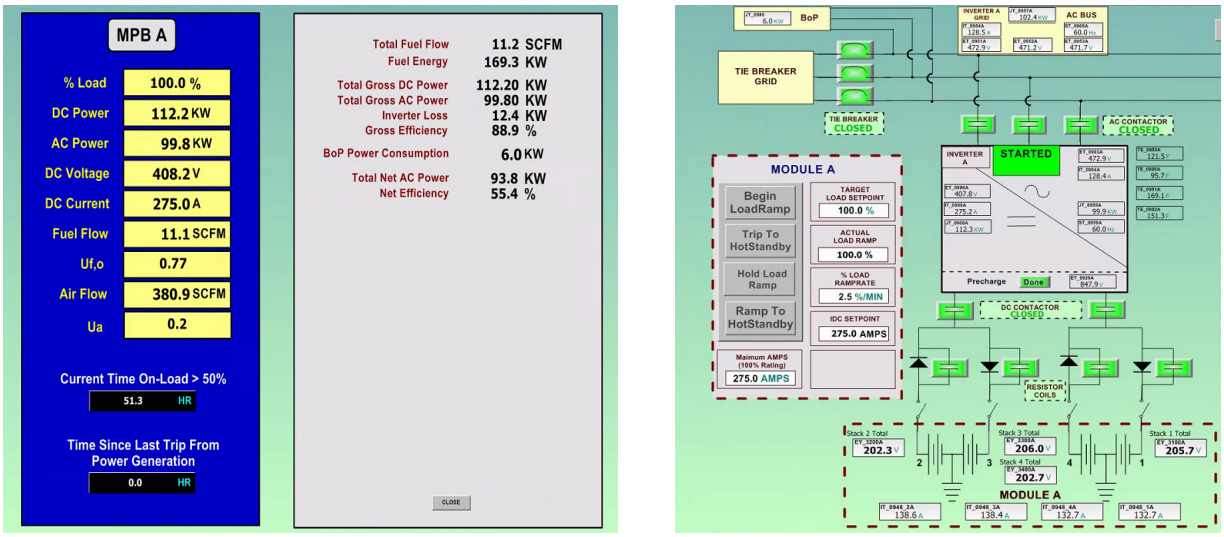

Figure 4-14 MPB-A Full Power – Plant Summary & One-line Screen

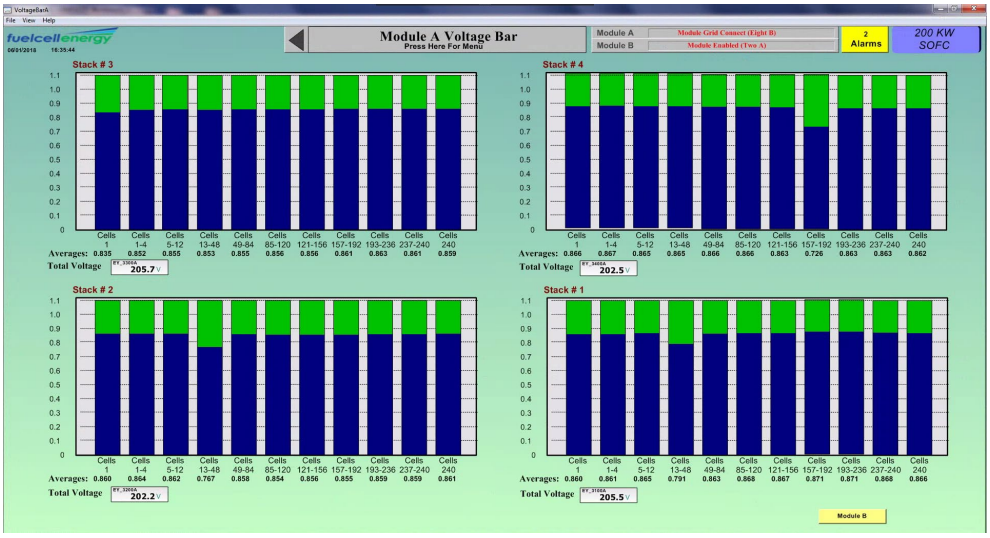

Figure 4-15 MPB-A Full Power – Cell Voltages

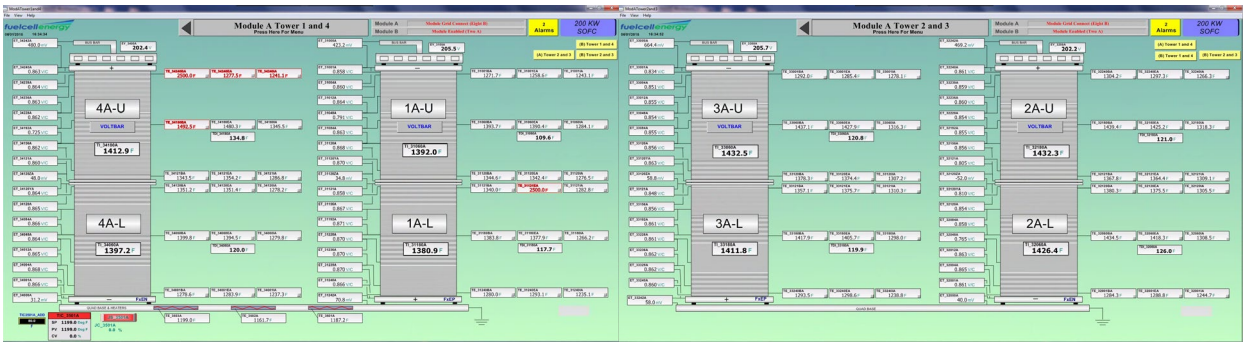

Figure 4-16 MPB-A Full Power – Stack Towers

A damaged cell was likely on MPB-A so the affected stack (4A Upper) was replaced with a spare that FCE had in house. Stack swap procedure can be found in Section 5.

The failed thermocouples on MPB-B were replaced with new ones that have no transition junction to lower the risk of failure, as they are more robust. Some critical thermocouples on MPB-A were also replaced with the more robust ones as well to increase reliability.

Total factory testing comprised 380 hours of hot operation (≥ 500°C), with 68 hours of power generation testing. Once the final rework activities were completed for the modules, each module was independently heated up and operated at full load for several hours at a stable condition. The final heat-up was done independently to minimize any further delay, as one module was ready while the other was still going through final repairs. Simultaneous heat-up of both modules has been tested previously. Performance and cell voltages for both modules are shown below in Figure 4-17, Figure 4-18, Figure 4-19 and Figure 4-20. Each module was able to deliver 97.4 kW to 98.5 kW of net AC power to the grid at an electrical efficiency (LHV) of 53.9% to 54.7%. These results reflect the tuned operating parameters made throughout the FAT to improve stack performance. Further improvements are likely achievable through continued operating parameter optimization during the planned on-site testing.

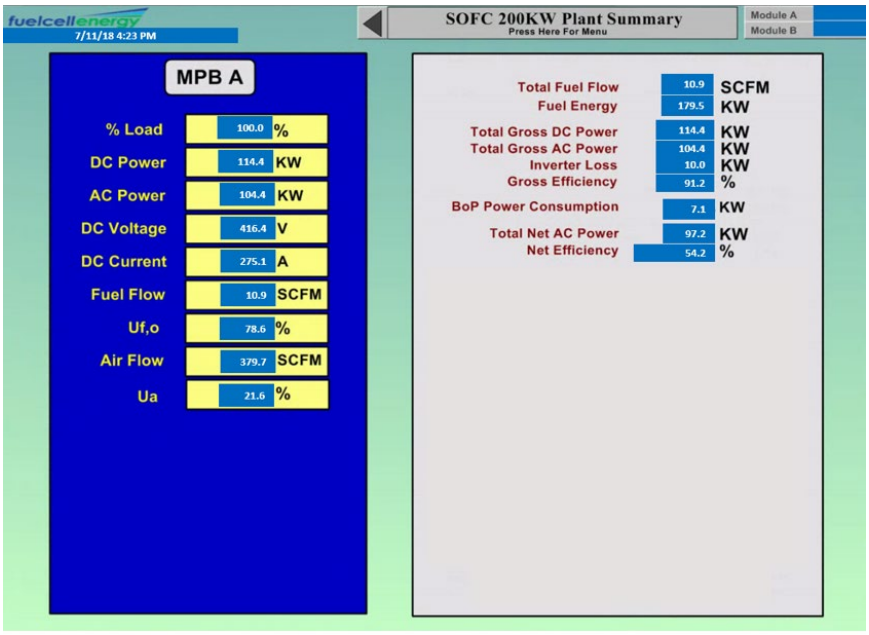

Figure 4-17 MPB-A Full Power – Plant Summary

Figure 4-18 MPB-A Full Power - Voltages

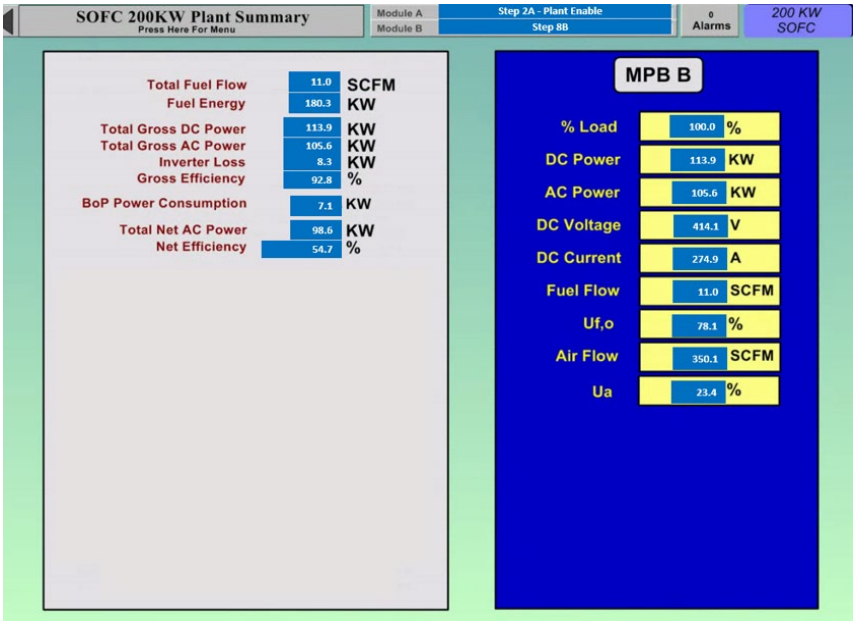

Figure 4-19 MPB-B Full Power – Plant Summary

Figure 4-20 MPB-B Full Power - Voltages

Host Site Commissioning

Commissioning activities included leak checks, rework of some instrumentation, broadband setup and communication troubleshooting (e.g. Airgas telemetry). The system was heated up and ramped on load to 75% for approximately two hours, which was the maximum allotted time to generate power prior to the witness test and approval per the interconnect agreement. The system performance and cell voltages at 75% load can be seen in Figure 4-21 and Figure 4-22, respectively.

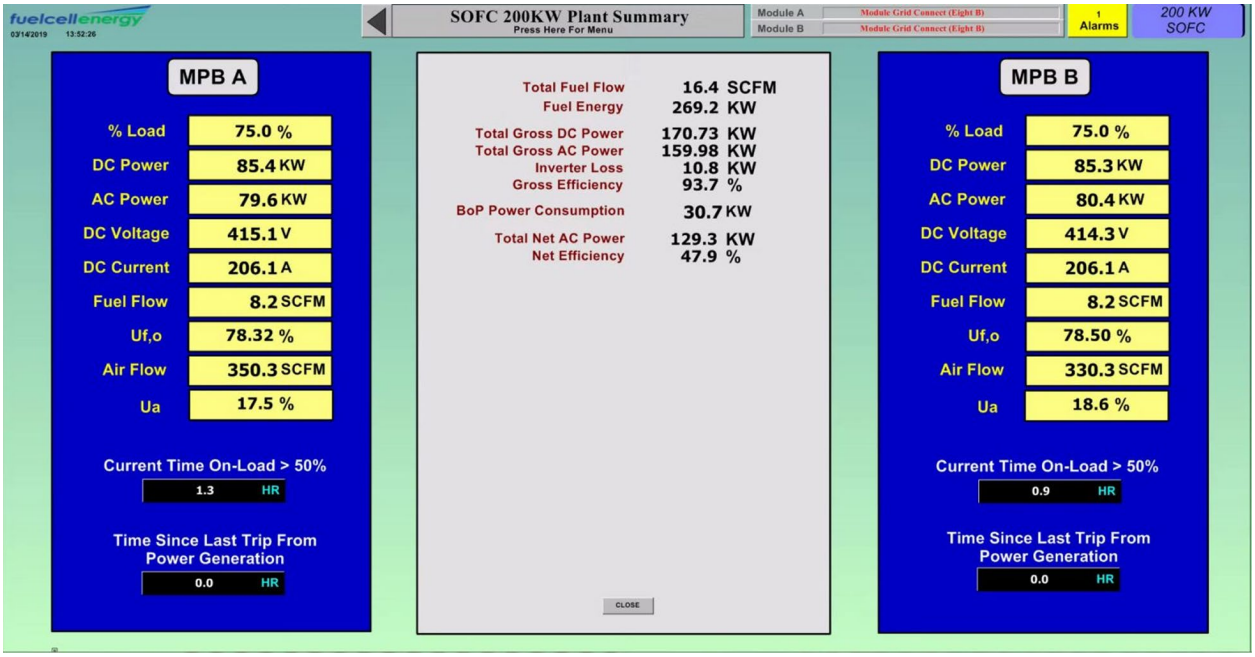

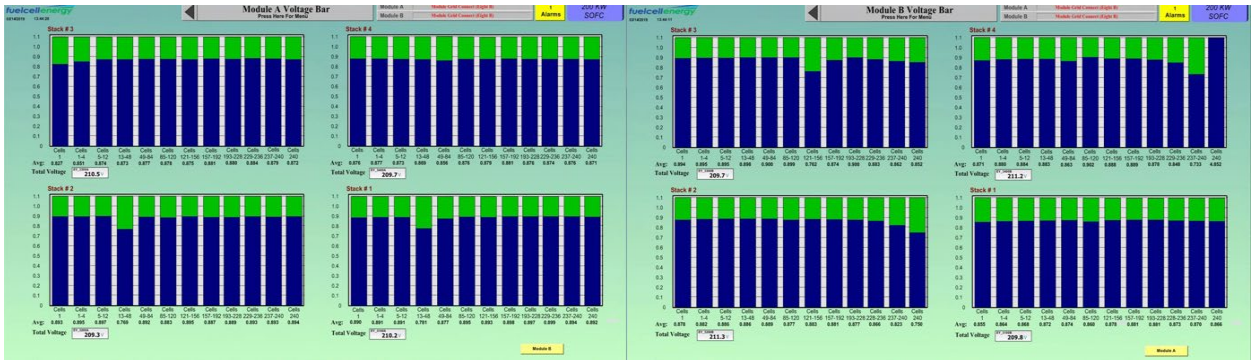

Figure 4-22 Cell Voltages at 75% Load

Afterwards, the witness test was scheduled and successfully performed with FCE and DLC personnel onsite. DLC replaced an existing billing meter at Clearway Energy's facility for one with bidirectional functionality early the next quarter.

SYSTEM TEST DEVIATIONS

Summary of test plan deviations are found below. However, a detailed overview of the test plan was submitted as a topical report under this project.

New permitting requirements by the City of Pittsburgh was the cause of the delay to plant commissioning/startup. The zoning approval was received after complications with the site's address were resolved. The electrical permit was then resubmitted and approved by the City one month later. At this time, the City stated that the HVAC/mechanical permit was no longer required. The approved electrical drawing requires additional grounding from the SOFC system to the steel frame of the building, which will be completed by the contractor prior to the electrical inspection.

After passing the electrical inspection, FCE will then send out a team to the site to commission and startup the system. In parallel, the host site (Pittsburgh Thermal), with support from FCE and the installation contractor, will prepare and submit the next stage of application required by the local utility and schedule an interconnect witness test. Following successful completion of the witness test as required by the interconnect agreement, the utility will install a new electrical meter, allowing for the start of the 5,000 hour test period.

Due to the sulfur breakthrough incident that occurred during the project at the host site, referred to in Section 5. Activities were continued during the quarter of July – September 2020. FCE received Modification 4 of the cooperative agreement on January 31, 2020. The modification includes additional scope to bring back the SOFC Prototype System to FCE's facility in Danbury, CT for continued operations. FCE has also requested a 3-month project extension to move the project end date until December 31, 2020 to allow more time for system operation. This no-cost extension request was approved by DOE/NETL.

Also due to the sulfur breakthrough, during returned operation at FuelCell Energy, Inc. facility in Danbury, CT, and a concern for stack health 90% load was the operational target, as the limiting factor in increasing load was the high stack temperatures as a direct result. This required a higher air flow to provide further stack cooling, which was still within the capacity of the fresh air blower. Around hour 1400 of the Danbury operation, the cathode inlet temperature was lowered by 10˚C which lead to more manageable stack temperatures and lower air flow in order to improve system efficiency.

5. PROBLEMS/DELAYS AND ACTIONS/PLANS:

FACTORY ACCEPTANCE TEST

The factory acceptance test (FAT) included heating up both modules and exporting AC power to the grid. Gas Chromatography (GC) samples were also taken at various operating modes to compare test results to process simulations. Throughout the test, operating parameters were adjusted to improve stack performance. Some issues were encountered, which required bringing the modules back inside the facility to undergo slight rework. These issues have caused a delay to the completion of the FAT. However, the rework activities were ultimately expected to result in a more reliable system.

Upon initial startup of the FAT, ground shorts were evident on MPB-B which were noticed at intermediate temperatures (approximately 400˚F). Because they were discovered immediately at relatively low temperatures, the stacks seemed unlikely to have experienced any damage.

While MPB-B was cooling down, MPB-A progressed through heat-up and was determined to have a fuel leak within the module due to a disconnected pressure sensing tube. This was noticed through a faulty pressure measurement and unusual GC samples. As a result, both modules were brought inside for further evaluation and repair.

Once the vessel lid on MPB-A was removed, the disconnected pressure tap at the Radiative Fuel Reformer inlet was confirmed, which is shown in Figure 5-1. The tubing was reconnected and there were no signs of any damage.

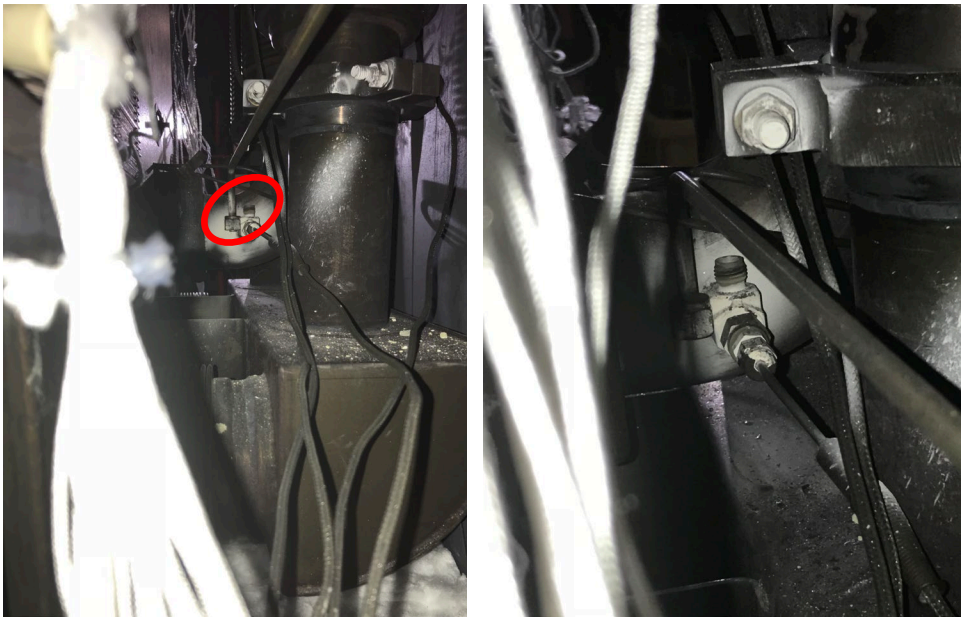

Figure 5-1. Anode Fuel Leak Due to Disconnected Pressure Tap

Once the tubing was reconnected, the anode loop underwent a leak test that revealed an additional leak. The leak test utilized cover gas (4% Hydrogen, balance Nitrogen) which could be detected by a handheld gas detector. The gas detector sensed a leak around the anode recycle blower. The blower casing insulation was removed for further investigation. Multiple leaks were found on the blower, including a crack on the casing which is shown below in Figure 5-2. It was determined that these leaks were a factory defect, as the blower was the first prototype unit fabricated and has subsequently been upgraded. The blower was swapped with an upgraded spare unit that FCE already had in house, while the damaged unit was sent back to the manufacturer for repair.

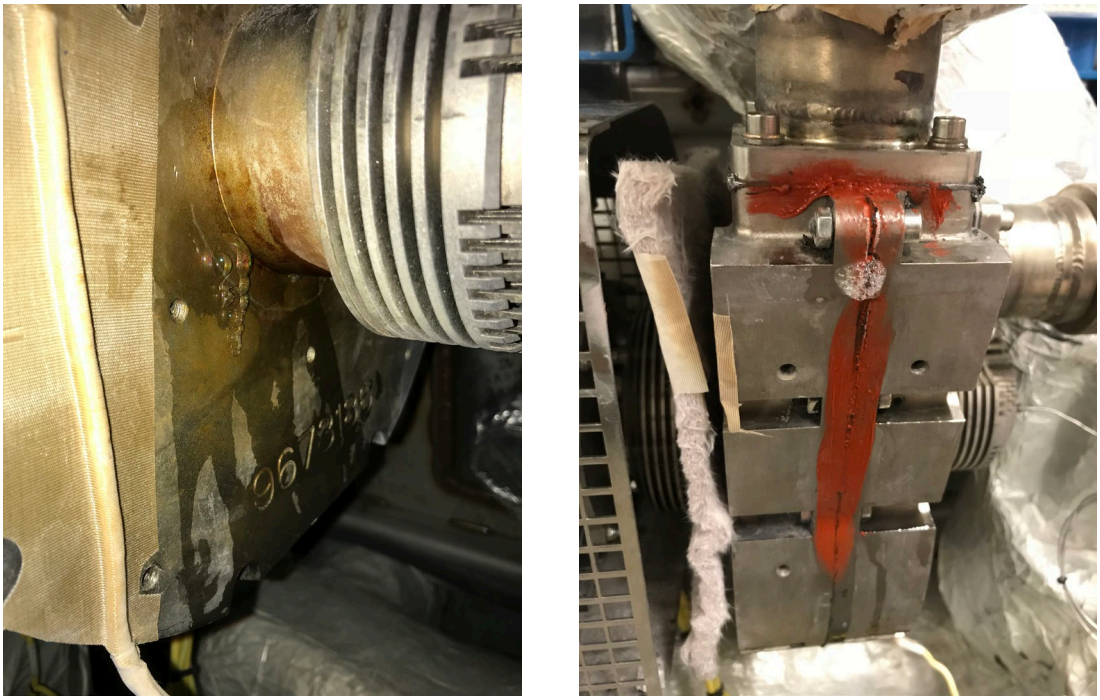

Figure 5-2. Anode Recycle Blower Crack and Casing Joint Leak

Upon initial inspection of MPB-B, no clear cause of the short was evident as it disappeared once the vessel lid was removed. To decrease the likelihood of voltage leads shorting to ground, the method of connecting and routing the voltage leads were modified. The short was determined to likely be occurring at or near the Weidmuller terminals, shown in Figure 5-3, so they were replaced with simple crimp-on snap plugs. This new method allowed the connection point between the high temperature leads and the low temperature harness wires to exist below the deck insulation instead of within the insulation. Additionally, the leads penetrated the insulation further away from the base perimeter where the enclosure is less likely to induce strain in the leads when sealed to the base. This was applied to both modules since the vessel lids were both removed.

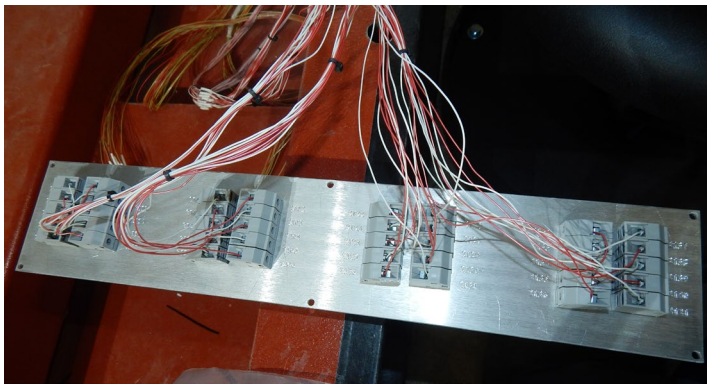

Figure 5-3. Original Weidmuller Terminals for Voltage Leads

While the modules were being reworked, the motor for the desiccant rotor on the balance of plant was replaced with a more robust one to withstand the higher temperatures experienced

within the desiccant system. The manufacturer provided a replacement motor as a warranty claim, which required only minimal modifications to install it in the unit.

Once MPB-B was on-load, multiple thermocouples began to fail including critical ones used for control. Since both modules experienced issues, they were both cooled down and brought back inside the facility for final repair.

A damaged cell was likely on MPB-A so the affected stack (4A Upper) was replaced with a spare that FCE had in house. While keeping the Quad Tower Assembly integrated in the outer base, the following process was executed in order to execute this stack swap.

1. Remove Cathode Inlet Distributor
2. Remove hot bus bars
3. Remove Radiative Fuel Reformer
4. Install turnbuckles to both stacks in Tower 4A
5. Release the tower compression on Tower 4A
6. Remove the Top Compression Plate, Tower 4A
7. Remove the upper stack while leaving the tower tie rods in place but unloaded
8. Remove the gasket assembly from the top plate on the lower stack and clean the surface
9. Install new gasket assembly
10. Hoist and install the replacement stack
11. Install the gasket assembly on the top plate of the upper stack
12. Install Top Compression Plate
13. Re-establish tower compression by applying tensile load on the tower tie rods
14. Remove turnbuckles
15. Reinstall Cathode Distributor
16. Reinstall Radiative Fuel Reformer

The failed thermocouples on MPB-B were replaced with new ones that have no transition junction to lower the risk of failure, as they are more robust. Transition junction thermocouples are perceived as less robust because the transition from the probe to the sheath is exposed to high temperatures within the hot zone. However, the ones without the transition junction can be routed through the hot zone without having the transition exposed to high temperatures. Some critical thermocouples on MPB-A were also replaced with the more robust ones as well to increase reliability.

Upon further inspection with the vessel lid removed, exposed in-cell thermocouple wires were discovered near the quad base on MPB-B. Since the in-cell thermocouples are electrically hot, it is critical for the Nextel sheath to be intact to provide dielectric isolation. To lower the risk of these thermocouples from shorting, the sheaths were reworked and re-routed to provide less strain. All exposed and faulty in-cell thermocouples were also removed to eliminate the high-risk short paths.

INVERTER FAULT, MPB-A

FCE utilized field support from Princeton Power to evaluate, repair and commission the two inverters at FCE's facility, as the sensor isolation boards of both inverters were damaged during initial testing. With the help of Princeton Power's field service engineer, the root cause was determined to be leaving certain connectors on the boards in place that should have been unplugged. The sensor isolation boards were replaced and the proper connections were made. The inverters were then successfully validated by using DC power supplies and sending various power demands locally to each inverter to export power to the grid (Table 4-1); the pre-charge assemblies for each inverter were also tested for proper operation. A Master-Master configuration for the inverters was used to allow either inverter to run without the other.

Issues were noticed with Inverter A when commanded to start and draw current at the later phases of commissioning when the field service engineer was no longer onsite. The inverter went through a fault and re-engaged several times before finally clearing the fault. Princeton Power was contacted to determine what may be causing the inverter to fault.

SITE INSTALLATION

Due to improper submission of the final application by the contractor and electrical inspector to the local utility, Duquesne Light Company (DLC, some delays were encountered with getting scheduling the witness test and receiving approval. The final application was eventually circulated to all parties to obtain the required signatures for submittal to DLC.

While the contractor was getting the final application prepared to be submitted to DLC, FCE's team traveled onsite to Clearway Energy (formerly NRG) to commission the plant and prepare for the anticipated utility interconnect witness test.

Upon inspection of the contractor's work, the pass through locations were not in the proper positions as shown on the FCE drawing. FCE's engineers worked closely with the contractor, as well as NRG personnel, to ensure the modifications would not compromise the weather barrier or the integrity of the new concrete pad. The concrete piers that would support the fuel cell were spaced at equal intervals (4.5ft) in line with the support structure of the building below. These supports did not line up with the support locations that were designed into the fuel cell. To remedy this situation, an interface support rail was designed by FCE to translate the load of the fuel cell to the appropriate support locations of the concrete piers. These rails were designed, constructed, test fit and shipped to the site.

Figure 5-4 New Concrete Upper Deck, Fuel Cell Pier Supports & Pass Throughs

Afterwards, the witness test was scheduled and successfully performed with FCE and DLC personnel onsite. DLC replaced an existing billing meter at Clearway Energy's facility for one with bidirectional functionality.

SULFUR BREAKTHROUGH – HOST SITE

During operation at the host site, around 1900 hot hours, high temperatures in the fuel reformer led to concern. Module B demonstrated stable operation at 100 kW and Module A continued to show slight improvements over time, allowing its power output to slowly be increased. At one point, high temperatures in the fuel reformer were observed in both modules followed by rapid performance degradation as shown in Figure 5-5 and Figure 5-6 for Module A and B, respectively. The progressive increase in reformer temperatures and decline in cell voltages were seen simultaneously in both modules, which strongly indicated sulfur breakthrough into the system. As a result, both modules were cooled down to prevent any further harm and to develop a plan to continue operation.

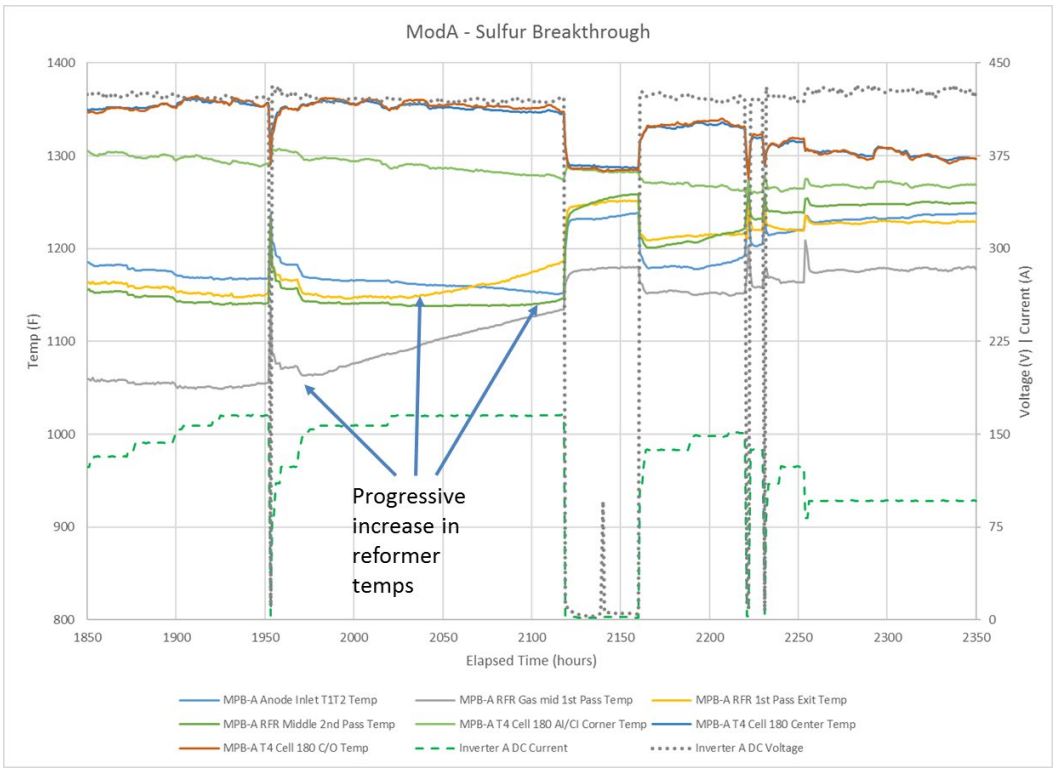

Figure 5-5. Module A 1st Sulfur Breakthrough

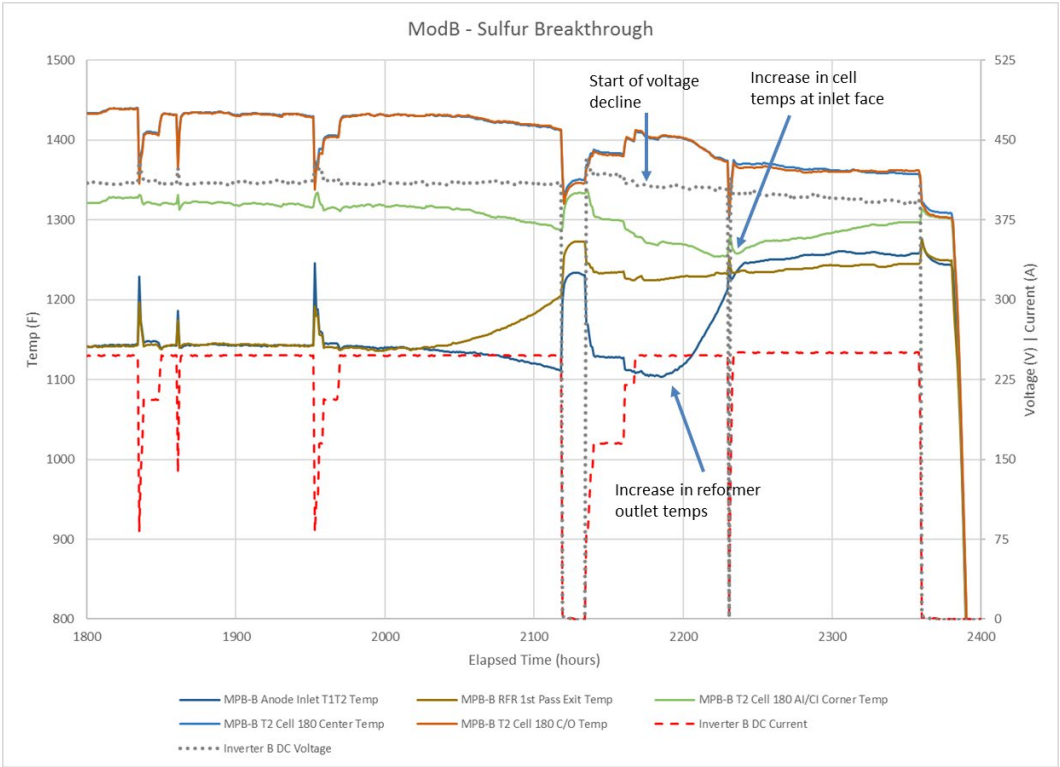

Figure 5-6. Module B 1st Sulfur Breakthrough

FCE dispatched a technician to the Clearway Energy Center site in Pittsburgh to take natural gas samples around the desulfurizer beds in order to analyze the natural gas feed composition and performance of the adsorbents before replacing them with fresh adsorbents. Once the adsorbents were changed out, the system was restarted and the samples were brought back to FCE's facility for analysis. High amounts of sulfur species were discovered in the natural gas supply, exceeding FCE's fuel specification for certain sulfur species. Higher than desired amounts were also seen in samples taken between and after the desulfurizer beds. FCE contacted the local natural gas utility and they were unaware of any changes made on their side.

Upon restart, the system was stable and showed slight improvements compared to the performance observed prior to the shutdown. However, the stacks did not show signs of continuous improvement as is expected with the reversible nature of sulfur poisoning when the sulfur is removed. Another natural gas sample was taken from a separate feed line at the site and sent to a third-party lab for further analysis and validation of FCE's initial findings. After only a few weeks of operation following the desulfurizer adsorbent media change-out, a second sulfur breakthrough event was observed via module performance monitoring. The system was then shut down to prevent further damage. The gas analysis from the third-party confirmed the high amounts of sulfur species in the supply, as well as high amounts of moisture which is detrimental to the performance of the adsorbents. Such severely out-of-specification natural gas, in terms of high levels of certain sulfur species, has not been observed at any other plant sites in FCE's cumulative experience operating hundreds of MWs of fuel cell systems. No explanation for the out-of-specification gas was available from the gas supplier. Higher than desired amounts of sulfur were also found in gas samples taken downstream of the desulfurizer beds, confirming that sulfur was indeed reaching the stack modules. Due to the gas quality issue, restart of the system at the site is not planned at this time.

Once the system was back to normal operating conditions following the media change, cell voltage and temperatures were stable as shown in Figure 5-7. The reformer temperatures were slightly lower than what they were prior to the previous shutdown, which signified increased catalyst activity (i.e. less sulfur poisoning). FCE experience shows that sulfur poisoning is somewhat reversible (albeit slowly) when the sulfur is completely removed from the feed gas, which was the desired result with the fresh adsorbents. This was not evident while the system continued to run. Another natural gas sample was taken from the feed to one of Clearway's boilers and sent to a third-party lab for further analysis and validation of the initial results.

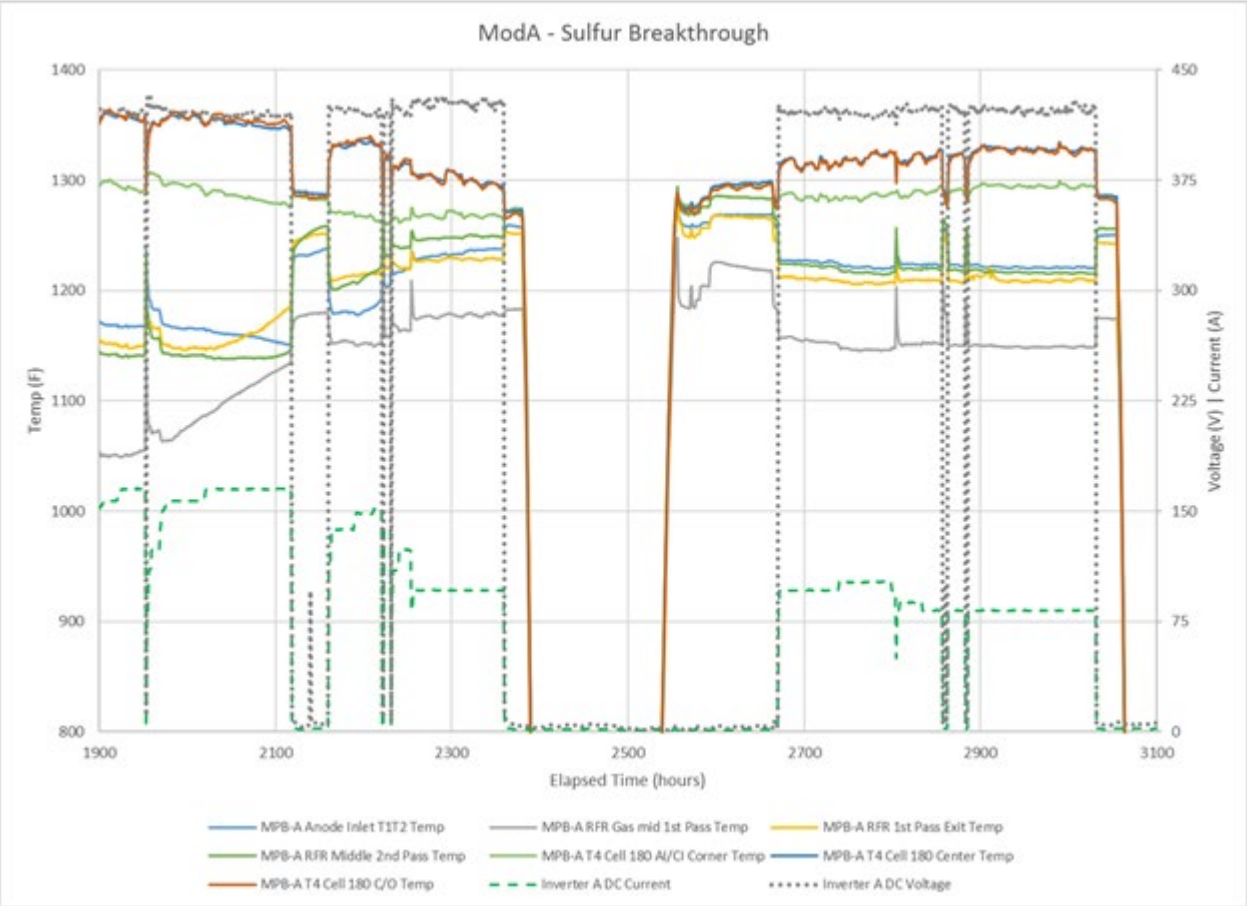

Figure 5-7. Module A – After Replacement of Desulfurizer Adsorbents

The anode recycle blower on Module B failed during the subsequent startup after the desulfurizer media change-out. While Module A was running, the anode recycle blower on Module B was replaced with a spare unit and started back up. Performance on Module B was similar to what was seen on Module A (slight improvement compared to prior to the trip but no signs of continued improvement). FCE believed that sulfur breakthrough was still occurring based on the initial gas sample results, although there was no system data confirming the theory at this point. Therefore, Module A was cooled down to preserve the weaker cells while Module B continued to run. After only a few weeks of operation following the desulfurizer adsorbent change-out, signs of sulfur breakthrough were observed for the second time as shown in Figure 5-7 (evident by the spike in anode inlet temperature and decline in cell voltage), resulting in a plant shut down. The third-party natural gas sample analysis also confirmed the high amounts of sulfur as well as high moisture content, which was ten times greater than what is allowed by FCE's fuel specification. Water contamination in the gas makes the control of sulfides extremely difficult even with normal sulfide levels. This explains why the reversible nature of the sulfur poisoning was not observed, as the natural gas supply continued to exceed FCE's fuel specification and thus, caused the sulfur to break through significantly quicker (in a matter of days) than designed. The system cannot operate under these conditions without significant design modifications.

Module A was removed from the skid and brought inside FCE's facility for stack de-integration. Five stacks were selected for post-test analysis. The stacks were selected based on a review of testing data, and were chosen to cover a wide sampling range in order to provide useful information on stack decay/damage causes and mechanisms. The five stacks were crated and sent to FCE's Calgary facility for analysis.

To resolve this issue, the plant has been relocated to FCE's Danbury, CT facility to complete testing.

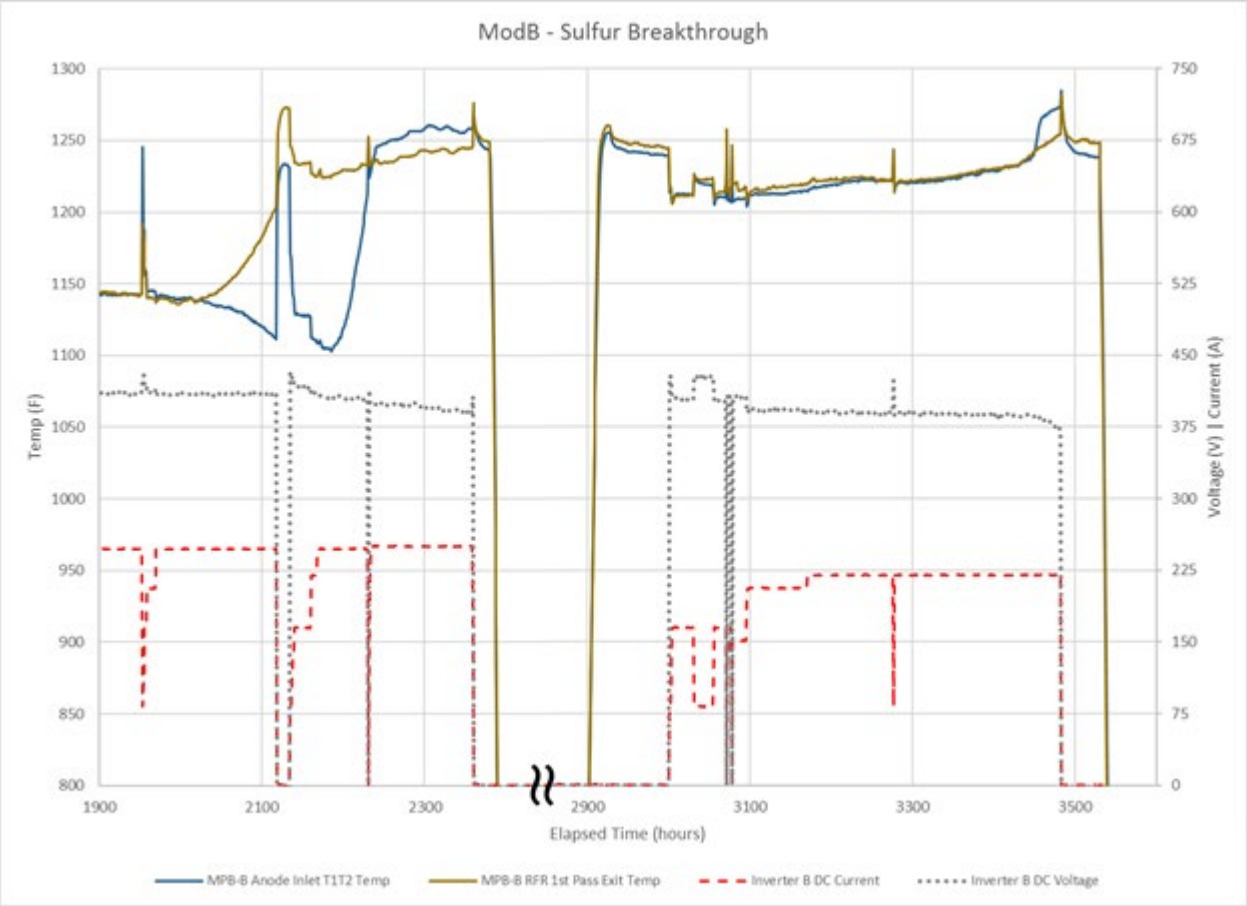

Figure 5-8 Module B – 2nd Sulfur Breakthrough

DANBURY, CT FACILITY INSTALLATION

FCE executed the removal of the 200 kW SOFC Prototype System from the Pittsburgh site and its shipment back to Danbury, CT. This included the following activities:

- FCE regained compliance to Adapt 1, Clearway Energy's safety and business compliance system, which allowed FCE personnel onsite to assist in the removal activities. This involved submitting updated business and safety documents to the satisfaction of Clearway Energy.

- Wayne Crouse Inc. (WCI) mechanical contractor was hired to disconnect the utilities and isolate the system at Clearway Energy Center in Pittsburgh, PA. WCI was responsible for hiring and managing the crane service for hoisting and loading the plant onto a truck.
- FCE hired H.W. Farren, which was the same trucking company that was used previously to deliver the system from Danbury to Pittsburgh.
- FCE personnel traveled to the site in Pittsburgh to decommission the system, which included purging and draining the necessary subsystems, removing the façade, preparing the system for transport, and assisting in hoisting activities (Figure 5-9).

Figure 5-9. Removal of SOFC Prototype System from Clearway Energy for Shipment

The unit was landed safely on Pad 4 of the outdoor test and conditioning facility at FCE's headquarters in Danbury, CT, as shown in Figure 5-10. Once landed, Module A was removed from the skid and brought inside FCE's facility to prepare for stack de-integration.

Figure 5-10. SOFC Prototype System Landed in Danbury, CT

The existing infrastructure surrounding Pad 4 required some rework to accommodate the prototype system operation, which included the following:

- Mechanical utilities were routed from their respective source and connected to the system (Figure 5-11).

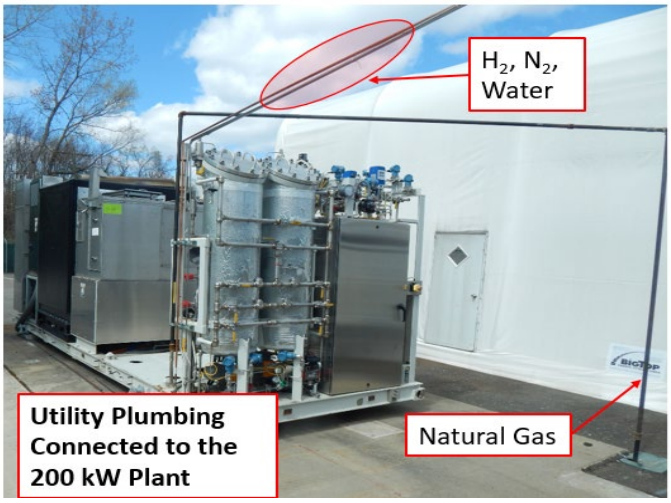

Figure 5-11. Mechanical Utility Tie-Ins Completed in Danbury, CT

- Power and communication have been established to Pad 4 and connected to the unit (
-
-

- Figure 5-12). An electrical services contractor was hired to re-establish 480V service and install a new 480V disconnect on Pad 4.

Figure 5-12. 480V Service Installed and Connected to the SOFC Prototype System in Danbury, CT

The SOFC Prototype System was then ready for utility and system check outs prior to startup. This included final leak checks of all utilities and functional checks of all instrumentation and equipment on the system.

COVID-19

Safety restrictions from COVID-19 were implemented across FCE's locations in March, 2020. The restrictions include reduced on-site staffing and reduced numbers of technicians working on the system installation to ensure proper distancing. Despite these restrictions, plans were implemented to enable Module B of the 200kW Plant in Danbury, CT in May 2020. Heat-up was completed and the plant was producing power and water independent by mid-May 2020.

CONNECTICUT TROPICAL STORM

There were very few plant trips during operation in Danbury that lead to significant stack cooling, as most were related to grid disturbances and were quickly recovered from a Hot Standby state (i.e. load cycle). However, on August 4, 2020 there was a tremendous tropical storm in the CT area which lead to the loss of power at FCE's facility in Danbury. At this time Module B tripped and cooled down, where it made a full thermal cycle. The facility was without power for approximately 6 days and the storm also caused a few equipment failures in the facility that required repair/replacement, which delayed restarting the system. Module B was heated back up and began ramping load on August 24th, 2020.

6. DEMONSTRATION TEST RESULTS

Early in the demonstration test, few low performing cell groups were seen on both modules and as a result, the modules were slowly ramped up on load to minimize any potential damage to the rest of the cells. Incremental step changes were made and held on a daily basis while carefully monitoring the concerning cell groups. All cell voltages are shown in Figure 6-1, which illustrates the performance of both modules. Module A had a few more low performing cell groups than Module B. Module B showed significant improvements over time, which allowed it to achieve 100 kW DC gross power output. Upon further detailed review of the Factory Acceptance Testing data, it is possible that the Module A stacks may have been damaged due to a redox cycle. As reported previously, at one point during factory acceptance testing in Danbury, abnormal gas compositions were measured in the anode-side of the process for Module A, indicating presence of combustion products. Upon cool-down and inspection of the module, it was discovered that a loose/disconnected sampling tube and a cracked anode recycle blower casing had allowed oxygen to enter the anode-side process. During cool-down of the module, it is suspected that the fuel and purge gas flows were not sufficient to maintain a reducing atmosphere at all points in the stacks given the amount of air intrusion. Refer to section 5 for more information.

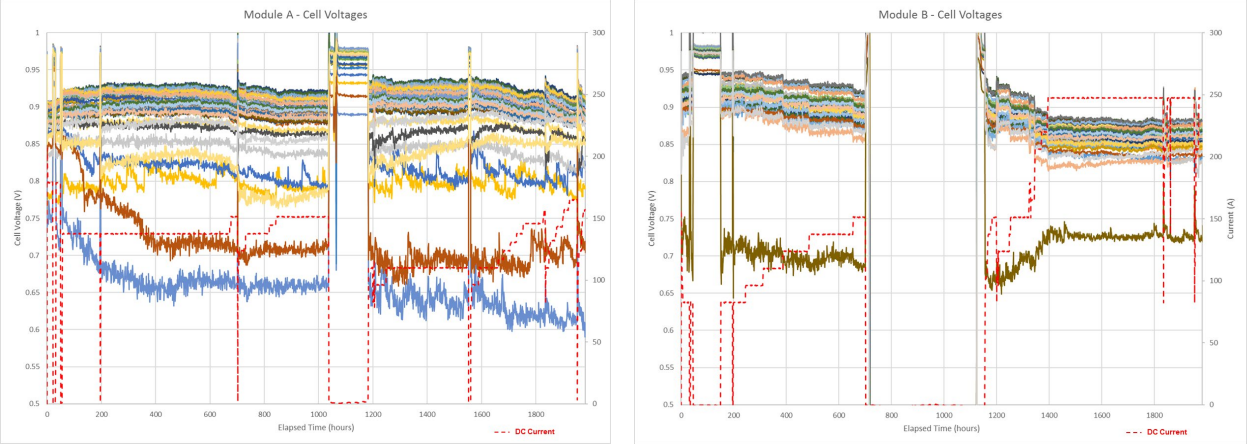

Figure 6-1. Cell Voltages

Once the ambient temperatures were getting warmer, the air system experienced hot temperatures which affected system performance and caused the blowers to approach their maximum capacity. To alleviate the issue, the desiccant system was turned off. This effectively improved plant output but allows any moisture in the ambient air to flow through the fuel cells.

Throughout the demonstration test, multiple grid disturbances were experienced which tripped the modules to Hot-Standby mode and hindered the progress made in ramping the modules up on load. This is shown in multiple instances in

Figure 6-2, where all current is suddenly lost and immediately recovered. This figure also depicts the average cell voltage of both modules.

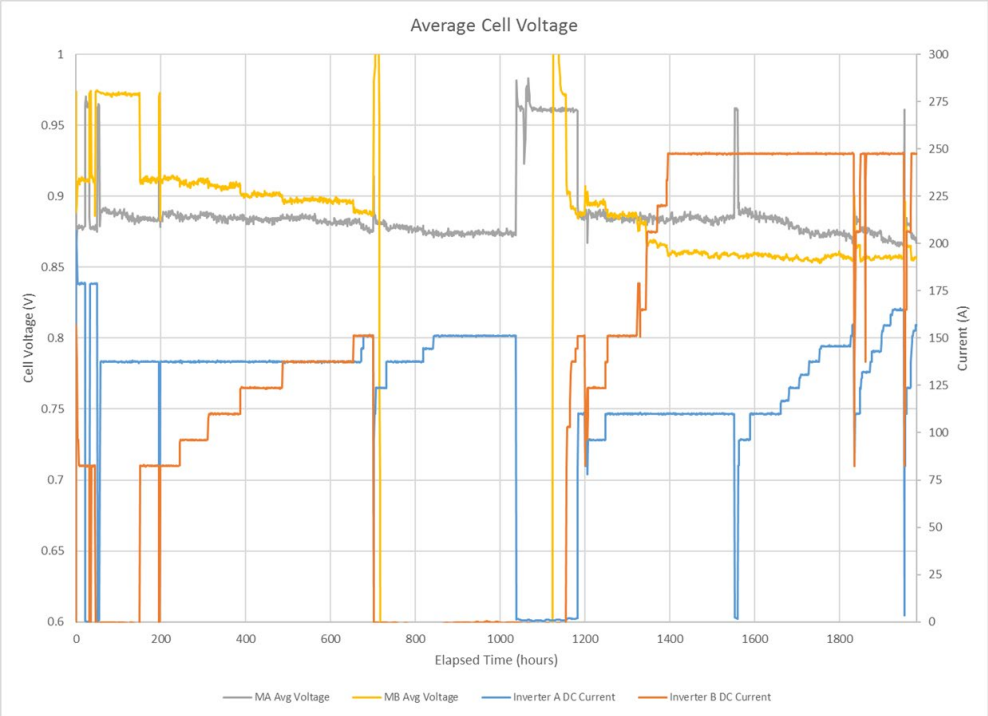

Figure 6-2. Average Cell Voltages

Module B experienced an issue with one of its electric heaters, which prompted the module to cool down. FCE personnel traveled to the site (Pittsburgh) to troubleshoot this issue, which was determined to be a failure of the SCR (silicon controlled rectifier), i.e. heater controller. The root cause was due to excessive temperatures in the electrical cabinet located in front of the module that housed the SCR. A design solution was implemented to prevent the electrical cabinets from getting too warm, which included adding insulation panels and installing new cooling air exhaust ports near the back of the cabinets. This solution was implemented on both modules and a replacement SCR was installed for Module B. This is indicated in

Figure 6-3 by an extended loss of power generation during the 700 to 1100 hour time frame. Once the system resumed normal operation, the design solutions proved effective. Noticeably cooler temperatures were measured inside of the electrical cabinets, even given the warm ambient temperatures.

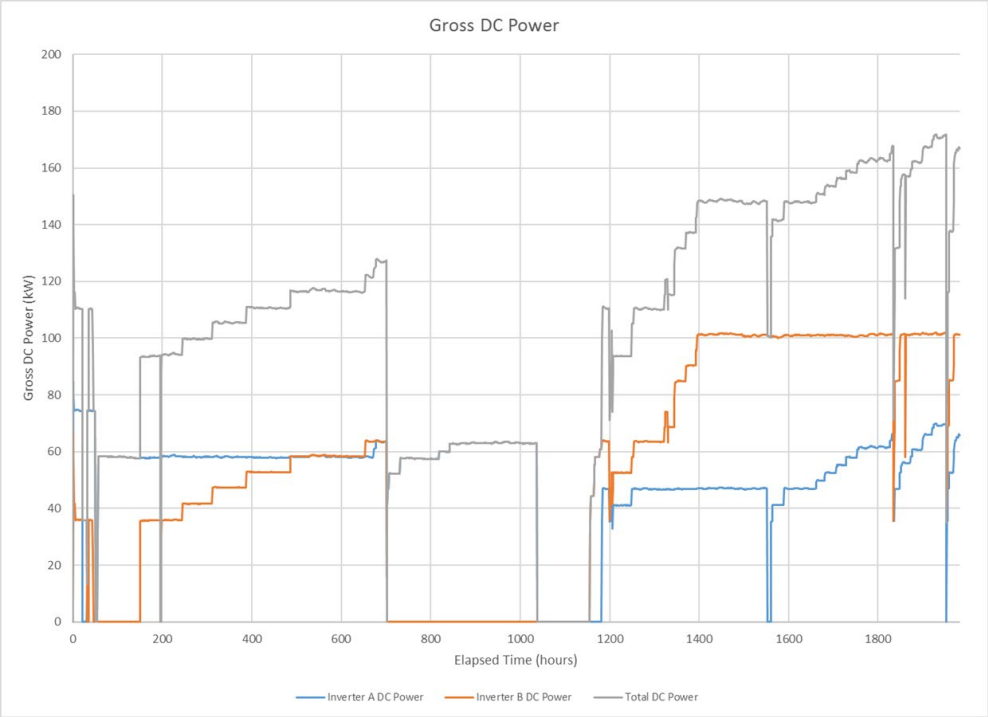

Figure 6-3. Gross DC Power Output

An overview of the demonstration operation in Pittsburgh is shown in Figure 6-4 and Figure 6-5, which shows the average cell voltages and gross DC outputs for both modules, respectively. The demonstration system had accumulated 3,384 hours of hot operation while at the Clearway site. In total, including Factory Acceptance Testing in Danbury, the system has completed 3,877 hours of hot operation.

Figure 6-4. Average Cell Voltages

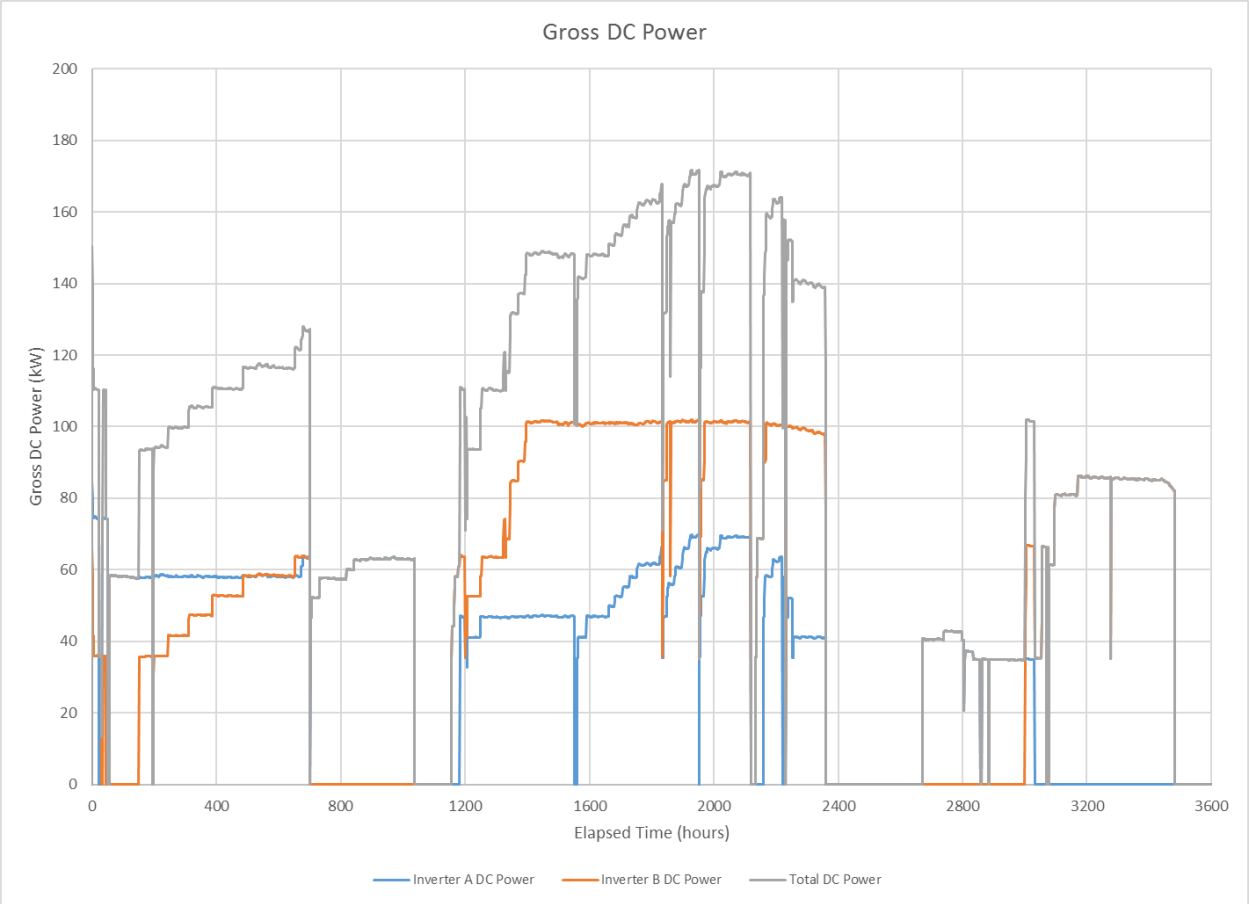

Figure 6-5. Gross DC Power Output

Following relocation of the SOFC Prototype System from Pittsburgh, PA to FCE's facility in Danbury, CT, reported in the last quarter, the unit was fully checked out and commissioned prior to starting back up. The natural gas desulfurizer beds were filled with fresh media to ensure no residual sulfur breakthrough from species absorbed during operations in Pittsburgh. The demonstration test officially resumed shortly thereafter and the progress is shown in Figure 6-6. The system was slowly ramped up to the same level of operation as in Pittsburgh, PA to ensure it was running as intended. The same low-voltage cell blocks were evident and stable, while the majority of the cells were stable at the levels seen after the second sulfur breakthrough in Pittsburgh. Very slight overall improvements were seen as time progressed but nothing significant to suggest recovery of the catalytic activity from the two separate sulfur poisoning incidents in Pittsburgh.

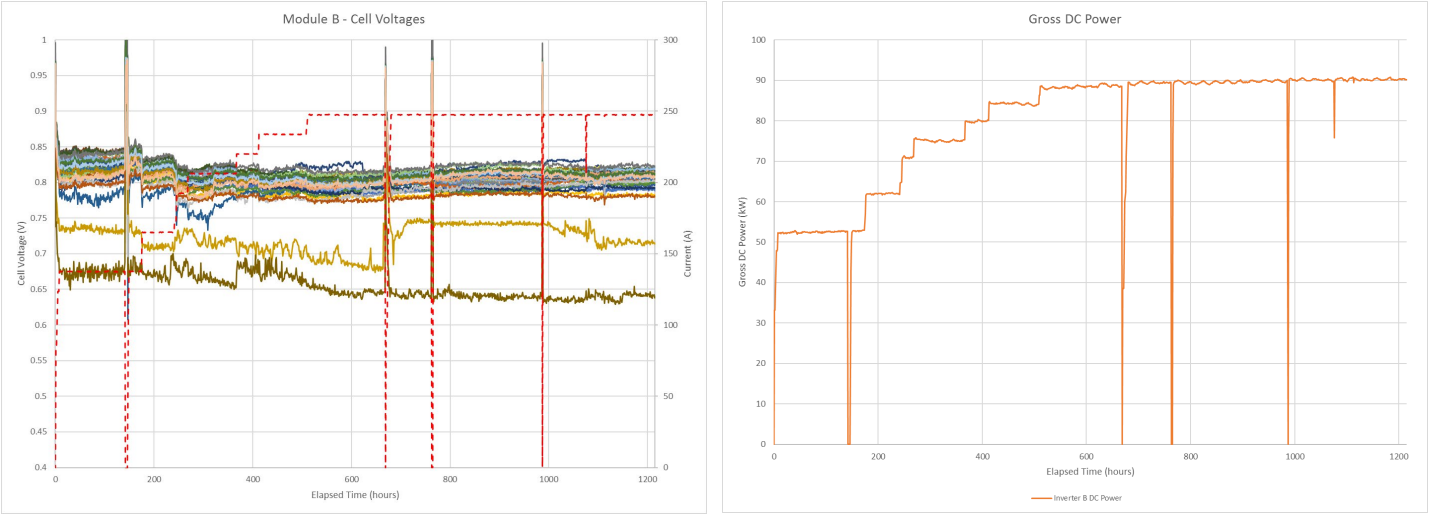

Figure 6-6. Module B Cell Voltages (*left*), Gross Power (*right*) – Danbury, CT

Natural gas samples have been analyzed in Danbury, CT once the system was generating power for an extended period of time to confirm the gas quality and effectiveness of the desulfurizers. The pipeline natural gas met FCE's fuel specification and no levels of sulfur were detected in the desulfurized natural gas (i.e. < 10 ppb).

GC samples were taken from the system during 60% load operation as shown in Table 6-1, which showed low levels of reforming due to the sulfur poisoning.

Figure 6-7 shows some temperatures around the reformer and stacks, which have been relatively stable at the same higher levels seen in Pittsburgh after the second sulfur breakthrough and further demonstrates no significant recovery from the sulfur poisoning.

Table 6-1. Module B 60% Load GC Results – Danbury, CT

5/19/20 5-6 PM| 60% Load | 6.57 SCFM NG | 277.5 SCFM Air | 92% Anode Recycle					
% Composition - GC					
Sample	3	1	2	4	5
	Anode Module In (u/s RFR)	RFR 1st Pass	Anode In (d/s RFR)	Anode Out	Cathode Exhaust
H2	15.167	16.944	21.516	18.100	0.000
O2	0.000	0.000	0.000	0.000	18.180
N2	12.608	12.101	11.565	15.327	81.411
CH4	20.373	18.804	16.837	5.643	0.000
CO	7.242	5.785	7.397	8.466	0.000
CO2	44.416	46.194	42.580	52.464	0.408
C2H6	0.193	0.172	0.105	0.000	0.000
Total	100.000	100.000	100.000	100.000	100.000

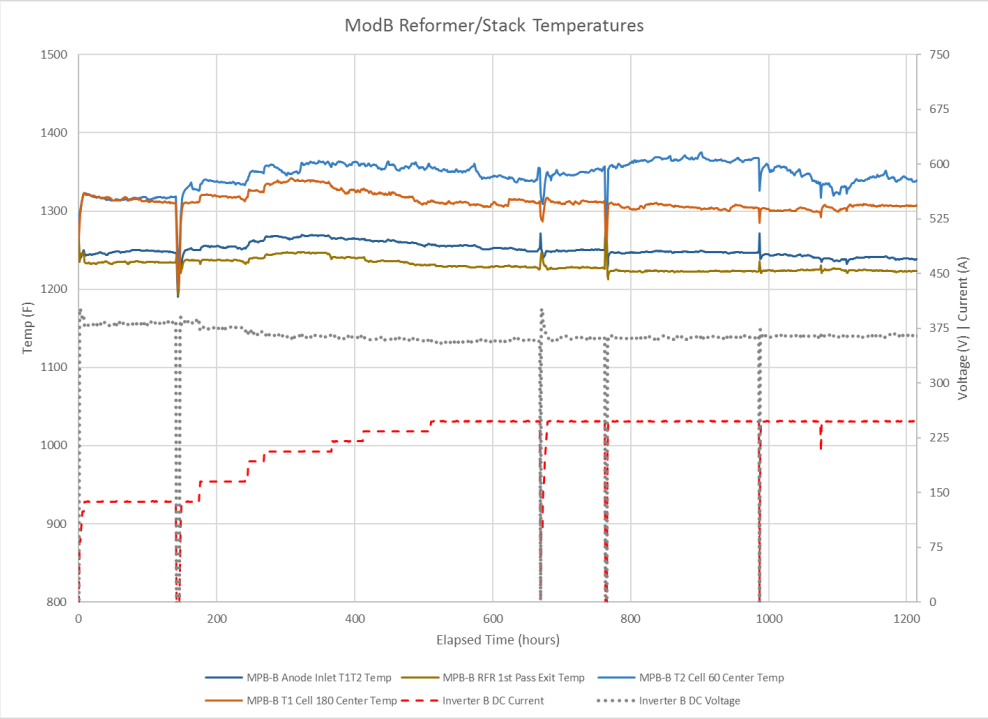

Figure 6-7. Module B Reformer/Stack Temperatures – Danbury, CT

Operating parameters have been tuned through the initial load ramp to satisfy stack requirements and deliver adequate and stable performance. As of the end of quarter 19 (June 2020), Module B has accrued an additional 1,215 hours of hot operation while running in Danbury, CT. In total, the SOFC Prototype System demonstration has 4,599 hours of hot operation including operation at Clearway Energy in Pittsburgh, PA.

Continued operations of the SOFC Prototype system led to the completion of the 5000 hour testing period fulfilling the final outstanding project milestone. Figure 6-8 provides a summary of the operational hours. This includes operation of both modules at Clearway Energy in Pittsburgh, PA and the continued operation of Module B at FCE's facility in Danbury upon its return from Pittsburgh.

From the start of Demo @ 1GPR 5/11/2020 – 10/14/2020 8:00AM	
Module B Gross Power	97.8 kW DC
Module B Hot Hours Accumulated:	3208 hours
Module B Hot Hours Net AC Generated:	3169 hours
Total Net Energy Output from System:	184, 047 kW-h
Last Plant On-Load %:	100 %

5000 hours of operation achieved ~9/9/2020

Total Summary 1GPR + Clearway Site 4/9/19 – 10/14/2020 8:00AM	
Module A Hot Hours Accumulated:	2910 hours
Module B Hot Hours Accumulated:	5808 hours
Total Hot Hours Net AC Generated(non-cumulative):	5895 hours
Total Net Energy Output from System:	299, 458 kW-h

Figure 6-8. SOFC Prototype System Operational Hours Summary

During operation at FCE's Danbury facility, due to the ongoing concern of stack performance and low-voltage cell blocks, most of the operation was at 90% load. This operating point was stable and provided relative data for direct comparison to operation in Pittsburgh, PA. There were very few plant trips during operation in Danbury that lead to significant stack cooling, as most were related to grid disturbances and were quickly recovered from a Hot Standby state (i.e. load cycle). However, on August 4, 2020 there was a tremendous tropical storm in the CT area which lead to the loss of power at FCE's facility in Danbury for six days. At this time Module B tripped and cooled down, where it made a full thermal cycle. The facility delayed restarting the system due to some equipment failures from the power outage. Module B was heated back up and began ramping load on August 24th, 2020. Module B continued operation past 5000 hours (which was achieved approximately September 9, 2020) through October 14, 2020.

The same low-voltage cell blocks were evident and relatively stable during the 90% load hold (hours 500 – 1500 in Figure 6-9), while the majority of the cells were stable at the levels seen after the second sulfur breakthrough in Pittsburgh. Very slight overall improvements were seen as time progressed but nothing significant to suggest recovery of the catalytic activity from the two separate sulfur poisoning incidents in Pittsburgh. The lowest cell block began to show increased degradation around hour 1500 of Danbury operation, originally holding around 0.65 volts/cell down to ~0.6 volts/cell.

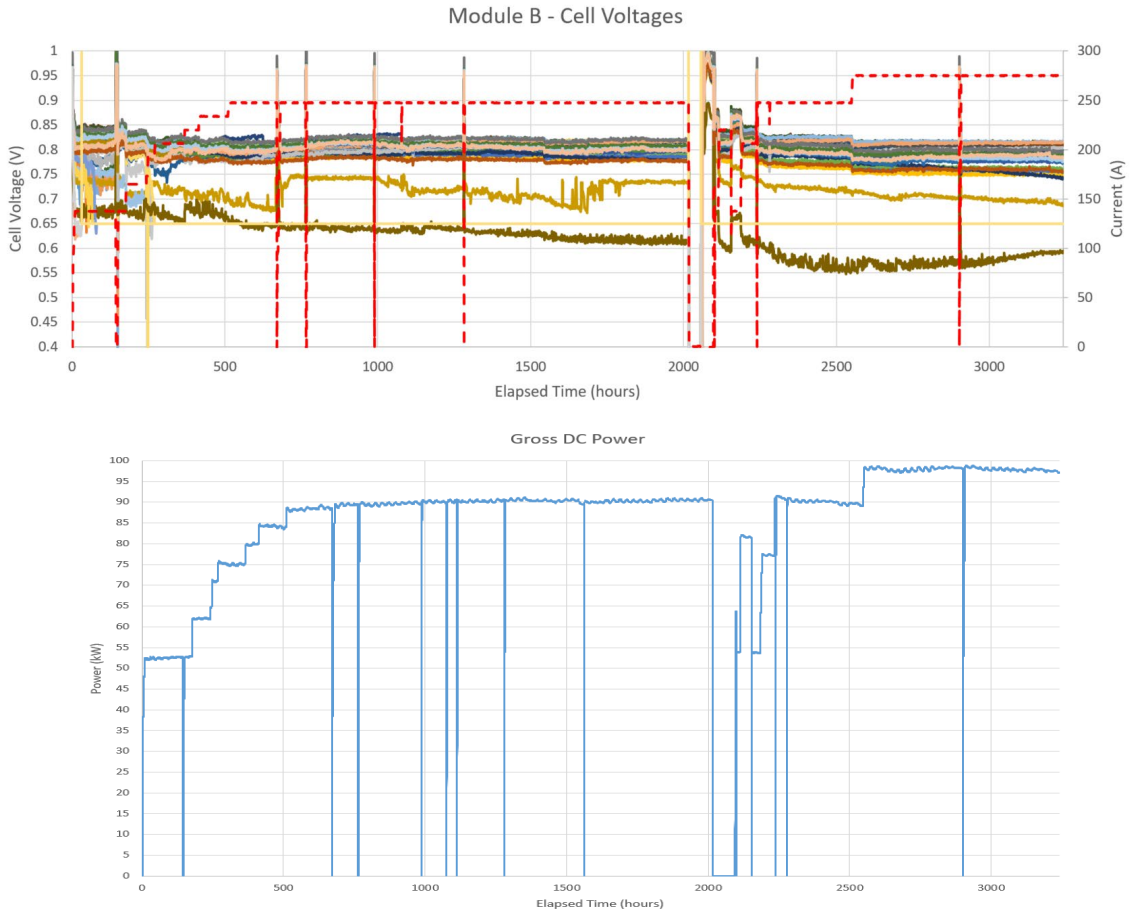

Figure 6-9. Module B Cell Voltages (*top*), Gross Power (*bottom)* – Danbury, CT

90% load was the operational target due to the sulfur poisoning in Pittsburgh, as the limiting factor in increasing load was the high stack temperatures as a direct result. This required a higher air flow to provide further stack cooling, which was still within the capacity of the fresh air blower. Around hour 1400 of the Danbury operation, the cathode inlet temperature was lowered by 10˚C which lead to more manageable stack temperatures and lower air flow in order to improve system efficiency. Once the 5000 hours were reached in September, the plant was brought up to 100% load and a majority of the cell voltages remained stable. The weakest cell group's performance worsened due to the thermal cycle caused by the loss of power from the tropical storm. This is evident in Figure 6-9 as the lowest cell group voltage eventually recovers to ~0.6 volts/cell where it was prior to the shutdown.

GC samples were taken from the system at 100% load operation as shown in

Table 6-2. Low levels of reforming were still evident due to the sulfur poisoning in the Radiative Fuel Reformer (RFR) but improved levels of stack reforming were seen compared to the previous 60% load GC's taken in May 2020. Figure 6-10 shows some temperatures around the reformer and stacks, which have been relatively stable at the same higher levels seen in Pittsburgh after the second sulfur breakthrough and further demonstrates no significant recovery from the sulfur poisoning.

Table 6-2. Module B 100% Load GC Results – Danbury, CT

9/28/2020 1-2 PM| 100% Load | 10.5 SCFM NG | 373 SCFM Air | 92% Anode Recycle					
% Composition - GC					
Sample	3	1	2	4	5
	Anode Module In (u/s RFR)	RFR 1st Pass	Anode In (d/s RFR)	Anode Out	Cathode Exhaust
H2	20.128	26.353	32.555	25.263	0.000
O2	0.000	0.000	0.000	0.000	17.068
N2	8.820	7.840	8.158	11.585	82.413
CH4	20.192	18.589	13.346	0.480	0.000
CO	8.707	8.069	10.501	10.802	0.000
CO2	41.758	38.936	35.353	51.870	0.519
C2H6	0.396	0.213	0.087	0.000	0.000
Total	100.000	100.000	100.000	100.000	100.000

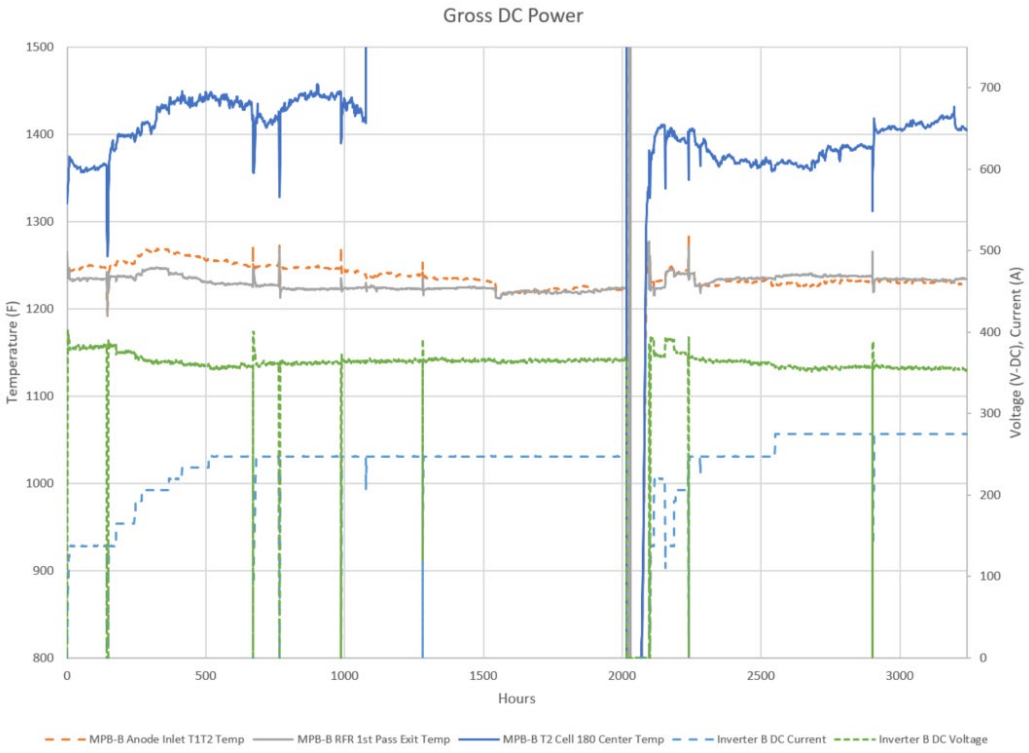

Figure 6-10. Module B Reformer/Stack Temperatures – Danbury, CT

During the 90% load operation at Danbury for Module B, gross fuel efficiency was ~58% instead of the simulated values of 64-65% and net fuel efficiency was well below target at around 36-38%. This was a direct consequence of the sulfur poisoning events in Pittsburgh. As shown in Figure 6-9 above, the average cell voltage for most of the cell groups is ~0.8 volts/cell, below the initial 0.85-0.875 volts/cell design. The sulfur poisoning also resulted in higher stack temperatures, increased air flow, and less cathode air preheater effectiveness. As a result of the increased air flow, which resulted in approximately 20-22% air utilization instead of the beginning of life target of 40%, the cathode air preheater was not capable of maintaining a cathode inlet temperature within a suitable range by itself. In order to make up the excess heat

duty, the startup electric heaters were required to achieve the desired cathode inlet temperature which consumed a total of approximately 8 kW. Figure 6-11 plots a “Projected Net Efficiency”, which is the calculated net efficiency without the added parasitic loads of the startup electric heaters. The projected net efficiency was 46-48% at these conditions.

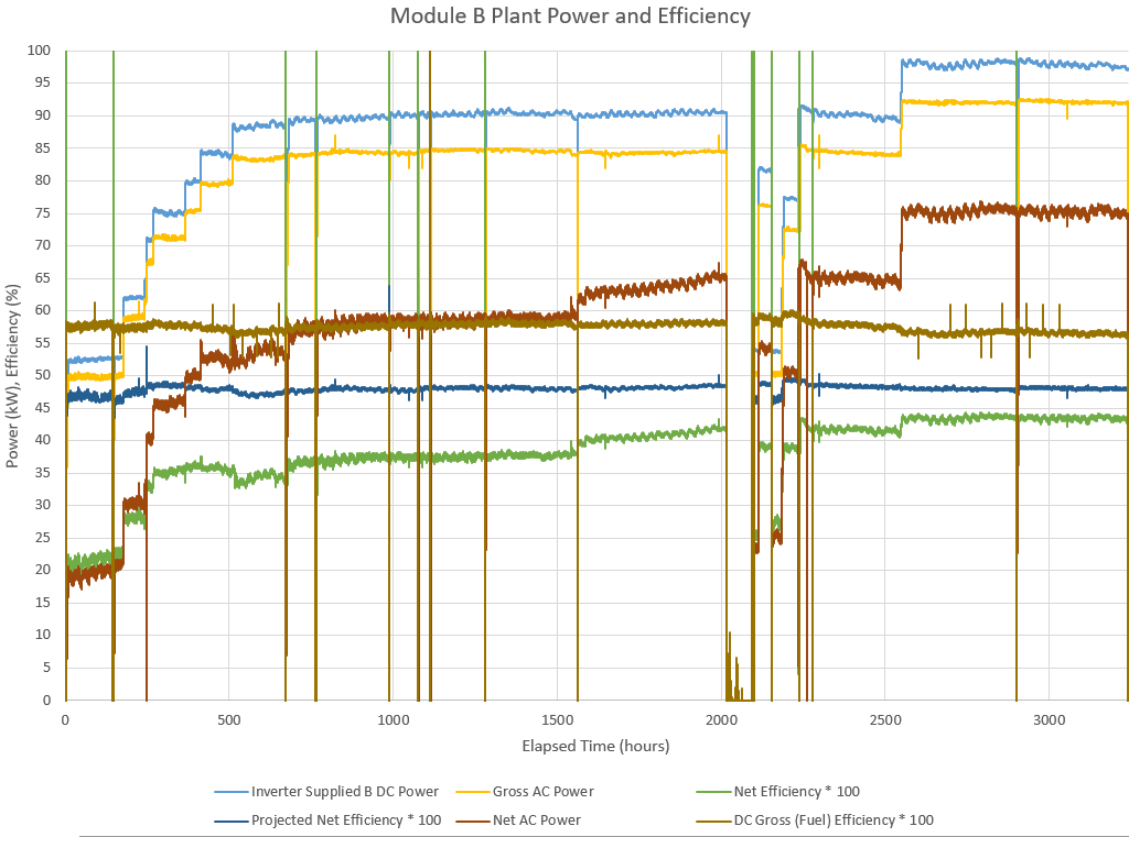

Figure 6-11. Module B Plant Power and Efficiency at Danbury Facility

Since Module B achieved milestone operation hot hours, the load was ramped to 100%. This was because the system could be monitored carefully as the load ramp held in case the temperatures of cell voltages had shown any further degradation. Figure 6-12 shows the same power plant and efficiency of Module B over the course of its full 5000+ hot operation between FAT, commissioning, Pittsburgh operations, and Danbury, CT operations. Holding at 100% load was stable for a couple weeks before the decision was made to begin cooling down the plant in order to prepare for future obligations with Mohawk Innovative Technology (MiTi) through sub-contract under project DOE - FE0027895 to operate the 200kW Reliable SOFC Module B with their high efficiency high temperature anode recycle blower. More on this project can be found in Section 10.

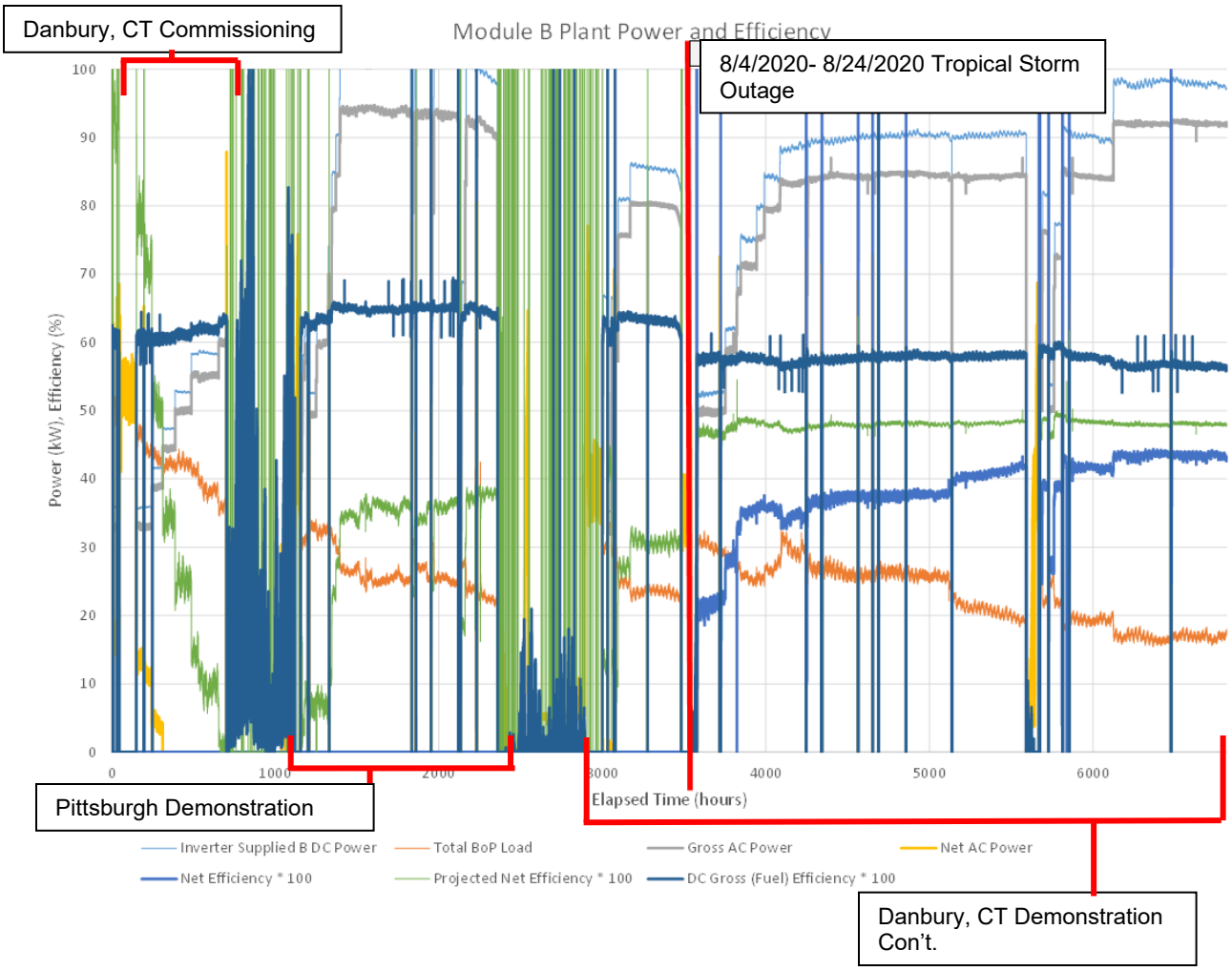

Figure 6-12 Module B 5000+ Demonstration Test Operational Data

7. POST-TEST STACK ANALYSIS

Module A was de-integrated inside FCE's facility. Temporary compression was established on each individual stack, and each tower was decompressed sequentially. All stacks were removed and five of them were crated for shipment to Calgary for post-test analysis, while the rest were stored and sealed in a separate crate for longer term storage. The five stacks sent for post-test analysis were selected to cover a wide sampling range after reviewing test data from Module A, which includes:

- Both flipped and non-flipped stacks
- Stacks with weak cell groups
- One stack with no low voltage cell groups (except single end cell)

Stacks are built and tested in a cathode down orientation. Due to the necessary voltage built up and polarities in the stack module, four of the eight stacks are mechanically flipped after conditioning for the module build. The flipped stacks are contained in Towers 3 and 4. The stack selection is outlined in Table 7-1. Module A Stack Selection and illustrated in Figure 7-1 (highlighted in yellow).

Table 7-1. Module A Stack Selection

Req'd Stack	Stack ID	Module	Tower Location	Flipped / Non-Flipped Currently	Rationale / Comments for Selection
1	GT060322 -0001	A	2B (lower)	flipped (+ or cathode up)	One of the lower cell groupings ~0.56V (32048)
2	GT060322 -0006	A	3A (upper)	Non-flipped (- or anode up)	One of the strongest stack overall with only the top cell (33001) low
3	GT059875 -0006	A	4A (upper)	flipped (+ or cathode up)	4A was replacement stack & interesting to autopsy as different test history
4	GT060322 -0003	A	4B (lower)	flipped (+ or cathode up)	One of the lower cell groupings ~0.66V (34084)
5 (Bonus)	GT060322 -0004	A	1A (upper)	Non-flipped (- or anode up)	2 low cell groupings in the same stack ~.740V, 0.840V (31048, 31084 respectively)

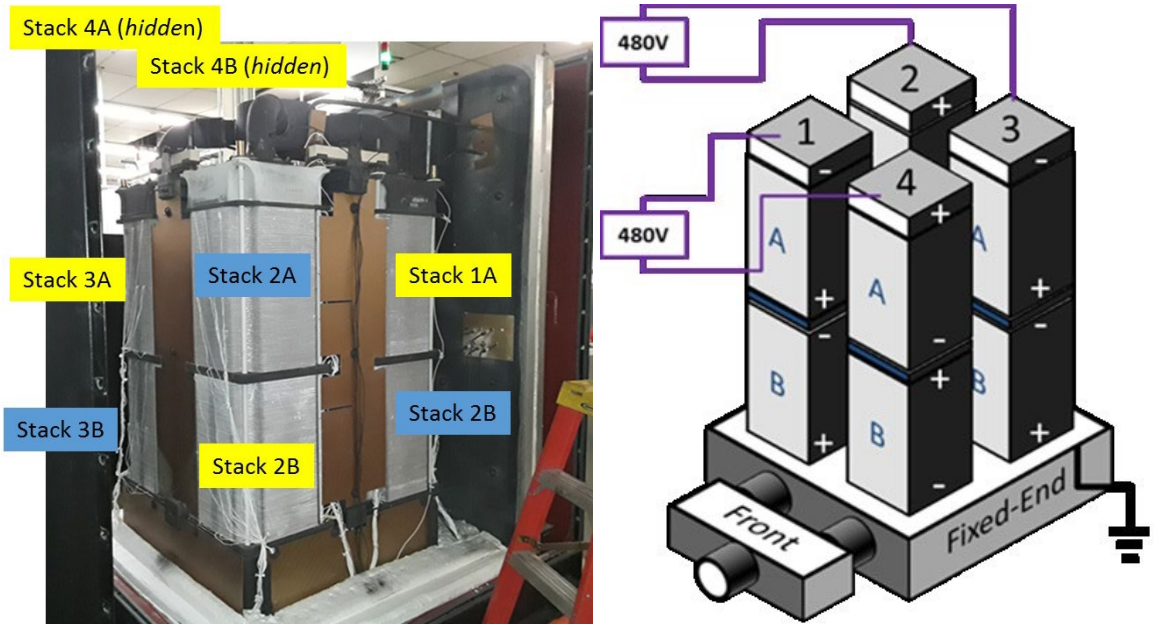

Figure 7-1. Module Configuration and Stack Selections

Analyses showed overall good electrical contact in all layers, no or small trace of carbon at the fuel inlets, and broken cells. Broken cells, which have been found in the low performing cells, were in pieces and oxidized (i.e. destroyed) or in a rounded crack. The round cracks are an indication of a mechanical root cause and is under further investigation. Stacks located at the top of the towers were severely damaged. The early hours of the initial factory acceptance testing proved to be detrimental as indicated by the direct comparison of the stack that was replaced to that of the new one prior to the Pittsburgh operation. Sulfur was found in the cells that operated in Pittsburgh, while the stack that only ran in Danbury showed no signs of sulfur. The analysis will be completed next quarter and detailed in a topical report.

Each stack was leak tested at three different times: i) after test at FCE Calgary (initial), ii) upon arrival at FCE Danbury (shipped) and iii) after completion of testing and shipment for post-test analysis at FCE Calgary (final). Leak rate was measured on the air side and fuel side then cross leak is determined. The table below shows the cross leak measurements for each stack at those

3 different times using air at 0.5 psid. The measurement are slightly lower after shipping due to different measurement apparatus and testing conditions.

Table 7-2. Leak Test Measurements (in SLPM)

Stack*	0001	0002	0003	0004	0005	0006	0007	0008	New
Initial	5775	5060	6525	5345	5310	6295	6206	5435	4505
Shipped	4810	4220	5440	4450	4430	5250	5170	4530	3898
Final	-------	16035	-----	Over	6945	-------	7140	12980	10940

*All 8 stacks are GT060322-xxxx. “New” stack is GT059879-0006

The final leak rate measurements were recorded for 6 stacks that were analyzed. Stacks -0005 and -0007 had a small increase whereas the 4 other stacks had their leak rate double or triple indicating a damage in those stacks.

STACKS AUTOPSY

All eight stacks plus the replacement stack were shipped back to Calgary. Upon visual inspection, the stacks did not show any outer damage. After leak test measurement was taken, the stacks were taken apart layer by layer while recording all observations. Common general features between stacks were:

- Very little to no solid carbon deposit at fuel inlets.
- Good contact on all layers.
- Many broken cells.

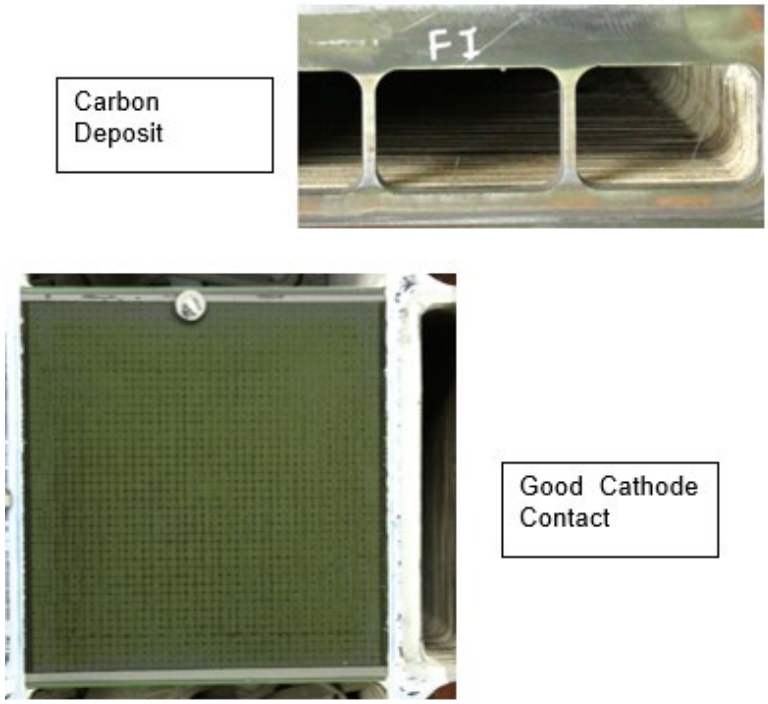

Figure 7-2 Common observations

The number of broken cells was high in some stacks (i.e. those with high leak rate). Cell breakage can be grouped in two different categories following the shape of the cracks and the severity of the damage:

- Rounded crack: this type of crack typically indicates a disruption of the mechanical stability of that layer.
- Destroyed: The origin of the damage is more difficult to determine. It could be similar to the first type but cracks were numerous that led to oxidation of large area of the cell.
- Other: This group includes cells with very small crack at cell edges or almost a straight line crack type. There were a small number of cells in that group and this could have happened at later stage in the testing.

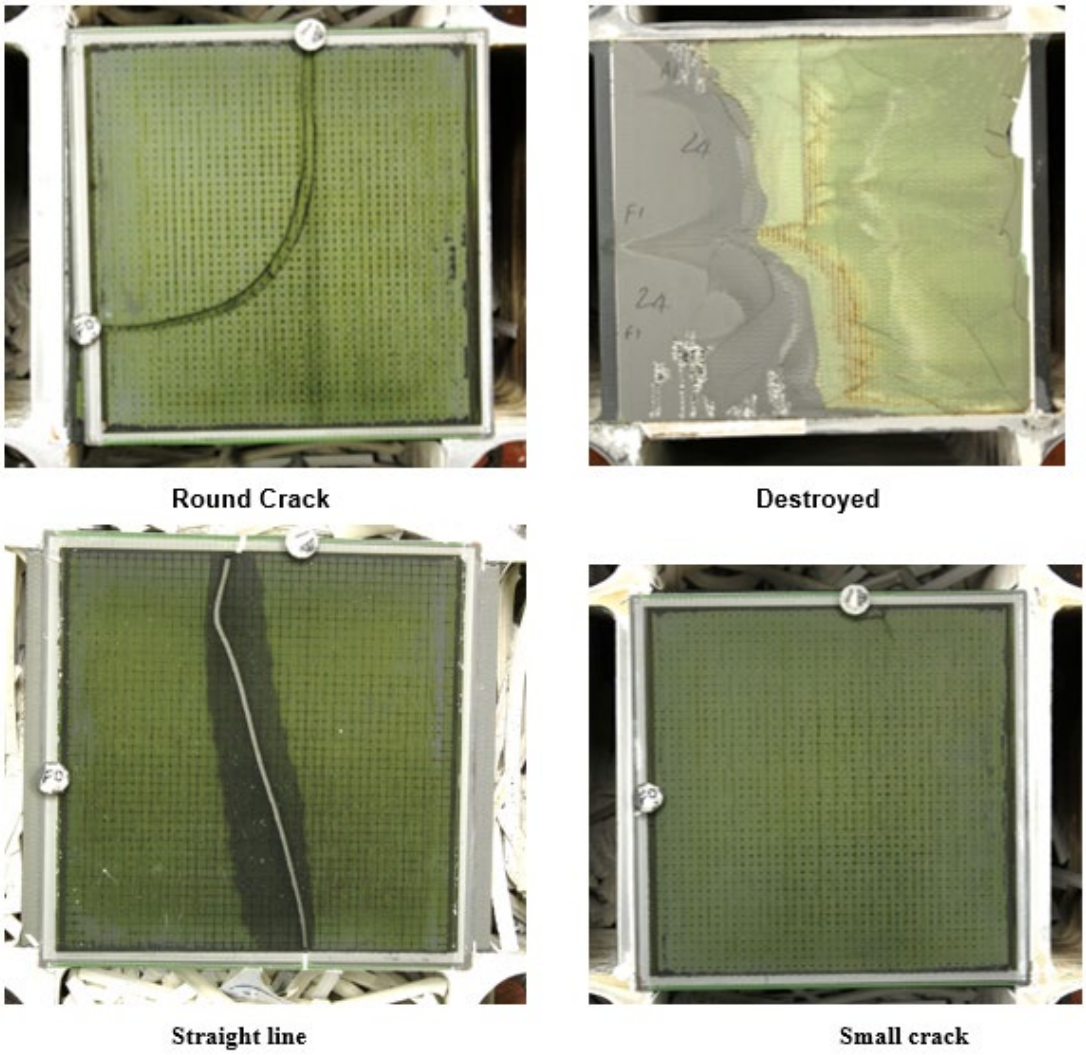

Figure 7-3 Types of cell damage seen in stacks

Table 7-3 Number of Broken Cells in Stacks

Stacks	Position	Broken Cells			
		Round	Destroyed	Other	Totals
GT060322-0002	4A Replaced	4	2	1	7
GT059789-0006	4A New	1	0	3	4
GT060322-0004	1A	8	4	3	15
GT060322-0005	3B	0	0	0	0
GT060322-0007	1B	0	0	0	0
GT060322-0008	2A	5	4	1	10

The replacement stack GT059789-0006 that was incorporated after 900 hours had 4 broken cells, and none of them were “destroyed”. The replaced stack (GT060322-0002) and 2 other autopsied stacks (GT060322-0004) and (GT060322-0008) had many broken cells with some of them “destroyed”. This indicates that initial testing events were destructive.

It is interesting to note that two stacks (GT060322-0005) and (GT060322-0007) with bottom position in towers had no broken cells.

CELLS ANALYSIS

Cross sections of broken cells were analyzed by scanning electron microscope (SEM). No manufacturing-type damage or defect was observed in those cells. Electrolyte layers were dense and with even thickness. Cell breakage was not related to cell fabrication or structure issues.

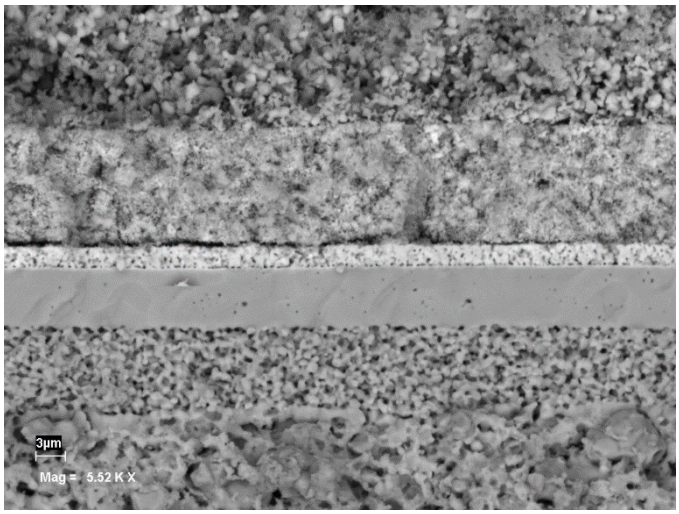

Figure 7-4 Cell Cross Section

SULFUR

Cross sections of broken cells were analyzed by Energy Dispersive Spectroscopy (EDS) to determine if any material reaction or any foreign element in the cells.

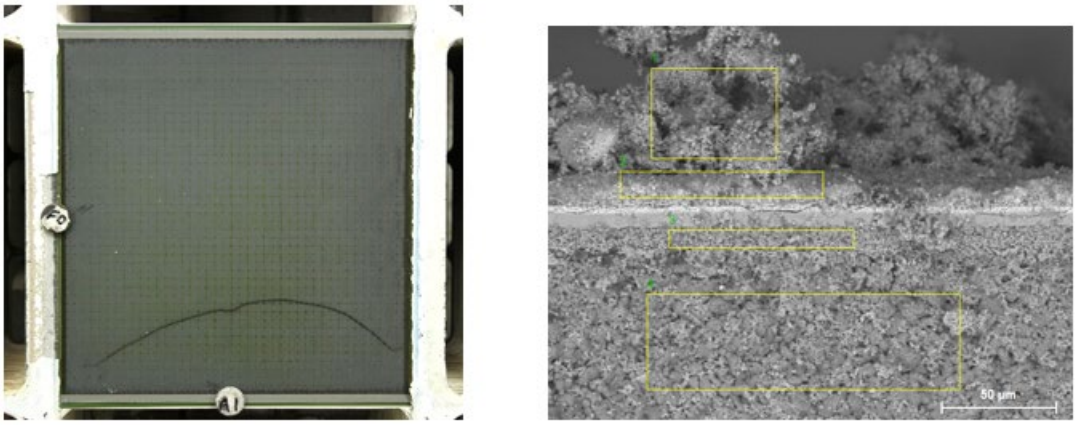

Figure 7-5 Cell 59-GT060322-0002

EDS results of cell 59 in stack GT060322-0002 (replaced after 900 hours of testing) did not have any sulfur on the crack surface. Some Nickel oxidation in AFL due to combustion was observed.

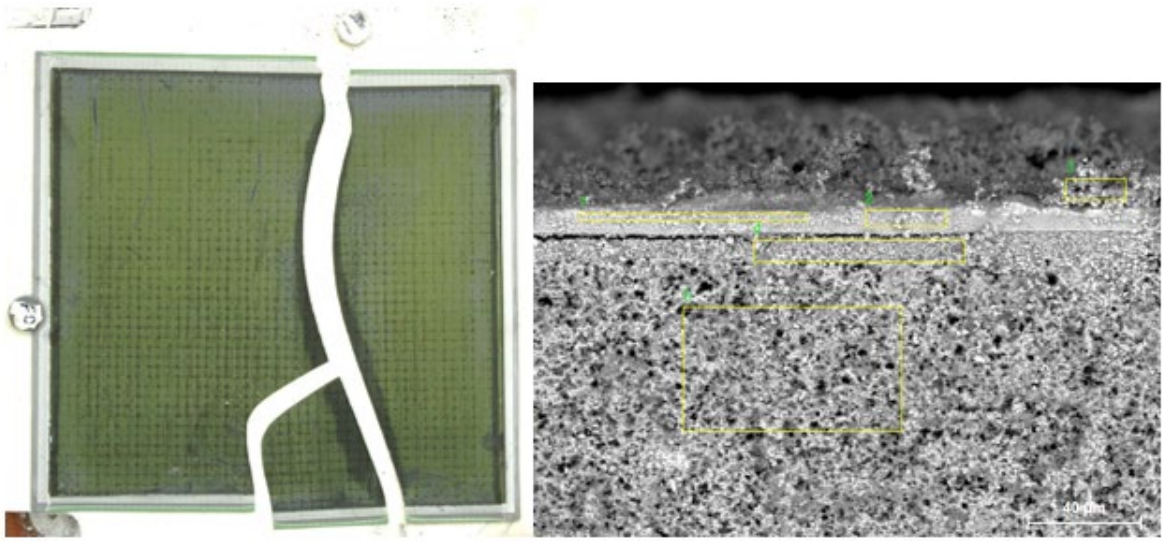

Figure 7-6 Cell 48-GT059879-0006

EDS results of cell 48 in stack GT059879-0006 (replacement stack, introduced post 900 hours of testing as replacement for GT060322-0002), showed presence of sulfur and oxidation of Nickel in anode. Similarly cells from other stacks had sulfur on the crack surface. All those stacks were tested in Pittsburgh and it confirms the sulfur breakthrough that occurred during the Clearway testing that affected the fuel cell performances.

ROOT CAUSE ANALYSIS

The main failure of the stacks in the module is the high number of broken cells. There were some system balance of plant component failures in the module test early on that may have created some damage or at least introduced an unplanned shutdown. From a review of the testing and the number of broken cells, most of the damage seems to have occurred early in the test. Also, the bottom stacks were not very affected; two of them did not have any broken cells.
The Figure 7-7 fishbone diagram lists all possible areas from cell, stack, compression system and testing that may have caused the high number of broken cells.

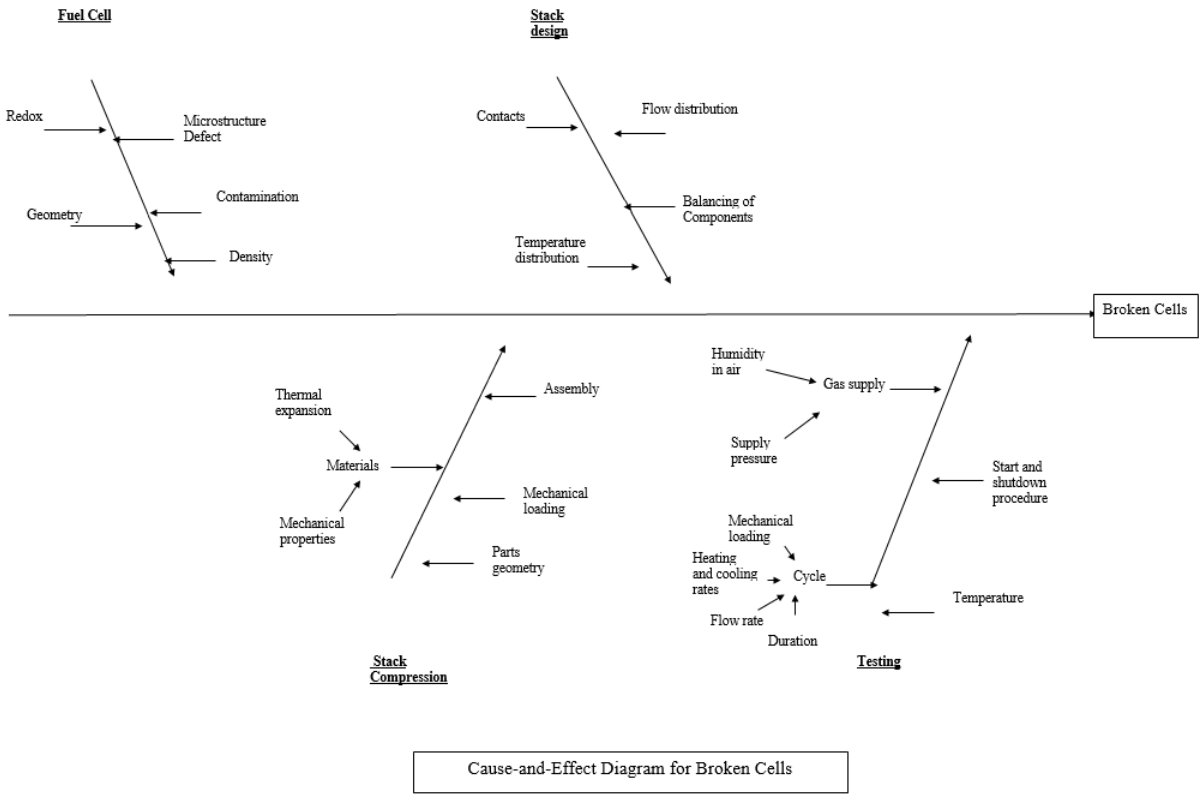

Figure 7-7. Fishbone Diagram for Broken Cells

Discussion

The Cause Effect diagram helps in looking at main contributors to the high number of broken cells and eliminate some of them after reviewing the testing results and post analysis observations.

Fuel Cells

The first category is “The Fuel Cell”. As mentioned above, cross sections of the cells and their analysis did not reveal any defect or foreign material. In fabrication, cells go through a thorough quality control program and follow strict criteria for acceptance. All data is recorded. No anomaly was found in cells geometry or density.

During the Module A system FAT, a fuel line was leaking and air was introduced in the fuel stream. This may have caused some oxidation and an abnormally high level of redox in some cells. Although, examination of broken cells did not show typical redox cracks that are usually very thin (hairline) at the fuel inlet edge of the cells and parallel to the fuel direction. The absence of those typical cracks eliminate Redox as main contributor of broken cells.

Stack

The second category in the Cause Effect diagram is “Stacks”. The design, build and conditioning of the stacks are very important in maintaining the mechanical stability of the fragile ceramic fuel cells. The selection of the components and the stack build follow strict quality criteria and procedures. Stacks went through acceptance testing including leak test which all stacks passed. Also among 6 stacks that were analyzed, two of them did not have any broken cells. So no issue with stack balancing or stack components are likely leading to broken cells.
Flow distribution and temperature distribution during FAT, may have caused some disruption. Particularly during heat up and cool down.

Compression System

The third category is “Compression system”. The compression system of the stacks consists of a rod and spring bolted at four corners of each stack tower. The assembly rod + spring is supposed to maintain a constant stack compression at every stage of the testing. Any overloading may cause breakage of cells and any loss of compression may lead to loss of contact. All four stack tower corners are supposed to be evenly loaded.
The material selection of the rod material is Inconel 718 a precipitation age hardening Superalloy. The long-term operating temperature is recommended to be maximum 1200F as the material can go through some changes that affect its stability at high temperatures. So the use of Inconel 718 can be risky.

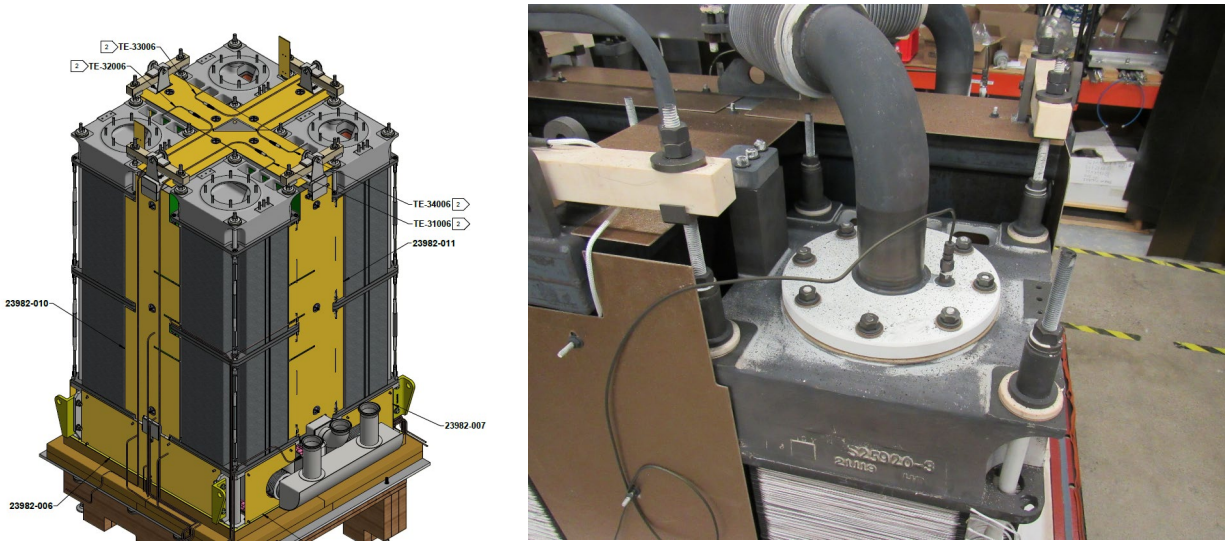

Figure 7-8 Compression System of Stack Towers

The other concern with the compression system is its assembly with other system components. Ideally, the stack compression system should be independent and free from other components and loading the stacks only. In the above picture, Figure 7-8, the rods are bolted to the exhaust plates that are connected to piping. Also two of the rods are connected by a ceramic bar to Radiant heat exchanger that will add weight and a variation in thermal expansion. It is adding a number of factors to thermal expansion matching between the rods system and the stack components. In summary, this type of mechanical design make the top of the tower less mechanically free to move and adapt to changes in the stack tower temperatures.

Testing

The last category in the Cause Effect Diagram is “Testing”. When comparing testing history and post-test analysis observations, it looks like events in the first hundreds hours of system FAT testing in Danbury were damaging to some stacks. The critical part of the testing is cool down and heat up. During FAT testing, the cool down followed three different procedures with some modifications each time:

Type A Recycle Cool down:

1. Electric heaters turned off, air flow to 225 scfm and cool at 70F/hr. Reformate and steam flowing until temperatures cool to ~550F (287C).
2. Steam and reformate turn off and Cover gas (4%H2N2) flows.
3. Turn off all fuel gases when all stacks drop below 450F (232C).
4. Turn off air when stacks are below 150F (66C).

Type B Non-Recycle Cool down:

1. Electric heaters, steam, fuel and anode blower turned off, air flow is 225 scfm and cool at 70F/hr.
2. Cover gas is flowing until the stacks drop below 450F.
3. Air flow stops < 150F.

Type C (Shutdown/ESD):

1. Cover gas (4%H2N2) flows and fuel side with ~2 scfm air purge air side for entire cool down to room temp.

Ideally, stacks should be cooled down using Type C but with reasonable flow of air down to room temperature to protect the cells.

CONCLUSION AND RECOMMENDATIONS

The system testing at Clearway NRG was successful hitting all required criteria. The two modules A and B had different performance. Module A had more issues first starting during FAT testing in Danbury. Premature ending of testing of Module A generated the interest in performing a post-test analysis and looking into a number of stacks from that Module. Common and general observation were collected and the main one was the high number of broken cells. The type of breakage was pointing to a mechanical cause. It was also noted that two of the bottom stacks had no broken cells.

After reviewing the testing data and performing a root cause analysis, few concerns were determined:

- Material selection of the rod in compression system. All materials in the hot zone of the module need to be stable for long term operation at 1400F.
- Loading the stack compression system with other system components mechanically. It is recommended to free the compression system from other components and ideally load the stack towers only.
- Different cool down procedures. Thermo-cycling is always a critical part of testing as the mechanical and material stability of the stack and its components can easily be disrupted leading to contact loss or cell breakage. A common safe cool down and heat-up procedure need to be adopted.

Another cause of low performing cells in Clearway testing was presence of Sulfur in gas feed. Sulfur affected both reforming and cells performance as seen present in cells crack surface.

8. LESSONS LEARNED

FACTORY ACCEPTANCE TEST

The Factory acceptance test (discussed in sections 4 &5) lead too many lessons learned that were able to be immediately implemented into the SOFC power plant system. Some lessons include utilizing a more meticulous checkout procedure prior to buttoning up the modules, including more intensive leak checks and resistance checks across the stacks. More detail can be found on the items below in section 5.

- Instrumentation Lessons
    - Voltage lead ground shorts found on MPB-B Tower 3 and Tower 4 lead to terminal blocks that were replaced with simple crimp-on snap plugs.
    - An in-cell TC ground shorts was found on MPB-B Tower 3 due to exposed TC wires near the quad base and all exposed/faulty in-cell TCs were removed.
    - Pressure sensing tube (Anode fuel) was disconnected inside the MPB-A enclosure and was reconnected/tightened
    - Multiple process TC's failed, and were replaced with more robust designs
- Anode recycle blower Lessons Learned:
    - Anode Recycle Blower seized due to differential thermal growth between impeller and casing during hot restart. This was solved with control logic implemented to limit blower ramp rate on restart and a design change implemented by the vendor to increase internal clearances
    - Anode Recycle Blower exhibited a crack/leak in the casing. Which lead to another design change implemented by vendor to strengthen casing.
- Initial testing showed weakness in MPB-A Tower 4-Upper
    - Swapped out with the spare stack
- A flexible hose feeding air to MPB-B overheated due to backflow of hot cathode gas caused by a pre-existing leak (poor seal between the hose and pipe) and closure of an upstream valve. The flexible hoses were replaced with SST flexible hoses with welded sanitary clamp connections.

REACTIVATION AIR SYSTEM

The reactivation air system's purpose in the BoP is to remove heat from the module and redirect it to the desiccant air dryer to reactivate the desiccant material used to dry incoming cathode air. The temperature of the hot reactivation air from the module that returns to the desiccant air dryer is controlled using a module bypass line that mixes cooler (unheated) air with the hot air from the module. The hot air (before the mix point) was near the upper end of the high temperature flexible hose's limit during normal operation. In order to allow for additional margin, a new corrugated stainless steel hose was designed, which can handle much higher temperatures. This allows more flexibility in the operating temperature of the anode recycle loop if desired; by allowing the operating temperature to be higher, reactivation air flow (and reactivation air blower power consumption) will be lower.

Having comprehensive process models of the 200kW prototype system helped diagnose issues in the BoP during testing. Models proved especially helpful when identifying issues with the desiccant system. The plant operator noticed that the reactivation air blower was operating at a higher speed than predicted by process modeling. After much troubleshooting, the root cause

was determined to be internal cross-leakage between the reactivation and cathode air streams within the desiccant system. The desiccant system was removed from the BoP and FCE technicians worked with the desiccant manufacturer to identify the locations where cross-leakage may occur. Additional sealant was applied to these areas and the desiccant was then re-integrated onto the BoP.
However, hot temperatures persisted and this resulting in the turning off of the desiccant system for a majority of the demonstration test. With better knowledge of available customer equipment and a better understanding of how the process models vary from what was seen during demonstration, a more effective desiccant system will be achieved.

MODULE PURGATORY ZONE

The compact product design of the 200kW Reliable SOFC system lead to hot temperatures within the electrical cabinets and air system. Module B experienced an issue with one of its electric heaters, which prompted the module to cool down. FCE personnel traveled to the site (Pittsburgh) to troubleshoot this issue, which was determined to be a failure of the SCR (silicon controlled rectifier), i.e. heater controller. The root cause was due to excessive temperatures in the electrical cabinet located in front of the module that housed the SCR. A design solution to install insulation panels and additional exhaust ports near the back of the electrical cabinets was implemented on both modules, which significantly reduced the temperatures inside of the cabinets. A heater controller was replaced inside one of the cabinets, which failed during operation due to the high cabinet temperatures.

CATHODE AIR PRE-HEATER

The BOP design of the SOFC Reliable System implements a catalytic cathode air pre-heater (CAP) that is designed as a priority heat exchanger to provide a majority of the cathode heat exchange, for on-load operation and especially during plant heat up. The hot side design of the CAP also has an oxidation catalyst coating to obtain more recuperative heat from the fuel cell anode/cathode exhaust.

The CAP was sized with process modeling for 40Ua (air utilization) during normal operation. Although stack cooling requirements during demonstration testing had air flow increased because of the sulfur breakthrough event, running closer to 20Ua on average. The increase in air flow made it so the cold side temperature control of the cathode fresh air was unable to achieve its target temperature. Because this would result in a low cathode inlet temperature, additional heat was from the electric heaters intended for start-up operations. With such operational data from the demonstration test, and future plans for a much less thermally dense CSA stack design (section 8), a wider range of conditions can be more accurately anticipated and incorporated into the cathode heat exchange design.

9. RESEARCH & TECHNOLOGY GAPS

CSA STACK DESIGN

The main research & technology gap is the LSA stack design used in the 200kW Reliable system in terms of power density and manufacturing cost. When considering the relative comparison, the newly designed CSA stacks under multiple previously mentioned projects including Next-Gen SOFC are driving a comparatively more efficient module.

Compression System

The CSA stacks have a different design from the LSA stacks that use an integrated compression system that eliminates system level compression system for design and structural simplifications. The integrated compression system is also easier (faster) to assemble.

This spring-like stack core design's construction is also well able to manage thermal and pressure transients while maintaining electrical contact on unit cells.

Higher Power Density Design

A simple, yet critical cost and operation impact is the CSA design is it's relatively higher power density (a 6 or 7-fold improvement) design. With a higher power density, and overall less thermal mass per stack. With stacks that hold less thermal mass the hope is to lower air flow requirements (operation at higher air utilization percentages). This would decrease all the air side hardware sizing and cost. However, this has not been successfully demonstrated this yet.

A more compact module means less insulation. Insulation can be a relatively large expense for such high temperature operations of solid oxide fuel cells. Also, a smaller module with less thermal mass compounds savings by: requiring less thermal energy to heat of the module relative to the LSA stack, lowering the heat duty requirements of the surrounding module heat exchangers or the possibility of removing certain heat exchangers; especially those used primarily during start-up/heat-up steps. Also with reduced thermal mass (faster heat shedding), resources would be saved requiring less cover gas due to a smaller window of higher temperatures where the module is at risk of oxidation without cover gas.

A smaller module footprint would also have a more compact packaging meaning less material (i.e. piping, framing) in the module for cost savings.

Anode/Cathode Seal

The CSA stack design has improved glass seal that is near hermetic further preventing anode/cathode leaks. By retaining the seal between the anode and cathode; less cover gas is required from the BOP during certain plant heat-up steps, and hot plant load upset conditions. This transition to near-hermetic glass seal technology from sliding ceramic type seals further enables pressurized operation, minimizes gas leakage (and extra heat) and is able to produce high quality hydrogen in electrolysis operation.

Site Installation & Maintenance

The CSA stack design is physically smaller and the lighter modules makes it easier for on-site assembly. Currently other project plant layouts utilizing the CSA stack design eliminate the requirement for cranes during installation saving lot of time and expense.

Granular (stack or string level) power control would allow current control of individual stacks. Such an improvement would allow each stack/module to be able to perform to their peak efficiency based on stack life contributing to cell degradation. This could offer up to 50% - 100%

longer useful system lifetime. Also, the generally higher voltage, lower current configuration, makes for easier power electronics.

The CSA within the future SOFC power plants would be a relatively good fit with existing and cost optimized solar inverter technology.

Stack Manufacturing & Assembly

All CSA stacks are robotically built, and many of the manufacturing steps either have automation/ semi-automation as part of current manufacturing or near term future. Repeat parts are the same diameter as CD/DVDs allows for ease of robotic manipulation and processing.

Other SOFC Projects

As mentioned in the CSA anode/cathode glass seal improvement, the new stack design can be used amongst a wide variety of fuel cell applications. This includes high-pressure power generation, electrolysis, and reversible modes of operation. With relatively small active area and pseudo-counter flow geometry there is a wider operating window and flexible operation on reformate as well as pure hydrogen fuel for fuel cell operation and also well manage endo- and exotherms of electrolysis operation.

Conclusion

Now that we are testing at full height, the key gaps are to realize the unit cell technology capability (voltage, lifetime, reliability, etc.) at the stack level. There are challenges here seeming regarding misdistribution of thermals and flow distribution still to be addressed within the CSA stack. In addition, we have yet to test a multi-stack module, and there is much work to do here. Cell yield is still unacceptably low (<50%), and needs to be improved. Some of this has to do with the dimensional requirements that the CSA design imposed on the cell; however, additionally a better understand is needed to refine the cell manufacturing processes.

10. STEPS FORWARD

Despite the 200kW Reliable SOFC System reaching the end of its 5000 hour demonstration testing, there is still more to learn on the horizon. By levying the existing plant equipment, FCE is always looking for strategy's to move SOFC and energy technology forward. Work on other DOE FE awarded projects and working with other businesses/vendors to increase future product equipment reliability.

MOHAWK INNOVATIVE TECHNOLOGY (DOE FE0027895)

In the short term FuelCell Energy, Inc. is sub-contracted under Mohawk Innovative Technology (MiTi) Blower to work on DOE project FE0027895. FCE's involvement will be limited to the installation of MiTi's high temperature high efficiency blower. The blower will replace the Anode recycle blower, and the MPB-B 100kW section of the Reliable SOFC system with a goal of 1000

hours of demonstration operation. As data is collected from the anode recycle blower, FCE will generate a CSV file of data for Mohawk. Work under this project will help verify more reliable equipment for the future of SOFC Reliable system as a potential commercial product.

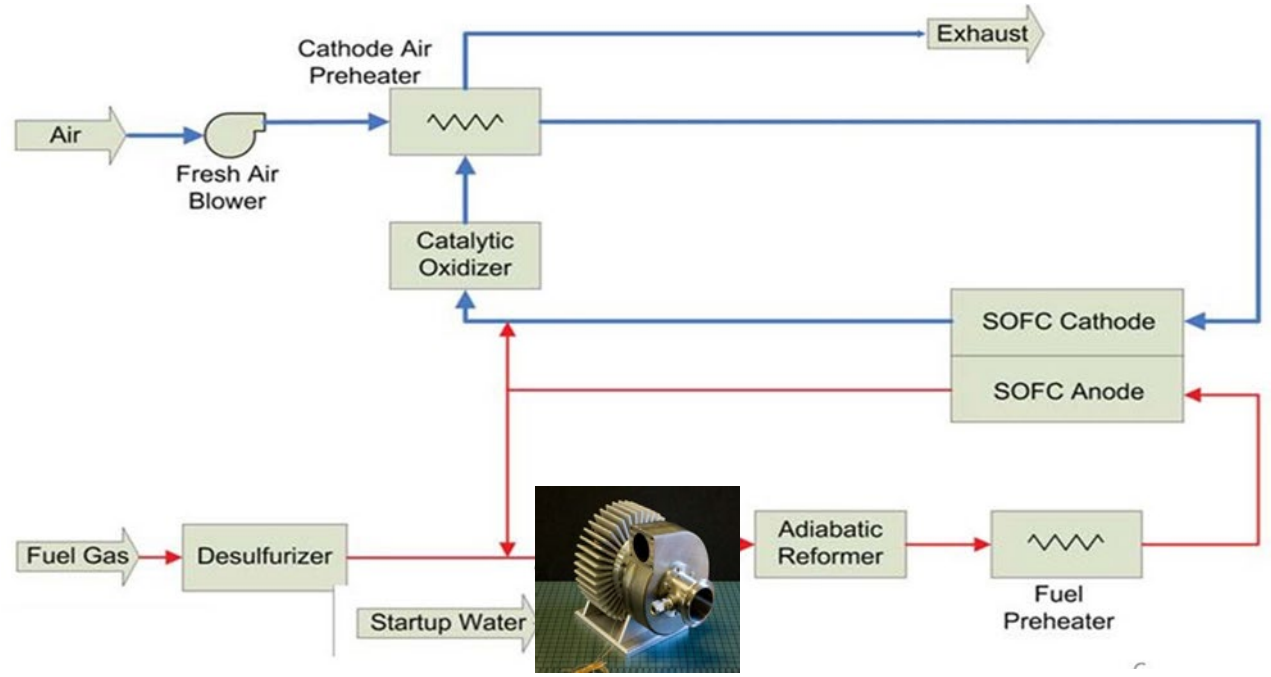

Figure 10-1 Simplified 100kW Block Flow Diagram with MiTi Blower

MW-CLASS SOFC PILOT SYSTEM DEVELOPMENT

Under DE-FE0031639 FCE is working on 1MWe-class distributed generation (DG) applications in the 2020's timeframe. The specific project objectives are to develop the conceptual design of a MWe-class SOFC power system, and to complete a techno-economic analysis (TEA) to demonstrate that the system can meet a cost target of ≤$6,000/kWe at low-volume production levels. The nominal 1 MWe system will utilize FuelCell Energy's next-generation of reliable and low-cost SOFC cell and stack technology that is the compact stack area (CSA) design. The module design change has minimal impact on the surrounding SOFC system balance of plant. Only minor changes to the BOP process may occur, because the same fuel and air requirements are present in the CSA design the same control strategy can be leveraged for the larger plant. Equipment sourcing and selection also becomes heavily based on existing equipment vendors and lessons learned from demonstration testing, referred to in Section 7. Plant layout can also use insight from the existing SOFC system layout to create a efficiently packaged system. Figure 10-2 & Figure 10-3 below is the current preliminary CAD model layout design for the 1MWe-class SOFC Power Plant, utilizing the CSA stack design in 40kW module sizes, grouped together in 250kW hot BOP sub-systems.

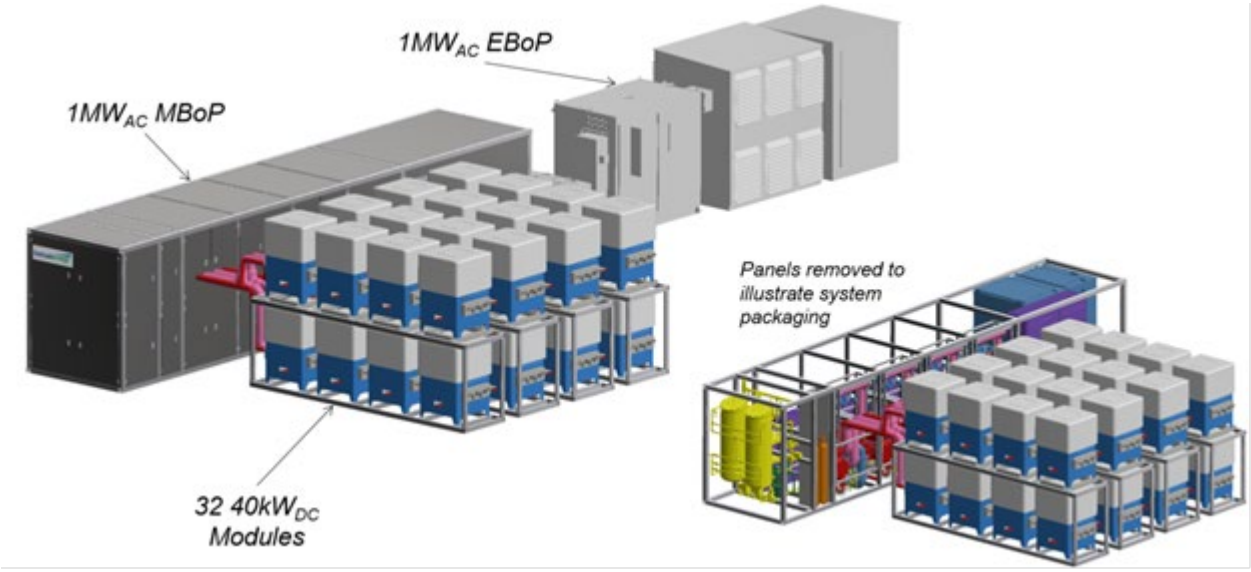

Figure 10-2 3-D CAD Model Layout of 1 MWe SOFC Plant, 40kW$_{DC}$ Modules

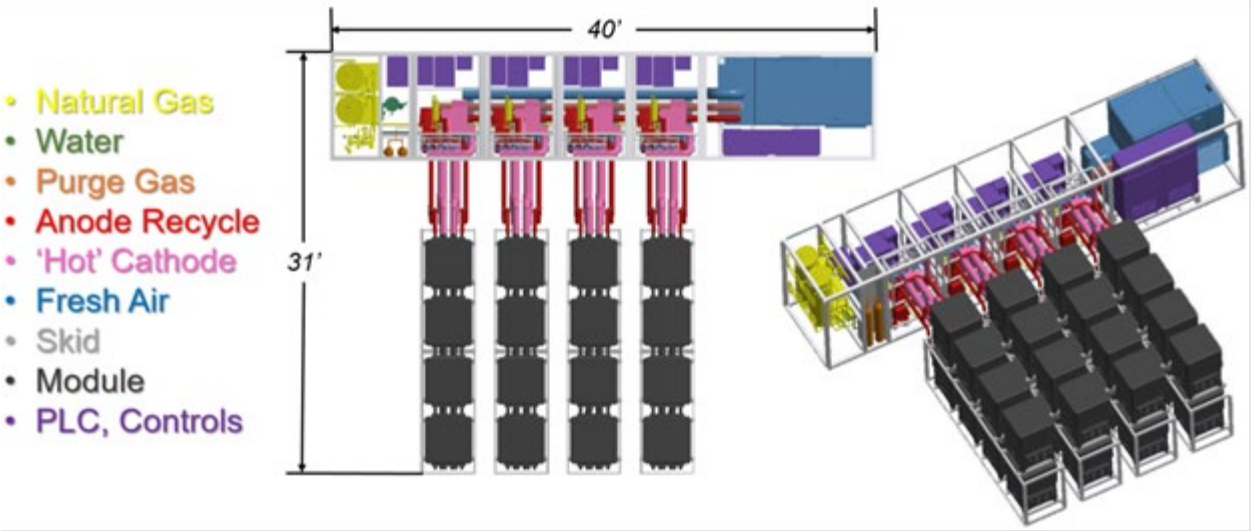

Figure 10-3 3-D CAD Model Layout of 1 MWe SOFC Plant, 40kW$_{DC}$ Modules

The project requires the conceptual design of a MWe-class SOFC pilot distributed generation system, design a compact low-cost stack module building block based on 2nd-generation SOFC technology, and to complete a TEA showing MWe-class system cost ≤$6,000/kWe.

11. STACK & SYSTEM COST ANALYSIS

The power block and stack capital costs will be estimated for mature market production of the fuel cell system (excluding coal gasification, syngas clean-up and CO_2 separation subsystems, if applicable), and de-escalated to 2011 dollars for easy comparison with DOE targets. The system will be based upon the power block of the FCE's ≥100 MWe Integrated Gasification Fuel Cell System with CCS, which was developed under previous cooperative agreements with DOE.

The IGFC system configuration includes a low-temperature catalytic gasifier, humid gas contaminant removal processes, a near-atmospheric pressure SOFC power block, a steam bottoming cycle, and provisions for CO2 purification and compression. The systems analysis will be updated based on the SOFC stack performance at NOC realized in the 200 kW prototype system test.

Objective:

- Estimate SOFC stack capital cost for use as the basis for fuel cell system power block capital cost

Approach:

The denominator for the calculation of stack cost ($/kW) will be the net AC power of the IGFC system. FCE will also characterize the stack cost based on peak power. The cost estimate will be performed in accordance with the "Stack Metric Test and Cost Estimation Guidance", included in DE-FOA-0001244 Section I-C.

The cost estimate will include the following fixed and variable cost elements:

- Equipment and Plant Depreciation
- Tooling Amortization
- Equipment Maintenance
- Utilities
- Indirect Labor
- Cost of Capital
- Manufactured Materials
- Purchased Materials
- Fabrication Labor
- Assembly Labor
- Indirect Materials

The following costs shall not be included:

- Research and Development
- Sales and Marketing
- General and Administration
- Warranty
- Taxes

Results & Discussion:

FACTORY COST ESTIMATE

FCE updated the Factory Cost Estimate of a 671.8 MW high efficiency IGFC system that was developed previously under DOE supported cooperative agreements DE-FC26-04NT41837 and DE-FE0011691. The cost updates reflect the latest stack design and manufacturing improvements to align with the current stacks utilized in the prototype system. The cost year basis was also adjusted from 2007 USD to 2011 USD. The updated SOFC stack cost estimate for a 120-cell stack block is 212 $/kW (based on net AC output from the system) and the total

power island Factory Equipment Cost is 681 $/kW, assuming a high volume stack production rate of ~250 MW per year. Both costs are lower than the DOE cost targets of 225 $/kW and 900 $/kW for stack cost and power island Factory Equipment Cost, respectively.

A detailed update of the Large Area Stack (LAS) SOFC Factory Cost Estimate was developed. The stack costs were then incorporated into FCE's previously-developed large-scale (≥100 MWe) high efficiency Integrated Gasification-Fuel Cell (IGFC) power plant techno-economic analysis. Prior to this report under DE-FE0011691, FCE released a Topical Report - Baseline Plant SOFC Stack Block Factory Cost Estimate Rev.1 (February 23, 2015), which included bottom-up techno-economic analyses to estimate stack production cost ($/kW$_{system\ net\ AC}$ [2011 $]) at volumes of >250 MW/year. In this previous report, the 120-cell stack was projected to cost $4,748 (2011 USD) at a production volume of 53,760 stacks per year. This cost translated to $241 per kW DC gross stack (based on stack nominal power rating of 19.69 kW DC gross) or $189 per kW AC (applying the Net AC to Gross DC ratio of 1.272) which is lower than (and hence surpasses) the DOE cost target of $225/kW AC (2011 USD). FCE reviewed this previous estimate in detail and updated the stack design and manufacturing process assumptions to align with the current stacks utilized in the 200 kW demonstration system. The stack and IGFC system cost estimates are discussed in the following sections.

FUEL CELL STACK COST BASIS

The updated Factory Cost Estimate for Solid Oxide Fuel Cell (SOFC) used the same large area stack basis as previously discussed, that is, the SOFC stack block features an internal manifold design and consists of 120 TSC-3 cells (550 cm^2 cell active area) and generates 19.68 kW DC (gross) at nominal power conditions (normal operating conditions of 298 mW/cm^2). The high level parameters and assumptions for stack block cost are shown in Table 11-1. The analysis framework is identical to the previous report, where the only difference is the assumption surrounding the building space areas. The new calculation was computed based on the total equipment footprint plus 200% for additional work space area.

Table 11-1. Stack Cost Derivation Parameters

Physical Characteristics	Value	Units	Notes
Cell substrate area	645	cm^2	
Active area	550	cm^2	
Cell substrate thickness	0.6	mm	
Cells per stack	120		
Half cell weight	193	g	
Power Characteristics			
Cell power density, nominal	0.2985	W/cm^2	
Cell power density, peak	0.2985	W/cm^2	
DC power output, nominal	19.70	kW	
DC power output, peak	19.70	kW	
DC power output, nominal per cell	164.16	W	
Production			
Stacks per year, net	53,760		
Stack yield	97.7%		Long-term three-sigma process
Stacks per year, gross	55,026		
Cells per year, delivered	6,451,200		
Cells per year, net	6,603,120		Into stacks, post cell and ass'y yield
Cell yield	97.7%		Long-term 3.5-sigma process
Assembly yield	97.7%		Long-term 3.5-sigma process
Cells per year, gross	6,917,674		
Cost Structure			
Cell fabrication maintenance rate	3.5%		% of capital
Cell fabrication consumables rate	20.0%		% of maintenance
Cell fabrication QA/QC rate	20.0%		% of fabrication labor
Stack assembly consumables rate	20.0%		% of maintenance
Indirect labor rate	20.0%		% of direct labor
Overhead rate	60.0%		% of maint + labor
Discount rate for capital recovery	11.0%		
Capital recovery period	10	yrs	
Capital recovery factor	17.0%		
Building cost	26.79	$\$/ft^2/yr$	
Cell Fabrication space	192,903	ft^2	
Seal Fabrication space	66,547	ft^2	
Stack Assembly space	3,120	ft^2	
Stack Outgoing QC space	90	ft^2	
TOTAL space	262,660	ft^2	
Labor Rates			
Cell fabricator	20.71	$/hr	
All other direct labor	19.87	$/hr	
Financial Assumptions			
US cost evaluation year	2011		

STACK DESIGN AND COMPONENTS

The baseline stack utilizes thin (0.6 mm) anode-supported planar solid oxide fuel cells with compressible ceramic seals and sheet metal interconnects in a cross-flow, internally manifold design. The stack block is shown in Figure 11-1.

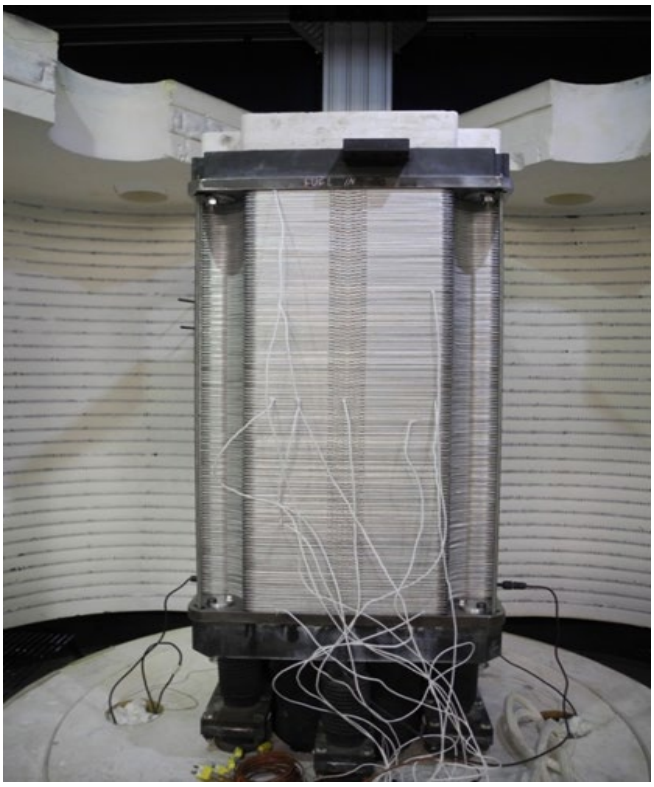

Figure 11-1. Stack Block

The stack consists of 120 repeat units and a set of non-repeat parts. A repeat unit includes one ceramic cell and metallic cell holder, anode flow field, nickel mesh, thermal spreader, cathode flow field, cathode exmet, anode and cathode seals, shims and an interconnect. There are 119 interconnects as they reside "between" cells. Non-repeat parts include two current collecting end plates. The component summary list along with the quantity and cost is shown in Table 11-2. As noted earlier, the revised stack cost is projected at $5,317 (2011 USD), whereas the 2015 stack cost estimate was $4,748 (2011 USD).

Table 11-2. Stack Cost ($/stack) Roll-up

(Original Costing on Left & Updated Costing on Right)

Description	Qty	Unit Cost	Total
Cell	120	$8.27	$992.23
Cell Fabrication	120	4.01	481.02
Cell Holder	120	2.60	311.77
Anode Shims	120	2.60	311.77
Anode Seals	242	0.88	213.21
Anode Flow Field	120	4.20	504.29
Cathode Shims	120	4.11	493.56
Cathode Seals	242	0.88	213.21
Cathode Flow Field	120	4.27	511.82
Interconnects	119	3.80	452.65
End Plates	2	57.40	114.80
Intermediate Plate	0	57.40	0.00
Stack Assembly		93.32	93.32
Building Cost		54.83	54.83
Totals Parts	**1325**		**$4,748.48**

Description	Qty	Unit Cost	Total
Cell	120	$9.18	$1,101.29
Cell Fabrication	120	5.04	605.09
Cell Holder	120	2.60	311.77
Anode Shims	120	2.02	242.82
Anode Seals	242	1.12	271.48
Anode Flow Field + contact	120 (x3)	5.76	691.28
Cathode Shims	120	4.11	493.56
Cathode Seals	242	1.12	271.48
Cathode Flow Field + contact	120 (x2)	5.12	614.18
Interconnects	119	2.68	318.79
End Plates	2	57.40	114.80
Intermediate Plate	0	--	--
Stack Assembly		149.09	
Building Cost		130.91	130.91
Totals Parts	**1685**		**$5,316.56**

The total cell fabrication cost has been updated to $605 per stack incorporating all related direct labor, indirect labor, allocated utilities, indirect costs, and capital recovery. In this new estimate, the cell cathode barrier layer has been added. The seal fabrication cost is also included in the cost for anode and cathode seals at $543 ($271.48 x 2) per stack. It also incorporates all related direct labor, indirect labor, allocated utilities, indirect costs, and capital recovery. Additionally, the unit cell design, including nickel mesh, thermal spreader, and cathode exmet, has been more detailed. Of the total stack cost of $5,317, $2,787 is for procured components and $2,529 is for in-house fabrication of cells, stack assembly, and building expenses. The new estimated cell material cost is $1,101 per stack. A change was made to the detailed calculation of the nickel oxide usage in the anode substrate and anode functional layer from the previous cost estimate which increases cell material cost.

PRODUCTION (MANUFACTURING) EQUIPMENT

The projected installed cell-related manufacturing equipment costs for cell and seal fabrication at high production volume is estimated at $76.9 million and shown in Table 11-3.

Table 11-3. Projected Production Equipment Costs, High Volume Production

Production Area	Equipment Cost	Installation	Installed Cost
Slurry Preparation	853,668	170,612	1,024,280
Tape Casting	4,540,822	1,708,869	6,249,691
Paste Preparation	1,241,209	247,862	1,489,070
Screen Printing	8,471,833	3,340,781	11,812,614
High Temperature Firing	19,314,489	7,148,166	26,462,656
Cell QC	2,041,586	408,317	2,449,903
Seal Production	20,198,437	7,242,507	27,440,944
Total	56,662,044	20,267,114	**76,929,158**

The increase in total installed capital cost was due to the following changes:

- Adjustment of unit cost of some equipment
- Adjustment of total quantity of equipment needed when applying 90% maximum capacity limit, extending work shift operation for some processes, and fine tuning of equipment throughput
- Inclusion of missing equipment and tools or accessories such as: slurry pots, 3 screen printers, scales, and fume hoods
- Removal of excess kiln that was not required

PRODUCTION DIRECT LABOR AND INDIRECT LABOR

Table 11-4. Indirect labor for cell production is assumed to be 20% of direct labor charges. The total full time employees (FTE) needed for cell and seal manufacturing is 228.

Table 11-4. Cell and Seal Production Direct Labor

Production Direct Labor	FTEs	Hrs/yr	DLH/unit	$/hr	$/unit	$/stack
Slurry Preparation	9	2,190	0.0031	20.71	0.063	7.59
Tape Casting	32	2,190	0.0109	20.71	0.225	27.00
Paste Preparation	7	2,190	0.0024	20.71	0.049	5.91
Screen Printing	60	2,190	0.0204	20.71	0.422	50.62
High Temperature Firing	12	2,190	0.0041	20.71	0.084	10.12
Cell QC	8	2,190	0.0027	19.87	0.054	6.48
Seal Production	100	2,190	0.0084	20.71	0.174	84.36
Total	**228**		**0.0519**		**1.072**	**192.07**

* FTE is full time employees, DLH is direct labor hours and $/unit is $/cell

STACK ASSEMBLY

Stack assembly is a significant in-house manufacturing activity. Based on the component list as shown in Table 11-5 and adjusting for some sub-assembly work before parts reach final assembly, there are approximately 840 final assembly pieces in a 120-cell stack. The high part count in the stack effectively moves stack assembly into the tens of millions of units per year range which justifies the proposed automation investment. Further detailing the unit cell components has led to increased costs in both anode side and cathode side sub-assembly spot welding. The estimated stack assembly cost per stack is now at $149.09 as shown in Table 11-2.

STACK ASSEMBLY EQUIPMENT

The projected installed equipment costs for stack assembly at high production volume is $7.3 million, as shown in Table 11-5.

Table 11-5. Projected Stack Assembly Equipment Costs, High Volume Production

Stack Assembly Area	Equipment Cost	Installation	Installed Cost
Stack Assembly, Welding and Material Handling	6,424,584	684,109	7,108,693
Corner Seal Application	146,201	38,987	185,188
QC Stack Outgoing	195	39	234
Total	6,570,979	723,135	**7,294,114**

Combining this with the cell-related production equipment cost, the total stack production factory capital cost for equipment is estimated at $84.2 million.

STACK ASSEMBLY DIRECT LABOR AND INDIRECT LABOR

The direct labor new estimates for high volume stack assembly are also based on adjustments made on operator-to-machine ratio, work shift operation, and total equipment needed. Stack assembly labor activities are grouped into major areas as shown in Table 11-6. Indirect labor for cell production is assumed to be 20% of direct labor charges. The total full time employees (FTE) needed for stack assembly is 59. Combining this with the production FTE needs, the total full time employees required for overall operation is 287.

Table 11-6. Stack Assembly Direct Labor

Stack Assembly Direct Labor	FTEs	Hrs/yr	DLH/unit	$/hr	$/unit	$/stack
Stack Assembly , Welding and Material Handling	48	315	2.2500	19.87	44.715	44.71
Corner Seal Application	9	315	0.4219	19.87	8.384	8.38
QC Stack Outgoing	2	315	0.0938	19.87	1.863	1.86
Total	**59**		**2.7656**		**54.962**	**54.96**

* FTE is full time employees, DLH is direct labor hours and $/unit is $/cell

STACK MANUFACTURING AND ASSEMBLY BUILDING EXPENSES

Building expenses, including general (indirect) building expenses such as lighting and space conditioning, are based on a total lease plus expenses cost of $26.79 per square foot. Stack manufacturing and assembly building is now estimated to require 262,660 square feet area after the adjustment on the total equipment needed. The estimated building cost per stack is at $130.91 as shown in
Table 11-2.

FACTORY STACK COST SUMMARY

In summary, the new estimate for a 120-cell stack block is $5,317 (2011 USD), which is 12% higher than the previous estimate. This new cost translates to $270 per kW DC gross power (based on stack nominal power rating of 19.69 kW DC gross) or $212 per kW AC (applying the Net AC to Gross DC ratio of 1.272 as realized in the IGFC system design). This cost prediction is still lower than the DOE cost target of $225/kW AC (2011 USD) for a high volume production rate of ~ 250 MW per year.

≥100 MW IGFC SYSTEM COST

Objective:

- Estimate capital cost of the ≥100 MW IGFC system Power Block and prepare Factory Cost Report

Approach:

The denominator for the calculation of the IGFC system cost ($/kW) will be the net AC power of the IGFC system. FCE will also characterize the system cost based on peak power. The cost estimate will establish and fully justify a reasonable estimate of the size and number of systems that must be manufactured per year to support the DOE cost goals outlined in Section A (Objectives) of the project SOPO.

Results & Discussion:

FCE previously developed the Solid State Energy Conversion Alliance (SECA) Coal-Based Factory Cost for the power block of an Integrated Gasification Fuel Cell (IGFC) system under a DOE supported cooperative agreement (DE-FC26-04NT41837). FCE released a Topical Report – Phase III Baseline SOFC Power Block Factory Cost Estimate Rev.3 (November 1, 2011), which included the cost estimation analysis to estimate the factory cost for the high efficiency IGFC power plant, utilizing a coal based gasification process and SOFC to generate electric power in a combined cycle. The IGFC plant has a capacity of 671.8 MW net electric output with an efficiency of 58.70% at Normal Operating Conditions (NOC) and a peak power efficiency of 53.85% based on coal HHV, exclusive of CO_2 compression power requirements. The IGFC system is shown in Figure 11-2. The figure also shows the power block cost estimate boundary. The Factory Cost Estimate is based on high-volume production of the fuel cell system (excluding coal gasification, syngas clean-up, and CO_2 separation subsystems). The denominator for the calculation of the Factory Cost ($/kW) is the power rating (net peak power) of the IGFC power plant (exclusive of CO_2 compression), using experimentally observed SOFC stack performance as the input. The non-stack cost estimates contained in this report are based on an annual production level that represents two power plants (671.8 MW each) per year.

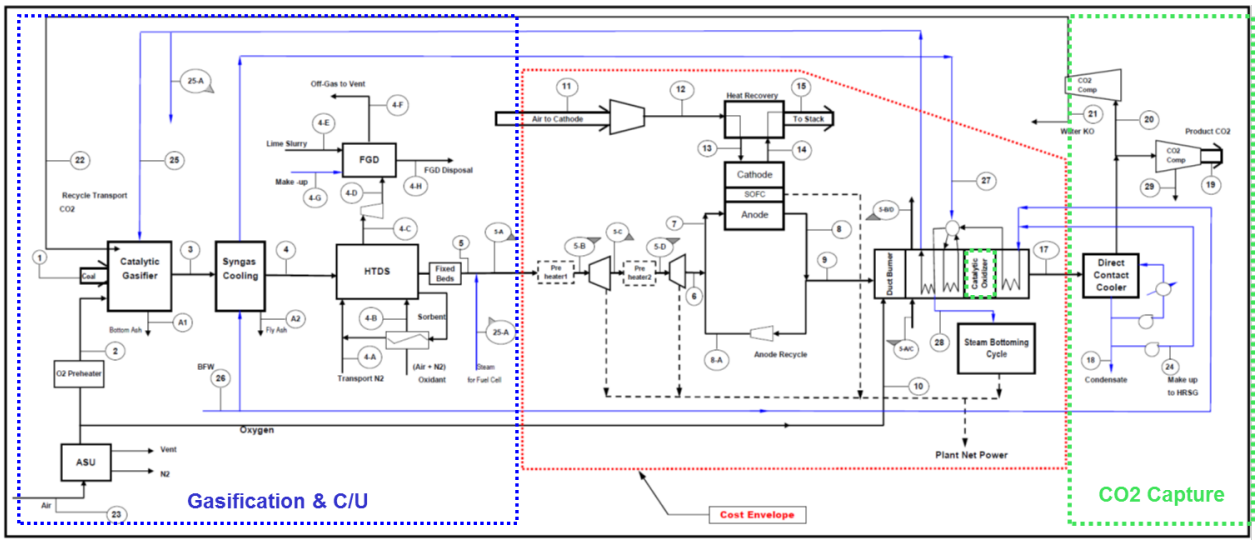

Figure 11-2. High Efficiency Coal Gasification / SOFC Power Plant – Block Flow Diagram

Cost estimating battery limits indicated with dashed red boundary (blue and green excluded)

The approach taken to develop this estimate was simply to revise the cost year basis (from 2007 USD to 2011 USD) and the stack cost to align with the current stacks utilized in the prototype system (as provided in Section 10). All other parameters and assumptions are the same as the previously-developed study.

The Factory Equipment Cost estimate overview is shown in Table 11-7. The SOFC stack cost estimate is 212 $/kW AC and the power island Factory Equipment Cost is 681 $/kW AC. Both costs meet the DOE cost targets of 225 $/kW and 900 $/kW for stack cost and power island Factory Equipment Cost, respectively.

Table 11-7. SOFC Plant Factory Equipment Cost

Item/ Description	Estimated Cost (2011 USD)	$/kW
Cost per Fuel Cell Block	$ 5,317	
Total Fuel Cell Block Cost	**$ 142,580,084**	**$ 212**
Inverter Cost	**$ 57,501,685**	**$ 86**
Cost per Module Enclosure	$ 60,238	
Total Module Enclosure Cost	**$ 20,240,115**	
BOP Cost	**$ 257,642,410**	**$ 383**
Total SOFC Plant Factory Equipment Cost		**$ 681**

12. CONCLUSION

The SOFC Prototype System has achieved 5000 hours of hot operation as of September 9, 2020 fulfilling the final outstanding project milestone. After the 5000 hours was achieved, the system was brought up to 100% load where overall stack performance continued to remain stable. The system continued to operate at 100% load through the end of the test campaign.

This Final report includes a full project test report as requested by D.O.E. The report encompasses several topics over the course of this project, including final results from demonstration testing and post-test stack analysis. Below is a comprehensive list of the requested test report topics:

- History/Background
- Project Purpose
- R&D On-Cell Development
- Cell Manufacturing
- Cell Yield
- Test plan, test deviations
- Issues and Problems
- Test Results (Relevant Test Data)
- Post Test Final Analysis of the system
- Lessons Learned
- Research and Technology Gaps
- Steps forward
- Stack and system cost analysis

Operation in Danbury was focused at 90% load to provide direct comparison to the operation in Pittsburgh and due to the lingering effects of the sulfur poisoning experienced there. As a result, higher stack temperatures were experienced which demanded higher air flow to provide additional cooling. The gross fuel efficiency was ~58% instead of the projected values of 64-65% and net fuel efficiency was around 36-38% during operation in Danbury as a direct consequence of the sulfur poisoning. The “projected net efficiency” which removes the added parasitic loads of the startup electric heaters was 46-48%.

GC samples were taken from the system at 100% load operation, which continued to show low levels of reforming in the reformer due to the sulfur poisoning. However, stack reforming did improve compared to the GC’s taken previously at 60% load. Temperatures inside the reformer and stacks remained high and stable, which suggests no significant recovery from the sulfur poisoning.

Post-test analysis for the five stacks from Module A have begun. Analyses showed overall good electrical contact in all layers, no or small trace of carbon at the fuel inlets, and broken cells. The early hours of the initial factory acceptance testing proved to be detrimental as indicated by the direct comparison of the stack that was replaced to that of the new one prior to the Pittsburgh operation. Sulfur was found in the cells that operated in Pittsburgh, while the stack that only ran in Danbury showed no signs of sulfur.

LIST OF ACRONYMS

A	Ampere
AC	Alternative Current
AFL	Anode Functional Layer
AI	Air In
AIC	Air In Center
AO	Air Out
AOC	Air Out Center
ASR	Area Specific (cell) Resistance
Atm	Atmosphere
BFD	Block Flow Diagram
BOL	Beginning of Life
BOP	Balance of Plant
CAD	Computer Aided Drafting
CBPP	Coal-Based Power Plant
CC	Current Collection (DC)
CDR	Component Development Requirement
CFD	Computational Fluid Dynamics
CFL	Cathode Functional Layer
COR	Contracting Officers Representative
CT	Cooling Tower
CTE	Coefficient of Thermal Expansion
CTF	Critical-To-Function
CTP	SECA Core Technology Program
CW	Cooling Water
CWP	Cooling Water Pump
DC	Direct Current
DFC	Direct Fuel Cell (FCE Molten Carbonate Fuel Cell)
DIR	Direct Internal Reforming, meaning in-stack reforming
DOE	United States Department of Energy
EOL	End of Life
FCE	FuelCell Energy, Inc.
FEA	Finite Element Analysis

FGD	Flue Gas Desulfurization
FI	Fuel In
FIC	Fuel In Center
FO	Fuel Out
FOC	Fuel Out Center
GA	General Arrangement (Plant Layout)
GT	Gas Turbine
HAZOP	HAZard and OPerability analysis
HDS	Hydrodesulfurization
HEX	Heat Exchanger
HHCs	Heavier Hydrocarbons (C2+)
HHV	Higher Heating Value
HMI	Human Machine Interface
H&MB	Heat and Mass Balance
HP	High Pressure
HRSG	Heat Recovery Steam Generator
I	Electrical Current
IC	Interconnect or separator plate
IGFC	Integrated Gasification Fuel Cell
IIR	Indirect Internal Reforming, meaning in-stack, between-cell, reforming
IR	Internal Resistance, of the cell or stack, ohm-cm^2.
K	degrees Kelvin
kW	Kilo-Watt
LHV	Lower Heating Value
MF	Mineral Fiber (thermal insulation)
MT	Microporous (thermal insulation)
MW	Mega-Watt
NETL	National Energy Technology Laboratory
Ni/YSZ	Nickel – Yttria-Stabilized Zirconia
NOC	Normal Operation Condition
OCV	Open Circuit Voltage
PCI	Pre-commercialized Integrated
PFD	Process Flow Diagram
P&ID	Piping & Instrumentation Diagram

POC	Proof-of-Concept
PPC	Peak Power Condition
psi	Pound per square inch pressure
psid	pounds per square inch pressure differential (pressure drop)
Q	Quarter
Redox	Reduction - oxidation
SECA	Solid State Energy Conversion Alliance
SG	Syngas
SLPM, Slpm	Standard liter per minute (at conditions of 1 atm and 70°F (21.1°C))
SOFC	Solid Oxide Fuel Cell
ST	Steam Turbine
TSC	Tape casting Screen-printing Cofiring
UA	Total heat transfer coefficient times heat transfer surface area, a designation for heat exchanger design
Ua, U_o, UtO	Air (Oxygen) Utilization
Uf, UtF	Fuel Utilization
USA	United States of America
V	Volt
VFD	Variable Frequency Drive
VPS	Versa Power Systems Ltd.
W	Watts